Studies of the Active Constituents of *Angelica sinensis* and *Garcinia hanburyi* on Colon Cancer

KAN, Lai Ting Winnie

A Thesis Submitted in Partial Fulfillment of the Requirements for the Degree of

Doctor of Philosophy

in

Pharmacology

The Chinese University of Hong Kong

September 2010

ProQuest LLC
789 East Eisenhower Parkway
P.O. Box 1346
Ann Arbor, MI 48106-1346

Thesis/Assessment Committee

Professor Alaster Hang Yung Lau (Chair)
Professor Ge Lin (Thesis Supervisor)
Professor John Anthony Rudd (Thesis Co-supervisor)
Professor Kwok Pui Fung (Committee Member)
Professor Karl Wah Keung Tsim (External Examiner)

ABSTRACT

Abstract of thesis entitled:

Studies of the active constituents of *Angelica sinensis* and *Garcinia hanburyi* on colon cancer

Submitted by Kan Lai Ting Winnie

for the degree of Doctor of Philosophy in Pharmacology

at The Chinese University of Hong Kong (July 2010)

Colorectal cancer is the second leading cause of cancer-related mortality in Hong Kong and lack of selectivity has limited the success of conventional chemotherapy. Given the recent interest in the anti-cancer effects of traditional Chinese medicine (TCM), there are two approaches to studying its bioactivity: as a mixture of ingredients or as single compounds. The objective of the present study is to examine the anti-tumor effects of *Angelicae Sinensis Radix* (DG) and *Garcinia hanburyi* resin (TH) using both approaches, respectively, as they are traditionally used to treat inflammation. In the present study, their anti-cancer effects and the mechanisms of actions were examined for the development of potential novel chemotherapeutic drugs for colon cancer since inflammation is a predisposing factor for colon cancer.

DG extract and its three main bioactive phthalides: *n*-butylidenephthalide, senkyunolide A and *z*-ligustilide (LGT), were found to be cytotoxic to HT-29 cells

with IC_{50} values (24 h) of 20.70 ± 0.85, 72.51 ± 8.65, 18.74 ± 1.14 and 41.98 ± 3.64 μg/ml, respectively. The results evidenced that LGT induced G_0/G_1 arrest and apoptosis, triggering cleavage of PARP, pro-caspases-3, -8 and -9 and nuclear fragmentation. LGT and cisplatin synergistically reduced the viability of HT-29 cells. More interestingly, DG extract was more potent than individual phthalides, suggesting that there are other bioactive components and/or synergistic interactions.

Subsequently, the anti-proliferative effects of DG and *Chuanxiong Rhizoma* (CX) extracts and mixtures containing three phthalides in the proportions similar to their presence in both extracts were examined, since CX also contains the same phthalides, but in different proportions. DG extract was significantly more potent than its corresponding phthalide mixture to inhibit cancer cell proliferation and synergistic interaction was observed among the phthalides and other bioactive components, while the phthalides in CX extract interacted antagonistically with other components.

Individual compounds purified from TH were investigated because gambogic acid isolated from this herb has been used clinically to treat cancer, 30-Epicambogin (EPC) and guttiferone K (GUTK) showed the highest cytotoxic selectivity and potency on HT-29 cells among 15 isolated compounds. IC_{50} values (24 h) for EPC and GUTK in HT-29 cells were 5.36±0.25 and 5.39±0.22 μM, respectively, and both induced G_0/G_1 arrest by down-regulation of cyclins D1, D3, CDK4 and CDK6, while up-regulation of $p21^{Waf1/Cip1}$ and $p27^{Kip1}$. Both compounds triggered the activation of caspases-3, -8 and -9 in apoptosis. The *in vivo* anti-tumor effects of GUTK were further investigated by using a subcutaneous Colon-26 mouse tumor model. GUTK (10 mg/kg i.p.) reduced tumor volume by 33.6% and potentiated the anti-tumor

effects of 5-fluorouracil when administered concurrently.

Our findings revealed that DG rather than individual phthalides, is worthy for further study as a potential anti-cancer drug, due to the synergistic interactions among multi-components in the herb. On the other hand, EPC and GUTK, isolated from TH have potential to be developed as novel anti-tumor candidates for combination use with 5-fluorouracil. The results strongly support the use of different approaches to study TCM for chemotherapy, according to its traditional and empirical use.

論文摘要

當歸及藤黃的活性成分對大腸癌的抗癌作用研究

大腸癌位居香港由癌症引起死亡的原因的第二位。目前的常規化療，對癌細胞缺乏選擇性，限制了治療的成功率。而當歸及藤黃這兩味中藥對炎症及癌症有著很好的治療作用，因此本研究分別通過研究這兩味中藥中的主要活性單體以及混合物，探討其對抗大腸癌的作用機制，為研發新型抗癌藥物提供理論基礎。

當歸提取物及三種苯肽，正丁烯醯內酯，川芎內酯 A 和槁本內酯（LGT）與 HT-29 細胞作用 24 小時後，明顯降低了癌細胞的存活率，IC_{50} 值分別為 14.99±2.34，236.90±18.22，54.17±5.10 和 60.63±6.79 μM。LGT 和當歸提取物將癌細胞阻滯在 G_0/G_1 期，並引起 PARP，pro-caspases-3，-8 和-9 的裂解來引起癌細胞的凋亡。並且 LGT 與順鉑可以產生協同作用降低 HT-29 細胞的存活率。而當歸提取物可以在劑量小於 LGT 的情況下引起細胞變化，提示提取物中可能有其他的活性成分產生協同增效作用。

此外，當歸及川芎均含有三種苯肽但比例不同。 將三種苯肽以在當歸及川芎提取物中的比例進行混合，製成苯肽人工混合物，並比較不同比例的苯肽人工混合物的活性。當歸提取物比相同比例的苯肽人工混合物的效果更好，顯示苯肽與當歸中的其他活性成分產生協同作用，從而增強了其抗癌細胞增殖的效應。而川芎苯提取物比相同比例的苯肽人工混合物的效果要弱，顯示川芎中的其他活性成分與苯肽產生對抗作用。

15 種從藤黃中分離得到的化合物，其中又以 30-epicambogin (EPC）及藤黃酮 K（GUTK）這兩個化合物的效果最強。EPC 及 GUTK 與 HT-29 細胞作用 24 小時

後，IC_{50} 值分別為 5.36±0.25 及 5.39±0.22 μM。兩種化合物都將癌細胞阻滯在 G_0/G_1 期，下調 cyclins D1，D3，CDK4 及 CDK6，同時上調 $p21^{Waf1/Cip1}$ 及 $p27^{Kip1}$，並引起 pro-caspases-3，-8 和-9 的裂解。在小鼠皮下接種大腸癌細胞 Colon-26 腫瘤模型測試下顯示，腹腔注射 GUTK (10 mg/kg) 可以減少 33.6%的腫瘤體積，而且可以提高腹腔注射 5-氟尿嘧啶的抗腫瘤效果。

本研究的結果顯示：由於當歸提取物的抗腫瘤效應來自於不同化合物之間的協同作用，因此當歸提取物較單體而言更有價值進一步開發為新的抗癌藥物。而另一方面，藤黃中的 30-epicambogin 及藤黃酮 K 則為有潛力的活性成分， 並有價值進一步研究與 5-氟尿嘧啶組合使用的抗癌藥物。

ACKNOWLEDGEMENTS

My last four years in the Department of Pharmacology have been amazing and no amount of words can fully describe how much I appreciate everything that I have gained. Everyone that I have met here has touched me in his/her own special way.

I would first like to express my deepest and most sincere thanks to my supervisor, Professor Ge Lin. She has supported me every step of the way, from the moment that I walked into her lab to the final submission of my thesis. I would like to thank her for the endless support: her positive energy during the good times and her words of encouragement and comfort during the bad times. She has given me the freedom that I needed as a PhD student and I feel that she has equipped me well with what I need to face challenges in the future. I truly appreciate the enormous amount of time and attention she has given me during my thesis writing and revising. I would also like to thank Professor John Rudd and Professor Chi Hin Cho for their guidance and support. Despite their busy schedules, they have both been very helpful with comments and advice when I needed it the most. As well, I would like to say thanks to my other thesis committee members: Professor Karl Tsim, Professor Kwok Pui Fung and Professor Alaster Lau, for their valuable feedback and challenging questions.

I am very thankful to my labmates: Ma Bin, Li Yanhong, Stella Chai, Cherry Yin and Li Na, for their assistance. I have learned so much from each and every one of them. I would like to show my gratitude to Professor Helen Wise for her kind words and the chats in her office. I would like to say a big thank you to: Jessica Law, Joyce Lee, Dr. Wayne Lee, Clover Wong, Christina Poon, Johnson Ng, Barry Yeung and Ethel Ng. All of you have laughed and cried with me, thanks for being my "battle mates!" Thanks to Jacky Li, Kam Ming Chan, Becky Kwan, Joresa Ng and for their help.

I wish to give thanks to my parents - they have been nothing but supportive and they are always the motivation behind everything that I do. I would also like to thank Vicko, Carmen, Bernice and Buchy for helping me to "gear up." Without my family, I know the completion of this thesis would not be possible. I owe my greatest thanks to Dave Yip. Dave, thank you for everything: the love, smiles, assistance, support and thoughtfulness. You always inspire me and make me want to be a better person.

Lastly, I would like to thank CUHK for the post-graduate studentship, the CUHK Direct Grant for providing financial support for my project and HKJCICM for providing the compound samples for my study.

PUBLICATIONS

1. **Kan, W.L.**, Cho, C.H., Rudd, J.A., Xu, H.X., & Lin, G. *In vitro* and *in vivo* effects of guttiferone K on growth inhibition of colon cancer cells through G_0/G_1 cell cycle arrest and apoptosis. Manuscript in preparation.

2. **Kan, W.L.**, Cho, C.H., Rudd, J.A., Xu, H.X., & Lin, G. Cytotoxic and anti-proliferative effects of 30-epicambogin, isolated from twigs of *Garcinia cowa,* on human colon cancer cells via G_0/G_1 cell cycle arrest and apoptosis induction. Manuscript in preparation.

3. **Kan, W.L.**, Cho, C.H., Rudd, J.A., Chan, W.Y., Hou, H.J., & Lin, G. Cytotoxic and apoptotic effects of *z*-ligustilide, isolated from *Angelica sinensis*, on human colon cancer cells. Manuscript ready for submission.

4. Gang, X., **Kan, W.L.**, Zhou, Y., Song, J.Z., Han, Q.B., Qiao, C.F., Cho, C.H., Rudd, J.A., Lin, G., & Xu, H.X. (2010). Cytotoxic polycyclic polyprenylated acylphloroglucinols from the twigs of *Garcinia cowa*. *Journal of Natural Products, 73*, 104-108.

5. **Kan, W.L.**, Cho, C.H., Rudd, J.A., & Lin, G. (2008). Study of the anti-proliferative effects and synergy of phthalides from *Angelica sinensis* on colon cancer cells. *Journal of Ethnopharmacology, 120*, 36-43.

CONFERENCE ABSTRACTS AND PRESENTATIONS

1. **Kan W.L.,** Cho, C.H., Rudd, J.A., Xu, H.X., Lin, G. (2010). Induction of apoptosis and G_0/G_1 cell cycle arrest by guttiferone K, isolated from *Garcinia cowa*, on human colon cancer cells. Poster presentation at The 9th Meeting of the Consortium for Globalization of Chinese Medicine 2010.

2. **Kan, W.L.,** Cho, C.H., Rudd, J.A., Xu, H.X., & Lin, G. (2010). 30-Epicambogin, isolated from twigs of *Garcinia cowa,* induces G_0/G_1 cell cycle arrest and apoptosis in human colon cancer cells. Poster presentation at The SYSU-CUHK State Key Laboratory of Oncology in South China 2010 Retreat Conference.

3. **Kan, W.L.,** Cho, C.H., Rudd, J.A., & Lin G. (2009). Anti-proliferative and apoptotic effects of *z*-ligustilide and synergy of phthalides from *Angelica sinensis* on human colon cancer cells. Oral presentation at The 8th Meeting of the Consortium for Globalization of Chinese Medicine 2009.

4. **Kan, W.L.,** Cho, C.H., Rudd, J.A., & Lin, G. (2009). *z*-Ligustilide, isolated from Radix *Angelica sinensis*, inhibits proliferation of human colon cancer cells via apoptosis induction. Oral presentation at The 2009 Hong Kong-Macau Postgraduate Symposium on Chinese Medicine.

5. **Kan, W.L.,** Cho, C.H., Rudd, J.A., & Lin G. (2009). Anti-proliferative and apoptotic effects of *z*-ligustilide, isolated from *Angelica sinensis*, on human colon cancer cells. Oral presentation at The 12th Scientific Meeting of the Hong Kong Pharmacology Society, in association with the Liaoning Pharmaceutical Society and the 3rd Hong Kong (CU)-Singapore-Taiwan Meeting of Pharmacologists. Winner of the Best Student Oral Communication Award.

6. **Kan, W.L.,** Cho, C.H., Rudd, J.A., & Lin, G. (2008). Study of the anti-proliferative effects of phthalides from *Angelica sinensis* on human colon cancer cells. Poster presentation at The IXth World Conference on Clinical Pharmacology and Therapeutics (CPT) 2008.

7. **Kan, W.L.,** Cho, C.H., Rudd, J.A., & Lin G. (2007). *In vitro* anti-proliferative effects of phthalides of *Angelica sinensis* on colon cancer cell line HT-29. Oral presentation at The Annual Scientific Meeting of the Hong Kong Pharmacology Society 2007 Postgraduate Oral Presentation Symposium.

ABBREVIATIONS

AIF – Apoptosis-Inducing Factor
APAF-1 – Apoptotic Protease Activating Factor-1
APC – Adenomatous Polyposis Coli
ATM - Ataxia Telangiectasia Mutated
ATP – Adenosine-5'-Triphosphate
ATR - Ataxia Telangiectasia and Rad3-related
BAD – Bcl-2-Associated Death Promoter
BLP – *n*-Butylidenephthalide
BCNU - 1,3-bis-(2-chloroethyl)-1-nitrosourea
CAD – Caspase-Activated DNase
CAM – Complementary and Alternative Medicine
CDK – Cyclin-Dependent Kinase
c-FLIP – Cellular FADD-like interleukin 1β-converting enzyme-Inhibitory Protein
CX – *Chuanxiong Rhizoma*
DBT – Dang gui Buxue Tang
DISC – Death-Inducing Signaling Complex
DMSO – Dimethylsulfoxide
DG – *Angelicae Sinensis Radix*
DR – Death Receptor
EGFR – Epidermal Growth Factor Receptor
EPC – 30-Epicambogin
ERK – Extracellular Signal-Regulated Kinase
FADD – Fas-associated Death Domain
FDA – Food and Drug Administration
5-FU – 5-Fluorouracil
GUTK – Guttiferone K
hTERT – Human Telomerase Reverse Transcriptase
IAP – Inhibitor of Apoptosis
i.p. – intraperitoneal
JNK/SAPK – c-Jun NH_2-Terminal Kinase/Stress-Activated Protein Kinase
LGT – *z*-Ligustilide
LV – Leucovorin
MAPK – Mitogen-Activated Protein Kinase
MOMP – Mitochondrial Outer Membrane Permeabilization
NER – Nucleotide Excision Repair
NF-κB – Nuclear Factor κ-Light-Chain-Enhancer of Activated B cells

NOXA - Phorbol-12-myristate-13-acetate-induced protein 1
NSAID – Non-Steroidal Anti-Inflammatory Drug
PARP – Poly (ADP-ribose) Polymerase
PI3K – Phosphatidylinositol-3 Kinase
PUMA – p53 Upregulated Modulator of Apoptosis
Rb – Retinoblastoma gene susceptibility protein
ROS – Reactive Oxygen Species
SKA – Senkyunolide A
SMAC/DIABLO - Second Mitochondria-derived Activator of Caspases/Direct IAP Binding Protein with Low PI
TCM – Traditional Chinese Medicine
TH – Resin of *Garcinia hanburyi*
TNF-α – Tumor Necrosis Factor-α
TRAIL – TNF-related Apoptosis-Inducing Ligand
TS – Thymidylate synthase
VEGF – Vascular Endothelial Growth Factor
VSMC – Vascular Smooth Muscle Cell
XIAP – X-linked Inhibitor of Apoptosis

TABLE OF CONTENTS

CHAPTER 1 – INTRODUCTION

1.1 Colorectal cancer

Colorectal cancer is a disease identified by malignant neoplastic growths in the colon, rectum and appendix and it is characterized by highly proliferating epithelial cells that become invasive and metastatic. It is the third most common cancer diagnosed and the third leading cause of cancer-related deaths in both men and women in the United States (American Cancer Society, 2010). In Hong Kong, it is the second most common cancer and the third leading cause of cancer mortality (Center of Health Protection Hong Kong, 2007-08). The incidence of colorectal cancer in both men and women is increasing in parts of Asia, such as China, Japan and Korea and it is comparable to that of the West. Also, the incidence of advanced neoplasia (invasive cancer) is comparable to that in the West, with increasing mortality rates (Sung *et al.*, 2008).

1.1.1 Symptoms, Staging and Risk Factors

Although colorectal cancer in its early stages is often asymptomatic, some subtle signs include changes in frequency of bowel habits, prolonged constipation and diarrhea, abnormal bloody or black stool, abdominal pain, the feeling of not being able to empty bowel completely, fatigue, nausea, vomiting and weight loss. The disease is diagnosed through sigmoidoscopy, colonoscopy and tests for fecal occult blood and carcino-embryonic antigen, which examine the colon for adenomas and polyps, blood in stool and colon cancer biomarkers (Cutsem & Oliveira, 2009). Biopsy tumor samples from the colon allow for the classification of colon cancer into

stages according to the modified Dukes staging, TNM (tumor/nodes/metastasis) and stage number (I-IV) systems. Since one of the most important prognostic markers for survival is the stage of the tumor at diagnosis, the tumor biopsy sample must be accurately categorized (Wilkes, 2005). The tumor is classified according to its penetration into the intestinal wall, its invasion into neighboring lymph nodes and its metastasis into other body organs (Wilkes, 2005; Cutsem & Oliveira, 2009). In the earliest Dukes staging system, tumors were classified into stages A to D with sub-stages according to the penetration of the tumor into the mucosa (stage A) and muscularis propria (stage B) of the bowel wall, lymph nodes (stage C) and to other organs (stage D). In 2002, the American Joint Committee on Cancer introduced the TNM and stage number grouping system to fully describe the extent of invasion of the tumor into the bowel wall and its metastasis into neighboring lymph nodes and distant organs, which allows for patients to be divided into stages. Specifically, this differentiates between the risk of recurrence and survival rates in patients characterized as Stage II and III, where the main difference is whether the tumor has spread into lymph nodes (Wilkes, 2005). This is of significance because the spread of the tumor into surrounding lymph nodes is predictive of outcome after surgical tumor removal (Kosmider & Lipton, 2007). Details of the current TNM staging system for colon cancer are summarized in Table 1.1.

Table 1.1 Current TNM staging system for colorectal cancer

Tumor stage	Tumor penetration
T1	Invasion into submucosa of bowel wall
T2	Invasion into muscularis propria of bowel wall
T3	Invasion through the muscularis propria into subserosa or periocolic or perirectal tissues
T4	Invasion into other organs with or without perforation

Nodal stage	Invasion of lymph nodes
N0	No lymph node invasion
N1	Invasion into 1 to 3 neighboring lymph nodes
N2	Invasion into 4 or more neighboring lymph nodes

Metastatic stage	Extent of metastasis
M0	No metastasis into distant organs
M1	Metastasis into distant organs

Risk factors for the disease include increasing age, family history, male gender, obesity, smoking, lack of exercise and chronic alcohol consumption (Kosmider & Lipton, 2007; Seitz & Becker, 2007; Sung *et al.*, 2008; Weingarten *et al.*, 2008). Other diseases that increase the risk of colorectal cancer include diabetes, inflammatory bowel disease, personal history of polyps and genetic disorders that lead to early onset hereditary non-polyposis colorectal cancer (HNPCC) and familial adenomatous polyposis (FAP) (Kosmider & Lipton, 2007; Xie & Itzkowitz, 2008).

1.1.2 Current Treatment Options

The standard treatment for colorectal cancer is surgical resection, followed by adjuvant therapy as a combination of chemotherapy or radiation therapy (Wilkes, 2005; Chau & Cunningham, 2006; Julien & Thorson, 2010). Surgical resection provides a strong cure for the disease, as 15.9% to 58.1% of patients were cured after resection for a local tumor, and chemotherapy is often used as adjuvant therapy to reduce the recurrence of the disease (Guyot *et al.*, 2005; Chau & Cunningham, 2006). In patients with stage II tumors surgically removed, the relapse rate is 25%, while it is as high as 60% in stage III patients (Chau & Cunningham, 2006; Kosmider & Lipton, 2007). Chemotherapy is suggested to be the main form of adjuvant therapy post-surgery since radiotherapy is not as effective at reducing recurrence as drug treatment alone, and it is damaging to neighboring organs (Chau & Cunningham, 2006). In rectal cancer, radiation therapy is usually combined with anti-tumor drugs as adjuvant therapy to reduce local and distant extra-hepatic metastasis, as local recurrence occurs in almost 50% of patients within a year after surgery (Kosmider & Lipton, 2007). Even though survival rates were similar in many randomized clinical trials between those given chemoradiation or radiation therapy alone, the pre- and post- surgical use of chemotherapeutic drugs reduced the local recurrence of the tumor (Julien & Thorson, 2010). Hence, there is an immense amount of research on the discovery of new anti-cancer drugs. Whereas the standard protocol for stage III patients is chemotherapy as adjuvant therapy commencing within 6-7 weeks of surgery, chemotherapy is usually not recommended for healthy stage II patients (Chau & Cunningham, 2006).

The first drug used for the treatment of colorectal cancer was 5-fluorouracil (5-FU) in the 1960s and still remains in use today. It is an anti-metabolite pyrimidine uracil

analogue that is a non-competitive inhibitor of thymidylate synthase (TS) (Wilkes, 2005). 5-Fluorouracil is converted into the active metabolites, fluorordeoxyuridine monophosphate (FdUMP), fluorodeoxyuridine triphosphate (FdUTP) and fluorouridine triphosphate (FUTP), which disrupt RNA synthesis and thymidylate synthase activity. Normally, thymidylate synthase is responsible for the reductive methylation of deoxyuridine monophosphate (dUMP) to deoxythymidine monophosphate (dTMP) with 5,10-methylenetetrahydrofolate acting as a cofactor (Longley *et al.,* 2003). The metabolite FdUMP binds to TS and dTMP synthesis is inhibited. The low levels of dTMP lead to imbalances in levels of the other deoxynucleotides, which results in disrupted DNA synthesis and repair. The other 5-FU metabolites (such as FUTP) are mis-incorporated into RNA and DNA, which results in DNA strand breaks and errors in RNA processing and post-translational modification (Longley *et al.,* 2003). Therefore, DNA synthesis and proliferation of rapidly-dividing neoplastic cells are selectively inhibited by 5-FU, which lead to death of cancer cells by apoptosis (Longley *et al.,* 2003; Huerta *et al.,* 2006). However, resistance rate to 5-fluorouracil is high, and it is one of the contributing factors to failed therapy for colorectal cancer (Li *et al.,* 2010a). Thus, 5-FU has been used in combination with other anti-cancer drugs since the 1980s (Wilkes, 2005). The mainstay first-line therapy consists of a combination of 5-FU and leucovorin (LV) through intravenous injection for an average of six months, which has resulted in a median survival of 10-12 months (Wilkes, 2005; Chau & Cunningham, 2006; Huerta *et al.,* 2006). Leucovorin (also known as folinic acid) increases cellular folate levels, thereby increasing the binding of 5-FU to thymidylate synthase, further inhibiting DNA synthesis (Huerta *et al.,* 2006). The survival advantage and toxicity profile were better in patients treated with a continuous infusion of 5-FU/LV, rather than a bolus administration, so the preferred route of administration for 5-FU/LV is

continuous infusion by intravenous route (Wilkes, 2005; Chau & Cunningham, 2006). Since continuous infusion is inconvenient for the patient, capecitabine is also considered as a first-line drug for colorectal cancer which can be administered as an oral 5-FU prodrug that is converted into its active form in the tumor (Wilkes, 2005). Subsequently, irinotecan has also been approved as second-line treatment for advanced colorectal cancer in 1996. It is a topoisomerase I inhibitor which inhibits DNA winding, therefore leading to reduced DNA replication and transcription. In addition, oxaliplatin, a third-generation platinum analogue, was approved by FDA as first-line treatment for metastatic colon cancer (Wilkes, 2005; Huerta *et al.,* 2006; Kosmider & Lipton, 2007). In particular, it forms cross-linking DNA adducts which disrupt DNA replication, and has a mechanism of action similar to that of typical platinum analogues used for treating cancer.

Several randomized clinical trials have been done to examine the effects of combination chemotherapy on cancer patients after surgical resection. That is, a combination of oxaliplatin and infusional 5-FU and LV (also known as FOLFOX) induced a longer median time to progression, longer disease-free survival, higher overall response rate and median survival time and lower recurrence rate for patients with advanced colon cancer when compared to combinations of irinotecan, 5-FU and LV (also known as IFL) and bolus 5-FU/LV (also known s LV5FU2) (Wilkes, 2005; Chau & Cunningham, 2006; Sharif *et al.,* 2008). Clinical trials have shown that the addition of oxaliplatin to infusional and bolus 5-FU/LV improved disease-free survival after 3 years. For instance, FOLFOX increased the chances that a patient would be alive and disease-free after 3 years by 5.3%, relative to the same regimen without oxaliplatin (Sharif *et al.,* 2008). Therefore, oxaliplatin, in combination with 5-FU and LV is considered as first-line treatment for patients with metastatic colon

cancer and highly recommended for adjuvant therapy in stage III of the disease after surgical resection (Wilkes, 2005). On the contrary, irinotecan did not increase disease-free survival when added to bolus and continuous infusional 5-FU/LV (IFL) (Chau & Cunningham, 2006). Thus, irinotecan and IFL are not recommended for use in combination therapy or as adjuvant chemotherapy in stage III colon cancer, respectively.

The most recently developed drugs are bevacizumab and cetuximab, which are both monoclonal antibodies used to treat metastatic colon cancer and target intracellular pathways. Bevacizumab has a high binding affinity to VEGF-A, which prevents binding of VEGF-A to VEGF-1 and -2 receptors on the surface of tumor and blood vessel endothelial cells (Kohne & Lenz, 2009). Hence, the downstream signaling pathways of proliferation and migration of tumor and endothelial cells are inhibited, which reduces angiogenesis and tumor progression and metastasis (Wilkes, 2005). Phase II and III clinical trials demonstrated that bevacizumab combined with 5-FU/LV or IFL increased overall survival and time to progression (Kohne & Lenz, 2009). Bevacizumab was approved by the FDA for use in combination with 5-FU/LV or irinotecan for the first-line treatment of metastatic colon cancer (Wilkes, 2005; Kohne & Lenz, 2009). Since there is an over-expression of epidermal growth factor (EGF) receptors on the surface of tumor cells, cetuximab (a chimeric murine/human antibody) acts as an inhibitor of the receptor to suppress downstream signaling pathways involved in cell proliferation and cell cycle (Wilkes, 2005; Huerta *et al.*, 2006). Cetuximab has been approved by the FDA for use in combination with irinotecan or as a single agent in patients that cannot tolerate irinotecan as second-line drug treatment in patients with EGFR-expressing tumors (Wilkes, 2005; Kohne & Lenz, 2009). Clinical trials showed that cetuximab, in combination with

FOLFOX and FOLFIRI (5-FU/LV/irinotecan) reduced the risk to progression and increased progression-free survival (Kohne & Lenz, 2009). Panitumumab is a fully humanized monoclonal antibody that has been approved for use in EGFR-sensitive tumors as a single agent after the failure of 5-FU, irinotecan and oxaliplatin since it has been found to reduce time to progression (Kohne & Lenz, 2009). There are ongoing clinical trials to investigate the effects of combining bevacizumab and cetuximab or panitumumab or together with FOLFOX and with pre-operative radiation therapy in both colon and rectal cancers (Wilkes, 2005; Kohne & Lenz, 2009; Julien & Thorson, 2010).

1.1.3 Problems with Current Anti-cancer Drugs

Although surgical resection can cure 75% of patients with stage II colon cancer and adjuvant chemotherapy has increased the overall survival of patients with stage III colon cancer, the local and distant relapse of the tumor occurs at a high rate (Huerta *et al.,* 2006; Kosmider & Lipton, 2007). Up to 40% of stage III patients will experience relapse despite of adjuvant therapy and up to 8% of patients will develop a new primary colon tumor within four years (Kosmider & Lipton, 2007). As well, the tumor response rate to single agents is low. For example, the clinical response rate to single injection of bolus 5-FU is 10-20%, and even with the addition of leucovorin, the response rate is still under 30%. Furthermore, a combination regimen consisting of 5-FU/LV with irinotecan or oxaliplatin increased the response rate to only up to 60% (Longley *et al.,* 2003; Noordhuis *et al.,* 2004). Many people may have an inherent or developed resistance to anti-cancer drugs. Specifically, patients with high thymidylate synthase expression do not have a high response rate to 5-FU and prolonged 5-FU treatment can also upregulate TS expression. Overexpression of dehydropyrimidine dehydrogenase (DPD), an enzyme responsible for the catabolism

of 5-FU into its metabolites, has also been suggested to lead to 5-FU resistance (Longley *et al.,* 2003). In addition, tumors that displayed KRAS (a GTPase downstream of EGFR signaling pathway) gene mutation had a low response rate to cetuximab and panitumumab (Kohne & Lenz, 2009). Due to the low response rates of colon cancer to single agents, combination therapy is usually chosen for adjuvant therapy to reduce disease recurrence.

1.1.3.1 Adverse Effects of Current Anti-cancer Drugs

One of the major problems with current anti-tumor drugs that remains unsolved is their lack of selectivity for cancer cells. That is, the mechanism of action of almost all drugs targets rapidly-dividing cancerous cells, but affects normal cells as well. The adverse effects of most anti-cancer drugs are nausea and vomiting, hematotoxicity, neurotoxicity and gastrotoxicity (Wilkes, 2005; Li *et al.,* 2006a, 2006b; Kosmider & Lipton, 2007). The major adverse effects of 5-FU and capecitabine are gastrotoxicity, namely nausea, diarrhea and mucositis, which can be exacerbated in patients with low DPD expression (Kosmider & Lipton, 2007). Bolus injection of 5-FU/LV induces neutropenia and nausea, which can be improved by administration through continuous infusion (Chau & Cunningham, 2006). Palmar-plantar erythrodysesthesia (also known as hand-foot syndrome) occurs in 56% of patients taking oral capecitabine and 34% of patients with continuous infusions of 5-FU (Wilkes, 2005). The capillaries in the soles of feet and palms of the hands are compressed, which stimulates an inflammatory response mediated by cyclooxygenase II. The symptoms are tingling, erythema of the hands and feet, edema and pain, blistering and scarring, which can be relieved with a COX-II inhibitor (Wilkes, 2005; Kosmider & Lipton, 2007). Other side effects include granulocytopenia and neuropathy (Kosmider & Lipton, 2007). The main adverse

effect of oxaliplatin is dose-limiting neurotoxicity: acute and chronic peripheral sensory neuropathy. Acute neurotoxicity is due to over-stimulation of the peripheral nerves and the symptoms include paresthesia and muscle spasms (Wilkes, 2005; Kosmider & Lipton, 2007). Chronic sensory neuropathy involves the large-fiber and motor peripheral nerves and is manifested as paresthesias and a distorted sense of body spatial position. Neuropathy may be treated with celecoxib, gabapentin, calcium and magnesium infusions, changing regimen to infusional 5-FU/LV or alternating oxaliplatin with a drug holiday (Wilkes, 2005; Kosmider & Lipton, 2007). Extravasation of oxaliplatin leads to tissue and muscle necrosis and fibrosis, which can be treated with anti-inflammatory drugs such as dexamethasone (Wilkes, 2005). Moreover, hypersensitivity reactions such as rash, fever or anaphylaxis may occur after oxaliplatin administration, which are treated with steroids and histamine antagonists (Wilkes, 2005). Treatment of colon cancer with FOLFOX and FLOX (oxaliplatin with bolus 5-FU/LV) resulted in neutropenia, neuropathy, diarrhea, bowel wall thickening and ulceration (Chau & Cunningham, 2006; Sharif *et al.*, 2008). The administration of irinotecan induced acute and delayed diarrhea accompanied with neutropenia and sepsis (Wilkes, 2005). IFL induced myocardial infarction and pulmonary embolism in addition to gastrotoxicity, so its use as adjuvant treatment is not encouraged (Chau & Cunningham, 2006). Generally speaking, bevacizumab and cetuximab are well-tolerated in clinical use but it has been reported that bevacizumab with or without irinotecan induced hypertension that required medication, deep vein thrombosis and pulmonary embolism (Kohne & Lenz, 2009). Decreased wound healing, hemorrhage and perforation in the gastrointestinal tract may also occur (Chau & Cunningham, 2006). Facial hair growth, rash, dry skin and skin infection and inflammation occurs in at least 45% of patients using cetuximab and panitumumab (Chau & Cunningham, 2006; Kohne & Lenz, 2009).

The appearance of adverse effects occurs with all of the clinically used drugs for colon cancer, and often, combination therapy show greater efficacy, but also more toxicity to other organs. Thus, new drug candidates with higher selectivity for cancer cells are needed.

1.1.4 De-regulation of Cellular Pathways in Colon Cancer

Although the initiation and progression stages of colon cancer are complicated and cannot be attributed to one single cause, an enormous amount of research has been done to suggest that in most cases, there are defects in the proliferation, survival and DNA replication pathways inside the normal cell that facilitate its transformation into a malignant cell (Viglietto *et al.,* 2002; Dias & Bailly, 2005; Huerta *et al.,* 2006; Liu *et al.,* 2006).

1.1.4.1 De-regulation of Genetic Pathways Leading to Colon Cancer

Since FAP and HNPCC account for only 1% and 5% of colorectal cases, respectively, most colon cancers occur as a result of non-hereditary somatic genetic changes and epigenetic modifications (Liu *et al.,* 2006). There are three main genetic pathways associated with colon tumorigenesis: 1) mutation of the Adenomatous Polyposis Coli (APC) gene which accounts for more than 80% of sporadic colon cancer; 2) microsatellite instability which involves silencing of mismatch repair genes and 3) mutation of the BRAF gene (Liu *et al.,* 2006). A de-regulation of the Wnt pathway and mutation of the APC gene are the first genetic problems in FAP and are some of the earliest events in sporadic colon carcinogenesis (Huerta *et al.,* 2006; Liu *et al.,* 2006). Normally, Wnt ligand binds to the cell surface receptors of the "Frizzled" family, which in turn activates "Dishevelled" family proteins. The activated "Dishevelled" proteins inhibit the axin/glycogen synthase kinase-3β (GSK-3β)/APC

complex. Therefore, proteolytic degradation of β-catenin cannot occur and β-catenin accumulates in the cytoplasm (Liu *et al.*, 2006). In a similar fashion, a mutation of the APC gene also leads to the accumulation of β-catenin in the cytoplasm. β-Catenin migrates into the nucleus, where it can interact with transcription factors to induce the transcription of oncogenes such as c-myc and cyclins, which in turn leads to tumorigenesis (Huerta *et al.*, 2006).

1.1.4.2 De-regulation of Cell Proliferation Pathways and Colon Cancer

The division and proliferation of cells is governed by the cell cycle, which consists of G_1, S (synthesis), G_2, M (mitosis and cytokinesis) phases and a quiescent stage known as G_0 phase. As the cell goes through the phases, biosynthesis of various enzymes and proteins occurs to prepare for the coming phase and the successful division into two daughter cells. Up to the end of G_1 phase (G_1/S checkpoint), cells respond to extracellular stimuli and make the decision to advance to S phase for DNA replication or to leave the cell cycle to enter G_0 phase in the cases of DNA damage. Since the cell cycle progresses in a mitogen-independent manner after G_1/S checkpoint, anti-tumor drugs that target the G_1 phase are effective in reducing proliferation (Belletti *et al.*, 2005). The phases of the cell cycle with their respective regulators are outlined in Figure 1.1.

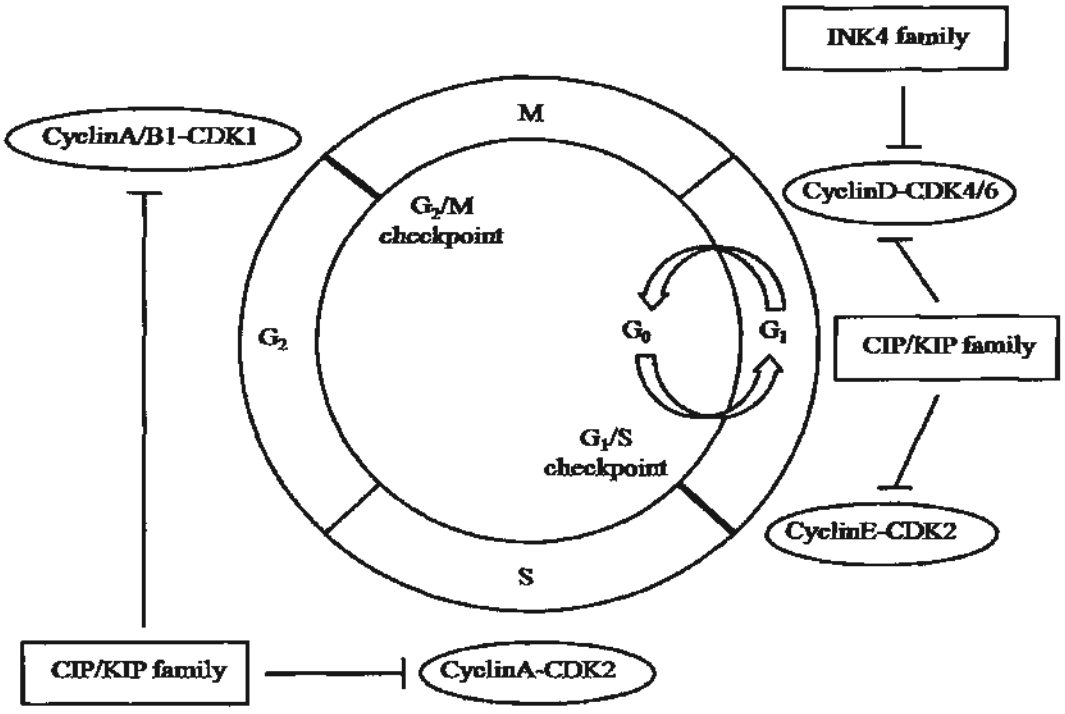

Figure 1.1 The phases of the cell cycle are regulated by cyclin-cdk complexes that are inhibited by cyclin-dependent inhibitors of two classes, INK4 family and CIP/KIP family.

It is well established that several proteins that control each phase of the cell cycle are mutated, deleted or over-expressed in various types of human cancers, which leads to uncontrolled cell division and proliferation (Viglietto *et al.,* 2002; Senderowicz, 2003; Belletti *et al.,* 2005; Lee & Kim, 2009). The regulation of the cell cycle is through controlling the activity of complexes composed of different cyclins and cyclin-dependent kinases (CDKs) in each phase. Specifically, proteins of the cyclin D family are produced in early to mid G_1 phase after the cell has encountered extracellular stimuli and various growth factors such as epithelial growth factor, IGF I and II and gastrointestinal hormones like gastrin. Many oncogenes, such as Ras, Src and β-catenin also induce cyclin D1 expression (Fu *et al.,* 2004). Once cyclin D is

produced, it binds to CDK4 or CDK6 (a class of serine-threonine kinases). Together, they form a holoenzyme in which the cyclin D is the regulatory subunit and the CDK is the catalytic subunit (Viglietto *et al.,* 2002; Fu *et al.,* 2004). Subsequently, the cyclin D/CDK4 or CDK6 complex phosphorylates the retinoblastoma gene susceptibility protein (Rb), which dissociates from the E2F/DP1/Rb complex. The free E2F acts as a transcription factor and facilitates the transcription of genes needed for S phase such as cyclins E and A, DNA polymerase and c-myc (Senderowicz, 2003). Similarly, complexes of cyclin E/CDK2, cyclin A/CDK2 and cyclin A or B1/CDK1 (also known as cdc2) form in G_1/S checkpoint, S phase and G_2/M checkpoint, respectively, to ensure that the cell progresses smoothly through all of the phases (Viglietto *et al.,* 2002; Senderowicz, 2003; Belletti *et al.,* 2005).

The first level of regulation of the cell cycle is through the regulation of cyclin and CDK mRNA and protein levels. Cyclins and CDKs may also be phosphorylated to enhance or inhibit their activity. For example, the activity of CDK4 may be inhibited by phosphorylation at the Y17 residue (Belletti *et al.,* 2005). Furthermore, the activity of cyclin/CDK complexes may be modulated by two classes of cyclin-dependent kinase inhibitors: 1) INK4 family and 2) CIP/KIP family (Lee & Kim, 2009). The INK4 family includes proteins $p15^{INK4B}$, $p16^{INK4A}$, $p18^{INK4C}$ and $p19^{INK4D}$ and they bind to CDK 4 or 6, which negatively affects the ability of cyclin D and ATP to bind and form the holoenzyme complex (Viglietto *et al.,* 2002; Belletti *et al.,* 2005). The CIP/KIP family includes proteins $p21^{Waf1/Cip1}$, $p27^{Kip1}$ and $p57^{Kip2}$ and they contain motifs in their N-termini that allow them to bind and inhibit both cyclins and CDKs (Viglietto *et al.,* 2002). Although CIP/KIP family can inhibit complexes containing cyclins D, E, A and the respective cdks, their main target is cyclin E/cdk2 at the G_1/S checkpoint (Viglietto *et al.,* 2002).

One of the most common alterations in cancer is the overexpression of cyclin D in early tumorigenesis, which allows for enhanced cell cycle progression and proliferation and de-differentiation of tumor cells (Senderowicz, 2003; Fu *et al.,* 2004; Mayo & Mayol, 2009). Amplification or overexpression of CDK4 has also been found in glioblastoma, melanoma and breast carcinoma (Senderowicz, 2003). The inactivation of the Rb pathway, by mutation of the Rb protein, or hyperphosphorylation of Rb, has also been found in many cancers (Senderowicz, 2003). Aside from changes in levels and activity of cyclins and cdks, dysfunction of the cyclin-dependent kinase inhibitors is also very common in cancer. It has been reported that a decreased expression of $p16^{INK4A}$ in primary colorectal cancer tissues was associated with large tumor size and metastasis into surrounding lymph nodes (Kim *et al.,* 2005). Furthermore, surgically-resected colon tumor samples that showed methylation of the promoter-associated CpG islands of $p16^{INK4A}$ was associated with increased disease recurrence and shortened cancer-related survival (Mitomi *et al.,* 2010). Likewise, the methylation of $p15^{INK4B}$ promoter was also more significant in primary colon cancer samples, and stage I and II patients with methylated $p15^{INK4B}$ showed lower survival rates (Ishiguro *et al.,* 2006). A large amount of work has been done on the effects of CIP/KIP proteins on cancer, especially $p27^{Kip1}$. $p27^{Kip1}$ Knock-out mice showed enlarged thymus and adrenal glands, with spontaneous induction of pituitary tumors (Nakayama *et al.,* 1996). In human colon cancer samples, there was an inverse correlation between tumor $p27^{Kip1}$ expression and the malignancy of the tumor according to tumor stage (Fredersdorf *et al.,* 1997). Loda *et al.* (1997) showed that low levels of $p27^{Kip1}$ in colorectal tumors were mediated by proteasomal degradation inside the cytoplasm, not by genetic means. Low $p27^{Kip1}$ levels were correlated with low survival and poor prognosis and $p27^{Kip1}$ has since become an independent prognostic marker for the disease (Loda *et*

al., 1997; Zhang & Sun, 2001). In addition, low $p27^{Kip1}$ is associated with metastasis of colon cancer, especially into lymph nodes (Thomas *et al.,* 1998; Li *et al.,* 2002).

1.1.4.3 Imbalance of Apoptosis in Colon Cancer

There are various modes of cell death, which includes apoptosis, necrosis and autophagy (Duprez *et al.,* 2009). Apoptosis is a type of energy-dependent genetically-programmed cell death that occurs naturally in embryogenesis, immune system development, tissue homeostasis and in response to physiological stresses (Sun, 2005). Apoptosis occurs in the development of the lens, four-chambered heart, skeletal muscle and limbs and digits in humans and animals (Penaloza *et al.,* 2006). It also eliminates the cells in the nervous system that fail to establish functional synaptic connections to aid in the development of the nervous system (Elmore, 2007). However, for cancer, most of the research has focused on apoptosis since cells that do not undergo apoptosis may become malignant; reduced apoptosis has been associated with resistance to chemotherapy and most of the current anti-cancer drugs induce apoptosis as their mechanism of action (Thonel & Eriksson, 2005; Huerta *et al.,* 2006; Huerta *et al.,* 2007). For instance, 5-FU and its active metabolite, FdUMP, both induce cell cycle arrest and apoptosis in human colon cancer cells (Matuo *et al.,* 2009). In cancer, the balance between cell proliferation and apoptosis determines the growth rate and metastasis of the tumor (Kim *et al.,* 2002). Normally, there is a tight balance in the mucosa in the colon between cell proliferation at the base of the crypt and apoptosis at the surface epithelium for cell turnover (West *et al.,* 2009). Disruption of this balance plays a major part in the progression of colon cancer, from normal tissue to adenoma to carcinoma. For instance, it has been demonstrated that resected colonic adenomas had reduced apoptotic index values, compared to normal mucosa (Anti *et al.,* 2001; Martin *et al.,* 2002; Keku *et al.,* 2008). There was a

progressive decrease in apoptosis as colon mucosa transformed into adenoma and subsequently, into carcinoma and reduced apoptosis has been correlated with increased recurrence (Bedi *et al.*, 1995; Keku *et al.*, 2008).

1.1.5 Apoptosis

The main morphological characteristics of apoptosis include condensed nuclear chromatin (pyknosis), reduction in cell size as organelles become tightly-packed, plasma membrane blebbing, DNA fragmentation (karyorrhexis), loss of adhesion to neighboring cells and intact membrane integrity (Kerr *et al.*, 1972; Wylie *et al.*, 1981; Elmore, 2007; Huerta *et al.*, 2007). Apoptosis can be induced by a variety of stimuli, such as heat, radiation, hypoxia, DNA damage, chemical toxins and cytotoxic chemotherapeutic drugs (Elmore, 2007; Duprez *et al.*, 2009). One of the main biochemical hallmarks is the activation of the caspase cascade, in which a series of cysteinyl aspartic acid-specific proteases are activated by cleavage of the zymogen form and the cell is then committed to apoptotic cell death (Elmore, 2007). So far, eleven human caspases have been discovered and are divided into three main classes: a) initiator caspases-2, -8, -9 and -10 which have long N-terminals, b) executioner/effector caspases-3, -6 and -7 which have short N-terminals and c) inflammatory caspases-1, -4 and -5. The remaining caspases are responsible for other functions such as cytokine processing and endoplasmic reticulum-mediated apoptosis (Huerta *et al.*, 2006; Elmore, 2007). There are two main apoptotic pathways, which are defined as the extrinsic death receptor-mediated and intrinsic mitochondrial-mediated pathways, as demonstrated in Figure 1.2.

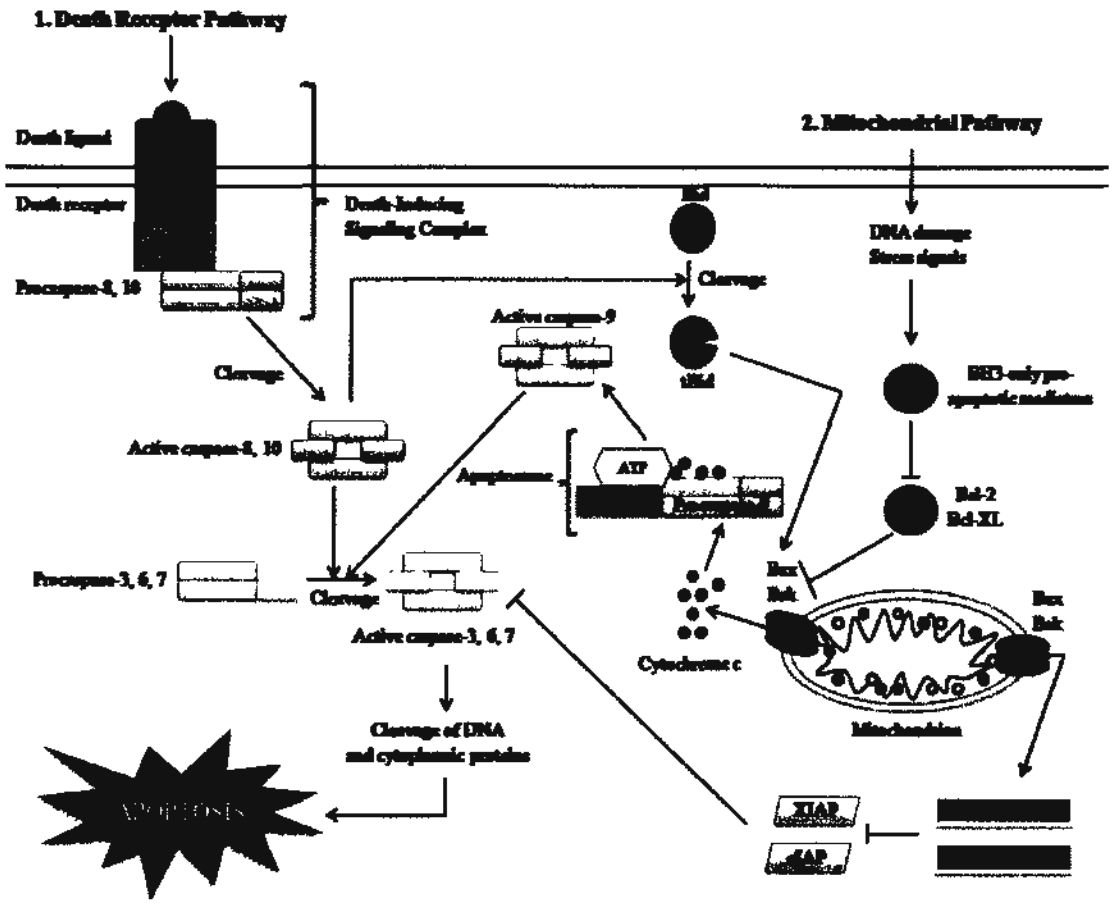

Figure 1.2 The two main pathways of apoptosis, death receptor and mitochondrial pathways, are initiated by different biochemical events and initiator caspases, but cross-talking can occur through tBid. Both pathways converge to activate the executioner caspases-3, -6 and -7, which in turn cleave DNA and cytoplasmic proteins to contribute to the cellular morphology that defines apoptosis. The sequence of events is described in detail below. Duprez *et al.* (2009).

1.1.5.1 Extrinsic Death Receptor-Mediated Apoptosis

In the extrinsic pathway, apoptosis is initiated by the binding of ligands to the death receptors on the cell surface. The transmembrane death receptors belong to the tumor necrosis factor (TNF) receptor gene superfamily, which have cysteine-rich

extracellular domains and cytoplasmic domains that contain 80 amino acids known as the "death domain" (Fulda & Debatin, 2003; Sun, 2005). The best-characterized death receptors are FasR (also known as CD-95 and APO-1), TNF receptor 1 (also known as TNFR1), TRAIL-R1 (also known as DR4) and TRAIL-R2 (also known as DR5). DR3 (also known as Apo-3) and DR6 are not well characterized. The corresponding ligands are FasL, TNF-α and TRAIL for both DR4 and DR5, respectively, and they are all type II transmembrane proteins that exist as soluble molecules (Fulda & Debatin, 2003). Once the death ligand binds to the respective death receptor, oligomerization of the receptors occur and adaptor proteins are recruited from the cytoplasm to the death domains (for instance, Fas-associated death domain, FADD) on the intracellular domains of the death receptors. Pro-caspase-8 is recruited to the adaptor protein through dimerization of the death effector domain on pro-caspase-8. The death-inducing signaling complex (DISC) is formed and this allows for the cleavage and auto-activation of caspase-8 (de Thonel & Eriksson, 2005; Huerta *et al.,* 2006). The activated caspase-8 cleaves downstream pro-caspase-3 and other executioner procaspases into their active forms.

1.1.5.2 Intrinsic Mitochondrial-Mediated Apoptosis

In the intrinsic pathway, various stimuli such as growth factor deprivation, radiation, DNA damage, viral infection, hypoxia and reactive oxygen species result in changes in the permeability of the mitochondrial membrane (Elmore, 2007; Youle & Strasser, 2008). The mitochondrial membrane permeability is determined by the ratio of pro-apoptotic and anti-apoptotic mediators (Huerta *et al.,* 2007). That is, the three main classes of Bcl-2 family members include: 1) anti-apoptotic mediators such as Bcl-2, Bcl-x, Bcl-XL, Bcl-XS, Bcl-W and Mcl-1; 2) pro-apoptotic mediators such as Bax and Bak, and 3) pro-apoptotic BH3-only proteins such as Bim, Bid, PUMA, Bad,

Bik and NOXA (Youle & Strasser, 2008). All three classes have structural homology as they share up to four domains of homology, called BH1, 2, 3 or 4 domains (de Thonel & Eriksson, 2005; Yip & Reed, 2008). Once the ratio of pro-apoptotic to anti-apoptotic mediators is high, mitochondrial outer membrane permeabilization (MOMP) occurs as there is an opening of the mitochondrial permeability transition pore and loss of the mitochondrial transmembrane potential (MMP) (Elmore, 2007; Nguyen & Hussain, 2007; Youle & Strasser, 2008). There are two well-established models for MOMP induction. The first is the formation of a transmembrane "megapore" that spans across both the outer and inner mitochondrial membranes, known as the permeability transition pore (PTP) complex. The PTP complex is composed of the adenine nucleotide translocase (ANT) in the inner membrane, the voltage-dependent ion channel (VDAC) in the outer membrane, the mitochondrial peripheral benzodiazepine receptor and the peptidyl-prolyl isomerase cyclophilin D (Hengartner, 2000; Green & Kroemer, 2004; Dias & Bailly, 2005; Nguyen & Hussain, 2007). When the pore is opened, water and solutes enter the mitochondrial matrix from the cytosol to trigger the swelling of the mitochondrial matrix. Then, the mitochondrial outer membrane is ruptured, which leads to the collapse of the mitochondrial inner membrane potential and proton gradient, further disrupting the respiratory chain function (Nguyen & Hussain, 2007). Ultimately, the disturbance of mitochondrial integrity leads to the release of cytochrome c and other pro-apoptotic factors (Kroemer *et al.,* 1998; Galluzzi *et al.,* 2006). In the second model of MOMP, the pro-apoptotic proteins Bax and Bak are recruited from the cytosol and mitochondrial outer membrane, respectively, upon activation and insert themselves after hetero- or homo-oligomerization into the mitochondrial outer membrane (Kim *et al.,* 2002; Chipuk *et al.,* 2006; Nguyen & Hussain, 2007; Youle & Strasser, 2008). Hence, formation of this pore allows for the leakage of cytochrome c and other

pro-apoptotic factors such as cytochrome c, SMA/DIABLO and AIF into the cytosol (Dias & Bailly, 2005; Youle & Strasser, 2008).

The exact mechanism for the altered permeability by Bax and Bak are still unclear but it is well-established that they can bind to Bcl-2 or Bcl-XL to neutralize their anti-apoptotic functions (Chipuk *et al.,* 2006; Huerta *et al.,* 2007). As well, BAD can heterodimerize with Bcl-XL and Bcl-2 to neutralize their functions and translocate to the mitochondria in its unphosphorylated form to enhance cytochrome c release (Yang *et al.,* 1995; Zha *et al.,* 1996). Other BH3-only proteins such as PUMA and NOXA have been shown to play a role in p53-mediated apoptosis by upregulation of pro-apoptotic mediators (Liu *et al.,* 2003a). The released cytochrome c binds to apoptotic protease activating factor 1 (APAF-1), ATP and pro-caspase-9 to form the apoptosome, which cleaves and activates caspase-9 through conformational change (Dias & Bailly, 2005; Shi, 2006; Yip & Reed, 2008). SMAC/DIABLO and HtrA2/Omi bind and neutralize the actions of a class of molecules called inhibitors of apoptosis (IAPs), which include XIAP, cIAP1 and cIAP2 (Du *et al.,* 2000). Thus, XIAP cannot interact with and inhibit the action of the executioner caspases and the two cIAPs cannot aid in the recruitment of the death receptors to the cell surface (Duprez *et al.,* 2009). Aside from the release of cytochrome c, other proteins such as apoptosis-inducing factor (AIF), endonuclease G and caspase-activated DNase (CAD) are released, but the first two proteins can act in a caspase-independent manner to induce other modes of cell death (Elmore, 2007).

The intrinsic and extrinsic pathways of apoptosis do not exist in a mutually-exclusive manner since there is an abundant amount of cross-talking between them. For example, caspase-8 can cleave Bid to produce a truncated form for Bid (tBid), which

translocates to the mitochondria to release cytochrome c (Roy & Nicholson, 2000; Sun, 2005). Also, the cleavage of caspase-6 downstream of the mitochondrial pathway can cleave and activate caspase-8 of the death receptor pathway (Cowling & Downward, 2002). Hence, apoptosis can occur due to a substantial amount of caspase-8 activation through the death receptor-mediated pathway or a minor activation of caspase-8 amplified by cross-talking with the mitochondrial pathway (de Thonel & Eriksson, 2005).

The two apoptotic pathways converge to cleave and activate the executioner caspases-3, -6 and -7. Activation of caspase-3 allows for the cleavage of many nuclear and cytoplasm substrate proteins, which leads to the morphological characteristics associated with apoptosis. For instance, caspase-3 cleaves the inhibitor of CAD (ICAD), which causes CAD to translocate to the nucleus and induce oligonucleosomal DNA fragmentation and chromatin condensation (Enari *et al.,* 1998). ACINUS (apoptotic chromatin condensation inducer in the nucleus) and AIF also migrate to the nucleus and induce DNA fragmentation and condensation of chromatin (Fulda & Debatin, 2003; Elmore, 2007). Poly (ADP-ribose) polymerase is also a common substrate for cleavage as it is used for DNA repair (Soldani & Scovassi, 2002). Furthermore, caspase-3 cleaves cytoskeletal proteins such as gelsolin, actin, fodrin and lamin A which leads to formation of apoptotic bodies, loss of cell shape, membrane blebbing and cell shrinkage (Kerr *et al.,* 1972; Kothakota *et al.,* 1997; Fulda & Debatin, 2003). The externalization of phosphatidylserine on the outer leaflet of the plasma membrane is a signal for macrophages to "engulf" and dispose of the apoptotic bodies through phagocytosis, which does not induce an inflammatory response as opposed to in necrosis (Fadok *et al.,* 2001; Elmore, 2007; Duprez *et al.,* 2009). Other modes of caspase-independent cell death may contribute

to apoptosis and involve AIF, endonuclease G, calpains and cathepsins (Broker *et al.*, 2005; Tait & Green, 2008).

Although it is well-established that apoptosis is dysfunctional in cancer, it is also a large factor in resistance to anti-tumor drugs (Fulda & Debatin, 2003). Normally, natural killer cells and cytotoxic T-cells of the immune system remove cancer cells by the binding of their own FasL to FasR on cancer cells (Sun, 2005; Huerta *et al.*, 2006). However, cancer cells usually have down-regulated death ligands and receptors, mutated death receptors or faulty death receptor signaling and they can "counterattack" immune cells by binding of their death ligands to the death receptors located on immune cells (O'Connell *et al.*, 2000; Fulda & Debatin, 2003; Sun, 2005). Cancer cells may also have a high level of decoy death receptors, which do not have a functional intracellular death domain and compete with other "normal" death receptors for ligand binding (Ashkenazi & Dixit, 1998). For instance, it has been demonstrated that there is an amplification of decoy receptors-3 that compete for binding with FasL in colon cancer samples (Pitti *et al.*, 1998). In this fashion, cancer cells can "escape" from apoptosis induced by immune cells and chemotherapeutic drugs that activate the death receptor pathway (Sun, 2005; Huerta *et al.*, 2006). Problems with transport of DR4, redistribution of death receptors in lipid rafts, caspase-8 and -10 mutations and inactivation and upregulated cellular FADD-like interleukin 1β-converting enzyme-inhibitory protein (c-FLIP) have contributed to resistance of colon cancer cells to TRAIL chemotherapy (Van Geelen *et al.*, 2004). c-FLIP binds to FADD and prevents its interaction with pro-caspase-8 at the DISC (Fulda & Debatin, 2003; Huerta *et al.*, 2006; Longley *et al.*, 2006). Resistance to FasL and TRAIL-induced apoptosis and tumor progression has been suggested to be due to an upregulation of c-FLIP in cancer cells (Tschopp & Irmler, 1998).

In colorectal cancer, the most common genetic abnormality is the absence or mutation of the p53 tumor suppressor gene (Debatin *et al.*, 2002; Wu, 2004; Huerta *et al.*, 2006; Slattery *et al.*, 2009). Normally, p53 leads to the upregulation of $p21^{Waf1/Cip1}$ and G_0/G_1 cell cycle arrest when DNA damage occurs, and subsequent apoptosis by upregulation of Bax, PUMA and NOXA and inhibition of survivin if the damage cannot be repaired (Huerta *et al.*, 2006; Elmore, 2007; Yip & Reed, 2008). Saleh *et al.* (2000) have demonstrated that Bcl-2 was higher in colon adenomas in comparison to carcinomas, which suggests that upregulation of Bcl-2 plays a role in early colon tumorigenesis. An increase in Bcl-2 and Bcl-XL expression in combination with a decrease in Bax expression in colon cancer also led to 5-FU resistance, regardless of the p53 status, which was also shown in other gastrointestinal cancers (Debatin *et al.*, 2002; Violette *et al.*, 2002). Although caspase mutations are rare, it may still occur in a minority of colon cancer cases and contribute to the pathogenesis of the disease (Oh *et al.*, 2010).

1.1.6 Nuclear Factor κ-Light-Chain-Enhancer of Activated B cells (NF-κB) Pathway and Apoptosis

NF-κB is a transcription factor found in the cytoplasm usually bound to IκB (inhibitor of κB). Once this pathway is activated by external factors such as TNF-α, ionizing radiation and anti-cancer drugs, IκB kinase (IKK) phosphorylates two serine residues on IκB, which causes the IκB to be ubiquitinated and targeted for degradation by the proteasome (Huerta *et al.*, 2006). The freed NF-κB translocates into the nucleus and acts as a transcription factor for the production of IAPs. For instance, it has been shown that there were higher levels of IAP survivin and Bcl-2, with reduced apoptotic rates in various stages of colon cancer as opposed to colonic epithelium, and this translated into worse patient survival rates (Kawasaki *et al.*,

1998; Sarela *et al.*, 2001).

1.1.7 Phosphatidylinositol-3 Kinase/Akt (PI3K/AKT) Pathway and Apoptosis

This pathway is mediated by the activation of the serine-threonine kinase AKT1, 2 and 3 (also known as protein kinase B) by phosphatidylinositol-3 kinase (PI3K) upon epidermal growth factor activation (Roos & Kaina, 2006). Specifically, PI3K phosphorylates inositol phospholipids to produce phsphatidylinositol-3,4,5-trisphosphate (PIP3), which phosphorylates AKT (Huerta *et al.*, 2006). The activation of this pathway is critical for cell survival, proliferation and growth (Vivanco & Sawyers, 2002; Huerta *et al.*, 2006; Elmore, 2007). In particular, BAD can be phosphorylated by AKT and sequestered by 14-3-3 proteins, hence, it cannot bind to Bcl-XL and neutralize its anti-apoptotic function (Datta *et al.*, 1997; Vivanco & Sawyers, 2002; Roos & Kaina, 2006). As well, AKT can phosphorylate and reduce the activity of caspase-9 (Cardone *et al.*, 1998). Furthermore, IKK can be phosphorylated and activated by AKT, which leads to release of IκB from NF-κB and allows for NF-κB to translocate into the nucleus and act as a transcription factor for IAPs (Romashkova & Makarov, 1999; Kane *et al.*, 1999). AKT also phosphorylates MDM2, a negative regulator of p53, which facilitates its translocation into the nucleus and binding to p53 to induce its proteasomal degradation (Mayo & Donner, 2001; Vivanco & Sawyers, 2002; Roos & Kaina, 2006). As well, ATM and ATR of the PI3K family can also phosphorylate and activate p53 at various serine residues to induce DNA repair after damage (Wu, 2004). Philp *et al.* have shown that the p85α-regulatory subunit of PI3K is often mutated in primary human colon tumors, which leads to constitutive activation (Philp *et al.*, 2001).

1.1.8 Mitogen-Activated Protein Kinase (MAPK) Pathways and Colon Cancer

The mitogen-activated protein kinases are serine-threonine kinases that convert extracellular stimuli to intracellular signals that mediate cell proliferation, differentiation, growth, survival and death (Kim & Choi, 2010). It contains three main members: extracellular signal-regulated kinase (ERK), p38 and c-jun NH_2-terminal kinase/stress-activated protein kinase (JNK/SAPK). The diagrammatic scheme for their activation is outlined in Figure 1.3. There are specific isoforms of each MAPK. That is, ERK exists as isoforms 1-8, JNK exists as isoforms 1-3 and p38 exist as isoforms α, β, γ, and δ (Dhillon *et al.,* 2007). Each MAPK signaling pathway works as a series of phosphorylations of the subsequent kinase. That is, extracellular stimuli activate MAP3K, which phosphorylates MAP2K, which activates MAPK (ERK, JNK or p38) (Kim & Choi, 2010). In turn, the MAPK phosphorylates and activates downstream transcription factors such as c-Jun, p53, c-myc and Elk-1 (Kim & Choi, 2010).

Mitogens and growth factors usually activate receptor tyrosine kinases through loading of the Ras GTPases and recruitment of the Raf kinases to the cell membrane for subsequent activation of ERK (Dhillon *et al.,* 2007). The ERK pathway is deregulated in almost one-third of human cancers and the end result is a constitutive activation of ERK and uncontrolled cell proliferation (Dhillon *et al.,* 2007). Some of the lesions in the pathway include over-expression or mutation of receptor tyrosine kinases, autocrine or paracrine over-production of receptor tyrosine kinase ligands, Ras mutations, B-Raf mutations and amplification of downstream effectors c-myc and AP-1 (Dhillon *et al.,* 2007).

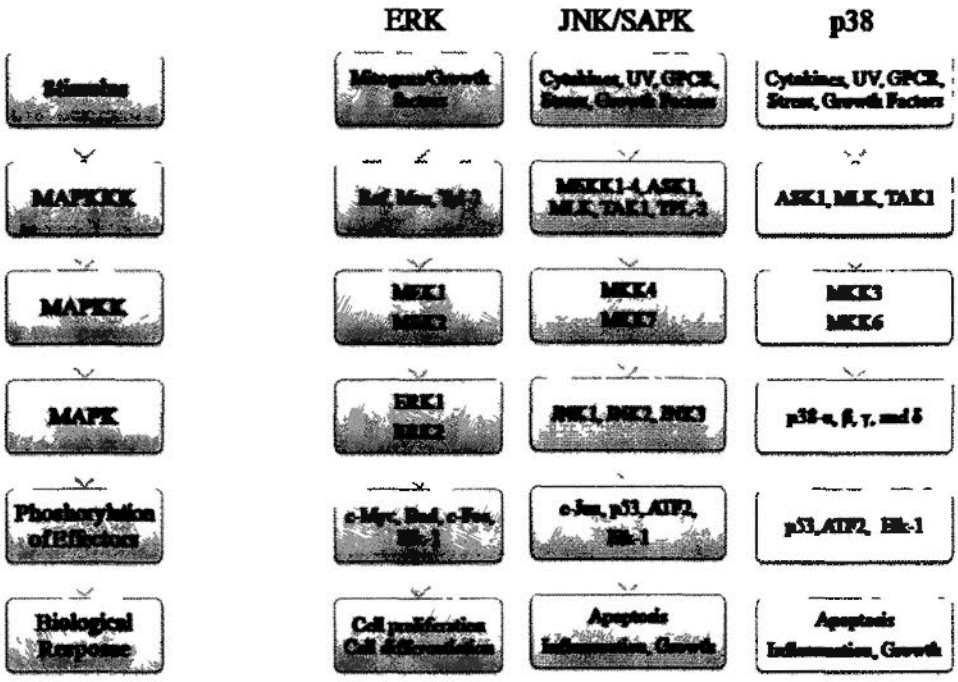

Figure 1.3 The activation of ERK, JNK/SAPK and p38 is through sequential phosphorylation of a series of MAP kinases followed by the phosphorylation and activation of intracellular effectors, such as transcription factors and pro- and anti-apoptotic mediators to regulate cell survival, proliferation, differentiation and death. Fan & Chambers (2001).

For instance, in colon cancer, K-Ras is frequently mutated and its oncogenic function is often activated (Malumbres & Barbacid, 2003; Schubbert *et al.*, 2007). Analysis of primary colon carcinoma indicated that mutations of the EGFR kinase domain occurred in approximately 10% of patients (Nagahara *et al.*, 2005). As well, ERK regulates the activity of pro- and anti-apoptotic mediators to enhance cancer cell survival (Balmanno & Cook, 2009).

The JNK family of kinases is mainly activated by inflammatory cytokines, UV

radiation, growth factor deprivation, DNA-damaging agents, GRPRs and environmental stress (Weston & Davis, 2002; Dhillon *et al.,* 2007). Through the three-tier kinase system (MAP3K → MAP2K → MAPK), JNK translocates into the nucleus and phosphorylates c-Jun, which in turn enhances the activity of transcription factor, AP-1 (Weston & Davis, 2002). Other targets of JNK phosphorylation include Elk-1, p53 and ATF-2 (Ip & Davis, 1998). Upon DNA damage by chemotherapeutic drugs or ionizing radiation, JNK has been shown to phosphorylate p53 at different serine and threonine residues to stabilize and activate p53 transcriptional activity to induce cell cycle arrest or apoptosis, which can be reversed in JNK1 and 2 knock-out cells (Davis, 2000; She *et al.,* 2002). It has been suggested that JNK has a tumor-suppressive function as drug-induced apoptosis is mediated by JNK activation (Mahalingam *et al.,* 2009; Zhang *et al.,* 2010a). However, it has been also suggested that the activation of JNK plays a role in colon carcinogenesis. Its activation has been associated with the transformation to cancer cells by Bcr-Abl and Met oncogene (Raitano *et al.,* 1995; Rodrigues *et al.,* 1997). For example, an increased number of aberrant crypt foci and proliferation in the colonic epithelium were detected in mice fed a high fat diet, which was associated with high JNK activity (Endo *et al.,* 2009). The controversial role of JNK in cancer progression and drug-induced cytotoxicity is still under investigation.

Similar to JNK, p38 is activated by DNA damage, ionizing radiation, inflammatory cytokines and oxidative stress and its phophorylation targets include nuclear transcription factors, p53, Elk-1, ATF-2, c-myc and members of the pro- and anti-apoptotic Bcl-2 family (Liu & Lin, 2005; Dhillon *et al.* 2007). However, p38 may also play a role in cell differentiation as it can be activated by extracellular stimuli such as fibroblast growth factor, platelet-derived growth factor and

insulin-like growth factor-1 (Dhillon *et al.*, 2007). Studies showed that the *in vivo* disruption of p38 activation by MAPKK mutants increased cell cycle progression and tumorigenesis (Brancho *et al.*, 2003). Even a subtle activation of p38 significantly reduced tumorigenesis *in vivo* (Timofeev *et al.*, 2005). After chemotherapeutic drug treatment, p38 phosphorylated and activated p53 to induce cell cycle arrest and apoptosis in cancer cells (Sanchez-Prieto *et al.*, 2000; Lee *et al.*, 2003; Shimada *et al.*, 2003; Liu *et al.*, 2006).

1.2. The Use of Traditional Chinese Medicine (TCM) in Chemotherapy

Even with many advances in drug development for colon cancer in the last decade, many problems still remain for current anti-tumor drugs. For instance, as discussed in the previous sections, one of the major problems is the lack of selectivity of current drugs for cancer cells as opposed to normal cells. Hence, this leads to adverse effects such as myelosuppression, neurotoxicity, nephrotoxicity, cardiotoxicity and gastrotoxicity, which can affect the patient's quality of life and severely reduce patient compliance (Wilkes, 2005; Chau & Cunningham, 2006; Li *et al.*, 2006a; Li *et al.*, 2006b; Xin *et al.*, 2007). Aside from this, many patients have an inherent or developed resistance to certain anti-cancer drugs and cross-resistance readily occurs (Kim *et al.*, 2010). As well, colon cancer has a high recurrent rate even after surgical resection and adjuvant radio- or chemotherapy (Chau & Cunningham, 2006). Thus, there is a high demand for new drug candidates for the treatment of colorectal cancer, for the general and elderly population (Kosmider & Lipton, 2007).

Recently, there is a large amount of public interest in the potential use of complementary and alternative medicine (CAM) in cancer. CAM is an alternate group of medical and health practices and products for the treatment of disease that

can be used in substitution or in combination with conventional medicine (Armstrong & Gilbert, 2008). It may include mind-body interventions such as meditation, biological therapies like herbal products and dietary supplements, body-based therapies such as massage and energy therapies such as tai-chi (Armstrong *et al.,* 2006). Many patients diagnosed with cancer use CAM in addition to conventional drug treatments, even though as much as 74% of users admitted that their physicians were not aware of this (Armstrong *et al.,* 2006). It has been shown that 63% of cancer patients use at least one type of CAM to treat adverse effects from conventional chemotherapy, such as insomnia, hair loss, nausea and vomiting, and the feeling of depression and anxiety from the disease diagnosis (Sparber *et al.,* 2000; Mok *et al.,* 2007). At least 90% of the users believed that their quality of life improved, with better skills at coping with stress (Sparber *et al.,* 2000). In another study, 87% of patients with cancer used CAM, in particular, 54% used herbal products (Bennett & Lengacher, 1999). There is a growing enthusiasm for the use of traditional Chinese medicine (TCM) in cancer chemotherapy since many patients used TCM to reduce the adverse effects associated with conventional chemotherapy, strengthen their immune system, improve their general health (vital energy, "qi,") by restoring balance in their bodies ("yin and yang") and restore their sense of hope and control (Ernst, 2000; Chang, 2002; Gerber *et al.,* 2006; Chiu *et al.,* 2009). There is ongoing *in vitro* and *in vivo* research to examine the selective anti-cancer mechanisms of action of single compounds or fractions isolated from Chinese herbs (Ruan *et al.,* 2006; Kim *et al.,* 2009; Li *et al.,* 2009; Lee *et al.,* 2010). For example, many polysaccharides from Chinese herbs have been shown to stimulate the immune system and exert their anti-tumor effects through inhibition of angiogenesis (Chang, 2002). According to TCM principles, drug treatment is administered as a formula that contains a combination of herbs, which is more effective than a single agent due

to synergistic interactions between different components in the formula (Xue & Roy, 2003; Ruan *et al.,* 2006). A mixture of ingredients also allows for reduction of toxicity due to "buffering" between the different components (Vickers & Zollman, 1999; Vickers, 2002). The type and dose of ingredients within the formula are adjusted according to the patient's health status and illness symptoms, which is a form of personalized medicine (Ruan *et al.,* 2006). Ruan *et al.* (2006) suggested that TCM can be combined with Western anti-cancer drugs for increased efficacy since Western drugs target the cancer locally while TCM targets the overall unhealthy state of the body.

There are two approaches to study TCM for drug development. The first approach is to study TCM as a mixture of ingredients in an herbal extract or in a "fu fang" formula, according to its traditional therapeutic use. The second approach is to study TCM as a single compound isolated from an herbal extract. In the current study, both approaches were used to study two herbs, *Angelica sinensis* and *Garcinia hanburyi,* which have both been traditionally used for the treatment of inflammation and gastrointestinal diseases such as gastric ulcers (Cho *et al.,* 2000; Ye *et al.,* 2001a; Ye *et al.,* 2001b; Ye *et al.,* 2001c; Liu *et al.,* 2003b; Ye *et al.,* 2003; Panthong *et al.,* 2007; Pedraza-Chaverri *et al.,* 2008; Han & Xu, 2009). Since there is a link between inflammatory diseases such as Crohn's disease and ulcerative colitis, and colon cancer, the objective of this study was to examine the potential anti-cancer effects of these two herbs on colon cancer (Feagins *et al.,* 2009; Triantafillidis *et al.,* 2009; Terzic *et al.,* 2010).

1.3 *Angelicae Sinensis Radix* - 當歸 (DG)

1.3.1 Plant Characteristics and Cultivation

Angelicae Sinensis Radix (當歸, Dang Gui) is derived from the root of *Angelica sinensis* (Oliv.) Diels (Family Apiaceae/Umbelliferae) and abbreviated as DG in this thesis. *A. sinensis* is a traditional Chinese medicinal perennial plant from branched taproot with radially symmetric flowers and fruit, as shown in Figure 1.4 (Upton, 2003). It is mainly cultivated in Minxian County, Gansu province, although it is also grown in the Hubei, Shaanxi, Sichuan and Yunnan provinces of China (Upton, 2003; Yi *et al.*, 2009). Scientists are interested in the roots of the herb, since most of the bioactive components are found in the roots (*Angelicae Sinensis Radix,* DG) Roots are grown in moist conditions, harvested after the second or third year and sliced and sulfured to remove contaminants. Then, the roots are smoke-dried at low temperature to avoid the loss of volatile oils in the root and sold in their sliced and pressed forms (Upton, 2003). There are actually many types of substitute herbs used instead of *A. sinensis*, such as *Angelica gigas* Nakai (Korean *Angelica*), *Angelica acutiloba* (Japanese *Angelica*) and *Levisticum officinale* (European *Angelica*) (Cho *et al.*, 2007; Piao *et al.*, 2007; Nunes *et al.*, 2009; Tianniam *et al.*, 2009). However, they contain different bioactive compounds such as coumarin derivatives and different secondary metabolites such as podophyllotoxin (Piao *et al.*, 2007; Tianniam *et al.*, 2009). Most importantly, DG contains the highest amount of phthalides and it is the most therapeutically effective compared to the other types of *Angelica* (Upton, 2003; Zhao *et al.*, 2003; Kim *et al.*, 2006; Yi *et al.*, 2009). For instance, Zhao *et al.* (2003) demonstrated that DG contained 10-fold higher levels of *z*-ligustilide (LGT) and ferulic acid than *A. gigas* and *A. acutiloba*.

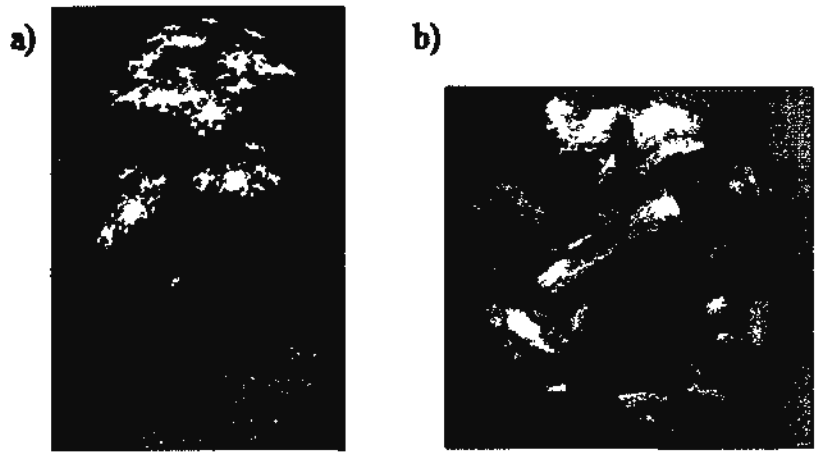

Figure 1.4 *Angelica sinensis* (Oliv.) Diels. is an herbaceous flowering plant that is cultivated in many parts of China (Figure 1.4A). The roots of the plant (known as Dang Gui, DG) are sliced and processed for medicinal use (Figure 1.4B).

1.3.2 Bioactive compounds – isolation and characterization

The phytochemistry of DG has been studied extensively (Lin *et al.*, 1998; Zhao *et al.*, 2003; Huang *et al.*, 2004; Dong *et al.*, 2005; Wang *et al.*, 2005; Yi *et al.*, 2005; Li *et al.*, 2006c, d). More than 70 compounds have been isolated from DG and these include mono- and dimeric phthalides, polysaccharides, organic acids and their esters, coumarins, vitamins, amino acids, aromatic compounds, terpenes and polyacetylenes (Upton, 2003; Yi *et al.*, 2009). The main bioactive components are phthalides, polysaccharides and ferulic acid (Upton, 2003; Beck & Chou, 2007; Li *et al.*, 2007; Kan *et al.*, 2008; Yi *et al.*, 2009). Some phthalides commonly found in DG are presented in Figure 1.5. Since phthalides present in the essential oil of this herb are non-polar, they are typically extracted with hexanes and pentane (Yi *et al.*, 2003). The current methods used for the extraction of phthalides and ferulic acid are supercritical-CO_2 fluid extraction, biomembrane extraction and pressurized liquid

extraction, which allow for simultaneous extraction of multiple volatile components at normal temperatures and automatic sample handling (Dong *et al.*, 2005; Li *et al.*, 2006c; Kim *et al.*, 2006). High performance liquid chromatography or gas chromatography coupled with mass spectrometry is frequently used to identify and quantify multiple compounds simultaneously (Lin *et al.*, 1998; Wang *et al.*, 2005; Yi *et al.*, 2005; Li *et al.*, 2006d; Shi *et al.*, 2006; Li *et al.*, 2007). The main phthalides isolated from DG include: *z*-ligustilide (LGT), *z*-ligustilide dimer, *n*-butylidenephthalide (BLP), senkyunolide A (SKA), senkyunolide H, senkyunolide I and butylphthalide (Lin *et al.*, 1998; Dong *et al.*, 2005; Li *et al.*, 2006c; Li *et al.*, 2006d). The chemical structures of the above compounds are shown in Figure 1.5.

Since *z*-ligustilide (LGT) is the most abundant phthalide isolated from the herbal extract, it is often considered as a primary reference compound, along with ferulic acid, for the identification and validation of DG (Zhao *et al.*, 2003; Upton, 2003, Dong *et al.*, 2005; Yi *et al.*, 2009). Polysaccharides have been separated and characterized by hot water extraction and anion-exchange chromatography or capillary zone electrophoresis. It has been shown that DG contained fucose, galactose, glucose, arabinose, rhamnose and xylose in a mole ratio of 1.0:13.6:15.0:8.7:21.3:3.7 and other studies also showed that the main monosaccharides were arabinose, glucose, rhamnose, galactose and galacturonic acid (Wang *et al.*, 2003; Sun *et al.*, 2005; Yang *et al.*, 2007a).

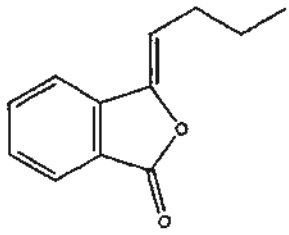

n-Butylidenephthalide (BLP)

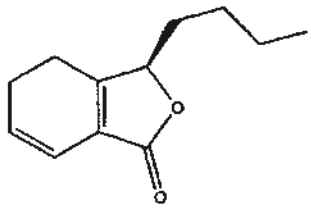

Senkyunolide A (SKA)

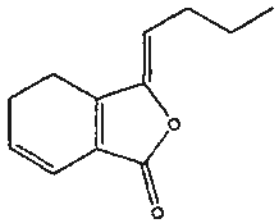

z-Ligustilide (LGT)

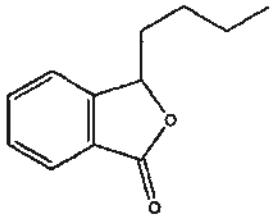

Butylphthalide

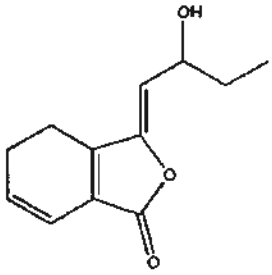

Senkyunolide F

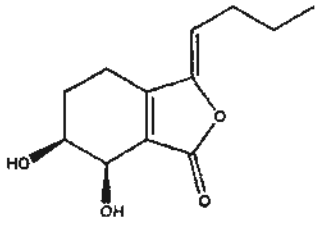

Senkyunolide H

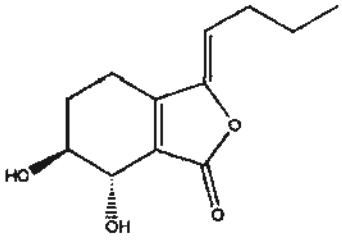

Senkyunolide I

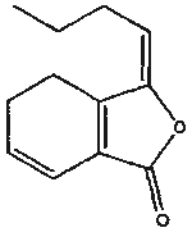

e-Ligustilide

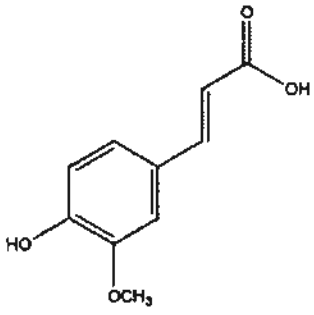

Ferulic acid

Figure 1.5 Chemical structures of compounds isolated from the DG extract. *n*-Butylidenephthalide (BLP), senkyunolide A (SKA) and *z*-ligustilide (LGT) are the three most common phthalides found in DG.

1.3.3 Therapeutics and Bioactivity

The use of DG dates back to the first known herbal text of China, called the Divine Husbandman's Classic of the Materia Medica (Shenlong Bencao Jing) in the Han dynasty from 200-300 A.D (Upton, 2003; Yi *et al.,* 2007). The traditional uses of this herb were to "nourish blood," regulate "qi," and to treat gynecological disorders, such as amenorrhea, dysmenorrhea, endometriosis and menopause (Ye *et al.,* 2001a; Wu *et al.,* 2004a; Tang *et al.,* 2006; Dietz *et al.,* 2008). Recent studies on DG have focused on its hepatoprotective, gastroprotective, neuroprotective, anti-oxidant, immunomodulatory, antispasmodic and anti-cancer effects, which will be briefly discussed in the following sections. The daily dose of DG extract is approximately 6-12 g daily prepared as a decoction (Upton, 2003).

1.3.3.1. Effects of DG on Cardiovascular Injury

Cardiovascular diseases such as atherosclerosis and hypertension are correlated with high proliferation of vascular smooth muscle cells (VSMCs) and DG has been prescribed in China for the treatment of these disorders (Hou *et al.,* 2005). In particular, the Fo Shou San formula, which contains a combination of DG and *Chuanxiong Rhizoma* (川芎, Chuanxiong), derived from the rhizomes of *Ligusticum chuanxiong* Hort. (Family Apiaceae/Umbelliferae) (abbreviated as CX in this thesis), has been clinically used in China (Hou *et al.,* 2004). Studies have shown that the mixture of these two extracts inhibited the proliferation of VSMCs, while it protected endothelial cells from oxidative stress (ROS) by increasing activities of anti-oxidant enzymes and induction of the endothelial nitric oxide synthase (Hou *et al.,* 2004; Hou *et al.,* 2005). A formula known as Dang-Gui-Shao-Yao-San, which contains DG, reduced platelet aggregation and reactive oxygen species production (Shen *et al.,* 2005). Moreover, a mixture of DG and *Astragali Radix*, known as Dang Gui Buxue

Tang (DBT), protected rats from myocardial ischemia-reperfusion injury by increasing glutathione levels in erythrocytes and myocardial mitochondria (Mak *et al.,* 2006; Chiu *et al.,* 2007). The phthalides have been suggested to be the active ingredients responsible for the therapeutic effects. For instance, LGT has been shown to inhibit vascular smooth muscle proliferation by inducing G_0/G_1 cell cycle arrest, to diminish the production of ROS and to reduce phenylephrine-induced aortic tension (Kobayashi *et al.,* 1992; Kobayashi *et al.*, 1993; Liang & He, 2006; Lu *et al.,* 2006; Du *et al.,* 2007). In addition, LGT and senkyunolide A had vasorelaxant effects in rat aorta with similar potencies And LGT also showed anti-thrombotic activity through inhibition of platelet aggregation in rats (Chan *et al.,* 2007; Zhang *et al.,* 2009). DG may also stimulate hematopoiesis by augmenting the expression of erythropoietin, hemoglobin, and iron content and stimulating the proliferation of bone marrow mononuclear cells (Chen *et al.,* 2006, Wang *et al.,* 2007; Gao *et al.,* 2008).

1.3.3.2. Effects of DG on Oxidative Stress

Overproduction of free radicals and peroxides from physiological reactions in the body results in oxidative damage, which may lead to diseases such as atherosclerosis, aging, neurodegenerative disorders and cancer (Droge, 2002). The extract of DG demonstrated anti-oxidant activity in several studies as it reduced lipid peroxidation, superoxide anion formation and increased free radical scavenging (Wu *et al.,* 2004a; Cai *et al.,* 2004; Cai *et al.,* 2006). DG reduced platelet aggregation and hemolysis in red blood cells by reduction of ROS (Shen *et al.,* 2005). A recent study showed that the lipophillic fractions of the herbal extract induced the activity of NAD(P)H:quinone oxidoreductase 1 (NQO1), which is an enzyme used to remove reactive electrophiles and prevent oxidative stress (Dietz *et al.,* 2008). Both LGT and ferulic acid contributed to the extract's anti-oxidant effects (Cai *et al.,* 2004; Dietz *et*

al., 2008). In addition, the polysaccharide fraction has been shown to reduce oxidative stress in liver toxicity induced by acetaminophen in mice (Ye *et al.,* 2001a).

1.3.3.3. Effects of DG on Gastrointestinal Injury

It has been demonstrated that DG had a protective effect on gastric injury induced by ethanol and indomethacin (Cho *et al.,* 2000). The polysaccharide-enriched fraction of the extract reduced inflammation and neutrophil infiltration and reduced hemorrhagic lesions in the gastric glandular mucosa (Cho *et al.,* 2000). The beneficial effects of DG on gastric wound healing was shown as the crude extract (which contained mostly polysaccharides) promoted wound healing by increasing cell proliferation, cell migration and EGF expression *in vitro*, while reducing gastric ulcer size and promoting ulcer healing *in vivo* (Ye *et al.,* 2001a; Ye *et al.,* 2001b; Ye *et al.,* 2001c; Ye *et al.,* 2003). The polysaccharide fraction from the extract reduced immunological colon injury and ulcerative colitis in rats, which may be due to its ability to reduce oxidative stress and increase wound repair (Liu *et al.,* 2003b; Wong *et al.,* 2008). It also attenuated the decrease in the number of proliferating cells induced by cyclophosphamide, an anti-cancer drug that is known for its adverse effects on gastric tissue (Hui *et al.,* 2006).

1.3.3.4. Effects of DG on Gynecological Disorders

Due to the traditional use of DG as a "female tonic" to treat menstrual disorders such as amenorrhea and pre-menstrual syndrome, many research groups have focused on its mechanism of action underlying the clinical observations (Piersen, 2003). Whether this herb acts as a phytoestrogen has been long debated and evidence has been contradictory (Rock & DeMichele, 2003). DG has shown only weak binding affinity to both estrogen receptors-α and –β subtypes as an agonist *in vitro* and an

increase in proliferation of estrogen receptor-positive and negative endometrial and breast cancer cells (Liu *et al.,* 2001; Lau *et al.,* 2005). Specifically, ferulic acid enhanced proliferation of MCF-7 (estrogen receptor-positive human breast cancer) cells and up-regulated expressions of HER2 oncogene and estrogen receptor-α (Chang *et al.,* 2006). Furthermore, ovariectomized mice treated with an ethanol extract of DG showed a reduction of serum luteinizing hormone, stimulation of uterine histo-architecture, such as an increase in the thickness of the luminal epithelium and development of uterine glands (Circosta *et al.,* 2006). The cervical and vaginal epithelium histo-architecture also showed cornification and stimulation, while the weight of the uterus increased after treatment with the extract (Circosta *et al., 2006*). The effects of the extract on vaginal cytology have been suggested to be due to LGT. On the contrary, Gao *et al.* (2007a) discovered that although DBT induced the phosphorylation of estrogen receptor-α and extracellular signal-regulated kinase (ERK), it had no mitogenic effect on the proliferation of MCF-7 cells. A double-blind, randomized, placebo-controlled clinical trial reported that DG extract taken daily did not change serum estradiol levels, endometrial thickness and vaginal cellular maturation and did not improve vasomotor flushes and other menopausal symptoms (Hirata *et al.,* 1997; Low Dog, 2005). However, a recent prospective clinical trial has demonstrated that DBT reduced the number of mild, hot flushes, which is the most common symptom associated with menopause (Haines *et al.,* 2008). The use of DG as a single agent in the treatment of menopause is controversial but the combined use of DG with other herbs may improve its efficacy and safety.

1.3.3.5. Effects of DG on Modulation of Immune System

DG stimulated the proliferation of murine and human lymphocytes (Wilasrusmee *et*

al., 2002a; Wilasrusmee *et al.*, 2002b). In particular, the polysaccharide fractions of the herb increased proliferation of macrophages and CD4+ helper T (Th1) cells, while increasing the production of interleukin-2 and interferon-γ. As well, the polysaccharide fraction triggered activation of macrophages and protected macrophages from *tert*-butylhydroperoxide injury by decreasing oxidative stress (Yang *et al.*, 2007b; Yang *et al.*, 2007c). Similarly, DBT treatment led to increased proliferation of T-lymphocytes and macrophages, release of interleukins-2, -6 and -10 and activation of ERK (Gao *et al.*, 2006; Gao *et al.*, 2007b). DG is a strong stimulator of immune responses, which is in accordance with its traditional use.

1.3.3.6. Effects of DG on Neural Injury and Degenerative Disorders

Many recent studies have examined the effects of DG and its active ingredients, especially LGT, on neurotoxicity and injury in the nervous system. That is, Yu *et al.* (2008) revealed that LGT pre-treatment attenuated the ROS and apoptosis induced by hydrogen peroxide injury in PC12 cell line. Besides, LGT protected mice and rats from brain damage and behavioral and cognitive deficits by anti-oxidant and anti-apoptotic mechanisms in murine models of transient forebrain, permanent focal and permanent forebrain ischemia (Kuang *et al.*, 2006; Peng *et al.*, 2007; Kuang *et al.*, 2008). Both the herbal extract and LGT have been suggested to be potential drug candidates for the treatment of Alzheimer's disease. That is, LGT reversed amyloid-β induced-morphological changes, neuronal loss and behavioral deficits, while the extract attenuated the reduction in cell viability by amyloid-β through its role as an anti-oxidant (Huang *et al.*, 2008; Kuang *et al.*, 2009). Also, DG prevented neurotoxicity by inhibition of the apoptotic caspase cascade (Jia *et al.*, 2005).

1.3.3.7. Anti-cancer effects of DG

Recently, there has been increasing interest in the use of herbal medicine in the treatment of cancer. DG extracts induced cytotoxic and anti-proliferative effects in human lung adenocarcinoma, glioblastoma multiforme, hepatoma, colon adenocarcinoma and astrocytoma (Cheng *et al.,* 2004; Tsai *et al.,* 2005; Lee *et al.,* 2006). As well, DG induced cancer cell death by induction of G_0/G_1 cell cycle arrest and mitochondrial and death receptor-mediated pathways of apoptosis and down-regulation of tumor invasion marker cathepsin B and angiogenesis marker VEGF *in vitro* (Cheng *et al.,* 2004; Tsai *et al.,* 2005; Lee *et al.,* 2006). *In vivo* studies of mice bearing subcutaneous brain tumors illustrated that the herbal extract reduced tumor volume and cell proliferation, increased survival rates and induced apoptosis (Tsai *et al.,* 2005; Lee *et al.,* 2006). Subsequently, studies were focused on the active components of DG that contribute to its anti-tumor effects. A polysaccharide fraction increased survival rates of mice bearing leukemia and Ehrlich ascitic cancer and its sub-fractions reduced tumor metastasis and invasion (Shang *et al.,* 2003). A phthalide isolated from this herb, *n*-butylidenephthalide (BLP), induced G_0/G_1 cell cycle arrest and apoptosis, reduced tumor volume and cell proliferation and increased survival rates in a similar manner to the extract under *in vitro* and *in vivo* conditions (Tsai *et al.,* 2006). Further studies demonstrated that upon BLP treatment, the orphan nuclear receptor Nurr-77 was up-regulated and translocated from nucleus to cytoplasm and the activity of telomerase was inhibited (Chen *et al.,* 2008; Lin *et al.,* 2008; Wei *et al.,* 2009).

1.4. Resin of *Garcinia hanburyi* - 藤黄 (TH)

1.4.1. Plant Characteristics and Cultivation

The resin of *Garcinia hanburyi* Hook. f. (藤黄, Teng Huang) (Family Guttiferae/Clusiaceae) is derived from the trunk of the tree and used as herbal folk medicine and is abbreviated as TH in this thesis. The plants are in the forms of tropical evergreen trees and shrubs and many of the species also bear edible fruits (Figure 1.6). They are found in Africa, Polynesia, China, and parts of southeastern Asia, such as in Malaysia, Philippines, Thailand and Cambodia (Reutrakul *et al.*, 2007; Pedraza-Chaverri *et al.*, 2008; Obolskiy *et al.*, 2009). Most of the bioactive compounds are from gamboge, the brownish to orange gum resin found on the inside of the trunk of the tree (Feng *et al.*, 2007; Gu *et al.*, 2008; Han & Xu, 2009). Plants belonging to other species of *Garcinia* have bioactive compounds in the hull and pericarp of the fruit, seeds, trunk, stems, branches and leaves of the tree (Pedraza-Chaverri *et al.*, 2008; Obolskiy *et al.*, 2009). For instance, many of the bioactive xanthones of *Garcinia mangostana* have been isolated from the fruit (Obolskiy *et al.*, 2009). Other *Garcinia* species commonly extracted for active compounds include *Garcinia cowa, Garcinia oblongifolia, Garcinia subelliptica and Garcinia yunnanensis* (Xu *et al.*, 2008; Huang *et al.*, 2009; Xu *et al.*, 2010; Zhang *et al.*, 2010b).

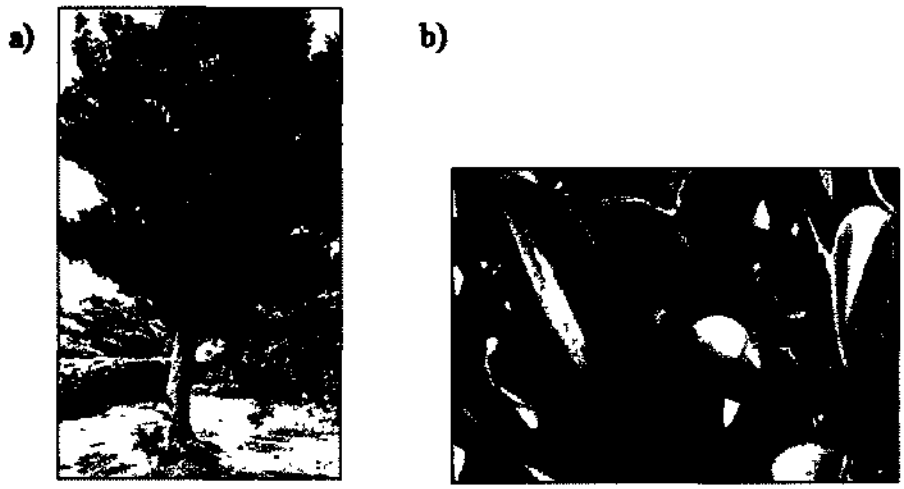

Figure 1.6 Plants of the *Garcinia* genus exist as fruiting trees or shrubs and are found in many parts of Southeastern Asia, including China (Figure 1.6A). The bioactive components of *Garcinia hanburyi* Hook. f. are mainly found in the gum resin (gamboge) of the trunk (TH), though they may also be found in the fruits, leaves and stems of the herb (Figure 1.6B).

1.4.2. Bioactive Compounds – Isolation and Characterization

Xanthones are the main bioactive compounds of TH and the xanthone found in highest quantity is gambogic acid, which is the major contributor to the color and bioactivity of the resin (Han *et al.*, 2006a; Han *et al.*, 2006b; Han & Xu, 2009). Plants of the *Garcinia* genus have caged xanthones and classical xanthones. Caged xanthones are hardly found in plants outside of the *Garcinia* genus (Han & Xu, 2009). In caged xanthones, there is a 4-oxa-tricyclo[4.3.1.$0^{3,7}$]dec-8-en-2-one scaffold built into a common xanthone backbone, with substitutions on the aromatic residue and peripheral oxidations (Han & Xu, 2009). The first caged xanthones

isolated from TH included gambogic acid, gambogin, moreollic acid and gambogenic acid (Asano *et al.*, 1996). Gambogic acid has been separated into R- and S- epimers (Han *et al.*, 2006a; Han *et al.*, 2006c). Many recent studies have identified various novel caged polyprenylated xanthones isolated from this plant species, such as gaudichaudic acid, 7-methoxydesoxymorellin, 10-methoxygambogic acid and desoxymorellinin (Han *et al.*, 2006b; Feng *et al.*, 2007; Reutrakul *et al.*, 2007). Triterpenoids have also been isolated, such as betulinic acid and messagenic acid (Wang *et al.*, 2008a). Interestingly, almost all of the isolated polyprenylated xanthones show cytotoxicity in various cancer cell lines at low concentrations, such as leukemia, hepatoma, gastric and breast cancer (Han *et al.*, 2006a; Feng *et al.*, 2007; Reutrakul *et al.*, 2007; Ee *et al.*, 2008). To date, there are approximately 30 caged xanthones isolated from the TH and fruits of *Garcinia* species (Han & Xu, 2009). In addition, other prenylated xanthones like oblongifolins, α-, β-, and γ-mangostins, garcinialiptones, garcicocowins and garciyunnanins have been isolated from various *Garcinia* species and are shown in Figure 1.7 (Xu *et al.*, 2008; Ha *et al.*, 2009; Han *et al.*, 2009; Huang *et al.*, 2009; Zhang *et al.*, 2010b; Xu *et al.*, 2010).

1.4.3 Therapeutics and Bioactivity

TH has been used since the 8th century where it was used as a yellow dye and watercolor pigment in Thailand (Wang *et al.*, 2008a; Han & Xu, 2009). It was used as folk medicine to treat wounds, chronic dermatitis, hemorrhoids and bedsore (Asano *et al.*, 1996; Han & Xu, 2009). As a TCM, it is used to promote detoxification and hemostasis and to act as a purgative to treat tapeworms (Han *et al.*, 2006b; Feng *et al.*, 2007). The mangosteen fruit from *G. mangostana* has been traditionally used as a general health tonic and for the treatment of inflammation, skin infections and wounds, diarrhea and amoebic dysentery (Pedraza-Chaverri *et al.*,

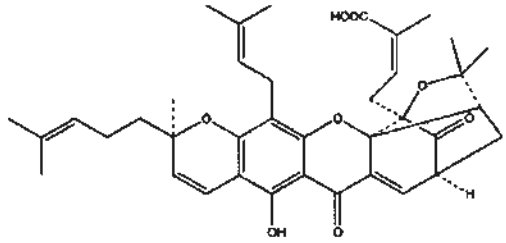

R-gambogic acid

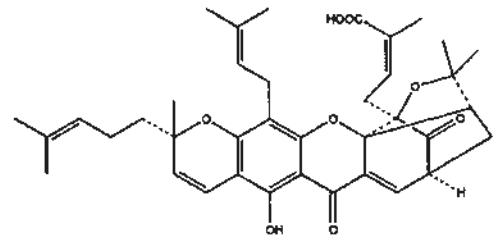

S-gambogic acid

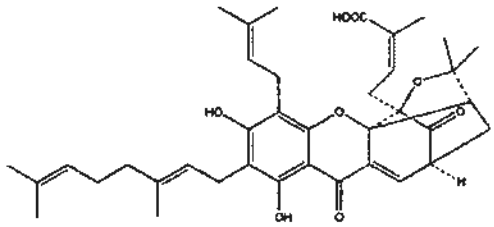

Gambogenic acid

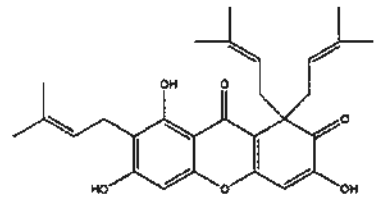

Allanxanthone C

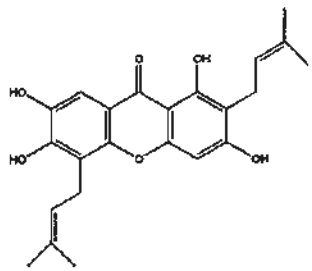

γ-Mangostin

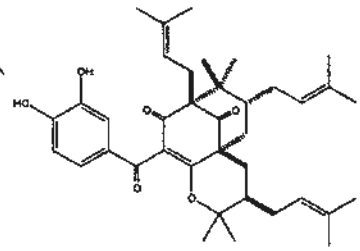

(-)30-epicambogin (EPC)

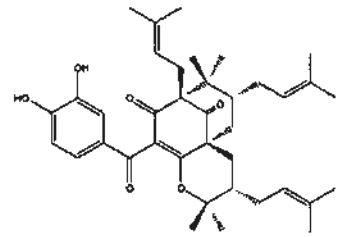

Cambogin

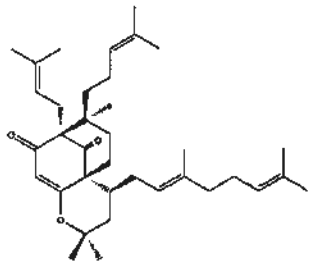

Garcicowin A

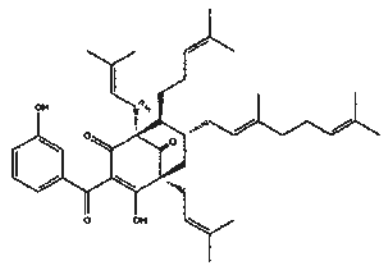

Garcicowin B

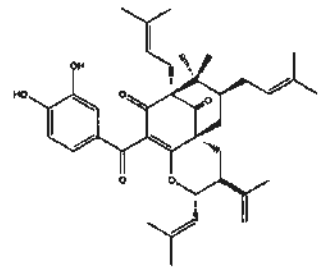

Garcicowin C

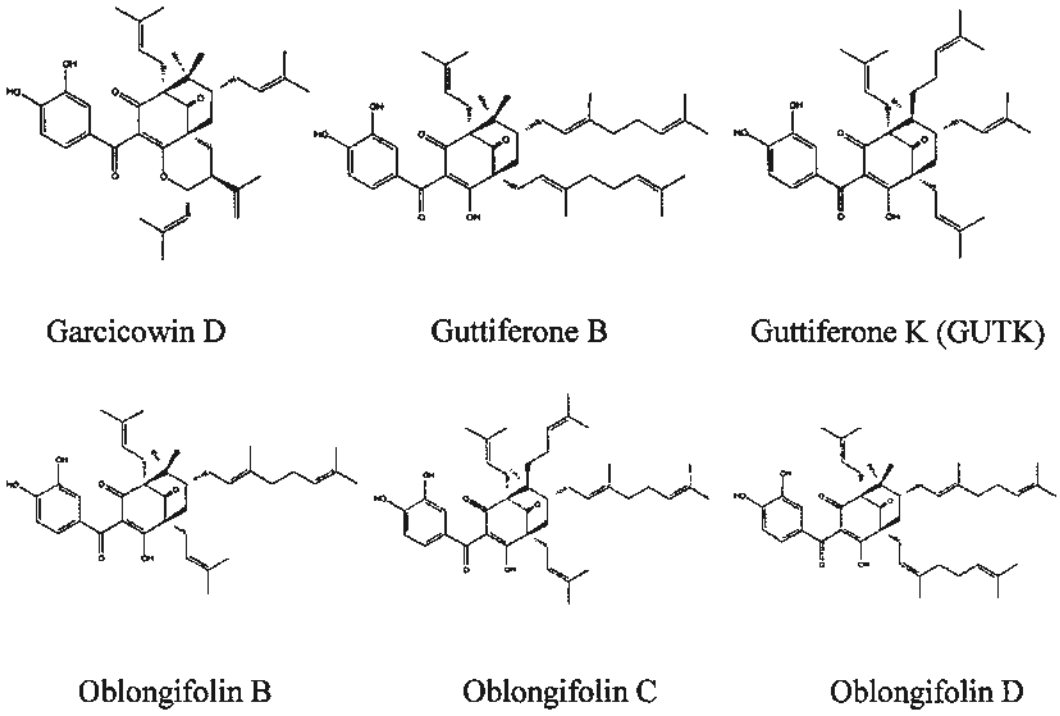

Figure 1.7 Chemical structures of caged xanthones and benzophenones isolated from TH and various other *Garcinia* species. Gambogic acid is the most common caged xanthone found in the brown-yellow gum resin (gamboge) on the inside of tree trunks of *G. hanburyi*.

2008; Obolskiy *et al.*, 2009). Although modern uses of TH include its anti-bacterial, anti-viral activity and neurotrophic activity, most of the research has focused on its potential use in anti-cancer therapy (Han & Xu, 2009).

1.4.3.1 Anti-bacterial and Anti-viral activity of *Garcinia* species

Caged xanthones isolated from *Garcinia scortechinii* had anti-bacterial effects against methicillin-resistant *Staphylococcus aureus* and xanthones with intact caged structure showed higher anti-bacterial activity (Rukachaisirikul *et al.*, 2005). TH has been used as folk medicine to treat herpes virus (Han & Xu, 2009). Several caged

xanthones isolated from TH, such as gambogic acid, morellic acid, dihydroisomorellin and 8,8a-epoxymorellic acid, showed inhibitory effects on HIV-1 (Reutrakul *et al.*, 2007). However, further studies are needed to illustrate the mechanisms underlying the anti-bacterial and anti-viral effects.

1.4.3.2 Neuroprotective effects of *Garcinia* species

Jang *et al.* (2007) demonstrated that gambogic amide was able to bind to neurotrophin receptor A and activate its downstream pathways such as MAPK and AKT by interacting with the juxtamembrane domain of neurotrophin receptor A. The gambogic acid derivative attenuated glutamate-induced neuronal cell death and enhanced neurite outgrowth *in vitro* and reduced kainic acid-induced neuronal death *in vivo* (Jang *et al.*, 2007).

1.4.3.3 Anti-oxidant and Anti-inflammatory effects of *Garcinia* species

Cardiovascular diseases are associated with increased levels of oxidative stress and weakened endogenous anti-oxidant systems. A recent study showed that α-mangostin had a protective effect on isoproterenol-induced myocardial necrosis in rats by increasing levels of mitochondrial anti-oxidants, such as superoxide dismutase and catalase, and restoring levels of cardiac endothelial nitric oxide synthase and nitric oxide (Sampath & Kannan, 2009). Camboginol, isolated from *Garcinia dulcis*, had anti-oxidant effects on Fe^{2+}- and non-metal-mediated oxidization of human low-density lipoprotein, which suggests its potential use as a preventive agent in atherosclerosis (Hutadilok-Towatana *et al.*, 2007). A xanthone-rich mangosteen liquid, with α-mangostin as its active ingredient, had anti-oxidant effects in human plasma (Kondo *et al.*, 2009).

In accordance with traditional use of TH, recent evidence revealed that an ethyl acetate extract of TH inhibited chemically-induced acute inflammation, pain and hyperthermia in rats, which may be due to its inhibition of synthesis or release of inflammatory mediators (Panthong *et al.*, 2007).

1.4.3.4 Anti-cancer effects of *Garcinia* species and its active components

There is increasing attention paid to the xanthone class of compounds for their anti-cancer activity, regardless of their plant origin. That is, caged xanthones naturally exist as secondary metabolites in TH and various *Garcinia* species (Na, 2009; Han & Xu, 2009). Traditionally, TH has been used to treat skin cancer in China and research in the 1980s demonstrated that gamboge in injection, tablet and ointment forms were effective at treating a wide spectrum of cancer types (Han & Xu, 2009). The dose recommended for clinical trials is 25 mg/60 kg every other day (Han & Xu, 2009). Nowadays, the injectable form of gambogic acid, the major component of gamboges, is undergoing phase II clinical trials in China (Han & Xu, 2009). Based on the empirical anti-cancer efficacy, there have been many *in vitro* and *in vivo* studies on the mechanism of gambogic acid and its derivatives on various types of cancer.

The majority of studies have been done on the anti-cancer effects of gambogic acid as it is the major bioactive compound of gamboge, its traditional use for treatment of cancer is well-known in China, it is easily isolated and it can even be bought from a commercial source. It has been shown in many studies that gambogic acid selectively induced apoptosis in gastric, hepatic, leukemia and melanoma cancer cells as opposed to normal non-cancerous cells (Zhao *et al.*, 2004; Yang *et al.*, 2007d; Wang *et al.*, 2008b; Xu *et al.*, 2009). Gambogic acid and its derivatives induced G_2/M cell

cycle arrest and apoptosis with up-regulation of pro-apoptotic Bax and down-regulation of anti-apoptotic Bcl-2 and survivin in Jurkat T, gastric, hepatic and skin cancer cells (Zhao *et al.*, 2004; Liu *et al.*, 2005; Tao *et al.*, 2007; Yu *et al.*, 2007; Wang *et al.*, 2008c; Xie *et al.*, 2009; Xu *et al.*, 2009; Mu *et al.*, 2010). Zhai *et al.* (2008) reported that gambogic acid directly inhibited anti-apoptotic Bcl-2 family members by competing with other pro-apoptotic proteins for binding to Bcl-2 members. The apoptosis induced by gambogic acid may be due to up-regulation of p53 protein expression in breast and hepatic cancer cells by down-regulation of MDM2, a negative regulator of p53 (Gu *et al.*, 2008; Gu *et al.*, 2009; Rong *et al.*, 2009). Both the mitochondrial and death receptor pathways were activated and led to the activation of caspase-3 (Liu *et al.*, 2005; Xie *et al.*, 2009; Mu *et al.*, 2010). Binding studies have demonstrated that gambogic acid can bind on to the transferrin receptor on the cell surface and potentiate TNF-α-induced apoptosis by down-regulation of anti-apoptotic proteins and invasion proteins (Kasibhatla *et al.*, 2005; Pandey *et al.*, 2005). Likewise, other polyprenylated xanthones and benzophenones isolated from other species of *Garcinia*, such as gambogenic acid, α- and β- mangostin, guttiferone E and H and garcinol, induced cell cycle arrest and extrinsic and intrinsic apoptotic pathways in a variety of human cancer cell lines (Pan *et al.*, 2001; Matsumoto *et al.*, 2003; Protiva *et al.*, 2008; Kikuchi *et al.*, 2010; Li *et al.*, 2010b; Prasad *et al.*, 2010; Watanapokasin *et al.*, 2010). However, most of the other xanthones induced G_0/G_1 cell cycle arrest, as opposed to G_2/M arrest seen for gambogic acid (Matsumoto *et al.*, 2005; Li *et al.*, 2010b).

In addition to the ability of gambogic acid to induce apoptosis in cancer cells, it had a detrimental effect on telomerase, an enzyme that adds DNA sequence repeats to the 3'ends of DNA to increase the number of cell divisions before a cell reaches

senescence (Artandi & DePinho, 2010). Gambogic acid reduced the mRNA expression of hTERT, one of the subunits of telomerase, and activity of telomerase in gastric, hepatic and lung cancer cells (Wu *et al.*, 2004b; Guo *et al.*, 2006; Yu *et al.*, 2006). As well, the expression of c-myc oncogene was diminished by gambogic acid, which led to the reduction of hTERT transcription (Guo *et al.*, 2006; Yu *et al.*, 2006). Gambogic acid inhibited angiogenesis by reduction of vascular endothelial growth factor (VEGF) levels and suppression of signaling pathways downstream of VEGF in lung and prostate cancer (Lu *et al.*, 2007; Yi *et al.*, 2008). Moreover, gambogic acid inhibition adhesion, migration and invasion of breast carcinoma cells by repressing the expression and activity of matrix metalloproteinases-2 and -9, which resulted in less invasion (Qi *et al.*, 2008a; Qi *et al.*, 2008b).

Many *in vivo* studies indicate that gambogic acid has great anti-tumor potential. Several studies showed that mangosteen xanthones, gambogic acid and gambogenic acid reduced tumor volume dose-dependently when administered to tumor-bearing mice in a schedule similar to the one used clinically for humans (Lu *et al.*, 2007; Rong *et al.*, 2009; Li *et al.*, 2010b; Watanapokasin *et al.*, 2010). Many *in vivo* studies revealed that gambogic acid and gambogenic acid reduced tumor volume to the same extent as conventional anti-cancer drugs by induction of apoptosis in tumor cells, suppression of angiogenesis and reduction of tumor invasion markers in lung cancer (Lu *et al.*, 2007; Qi *et al.*, 2008a; Rong *et al.*, 2009; Li *et al.*, 2010b). Gambogic acid and mangosteen xanthones decreased tumor volume in tumor-bearing mice by similar mechanisms in gastric, colon, brain, liver and prostate cancer at similar dose ranges (Guo *et al.*, 2004; Liu *et al.*, 2005; Yang *et al.*, 2007d; Qiang *et al.*, 2008; Yi *et al.*, 2008; Watanapokasin *et al.*, 2010).

1.5 Objectives of the Current Study

As discussed previously, colorectal cancer is a serious disease with high invasion and metastatic potential. Although there are many first-line drugs available as adjuvant chemotherapy after surgical resection, the drug response rates are low. Even with combination chemotherapy, resistance is still the major factor for treatment failure. In addition, it affects other normal body organs and many adverse effects, such as hematotoxicity and neurotoxicity, commonly occur. Therefore, there is a high demand for novel chemotherapy candidates that are potent and selective to colon cancer cells. In general, traditional Chinese medicine (TCM) is often well-tolerated. DG is a Chinese medicinal herb that has been traditionally used as a general health tonic and for treatment of gynecological disorders. TH is also a Chinese medicinal herb that has been used for anti-inflammatory and wound-healing purposes. Both herbs and their bioactive components have been screened for their anti-cancer potential but the specific mechanisms of action underlying their cytotoxic effects have not been studied before in colon cancer.

The objectives of the current study are:

1. Identify the bioactive compounds of DG extract that are cytotoxic to and have anti-proliferative effects on human colon cancer cells
2. Study the mechanisms of action underlying *in vitro* cytotoxic effects of LGT in human colon cancer cells
3. Examine the interactions between different phthalides in DG extract to contribute to the anti-proliferative effects
4. Identify the bioactive compounds of TH that are cytotoxic to human colon cancer cells
5. Investigate the *in vitro* cytotoxic and anti-proliferative mechanisms of action of two promising bioactive compounds, 30-epicambogin (EPC) and guttiferone K (GUTK) on human colon cancer cells
6. Investigate the *in vivo* anti-cancer effects of GUTK on colon tumor-bearing mice

CHAPTER 2: EFFECTS OF *ANGELICAE SINENSIS RADIX* AND ITS BIOACTIVE COMPONENTS ON VIABILITY AND PROLIFERATION OF HUMAN COLON CANCER CELLS

Angelicae Sinensis Radix (當歸, Dang Gui, DG) is derived from the root of *Angelica sinensis* (Oliv.) Diels (Family Apiaceae/Umbelliferae). The DG extract has been shown to have anti-cancer effects *in vitro* and *in vivo* in lung and brain cancer (Cheng *et al.*, 2004; Tsai *et al.*, 2005). However, its effects on colon cancer have not been studied before. Furthermore, the effects of various phthalides on the growth of cancer cells are not well-examined. Therefore, in this chapter, the focus is on the identification of the bioactive phthalides from the essential oil of DG extract that contribute to cytotoxic and anti-proliferative effects in human colon cancer cells. One of the phthalides, *z*-ligustilide (LGT), the most abundant and potent bioactive phthalide in the herbal extract, was examined for its selectivity towards cancer cells and the mechanisms of action underlying its cytotoxic and anti-proliferative effects in human colon cancer. Furthermore, the individual anti-proliferative effects of *n*-butylidenephthalide (BLP), senkyunolide A (SKA) and *z*-ligustilide (LGT) were compared to their combined effects in the DG and *Chuanxiong Rhizoma* extracts. *Chuanxiong Rhizoma* (川芎, Chuanxiong, CX) is derived from the rhizomes of *Ligusticum chuanxiong* Hort. (Family Apiaceae/Umbelliferae) and was also studied since it also contains BLP, SKA and LGT, but in different proportions than DG. The interactions between BLP, SKA and LGT and other bioactive ingredients in the two herbal extracts were studied for their contribution to the anti-tumor effects of the DG extract.

2.1 Materials and Methods

2.1.1 Chemicals, Materials and Reagents

All of the drugs, chemicals and reagents used were of analytical grade and were purchased from the companies listed in the tables below. All cell culture labware were purchased from TPP®.

Cell Culture/Drugs

Chemical/Reagent	Product Brand	Catalog Number
3-Butylidenephthalide	Sigma-Aldrich®	W333301
Cisplatin	Sigma-Aldrich®	479306
Dimethylsulfoxide	Sigma-Aldrich®	D8418
Dulbecco's phosphate-buffered saline	Gibco®	21600-010
Fetal bovine serum	Biosera	S1810
HEPES	Sigma-Aldrich®	H4034
Minimum essential medium (MEM)	Gibco®	41500-034
RPMI 1640 medium	Gibco®	23400-021
Penicillin G, sodium salt	Sigma-Aldrich®	P3032
Sodium bicarbonate	Sigma-Aldrich®	S5761
Streptomycin sulfate	Gibco®	11860-038
Trypsin, 0.25%	Gibco®	15050-065

DAPI Staining/Flow Cytometry

Chemical/Reagent/Equipment	Product Brand	Catalog Number
4',6-Diamidino-2-phenylindole (DAPI)	Sigma-Aldrich®	D9542

Absolute ethanol	Merck	1.00983.2511
Flow Cytometer	BD Biosciences	FACS Aria II
Phase-contrast and Fluorescent Microscope	Nikon	Eclipse TS100
Paraformaldehyde	Sigma-Aldrich®	158127
Propidium iodide	Sigma-Aldrich®	P4170
RNase A	Roche Applied Science	10154105
Sodium citrate	Sigma-Aldrich®	S1804

Immuno-blotting/Western Blot

Chemical/Reagent/Equipment	Product Brand	Catalog Number
40% Acrylamide solution	Bio-Rad	161-0141
β-Actin rabbit monoclonal antibody	Cell-Signaling Technology®	4970
Albumin from bovine serum (BSA)	Sigma-Aldrich®	A2153
Ammonium persulfate (APS)	Bio-Rad	161-0700
Anti-mouse IgG, HRP-linked antibody	Cell-Signaling Technology®	7076
Anti-rabbit IgG, HRP-linked antibody	Cell-Signaling Technology®	7074
2% Bis solution	Bio-Rad	161-0143
Blotting-grade non-fat dry milk	Bio-Rad	170-6404
Bromophenol blue	Sigma-Aldrich®	B0126
Caspase-3 (8G10) rabbit monoclonal	Cell-Signaling	9665

antibody	Technology®	
Caspase-8 (1C12) mouse monoclonal antibody	Cell-Signaling Technology®	9746
Caspase-9 (C9) mouse monoclonal antibody	Cell-Signaling Technology®	9508
α-Cholic acid	Sigma-Aldrich®	C1129
Complete mini EDTA-free protease inhibitor cocktail tablets	Roche Applied Science	11836170001
Ethylenediaminetetraacetic acid (EDTA)	Sigma-Aldrich®	E6758
Filter paper	Whatman	3030-392
Glycerol	Sigma-Aldrich®	G5516
Hybond™ ECL™ nitrocellulose membrane	Amersham/GE Healthcare	RPN303D
20X LumiGLO® reagent and 20X peroxide	Cell-Signaling Technology®	7003
MAPK family antibody sampler kit	Cell-Signaling Technology®	9926
2-Mercaptoethanol	Sigma-Aldrich®	M3148
Methanol	Merck	1.06007.2500
Microtube Thermo Shaker	Grant-Bio	PHMT
Mini-PROTEAN Tetra Cell	Bio-Rad	165-8001
Mini-Trans Blot Electrophoretic Transfer Cell	Bio-Rad	170-3930
Molecular Imager ChemiDocXRS+ System	Bio-Rad	170-8265

PARP antibody	Cell-Signaling Technology®	9542
Phospho-MAPK family antibody sampler kit	Cell-Signaling Technology®	9910
PowerPac HC Power Supply	Bio-Rad	164-5052
Protein assay dye reagent concentrate	Bio-Rad	500-0006
SeeBlue Plus2 pre-stained standard	Invitrogen™	LC5925
Sigma 7-9®	Sigma-Aldrich®	T1378
Sodium chloride	Sigma-Aldrich®	S5886
Sodium dodecyl sulfate	Bio-Rad	161-0301
N,N,N',N"-Tetramethylethylenediamine (TEMED)	Bio-Rad	161-0801
10X Tris/glycine	Bio-Rad	161-0771
10X Tris/glycine/SDS	Bio-Rad	161-0772
Triton X-100	Sigma-Aldrich®	T8787
Tween-20	Bio-Rad	170-6531

Caspase-3 Activity/LDH/MTT/[^{3}H]-Thymidine Incorporation Assays

Chemical/Reagent/Equipment	Product Brand	Catalog Number
Microplate Spectrophotometer	Bio-Rad	Benchmark Plus™
Caspase-3 Assay Kit, Colorimetric	Sigma-Aldrich®	CASP3C
Cytotoxicity Detection Kit (LDH)	Roche Applied Science	11644793001
Dimethylsulfoxide (DMSO)	Sigma-Aldrich®	D4540
Optiphase Hisafe 3 aqueous	PerkinElmer	1200-437

scintillation cocktail		
Thiazolyl blue tetrazolium bromide (MTT)	Sigma-Aldrich®	M2128
[^{3}H]-Thymidine	GE Healthcare	TRA306-1MCI
Tri-Carb low activity liquid scintillation analyzer	Packard Instrument Company	2900TR
Trichloroacetic acid (TCA)	Sigma-Aldrich®	T4885

Preparation of Specific Buffers

Buffer	Reagents needed
Radioimmunoprecipitation assay (RIPA) buffer	0.5% α-Cholic acid, 2mM EDTA, 10% Glycerol, 150 mM NaCl, 0.1% SDS, 50 mM Tris (pH 7.5), 1% Triton X-100, Distilled water to make up volume
4X Sample buffer	0.02% Bromophenol blue, 30% Glycerol, 10% β-Mercaptoethanol, 0.25M Tris-HCl (pH 6.8), 8% SDS, Distilled water to make up remaining volume
Stripping buffer (500 ml)	10 g SDS, 3.786 g Sigma 7-9® (pH 6.7)
1X TGS and 1X TG	Dilute 10X stock solution with distilled water
5% Non-fat dry milk	Dissolve with 1X washing buffer
1X Washing buffer	100 mM NaCl, 10 mM Tris (pH 7.5), 0.1% Tween-20

2.1.2 Methods

2.1.2.1 Cell Lines and Cell Culture

In the current study, the HT-29 human colorectal adenocarcinoma cell line was used as an *in vitro* model for colon cancer. The HT-29, SW1116 human colorectal adenocarcinoma cells and CCD-18Co human normal colon fibroblasts were purchased from American Type Culture Collection (Rockville, MD, USA). The HT-29 and SW1116 cell lines were grown in RPMI 1640 medium, supplemented with 10% heat-inactivated fetal bovine serum, 2.0 g/L sodium bicarbonate, 0.1 g/L streptomycin sulfate and 0.06 g/L penicillin G. The CCD-18Co cell line was grown in Minimum Essential Medium, supplemented with 10% heat-inactivated fetal bovine serum, 5.958 g/L HEPES, 2.2 g/L sodium bicarbonate, 0.1 g/L streptomycin sulfate and 0.06 g/L pencillin G. Both cell lines were maintained at 37°C in a humidified atmosphere with 5% CO_2.

2.1.2.2 Preparation of DG extract and phthalides

The crude oil extracts of DG and CX were prepared from CO_2-supercritical fluid extraction and purchased from Masson Pharmaceutical, Ltd. (Guangzhou, Guangdong, China). Both extracts contained phthalide derivatives and other organic soluble ingredients in oil form, but did not contain water-soluble components, such as polysaccharides. A previously-developed online high performance liquid chromatography-diode array detector-mass spectrometry (HPLC-DAD-MS) analytical method was used to separate and identify several phthalides from the herbal extracts (Li *et al.*, 2003; Li *et al.*, 2004). *n*-Butylidenephthalide (BLP), senkyunolide A (SKA) and *z*-ligustilide (LGT) were isolated from the two herbal extracts and determined to be the major phthalides present in both DG and CX

(Figure 1.5, Table 2.1). The purities of BLP, SKA and LGT were also assessed using HPLC-DAD-MS and determined to be as high as 96%, 95.5% and 98.16%, respectively. BLP was also purchased from Sigma-Aldrich®. The three phthalides were quantified using a previously-developed HPLC-UV method and Table 2.1 shows the proportion of each phthalide in DG and CX extracts (Yan *et al.*, 2005). In the following experiments, all of the herbal extracts and phthalides were dissolved in DMSO to produce stock solutions of 1.0 g/ml and then further diluted in culture medium prior to use. The concentrations of DMSO in culture medium for all experiments were under 0.01% and had no effect on the viability of HT-29 cells.

Table 2.1 The percentage content of BLP, SKA and LGT in DG and CX extracts

Herbal extract	Content of BLP (%)	Content of SKA (%)	Content of LGT (%)	Total content of three phthalides (%)	Ratio of BLP:SKA: LGT
DG	0.86	0.20	40.00	41.06	1:0.23:46.51
CX	0.59	7.70	15.70	23.99	1:13.05: 26.61

2.1.2.3 3-(4,5-Dimethylthiazol-2-yl)-2,5-diphenyltetrazolium bromide (MTT) assay

To determine the effects of phthalides and extracts of DG and CX on the viability of HT-29 and CCD-18Co cells, cell number was quantified using the standard colorimetric MTT assay. The MTT assay is based on the principle that active mitochondrial dehydrogenases of viable cells reduce the yellow MTT to insoluble purple formazan crystals, which can be re-solubilized with DMSO or an acidified solution. The absorbance of the colored solution can be analyzed using a spectrophotometer. MTT was prepared in 0.01 M phosphate-buffered saline (PBS) to

make a 5 mg/ml stock and stored at 4°C. Cells were seeded overnight in 96-well plates at a density of 8.0 x 10^3 cells per well with 100 µl of culture medium. Cells were treated with various concentrations of DG extract, BLP, SKA and LGT (0-200 µg/ml), along with the respective DMSO vehicle controls for 24 and 48 h. Culture media was aspirated and cells were rinsed with PBS. Then, 10 µl of MTT was added to each well with 100 µl of culture medium and incubated at 37°C for 3 h. The medium was removed and 200 µl of DMSO was added to each well to solubilize the purple formazin crystals for 15 mins on an orbital shaker set at 150 rpm. The absorbance of the solution was measured using a microplate spectrophotometer at a wavelength of 570 nm, with background subtraction at 620 nm. The absorbance of the untreated cells in medium was considered 100%. Cisplatin (0-350 µM), a commonly used anti-cancer drug, was dissolved in saline and used as a positive control. The assay was performed in triplicates. The concentration of each drug that reduced cell viability by 50% (IC_{50}) was estimated from a semi-logarithmic dose-response curve fitted by GraphPad Prism 5.0 (GraphPad Software, Inc., San Diego, CA, USA).

2.1.2.4 [^{3}H]-Thymidine incorporation assay

[^{3}H]-Thymidine uptake by cells is a standard method for measuring DNA synthesis and cell proliferation. Cells were seeded overnight in 24-well plates at a density of 4 x 10^4 cells/well in 1 ml of culture medium. Cells were treated with different concentrations of phthalides and herbal extracts with their respective vehicle controls in culture medium for 4 h and 24 h. Then, culture medium was aspirated and replaced with 0.5 µCi of [^{3}H]-thymidine dissolved in 1 ml of culture medium per well for 5 h at 37°C. The culture medium was removed and cells were washed with 0.5 ml/well of ice-cold 0.15 M sodium chloride. Cells were then incubated with 0.5

ml/well of 10% trichloroacetic acid solution for 15 mins at room temperature. Cells were washed with distilled water and lysed with 0.5 ml/well of 1% sodium dodecyl sulfate for at least 15 minutes at 37°C. Next, cell lysates were transferred to individual scintillation vials containing 6 ml of Optiphase Hisafe 3 aqueous scintillation cocktail per vial. A Packard Tri-Carb low activity liquid scintillation analyzer was used to measure the amount of [^{3}H]-thymidine incorporated into cellular DNA by liquid scintillation spectrometry. Cisplatin was used as a positive control and the assay were conducted in triplicates. The concentration that reduced the cell proliferation to 50% (IC_{50}) was estimated from a semi-logarithmic dose-response curve fitted by GraphPad Prism 5.0.

2.1.2.5 Lactate dehydrogenase (LDH) activity assay

The release of cytoplasmic lactate dehydrogenase into extracellular environment only occurs in dead cells or cells that have lost their membrane integrity. The released LDH reduces NAD^+ to $NADH^+$ H^+ by oxidation of lactate to pyruvate. Then, the 2 H are transferred from $NADH^+$ H^+ to yellow tetrazolium salt INT by a catalyst provided in the kit to produce a red solution. The assay was performed as indicated in the protocol of the commercially-available kit. Briefly, cells were seeded overnight in 96-well plates at a density of 8 x 10^4 cells/well in 100 µl of culture medium. Cells were treated with various concentrations of drugs and 1% Triton X-100 in 200 µl for 24 h. The microplate was centrifuged at 250 g for 10 mins. Then, 100 µl of culture medium supernatant was transferred to a well of a new 96-well plate. Next, 100 µl of the reaction mixture (provided by the kit) was added to the supernatant and incubated for 30 mins at room temperature. The absorbance of the solution was measured using a microplate spectrophotometer at 490 nm, with background subtraction at 620 nm. The experiment was conducted in triplicates. To calculate the percentage cytotoxicity,

the average of absorbance values for each treatment condition is first calculated. The value in the background control (culture medium only with no cells) was subtracted from all of the treatment mean values. The following equation was used:

Cytotoxicity (%) = (experimental value – low control)/(high control – low control)

where experimental value is the absorbance of cells treated with various drug concentrations, high control is the absorbance value of cells treated with 1% Triton X-100 and low control is the absorbance value of cells incubated with medium only

2.1.2.6 4'6-Diamidino-2-phenylindole (DAPI) staining assay

DAPI is a cell-permeable fluorescent dye that binds to the minor groove of double-stranded DNA and forms a stable complex that can be view using fluorescent microscopy ($\lambda_{excitation}$: 364 nm, $\lambda_{emission}$: 454 nm for DAPI-DNA complex). DAPI was prepared in PBS at a stock concentration of 10 mg/ml. Human colon cancer HT-29 cells were seeded overnight in 6-well plates at a density of 3.5 x 10^5 cells/well. Cells were treated with LGT for 12 h and 24 h. After the drug incubation period, the 6-well plate was centrifuged at 2000 g for 15 minutes at room temperature. Culture medium was aspirated and adherent cells were fixed with 4% paraformaldehyde for 10 minutes at room temperature. Cells were washed once with PBS and then incubated with DAPI solution (1 μg/ml in PBS) for 10 minutes at room temperature in the dark. Cells were washed three times with PBS and their nuclear morphologies were immediately viewed using the fluorescent microscope with 330-380 nm excitation filter.

2.1.2.7 Flow cytometry assay

The HT-29 cells were seeded overnight in 60 x 15 mm culture dishes at a density of 3.5 x 10^5 cells/dish with 3 ml of culture medium. Cells were treated with various concentrations of LGT and *Angelica sinensis* extract for 6, 12 and 24 h after overnight serum starvation. To examine the proportion of cells in different phases of the cell cycle, cellular DNA was stained with propidium iodide. Propidium iodide is a cell-inpermeable fluorescent dye that binds to double-stranded nucleic acids (both DNA and RNA) and can be quantified using a flow cytometer ($\lambda_{excitation}$: 493 nm, $\lambda_{emission}$: 630 nm) since the DNA content changes in different stages of the cell cycle. The propidium iodide, RNase A and sodium citrate were prepared as 5 mg/ml, 100 μg/ml and 380 mM stock solutions in PBS, respectively. After the drug incubation period, the culture medium was aspirated and cells were harvested by trypsinization. After the cell pellet was washed with PBS twice, cells were resuspended in 1 ml PBS, fixed with 75% ethanol and stored at 4°C or -20°C until analysis. On the day of analysis, cells were washed twice with PBS and stained with propidium iodide solution that contained 50 μg/ml propidium iodide, 10 μg/ml RNase A and 3.8 mM sodium citrate at room temperature in the dark for 30 mins. Stained cells were passed through a 40-70 μm filter and 10^4 events were analyzed per sample using a flow cytometer. DNA content was further analyzed using BD FACSDiva™ software.

2.1.2.8 Immuno-blotting/Western Blot

The HT-29 cells were seeded overnight in 60 x 15 mm culture dishes at a density of 3.5 x 10^5 cells/dish. Then, cells were treated with different concentrations of LGT (24.60-82.01 μg/ml) for various time points (3, 6, 12, 24, 36, 48 h). Floating and adherent cells were harvested by trypsinization and lysed with RIPA buffer containing a cocktail of protease inhibitors for 15-20 mins on ice. Supernatants of

cell lysates were collected by centrifugation at 15,000 g for 10 mins at 4°C and protein content was quantified using Bio-Rad protein assay dye concentrate (5x) diluted with distilled water according to Table 2.2. Samples were diluted in saline with a starting dilution factor of 1250 and adjusted according to their absorbance values. Samples were incubated at room temperature for 15-20 mins after the addition of the dye and the absorbance readings of the standard and samples were measured at 595 nm. A representative of the standard curve for protein concentration is shown in Figure 2.1. The correlation between absorbance values detected at 595 nm and protein concentration showed good linearity with $r^2 > 0.98$.

Table 2.2 Construction of the protein assay standard curve using BSA

	Well Number						
Reagent	1	2	3	4	5	6	7
0.1 μg/μl BSA (μl)	0	20	40	80	100	150	200
Normal Saline (μl)	1000	980	960	920	900	850	800
1X Assay Dye (μl)	1500	1500	1500	1500	1500	1500	1500
Amount of protein (μg/ml)	0	0.8	1.6	3.2	4.0	6.0	8.0

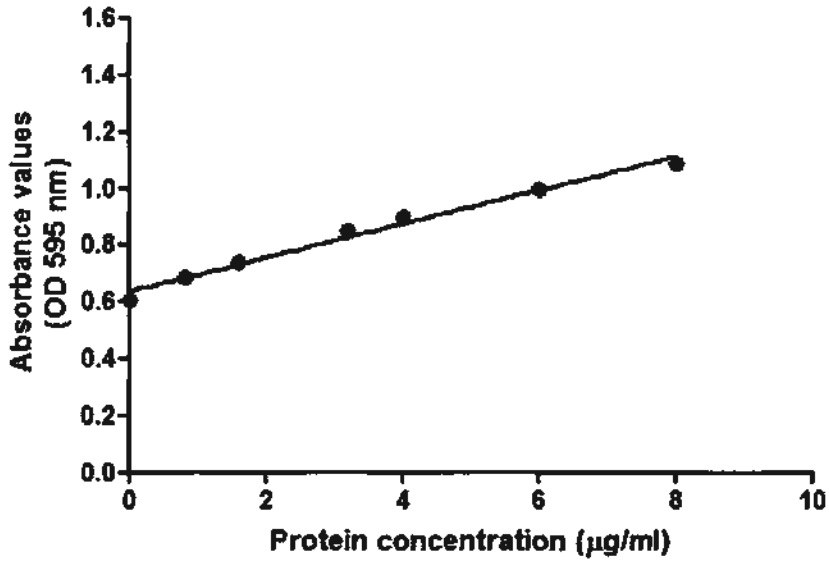

Figure 2.1 Representative standard curve for determination of protein concentration using Bio-Rad protein assay (Coomassie Brilliant Blue G-250) dye. The r^2 for this standard curve was 0.9844.

Cell lysates were dissolved in 4X sample buffer and heated at 95-100°C for 5 mins to denature proteins to their primary structure. Equal amounts of samples (at least 30-30 μg protein/lane) were loaded and proteins were separated by 7.5-15% sodium dodecyl sulfate polyacrylamide gel electrophoresis at constant 100 V until the target protein reaches the desired level on the gel. Then, proteins on the gel were transferred to a nitrocellulose membrane by electrophoresis at 100 V for 1-2 h, depending on the molecular weight of the target protein. The membrane was blocked with 5% non-fat dry milk in 1X Tris-buffered saline containing 0.1% Tween-20 for 1 h at room temperature with shaking. Then, the membrane was incubated with the primary antibody suitable for probing the target protein diluted in 5% non-fat milk or BSA in Tris-buffered saline containing 0.1% Tween-20 overnight at 4°C with shaking. The primary antibodies used included: anti-PARP, anti-caspase-3, anti-caspase-8, anti-caspase-9, anti-β-actin, anti-phospho-p44/p42, anti-p44/p42, anti-phospho-

SAPK/JNK, anti-SAPK/JNK, anti-phospho-p48 and anti-p38 at 1/1000 dilution. After overnight incubation, membranes were washed three times with washing buffer and incubated with horseradish peroxidase-conjugated anti-mouse or anti-rabbit secondary antibodies diluted in 5% non-fat dry milk in washing buffer for 1-2 h at room temperature with shaking. The antibody-bound proteins were detected by chemiluminescence using ECL reagent and ChemiDoc XRS Molecular Imager system. Band intensities were estimated by the Quantity One 1-D Analysis software and normalized using the following equation:

Normalized band density = (Band density of target protein)/(Band density of β-actin)

2.1.2.9 Caspase-3 activity assay

The activity of caspase-3, a key effector protease in apoptosis, was measured using a commercially-available kit according to the manufacturer's protocol. The kit is based on the principle that activated caspase-3 in cell lysates will cleave the peptide substrate acetyl-Asp-Glu-Val-Asp p-nitroaniline (Ac-DEVD-pNa) provided in the kit to produce Ac-DEVD and release of p-nitroaniline (pNa). p-Nitroaniline is a colored compound which can be detected spectrophotometrically. The HT-29 cells were seeded overnight in 60 x 15 mm culture dishes at 3.5 x 10^5 cells/dish with subsequent LGT and DG treatment for 24 h. Then, floating and adherent cells were harvested by trypsinization and incubated with lysis buffer provided in the kit overnight at 4°C. Protein content of each cell lysate was quantified by protein assay using Bio-Rad protein assay dye. Cell lysates were incubated with the peptide substrate, Ac-DEVD-pNa for at least 60 mins at 37°C in the dark. The absorbance of the released p-nitroaniline was measured by microplate reader at 405 nm every 60 minutes until 300 minutes. The experiment was conducted in duplicate. The quantity

of pNa produced was determined from a standard curve and is directly proportional to the amount of caspase-3 activity. The standard curve for p-nitroaniline was constructed as shown in Table 2.3.

Table 2.3 Construction of the p-nitroaniline standard curve

	Well Number					
Reagent	1	2	3	4	5	6
p-Nitroaniline (µl)	0	1	2	5	10	20
1X Assay buffer (µl)	1000	999	998	995	990	980
µmol p-nitroaniline per 100 µl	0	0.001	0.002	0.005	0.010	0.020

A representative of the standard curve for p-nitroaniline concentration is shown in Figure 2.2. The correlation between absorbance values detected at 405 nm and p-nitroaniline concentration showed good linearity with $r^2 > 0.999$. The standard curve was constructed each time along with the assay. Caspase-3 activity was calculated using the following equation:

Caspase-3 Activity (in µM pNa/min·ml) = (µM pNa x d)/(t x v)

where v is the volume of sample in ml, d is the dilution factor and t is the reaction time in minutes

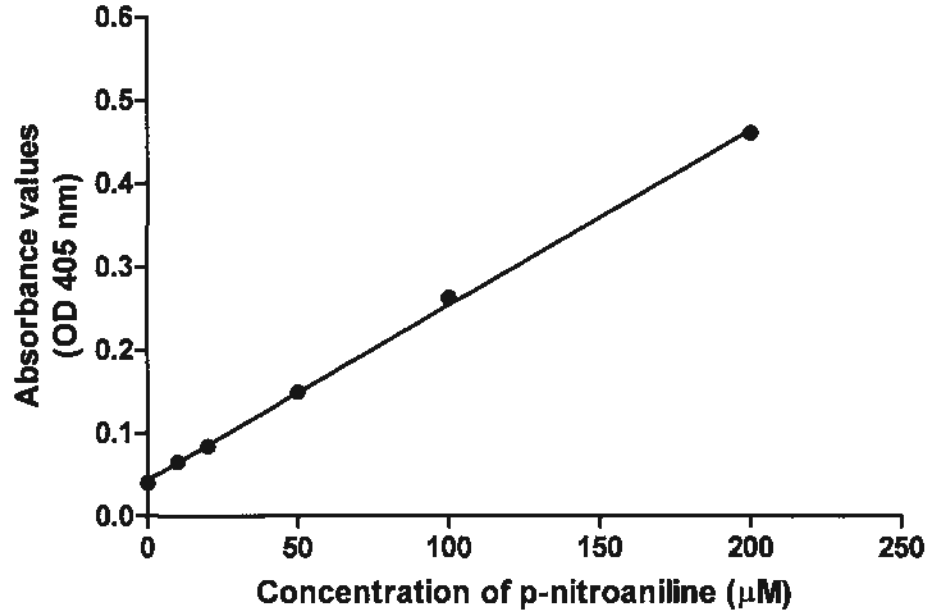

Figure 2.2 Representative standard curve for concentration of p-nitroaniline to examine caspase-3 activity. The r^2 for this standard curve was 0.9992.

2.1.2.10 Interactions between various components in DG and CX extracts

According to TCM principles, the effects of an extract or a combination of extracts are greater than that of a single agent. Therefore, TCM is almost always administered as a mixture of ingredients in a medicinal formula. However, the scientific evidence for the improved efficacy of a combination of ingredients is lacking. To investigate the interactions between different phthalides and other components in an herbal extract and their contributions to its anti-proliferative effects, the DG and CX extracts were employed. The CX extract also contains the same major phthalides as DG, but they exist in different proportions (Li *et al.*, 2003; Yan *et al.*, 2005), as illustrated in Table 2.1. Using the [^{3}H]-thymidine incorporation assay, the effects of BLP, SKA, LGT, DG and CX extracts on proliferation of HT-29 and CCD-18Co cells were examined after 24 h incubation. Semi-logarithmic dose-response curves were

constructed. Then, using pure phthalides, two phthalide mixtures were prepared to contain BLP, SKA and LGT in the composition ratios identical to that in the extracts of DG and CX (Table 2.1). The two mixtures were dissolved in DMSO and diluted with culture medium prior to use.

2.1.2.11 Analysis of multiple-drug effects

The equation used to calculate multiple-drug interactions is based on the median-effect principle and it is mathematically derived from the Michaelis-Menton equation of enzyme kinetics, the Hill equation for higher-order ligand-binding saturation, the Henderson-Hasselbach equation for pH ionization and the Scatchard equation for receptor binding (Chou, 2006). It is a well-established and scientifically-accepted method to analyze synergistic, additive and antagonistic interactions between different components in a mixture by calculation of the combination index (CI). The combination indices were calculated at 20, 30, 50, 70% cell proliferation (which corresponds to 80, 70, 50, and 30% inhibition of proliferation). The equation was as follows:

$$\text{Combination Index} = \frac{(D)_1}{(D_x)_1} + \frac{(D)_2}{(D_x)_2} + \frac{(D)_3}{(D_x)_3}$$

Where $(D_x)_1$, $(D_x)_2$ and $(D_x)_3$ in the denominators were the concentrations of pure BLP, SKA and LGT that was needed to induce 80, 70, 50 or 30% (or x%) inhibition of cell proliferation according to their individual dose-response curves, respectively. The $(D)_1$, $(D)_2$ and $(D)_3$ in the numerators were the concentrations of BLP, SKA and LGT that induced 80, 70, 50 and 30% (or x%) inhibition of cell proliferation, calculated according to each of their percentage contents in the two herbal extracts or

two artificial mixture of phthalides. A combination index value of less than 1 was considered synergistic, close to 1 was considered additive and greater than 1 was considered antagonistic interactions (Chou, 2006). The median-effect analysis was also used to calculate the type of interaction in drug combinations between various concentrations of BLP, SKA and LGT with various concentrations of cisplatin. Table 2.4 illustrates the type of interaction according to the calculated combination index value.

Table 2.4 Extent of synergistic and antagonistic interactions according to the calculated combination index values. Chou (2006)

Combination index range	Type of interaction
<0.10	Very strong synergism
0.10-0.30	Strong synergism
0.30-0.70	Synergism
0.70-0.85	Moderate synergism
0.85-0.90	Slight synergism
0.90-1.10	Nearly additive
1.10-1.20	Slight antagonism
1.20-1.45	Moderate antagonism
1.45-3.30	Antagonism
3.30-10.00	Strong antagonism
>10	Very strong antagonism

2.1.2.12 Statistical analysis

Data are expressed as mean value ± S.E.M. from at least three independent experiments conducted in at least duplicate. The data were analyzed by one-way analysis of variance (ANOVA) followed by Bonferroni's multiple comparison post hoc test, using GraphPad Prism 5.0. Differences were considered statistically significant at $p<0.05$.

2.2 Results

2.2.1 Effects of BLP, SKA and LGT on the viability of HT-29 cells

As shown in Figure 2.3, all three phthalides dose-dependently reduced viability of HT-29 cells and the IC_{50} values were 72.51 ± 8.65 μg/ml (385.24 ± 45.96 μM), 18.74 ± 1.14 μg/ml (97.60 ± 5.94 μM) and 41.98 ± 3.64 μg/ml (220.95 ±19.16 μM) for BLP, SKA and LGT, respectively. Cisplatin, a commonly used anti-cancer drug used to treat solid tumors, was used as a positive control. It also dose-dependently reduced cell viability and its IC_{50} value was 40.92 ± 3.23 μg/ml (136.38 ± 10.76 μM). While SKA and LGT significantly decreased the viability of HT-29 cells at 32.00 and 41.01 μg/ml ($p<0.001$) after 24 h, respectively, BLP only significantly decreased cell viability at 120.00 μg/ml ($p<0.01$) (Figure 2.4). As well, both SKA and LGT were cytotoxic to HT-29 cells in a time-dependent manner (Figure 2.4).

2.2.2 Effects of BLP, SKA and LGT on the viability of SW1116 cells

To ensure that the three phthalides indeed are cytotoxic to human colon cancer cells, another human colorectal adenocarcinoma SW1116 cell line was used to examine the cytotoxic activities of BLP, SKA and LGT. The IC_{50} values of BLP, SKA, LGT and cisplatin are summarized in Table 2.5 for both HT-29 and SW1116 cell lines. In both

HT-29 and SW1116 cells, the potency order for cytotoxicity is SKA > LGT >> BLP. In HT-29 cells, the cytotoxic effects of SKA were greater than that of the positive control, cisplatin, while LGT was similar to cisplatin in terms of potency. However, in SW1116 cells, cisplatin had a much lower IC_{50} value than any of the phthalides. Another interesting finding was the low cytotoxic effects of BLP in SW1116 cells; it was approximately 80-fold less potent than the positive control and approximately 20-fold less potent than SKA (Table 2.5). Since the potency order of phthalides was similar between both human colon cancer cell lines and SKA and LGT showed comparable activities in both cell lines, the phthalides were assumed to be a bioactive component of the DG extract for cytotoxicity against human colon cancer cells.

2.2.3 Effects of DG and CX extracts on the viability of HT-29 cells

The cytotoxic effects of the DG extract were also examined. As shown in Figure 2.5, the DG extract reduced viability of HT-29 cells in a dose-dependent manner after 24 and 48 h incubation, with IC_{50} values of 20.70 ± 0.85 μg/ml and 20.82 ± 2.05 μg/ml, respectively, but the time-dependent reduction of cell viability was not strong. The whole herbal extract had a lower IC_{50} value than BLP and LGT and similar IC_{50} to SKA (Table 2.5). However, after accounting for the fact that the DG extract is composed of 41.06% phthalides, the extract was much more potent at diminishing the viability of HT-29 cells than any one of the phthalides (Table 2.5). According to Table 2.1, the IC_{50} value of DG extract was 20.70 ± 0.85 μg/ml, which corresponds to IC_{50} values of 17.80, 4.14, and 8.28 μg/ml for BLP, SKA and LGT, respectively, as calculated according to their percentage content in the DG extract. Since the calculated IC_{50} values are much lower than the actual IC_{50} values of the phthalides, it suggests that the three phthalides may interact synergistically in DG extract to induce cytotoxicity in HT-29 cells. CX extract also contains BLP, SKA and LGT as major

bioactive phthalides. The phthalide content is lower in CX than in DG and BLP, SKA and LGT in CX have different proportions ratios than in DG (Table 2.1). The extract of CX did not significantly affect the viability of HT-29 cells, until at the highest dose tested (125 μg/ml, $p<0.01$, Figure 2.6B). However, DG extract significantly reduced the viability of HT-29 cells, even at the lowest dose tested (15 μg/ml, $p<0.001$, Figure 2.6A). The results suggest that two herbal extracts, with the same bioactive phthalides, but in different proportions, may have very different effects on the cell viability.

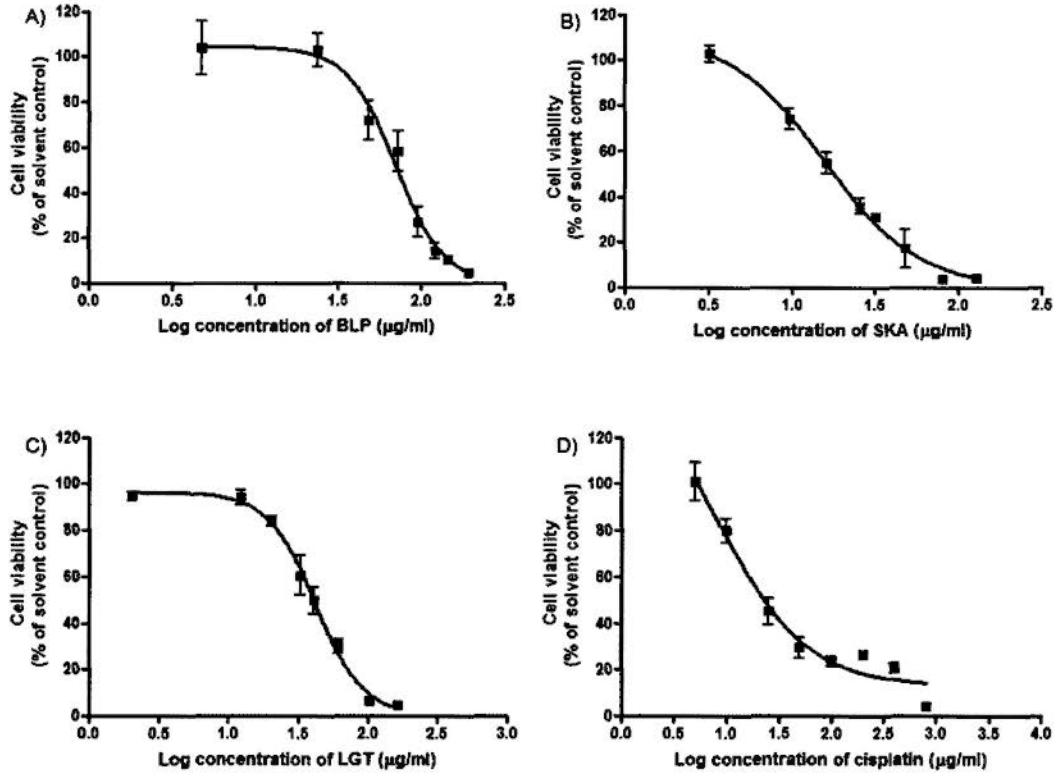

Figure 2.3 Effects of A) *n*-butylidenephthalide, B) senkyunolide A, C) *z*-ligustilide and D) cisplatin on the viability of HT-29 cells after 24 h treatment. Data are expressed as mean values ± S.E.M as a percentage of the solvent control. The solvent control was 0.01% DMSO, which had no effect on the viability of HT-29 cells. The experiment was performed in triplicate in three independent experiments.

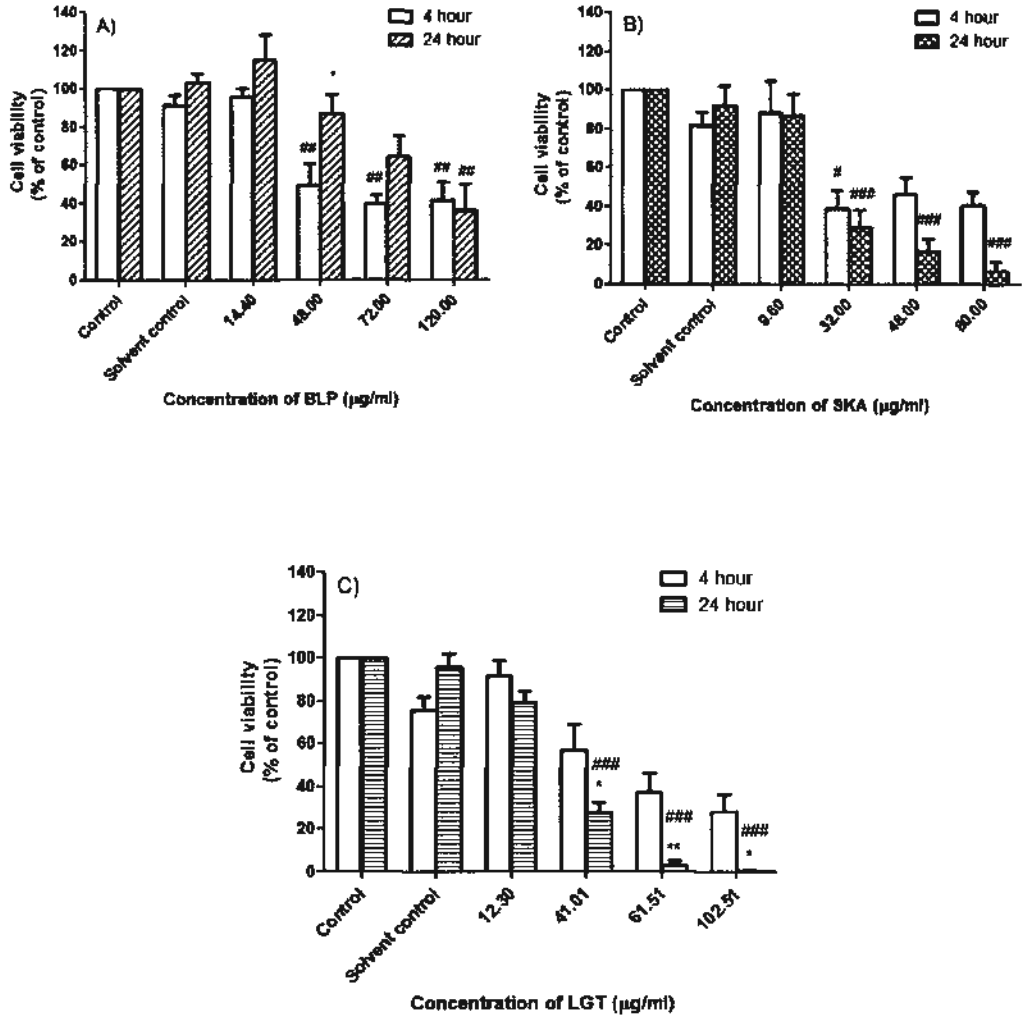

Figure 2.4 Effects of A) BLP, B) SKA and C) LGT on the viability of HT-29 cells after 4 h and 24 h treatment. Data are presented as a percentage of control (untreated medium) as mean values ± S.E.M. The solvent control was 0.01% DMSO. The experiment was performed in triplicate in three independent experiments. #$p<0.05$, ##$p<0.01$, ###$p<0.001$ compared with the corresponding solvent control; *$p<0.05$ and **$p<0.01$ compared with the 4 h treatment.

Table 2.5 Potency of cytotoxic effects of phthalides against HT-29 and SW1116 cell lines after 24 h drug treatment

	IC_{50} in μg/ml (μM)	
	HT-29	SW1116
BLP	72.51 ± 8.65	552.67 ± 68.07
	(385.24 ± 45.96)	(2936.30 ± 361.65)
SKA	18.74 ± 1.14	24.71 ± 12.36
	(97.60 ± 5.94)	(128.70 ± 64.38)
LGT	41.98 ± 3.64	65.90 ± 4.16
	(220.95 ± 19.16)	(346.84 ± 21.89)
DG extract	20.70 ± 0.85	N.D.
Cisplatin	40.92 ± 3.23	6.89 ± 1.33
	(136.38 ± 10.76)	(22.96 ± 4.43)

N.D indicates that the IC_{50} value was not determined in the cell line.

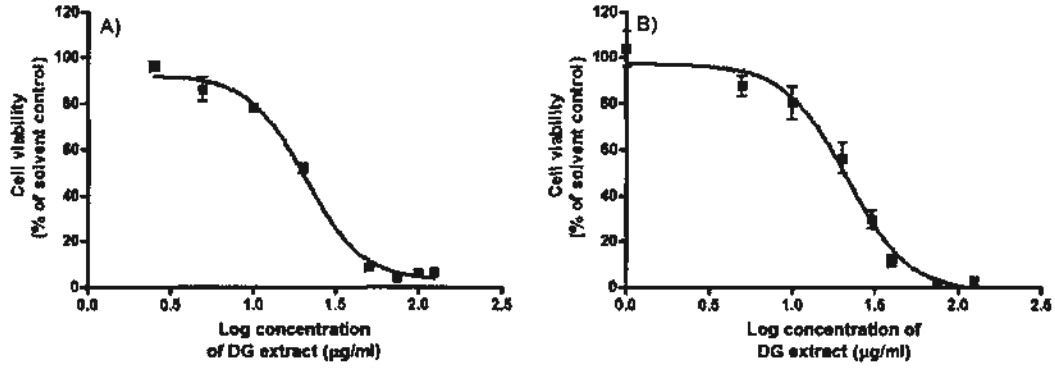

Figure 2.5 Effects of DG extract on the viability of HT-29 cells after A) 24 h and 48 h treatment. Data are presented as a percentage of solvent control as mean values ± S.E.M. The solvent control was 0.01% DMSO. The experiment was performed in triplicate in three independent experiments.

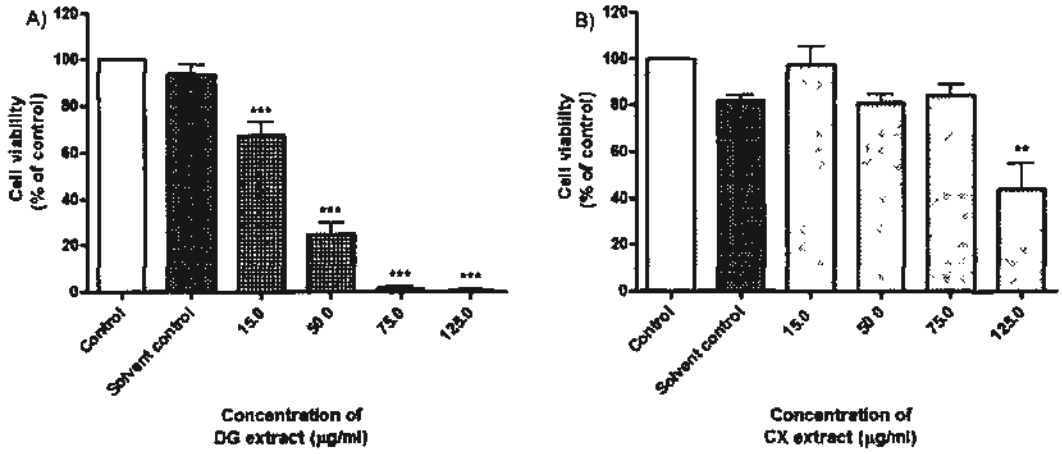

Figure 2.6 Effects of A) DG and B) CX extracts on the viability of HT-29 cells after 24 h treatment. Data are presented as a percentage of control (untreated medium) as mean values ± S.E.M. The solvent controls were 0.005% and 0.2% DMSO, respectively. The experiment was performed in triplicate in three independent experiments. **p<0.01, ***p<0.001 compared with the solvent control.

2.2.4 Cytotoxic selectivity of phthalides, DG and CX extracts on HT-29 cells

Since one of the drawbacks of using conventional anti-tumor drugs is the lack of selectivity for cancer cells, the cytotoxic effects of the three phthalides along with the two herbal extracts were studied in both human colon cancer HT-29 cells and normal human colon fibroblast CCD-18Co cells (Figure 2.7). All of the phthalides and the two herbal extracts showed significantly greater cytotoxicity in HT-29 cells, rather than in CCD-18Co cells at all concentrations tested ($p<0.05$). The effects of LGT and DG on viability of HT-29 cells were significantly different from CCD-18Co cells starting from the lowest dose tested, 12.3 and 15.0 μg/ml, respectively (Figures 2.7C, D). Unexpectedly, BLP and CX appeared to increase the viability of CCD-18Co cells by 10-20% at all of the concentrations tested (Figures 2.7A, E). Cisplatin was more cytotoxic in CCD-18Co cells at 50 μg/ml and higher (Figure 2.7F), which is in

accordance with the fact that many chemotherapeutic drugs used nowadays induce adverse effects due to lack of selectivity (Li *et al.,* 2006a; Li *et al.,* 2006b). From these results, BLP, SKA, LGT, DG and CX had good selectivity towards colon cancer cells.

2.2.5 Effects of phthalides, DG and CX extracts on viability and plasma membrane integrity of HT-29 and CCD-18Co cells

To re-confirm the findings on the cytotoxic effects of phthalides and DG, another cytotoxicity assay was carried out. Non-viable cells lose plasma membrane integrity in the late stages of cell death, which results in the release of cytoplasmic lactate dehydrogenase. None of the phthalides and herbal extracts induced significant loss of membrane integrity at concentrations close to their IC_{50} values (Figure 2.8; Table 2.5). This suggests that at IC_{50} concentrations, cell death occurs, but not to the point where membrane integrity is compromised. BLP, SKA and LGT showed significant increase in LDH release to approximately 40% at the highest doses tested, at 120, 80 and 102.5 μg/ml, respectively ($p<0.001$, Figures 2.8A-C). All of the phthalides and DG extract induced dose-dependent increase in LDH release after 24 h treatment. The decrease in viability of HT-29 cells was in accordance with an increase in LDH release (Figures 2.6-2.8). While the CX extract significantly reduced cell viability to 44.1%, it only increased the basal release of LDH to 0.9% (Figures 2.6B, 2.8E). BLP, SKA, LGT and the DG extract increased LDH release in CCD-18Co cells in a dose-dependent manner (Figures 2.9A-D). The CX extract showed no significant increase in LDH release at all concentrations tested (Figure 2.9E). The LDH release was higher in HT-29 cells than in CCD-18Co cells for BLP and DG extract at all concentrations tested (Figure 2.9A, D). At 120 μg/ml of BLP, the LDH release was 38.96% in HT-29 cells, while it was 8.2% in CCD-18Co cells (Figures 2.8A, 2.9A).

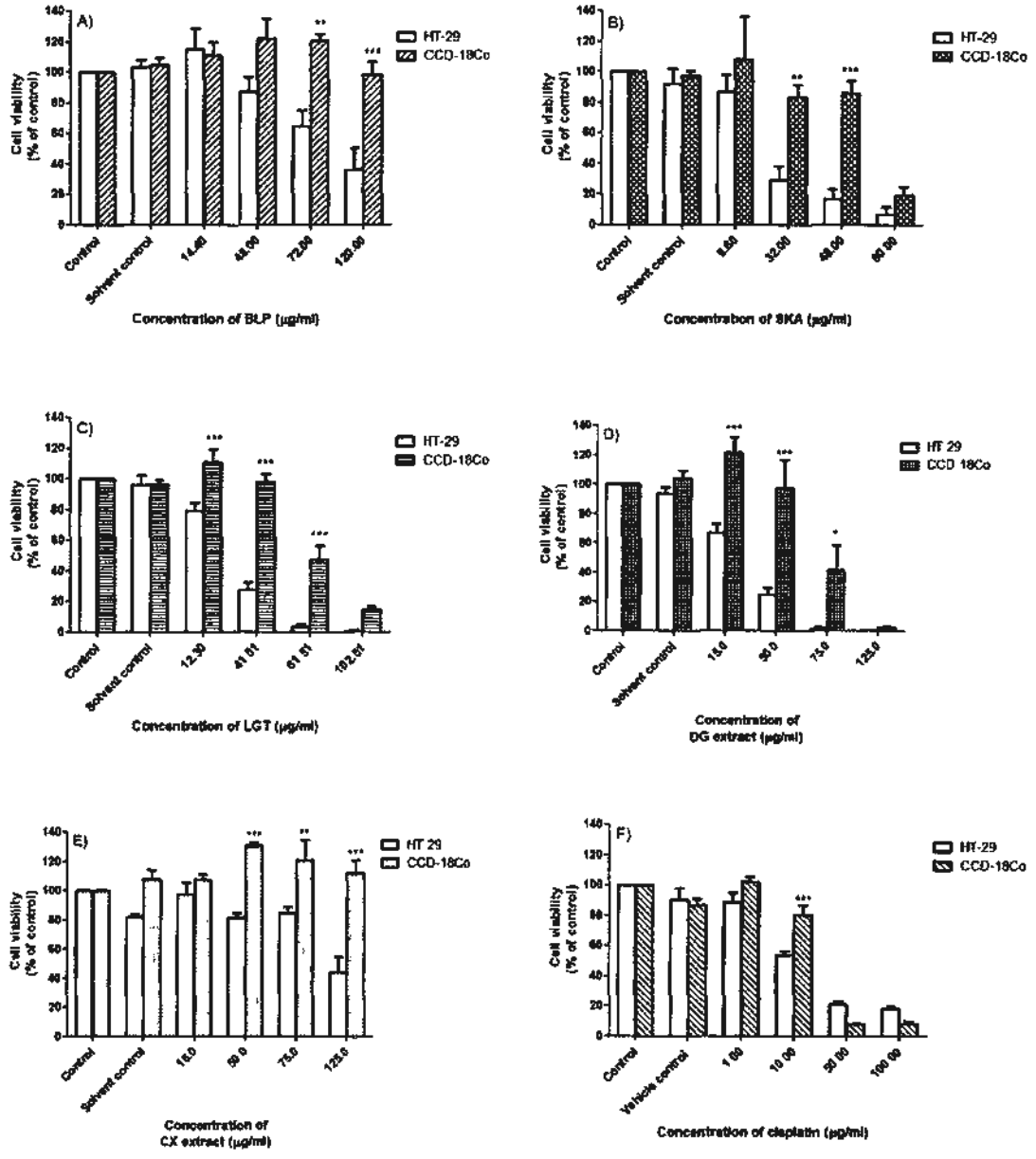

Figure 2.7 Effects of A) BLP, B) SKA, C) LGT, D) DG extract, E) CX extract and F) cisplatin on the viability of HT-29 and CCD-18Co cells after 24 h treatment. Data are presented as a percentage of control (untreated medium) as mean values ± S.E.M. The solvent controls were 0.2% DMSO. The experiment was performed in triplicate in three independent experiments. *$p<0.05$, **$p<0.01$, ***$p<0.001$ compared with HT-29 cell line.

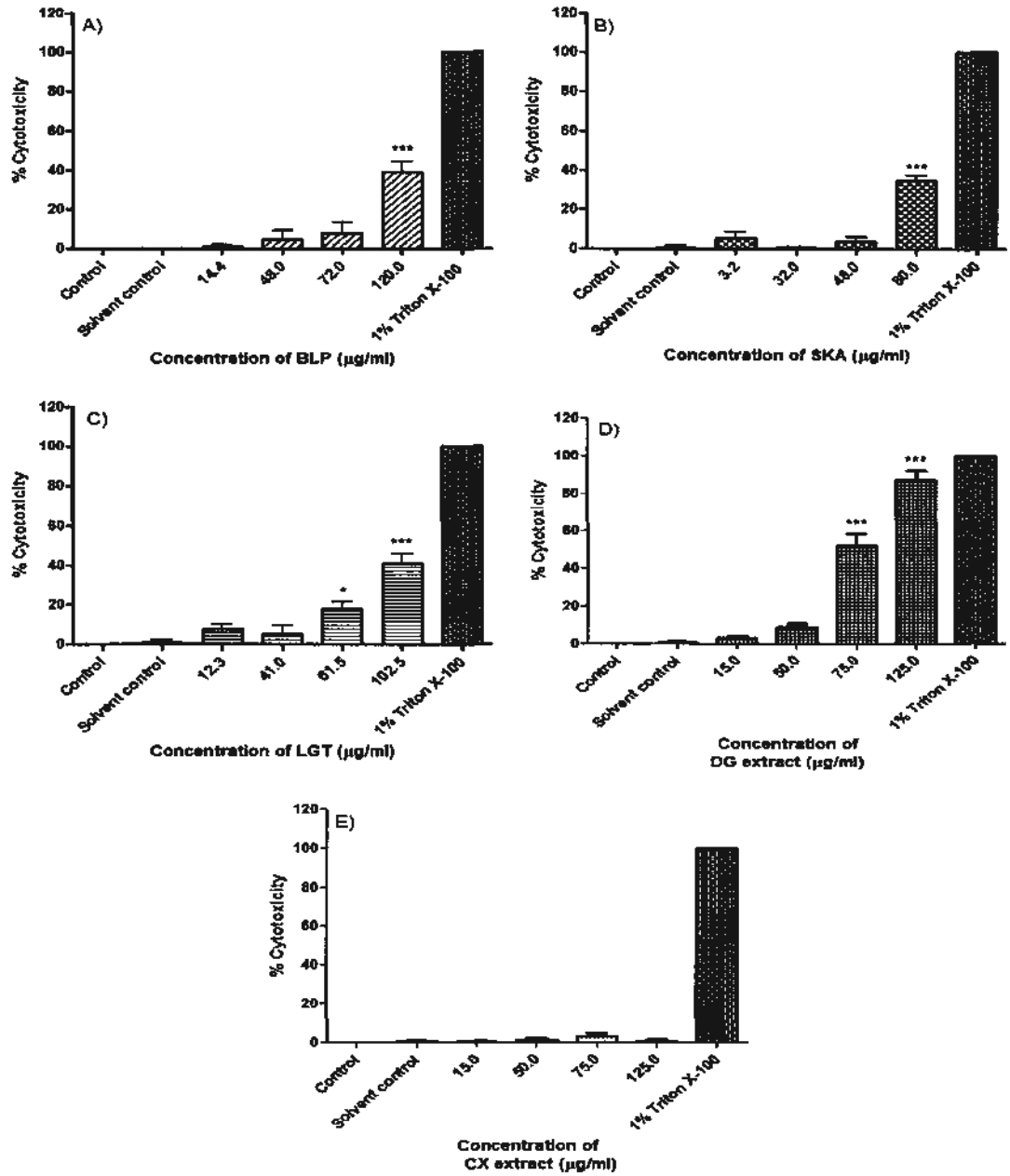

Figure 2.8 Effects of A) BLP, B) SKA, C) LGT, D) DG extract and E) CX extract on LDH release with loss of plasma membrane integrity in HT-29 cells after 24 h treatment. Untreated control cells were normalized as 0% cytotoxicity and Triton X-100-treated positive control cells were normalized as 100% cytotoxicity. The solvent control was 0.2% DMSO. The experiment was performed in triplicate in three independent experiments and data was presented as mean values ± S.E.M. *$p<0.05$, ***$p<0.001$ compared with the solvent control.

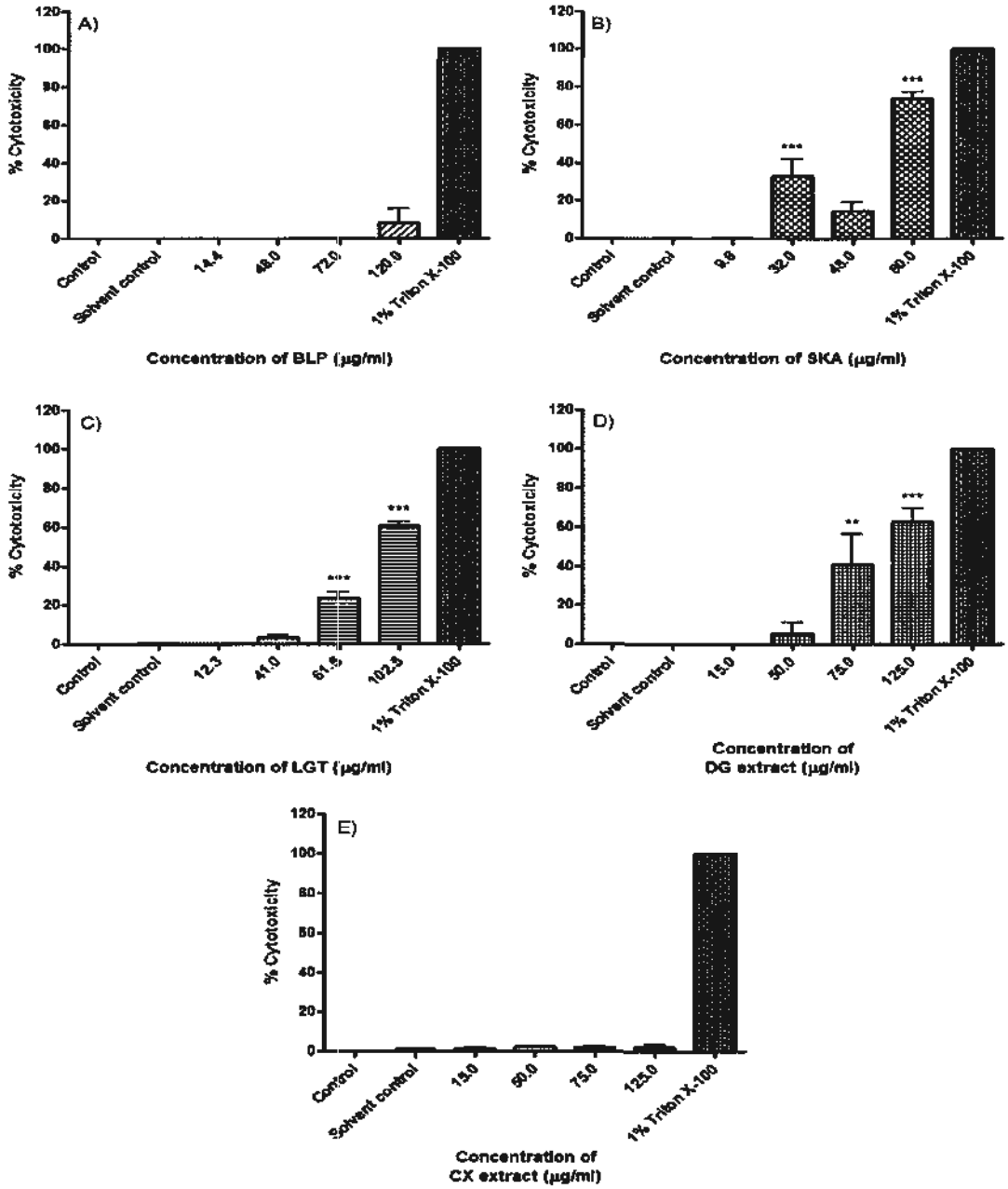

Figure 2.9 Effects of A) BLP, B) SKA, C) LGT, D) DG extract and E) CX extract on LDH release in CCD-18Co cells after 24 h treatment. Untreated control cells were normalized as 0% cytotoxicity and Triton X-100-treated positive control cells were normalized as 100% cytotoxicity. The solvent control was 0.2% DMSO. The experiment was performed in triplicate in three independent experiments and data was presented as mean values ± S.E.M. *$p<0.05$, ***$p<0.001$ compared with the solvent control.

At 125 μg/ml of DG extract, the LDH release was 24.75% higher in HT-29 cells than in CCD-18Co cells (Figures 2.8D, 2.9D). The LDH release was similar in both cell lines after LGT treatment (Figures 2.8C, 2.9C). SKA induced doubled the amount of LDH release in CCD-18Co cells relative to HT-29 cells (Figures 2.8B, 2.9B).

2.2.6 Effects of phthalides, DG and CX extracts on the proliferation of HT-29 cells

As shown in Figure 2.10, BLP, SKA and LGT dose- and time-dependently inhibited the proliferation of HT-29 cells after 4 and 24 h treatment, as examined by the [^{3}H] thymidine incorporation assay. At around the cytotoxicity IC_{50} values of each phthalide (Table 2.5), the proliferation of HT-29 cells were also significantly reduced, which suggests that the phthalides may target cell proliferation mechanisms in addition to cell death mechanisms (Figures 2.10A, C). Similar to the MTT results, both SKA and LGT were much more potent than BLP. Furthermore, both DG and CX extracts inhibited HT-29 proliferation in a dose-dependent manner. DG significantly reduced cell proliferation at the lowest concentration tested, 15 μg/ml ($p<0.001$, Figure 2.11A), while CX significantly reduced cell proliferation at 75 μg/ml and higher ($p<0.001$, Figure 2.11B). The positive control, cisplatin, almost completely abolished the proliferation of HT-29 cells starting from 20.0 μg/ml (Figure 2.11C).

2.2.7 Phthalides and DG and cell cycle distribution

2.2.7.1 Effects of incubation time and DMSO on cell cycle distribution of HT-29 cells

From the results, BLP, SKA, LGT and the DG extract were cytotoxic and

anti-proliferative to human colon cancer cells in a selective manner. Since the cell cycle has a crucial role in governing cell death and proliferation, the cell cycle distribution after treatment of HT-29 cells with the three phthalides and the herbal extract was analyzed using propidium iodide staining and flow cytometry.

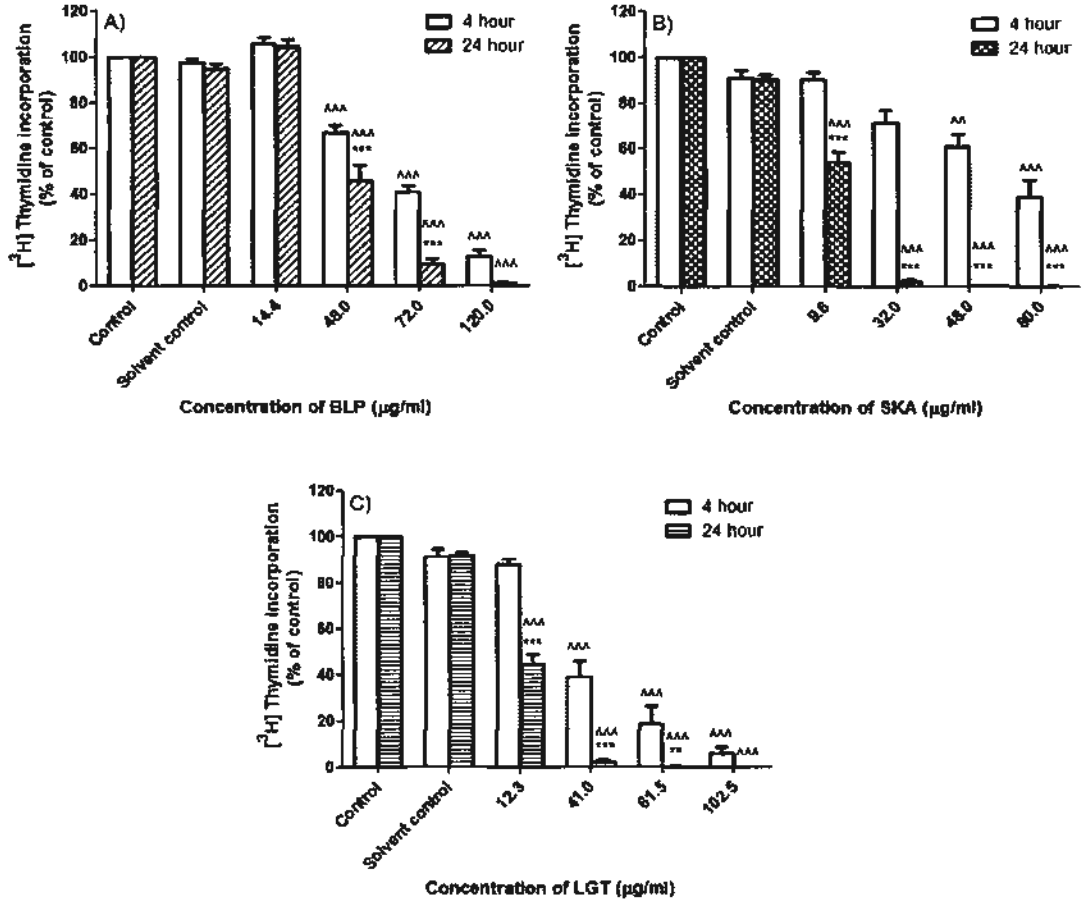

Figure 2.10 Effects of A) BLP, B) SKA and C) LGT on the proliferation of HT-29 cells after 4 and 24 h treatment as assessed by [^{3}H] thymidine incorporation assay. Data are presented as a percentage of control (untreated medium) as mean values ± S.E.M. The solvent controls were 0.2% DMSO. The experiment was performed in triplicate in three independent experiments. **$p<0.01$, ***$p<0.001$ compared with 4-h treatment of the respective group; ^^$p<0.01$, ^^^$p<0.001$ compared with the respective solvent control.

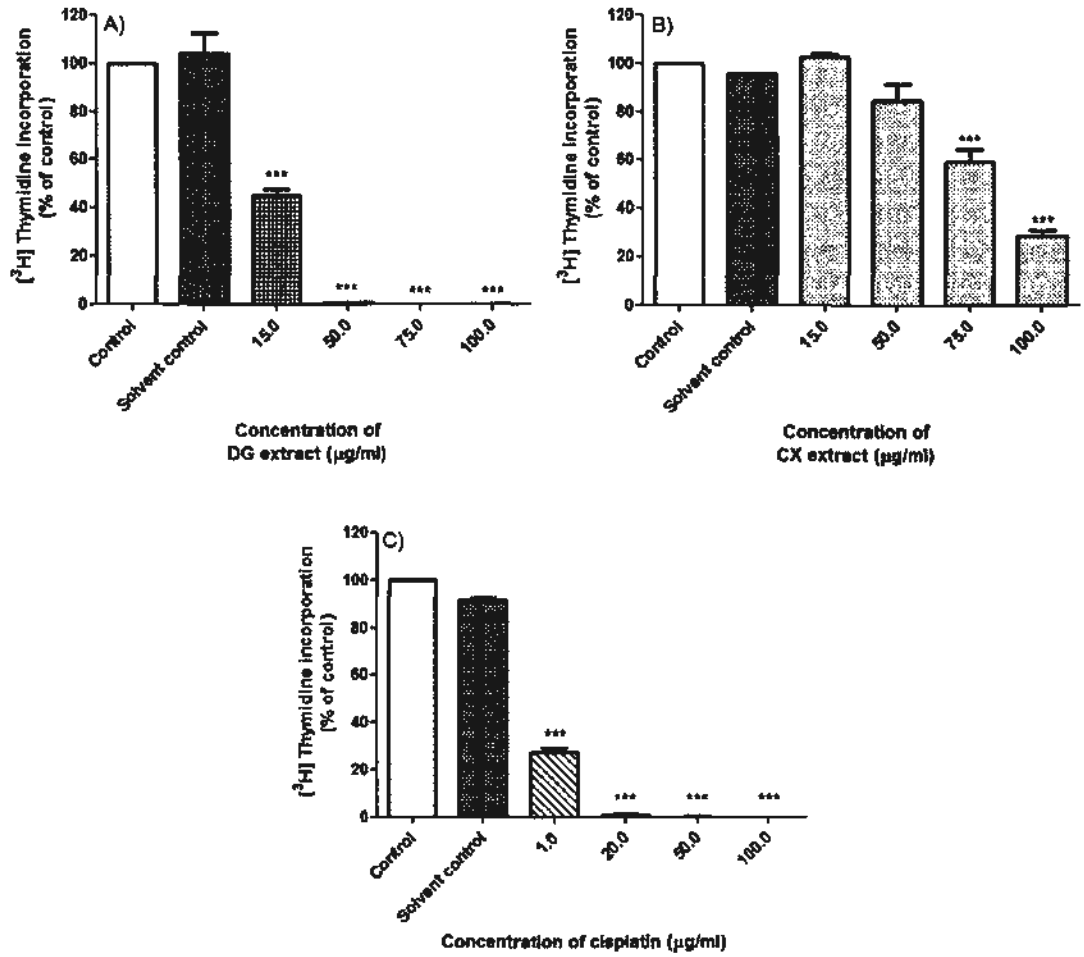

Figure 2.11 Effects of A) DG extract, B) CX extract and C) positive control cisplatin on proliferation of HT-29 cells after 24 h treatment as studied by [^{3}H] thymidine incorporation assay. Data are presented as a percentage of control (untreated medium) as mean values ± S.E.M. The solvent controls were 0.2% DMSO for phthalides and 5% normal saline for cisplatin. The experiment was performed in triplicate in three independent experiments. ***$p<0.001$ compared with the solvent control.

First, the effects of the solvent, 0.005% DMSO, on the cell cycle distribution were studied after 6, 12 and 24 h treatment. At all three time points tested, DMSO did not induce any significant change to any phase of the cell cycle (Figure 2.12). Hence, all subsequent statistical comparisons of treatment groups were made in comparison to the solvent control (0.005% DMSO). Then, the cell cycle distribution of cells after 6, 12 and 24 h in untreated medium was examined and shown in Figure 2.13. After 24 h of medium-only treatment, there was a significant reduction in the number of cells in G_0/G_1 phase as there was a concomitant increase in the number of cells in S phase as cells migrate through the cell cycle ($p<0.05$, $p<0.001$, Figure 2.13). Therefore, for flow cytometric analysis of cell cycle distribution, it is not feasible to make simple comparisons of treatment effects between time points. The statistical comparisons must be performed between treatment group and the solvent control group in the respective time point. The concentrations of BLP, SKA, LGT and CX extract used for the flow cytometry experiments were approximately 1 x IC_{50}, 2 x IC_{50}, 3 x IC_{50} and 4 x IC_{50} values according to their cytotoxicity IC_{50} values in Table 2.5. The concentrations of DG extract used were approximately 2 x IC_{50}, 3 x IC_{50} and 4 x IC_{50} values.

2.2.7.2 Effects of the phthalides, DG and CX on cell cycle distribution in HT-29 cells

After 24 h treatment, BLP induced a significant increase in the number of cells in G_0/G_1 at its cytotoxicity IC_{50} and 2 x IC_{50} values, with a dose-dependent decrease in the number of cells in S and G_2/M phases (Figure 2.14A). Simultaneously, there was a significant dose-dependent accumulation of cells, up to approximately 20%, in the sub-G_1 apoptotic phase ($p<0.01$, Figure 2.14A). Then, a time course experiment was performed to examine the effects of BLP on the cell cycle after 6, 12 and 24 h treatment.

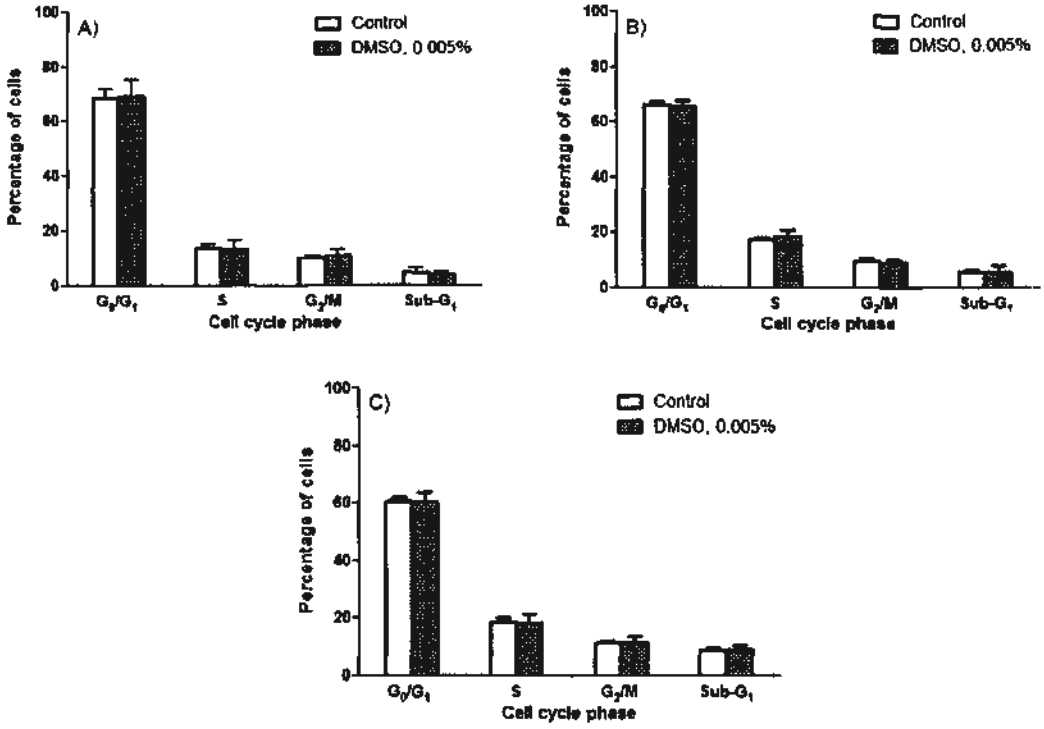

Figure 2.12 Effects of 0.005% DMSO on cell cycle distribution in HT-29 cells after A) 6 h, B) 12 h and C) 24 h treatment as assayed by propidium iodide staining and flow cytometry. Data are presented as a percentage of control (untreated medium) as mean values ± S.E.M from three independent experiments.

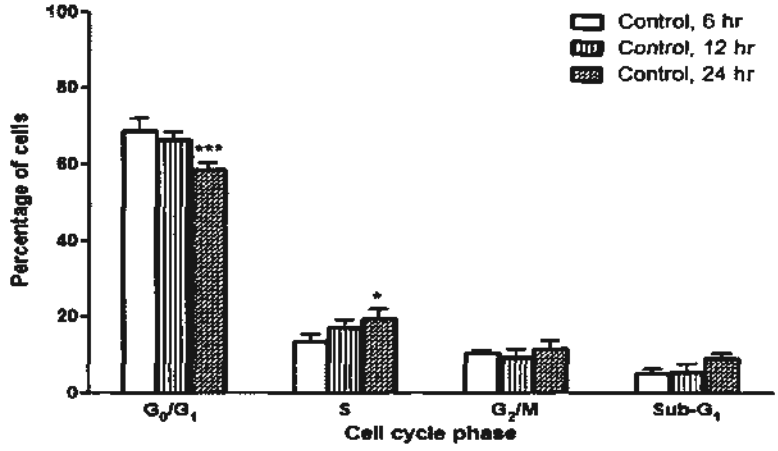

Figure 2.13 Cell cycle distribution of untreated control HT-29 cells after 6, 12 and 24 h. Data are presented as a percentage of control (untreated medium) as mean values ± S.E.M. from three independent experiments. *p<0.05, ***p<0.001 compared with control cells, 6 h.

While there was no significant change in cell cycle distribution after 6 h treatment, there was a significant reduction of cells in S phase and increase of cells in sub-G_1 phase by 12 h ($p<0.01$, Figures 2.14B, C). After 24 h, significant accumulation of cells in G_0/G_1 and sub-G_1 occurred, along with reduction in S and G_2/M phases ($p<0.01$, Figure 2.14D). SKA induced a dose-dependent accumulation of cells in G_0/G_1 phase and at 32.0μg/ml, SKA also significantly reduced the number of cells in S and G_2/M phases ($p<0.05$, Figure 2.15A). The G_0/G_1 cell cycle arrest and inhibition of S phase occurred after 12 h treatment in a time-dependent manner and was sustained after 24 h treatment (Figure 2.15B-D). However, there was no significant change in sub-G_1 phase, even after treatment with the highest concentration of SKA (Figure 2.15A). After 24 h treatment of HT-29 cells with 36.9 μg/ml LGT, G_0/G_1 arrest was induced with declines in S and G_2/M phases ($p<0.01$, Figure 2.16A). The accumulation of cells in sub-G_1 phase increased in a dose-dependent manner. For instance, at 102.5 μg/ml LGT, the sub-G_1 phase cell population increased by almost two-fold, from 8.4% to 15.7% (Figure 2.15A). At 102.5 μg/ml, the increase of cells in G_0/G_1 and sub-G_1 phases occurred after 6 h and 12 h treatments, respectively (Figures 2.16B, C). Further experiments with BLP, SKA and LGT treatments for 36 h and 48 h would confirm their effects on the cell cycle.

The DG extract induced G_0/G_1 cell cycle arrest, as the number of cells in G_0/G_1 phase significantly increased 15.1% after HT-29 cells were treated with 50.0 μg/ml of the extract ($p<0.001$, Figure 2.17A). This was accompanied with a significant reduction of cells in S phase and G_2/M phase, which were most prominent after 24 h treatment ($p<0.05$, Figures 2.17A, D). The concentration of DG needed to induce the arrest was 50.0 μg/ml, which is equivalent to approximately 20.5 μg/ml total phthalides, as calculated according to the phthalide content (41.06%) in DG.

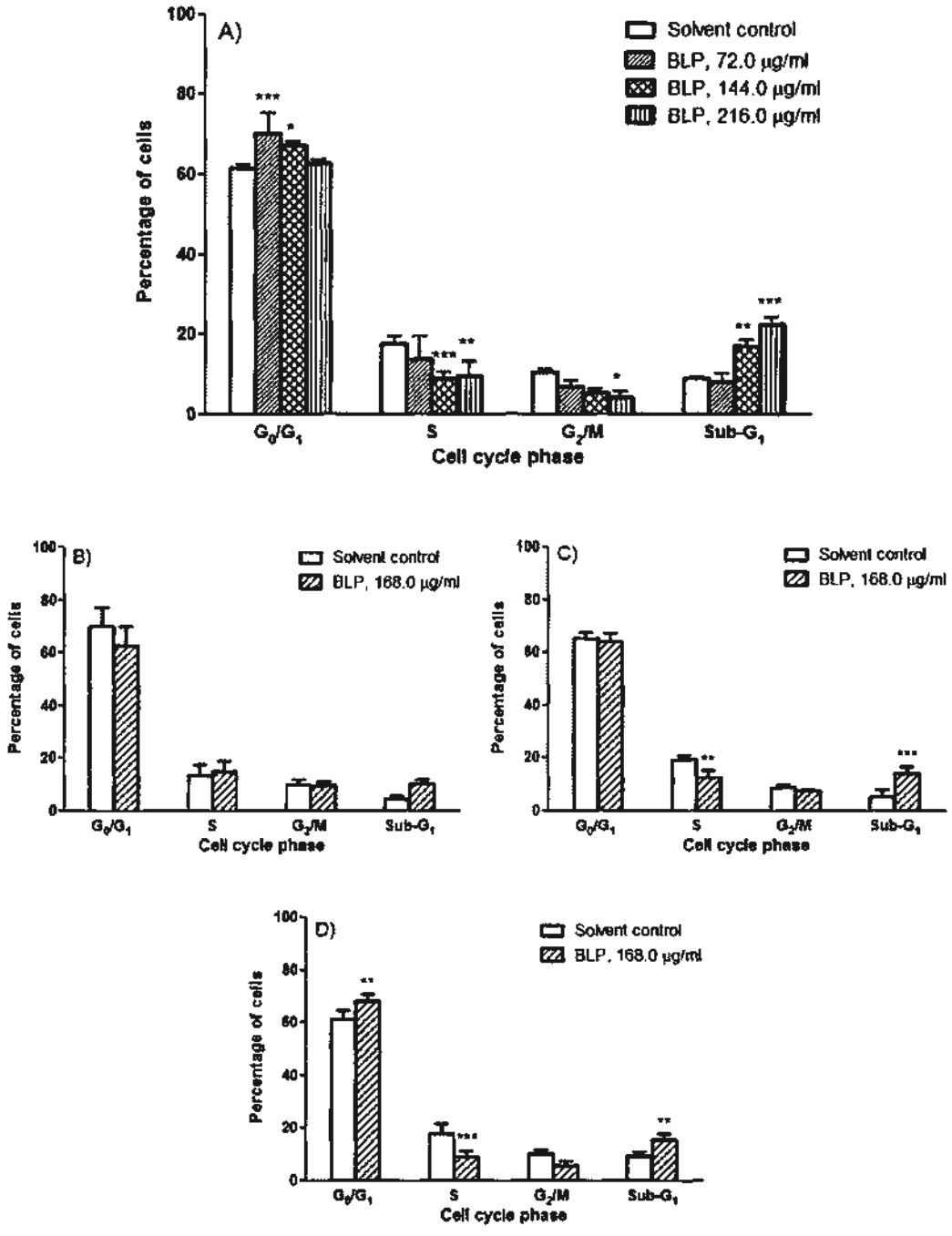

Figure 2.14 Effects of various concentrations of BLP on distribution of HT-29 cells in various phases of the cell cycle after A) 24 h treatment. The effects of BLP at 168.0 μg/ml on cell cycle after B) 6 h, C) 12 h and D) 24 h treatment were also examined. Data are presented as a percentage of control (untreated medium) as mean values ± S.E.M. from three independent experiments. **p<0.01, ***p<0.001 compared with solvent control in respective phase of cell cycle.

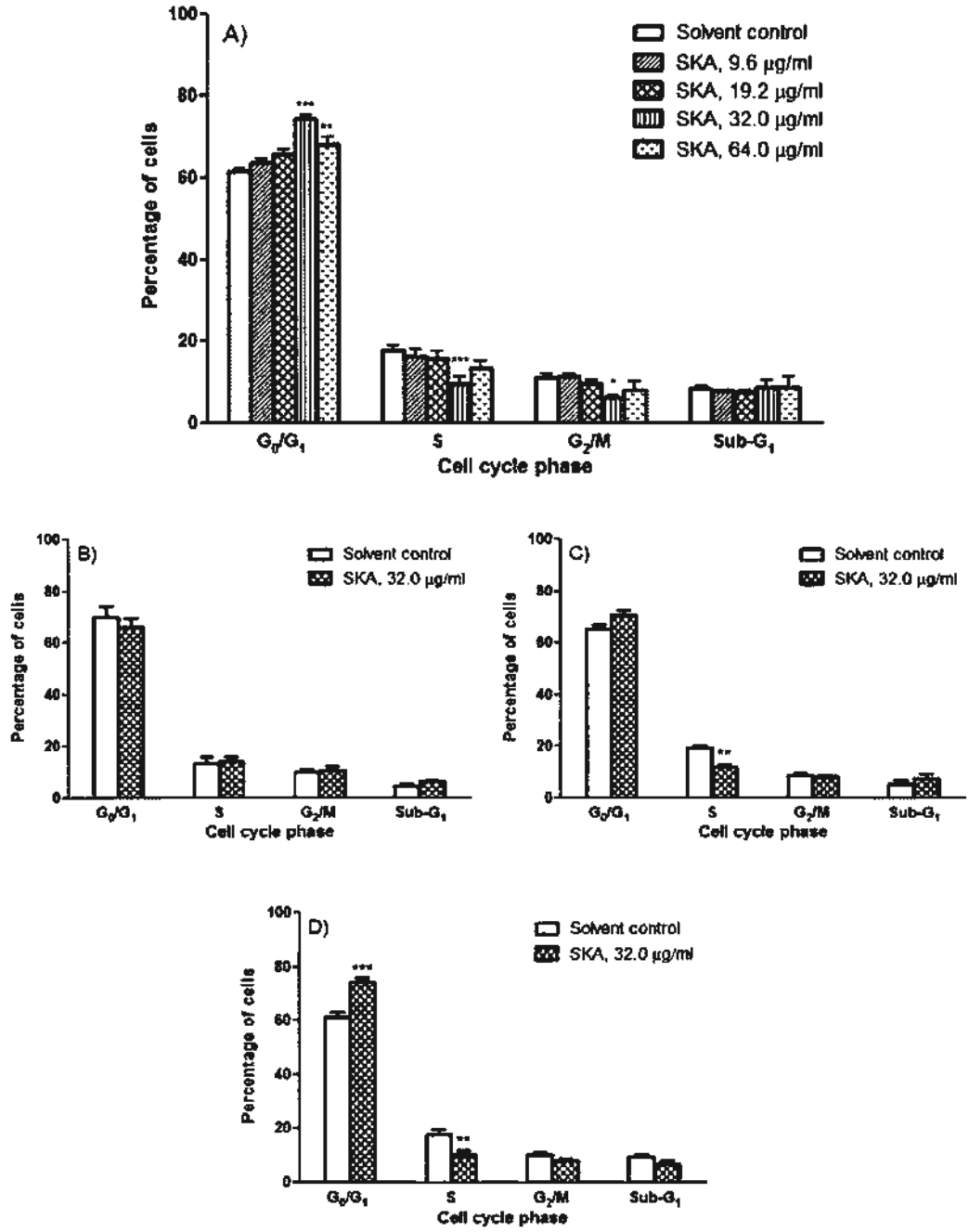

Figure 2.15 Effects of various concentrations of SKA on distribution of HT-29 cells in various phases of the cell cycle after A) 24 h treatment. The effects of SKA at32.0 μg/ml on cell cycle after B) 6 h, C) 12 h and D) 24 h treatment were also examined. Data are presented as a percentage of control (untreated medium) as mean values ± S.E.M. from three independent experiments. *p<0.05, **p<0.01, ***p<0.001 compared with solvent control in respective phase of cell cycle.

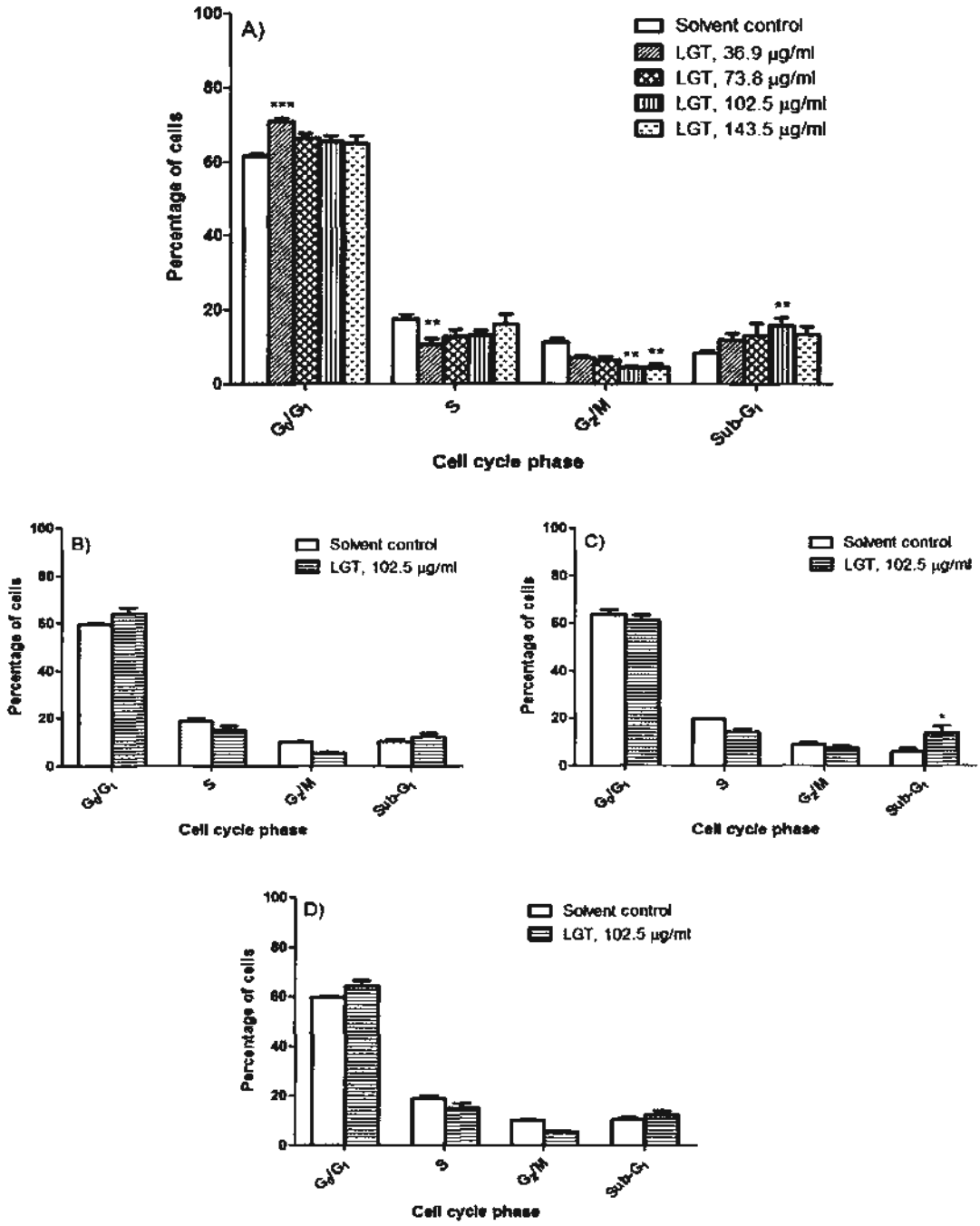

Figure 2.16 Effects of various concentrations of LGT on distribution of HT-29 cells in various phases of the cell cycle after A) 24 h treatment. The effects of LGT at 102.5 µg/ml on cell cycle after B) 6 h, C) 12 h and D) 24 h treatment were also examined. Data are presented as a percentage of control (untreated medium) as mean values ± S.E.M. from three independent experiments. *p<0.05, **p<0.01, ***p<0.001 compared with solvent control in respective phase of cell cycle.

The concentrations of BLP, SKA and LGT that induced G_0/G_1 arrest were 32.0, 36.9 and 72.0 μg/ml, respectively (Figure 2.14A, 2.15A, 2.16A), which were higher than the concentration of total phthalides in DG (20.5 μg/ml) needed for the same effect. A similar trend was also observed for the accumulation of cells in sub-G_1 phase. Specifically, A concentration of 102.5 μg/ml of LGT and 144.0 μg/ml of BLP triggered a significant accumulation of HT-29 cells in sub-G_1 phase, but 175.0 μg/ml of the DG extract (71.9 μg/ml of total phthalides) had a similar effect as LGT and BLP (Figure 2.14A, 2.16A, 2.17A). This suggests that the three phthalides may act in a synergistic manner to induce G_0/G_1 arrest or accumulation of cells in sub-G_1 phase or there may be other bioactive compounds in the DG xtract that have a similar effect. SKA did not increase the percentage of cells in sub-G_1 phase at any concentration tested (Figure 2.15A). For comparison, CX did not induce significant changes to any of the phases of the cell cycle at all of the concentrations tested and it even reduced the number of cells in sub-G_1 phase (Figure 2.19). It is interesting to note that although both DG and CX contained the same phthalides, 175.0 μg/ml of the DG extract (71.9 μg/ml phthalides) significantly induced accumulation of cells at sub-G_1 phase, while 375.0 μg/ml of the CX extract (90.0 μg/ml phthalides) did not (Figure 2.17). Cisplatin, the positive control, triggered an accumulation of HT-29 cells in sub-G_1 phase, in accordance with studies in other cancer types (Otto *et al.,* 1996; Fuertes *et al.,* 2003). It appears that BLP, SKA and LGT are bioactive phthalides in the DG extract for the induction of G_0/G_1 cell cycle arrest and increase of cells in sub-G_1 apoptotic phase. However, the greater effects of the DG extract may be due to synergistic interactions between the three phthalides or the presence of other bioactive components that also affect cell cycle. Due to different proportion ratios in the respective herbal extracts, the three phthalides may interact with each other and/or with other components in the extract to produce different effects on cell cycle.

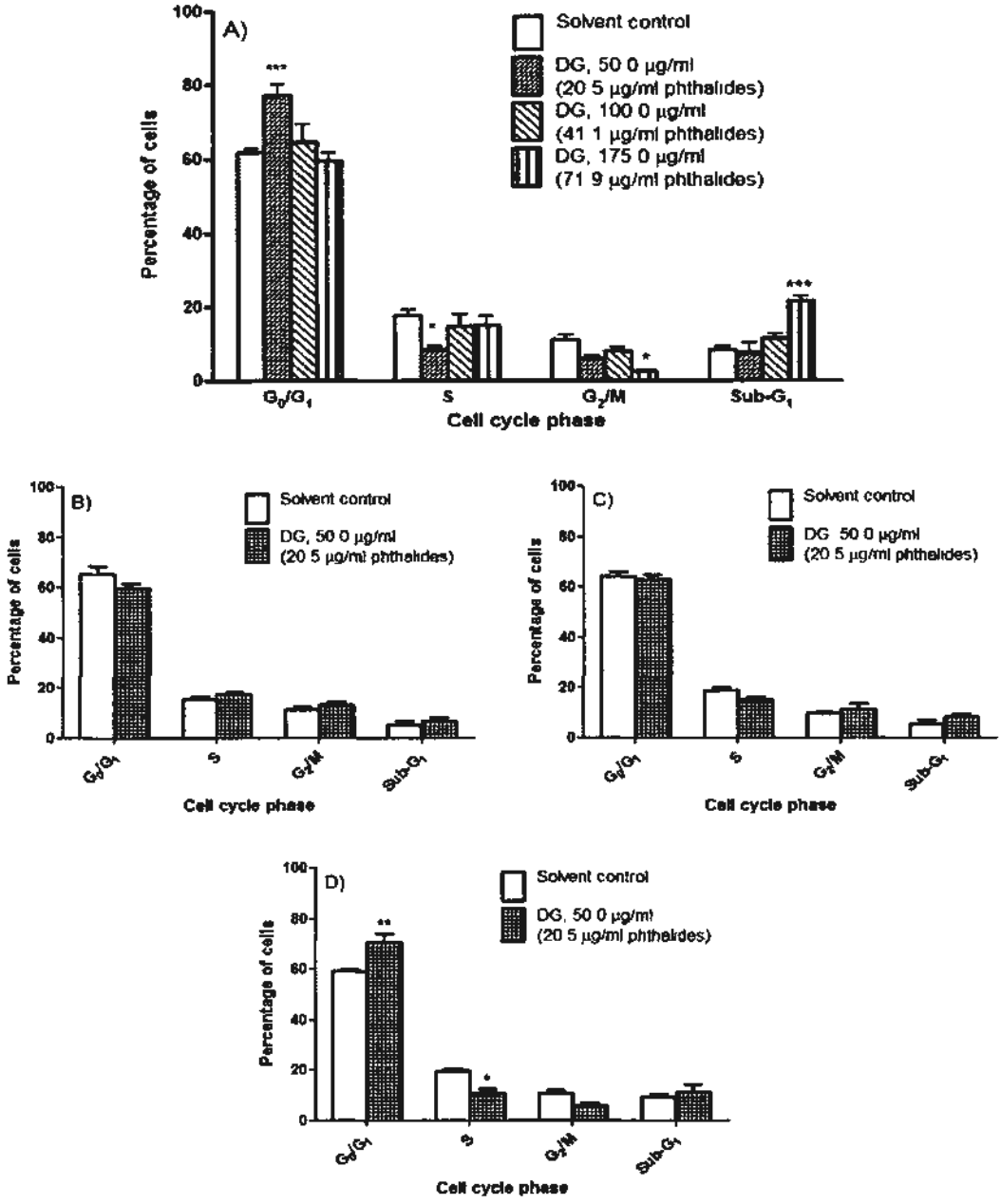

Figure 2.17 Effects of DG extract on distribution of HT-29 cells in various phases of the cell cycle after A) 24 h treatment. The concentration of phthalides in brackets is calculated according to the phthalide content in the extract as indicated in Table 2.1. The effects of DG extract at 50.0 µg/ml on cell cycle after B) 6 h, C) 12 h and D) 24 h treatment are also shown. Data are presented as a percentage of control (untreated medium) as mean values ± S.E.M. from three independent experiments. *p<0.05, **p<0.01, ***p<0.001 compared with solvent control in respective cell cycle phase.

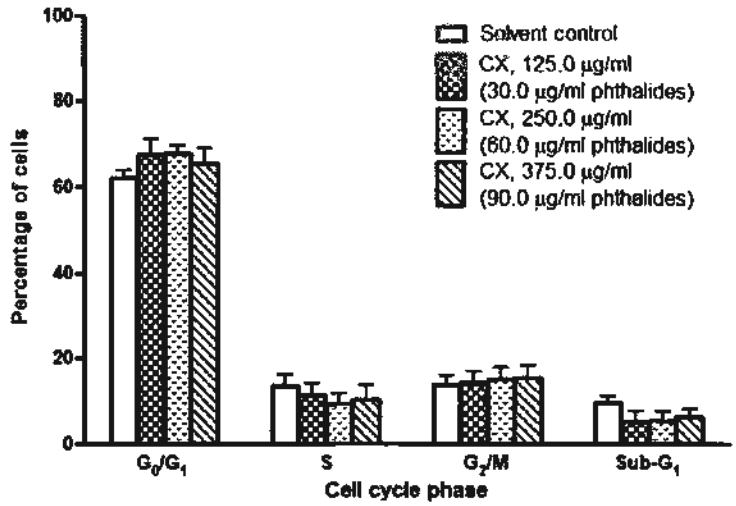

Figure 2.18 Effects of CX extract on distribution of HT-29 cells in various phases of the cell cycle after A) 24 h treatment. The concentration of phthalides in brackets is calculated according to the phthalide content in the extract as indicated in Table 2.1. Data are presented as a percentage of control (untreated medium) as mean values ± S.E.M. from three independent experiments.

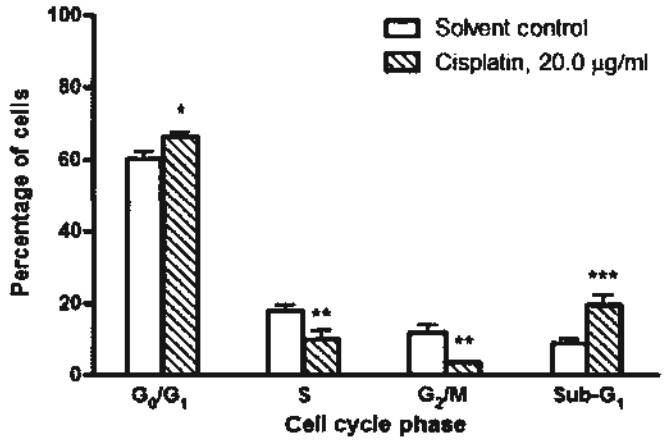

Figure 2.19 Effects of cisplatin at 20.0 μg/ml on distribution of HT-29 cells in various phases of the cell cycle after 24 h treatment. Data are presented as a percentage of control (untreated medium) as mean values ± S.E.M. from three independent experiments. *$p<0.05$, **$p<0.01$, ***$p<0.001$ compared with solvent control (5% saline) in respective phase of cell cycle.

2.2.8 Effects of BLP, SKA and LGT in combination with cisplatin on viability of HT-29 cells

Since conventional anti-cancer therapy is usually administered as a combination of cytotoxic drugs, the effects of BLP, SKA and LGT in combination with cisplatin were investigated by combining each of the phthalides with cisplatin in a 1:1 ratio at different concentrations (below, at and above IC_{50} values). Then, median effect analysis was used to calculate combination index values and to examine the type of interaction between each of the phthalides with cisplatin.

For both BLP and SKA, at each concentration of phthalide tested, as the concentration of cisplatin increased, the viability decreased in a concentration-dependent fashion (Figures 2.20A, 2.21A). However, for cisplatin concentrations higher than 50.0 μg/ml, increasing the concentration of BLP did not increase the toxicity of the BLP-cisplatin combination (Figure 2.20A). At 200.0 μg/ml of cisplatin, all concentrations of BLP used in the combination yielded strong antagonistic interactions, as all of the CI values were over 3.30 (Figure 2.20B, Table 2.4). At concentrations of cisplatin under or at its IC_{50} value (from 10.0-50.0 μg/ml), as the concentration of BLP is increased, the interaction between the two drugs changes from antagonistic to additive interactions (Figure 2.20B). Based on the combination index values, the best combination for cytotoxicity to HT-29 cells is greater than 96.0 μg/ml of BLP with lower than IC_{50} values of cisplatin (Figure 2.20B).

Likewise, none of the SKA-cisplatin combinations studied produced synergistic interactions. At each concentration of SKA tested, as cisplatin concentration was increased, the combination index value was also increased. However, at each

cisplatin concentration tested, as the SKA concentration increased, the combination index value decreased (Figure 2.21B). At 9.6 and 16.0 μg/ml of SKA, combinations with 200.0 μg/ml of cisplatin led to combination index values of 5.06 and 5.03, respectively, which indicated strong antagonistic interactions. Therefore, the best combination for cytotoxicity is <25.0 μg/ml of cisplatin combined with the highest concentration of SKA (48.0 μg/ml) (Figure 2.21B).

An interesting finding was made surrounding the combination of LGT with cisplatin. At all of the LGT concentrations tested, the lowest concentration of cisplatin (10.0 μg/ml) significantly decreased the viability of HT-29 cells (Figure 2.22A). Increasing the concentration of cisplatin higher than 25.0 μg/ml did not further potentiate the cytotoxic effects of LGT. Regardless of the LGT concentration, cisplatin at 200.0 μg/ml had antagonistic interactions with LGT, as shown by the CI values from 1.06-2.45 (Figure 2.40B). All of the remaining combinations resulted in synergistic interactions between LGT and cisplatin to generate potent cytotoxicity (Figure 2.22B). Unlike BLP or SKA combinations with cisplatin, low concentrations of both LGT and cisplatin can be used to achieve significant synergism in cytotoxicity. Lower than IC_{50} values of both LGT and cisplatin in combination reduced the viability of HT-29 cells to less than 20% (Figure 2.22A). The cytotoxic effects of the combination of LGT and cisplatin should be carried out also in normal human colon fibroblast CCD-18Co cell line to ensure that the synergistic effects are selective to colon cancer cells.

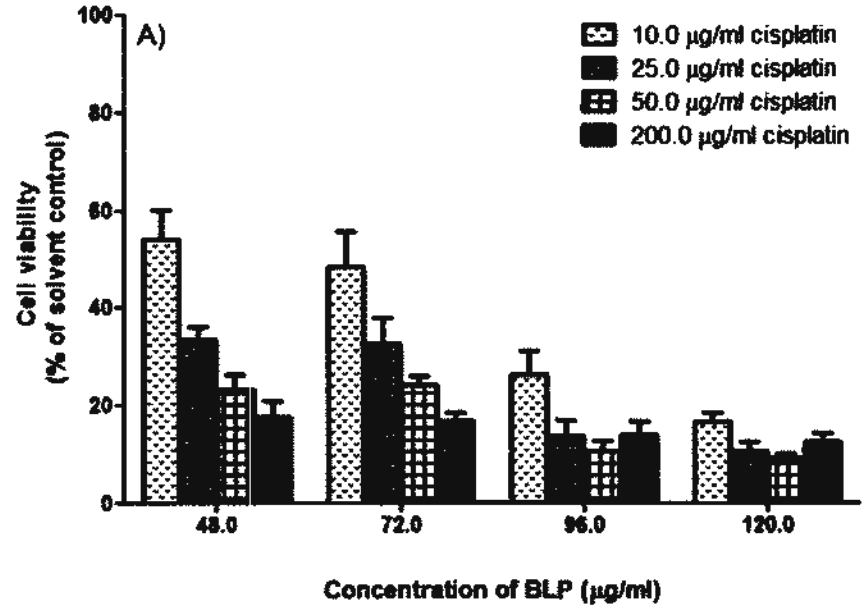

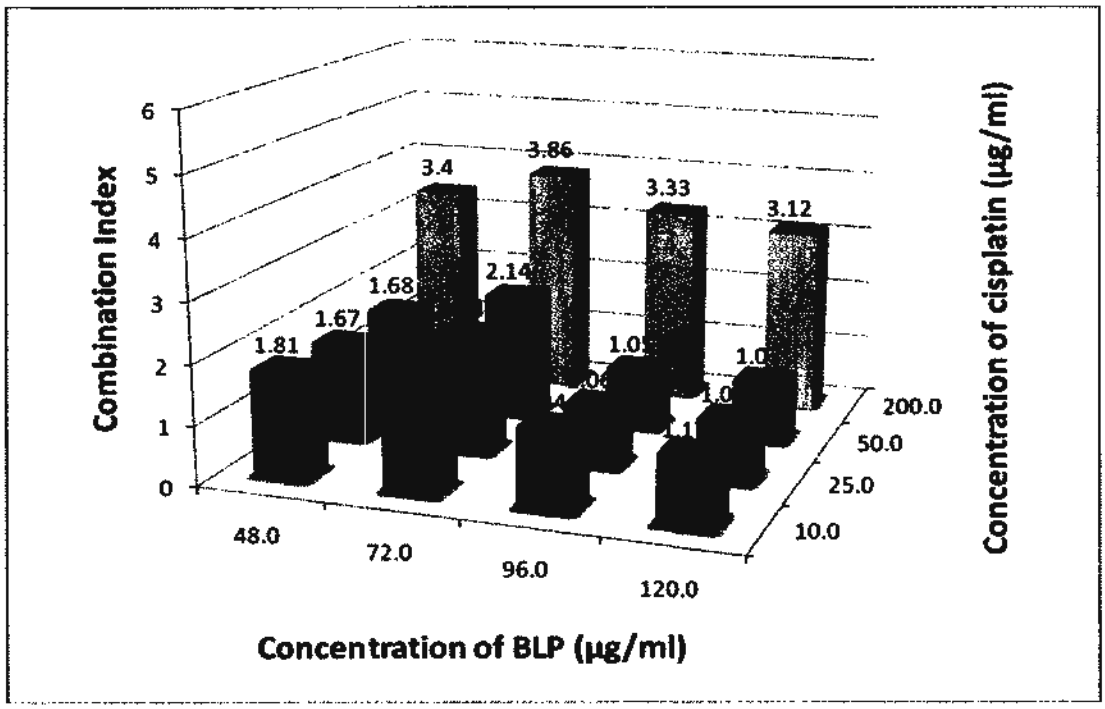

Figure 2.20 Effects of various combinations of *BLP* and cisplatin on the A) viability of HT-29 cells after 24 h treatment. Data are expressed as mean values ± S.E.M as a percentage of the solvent control. The solvent control was 0.01% DMSO mixed with saline, which had no effect on the viability of HT-29 cells. The experiment was performed in triplicate in three independent experiments. B) The combination index values were calculated from the mean of three independent experiments.

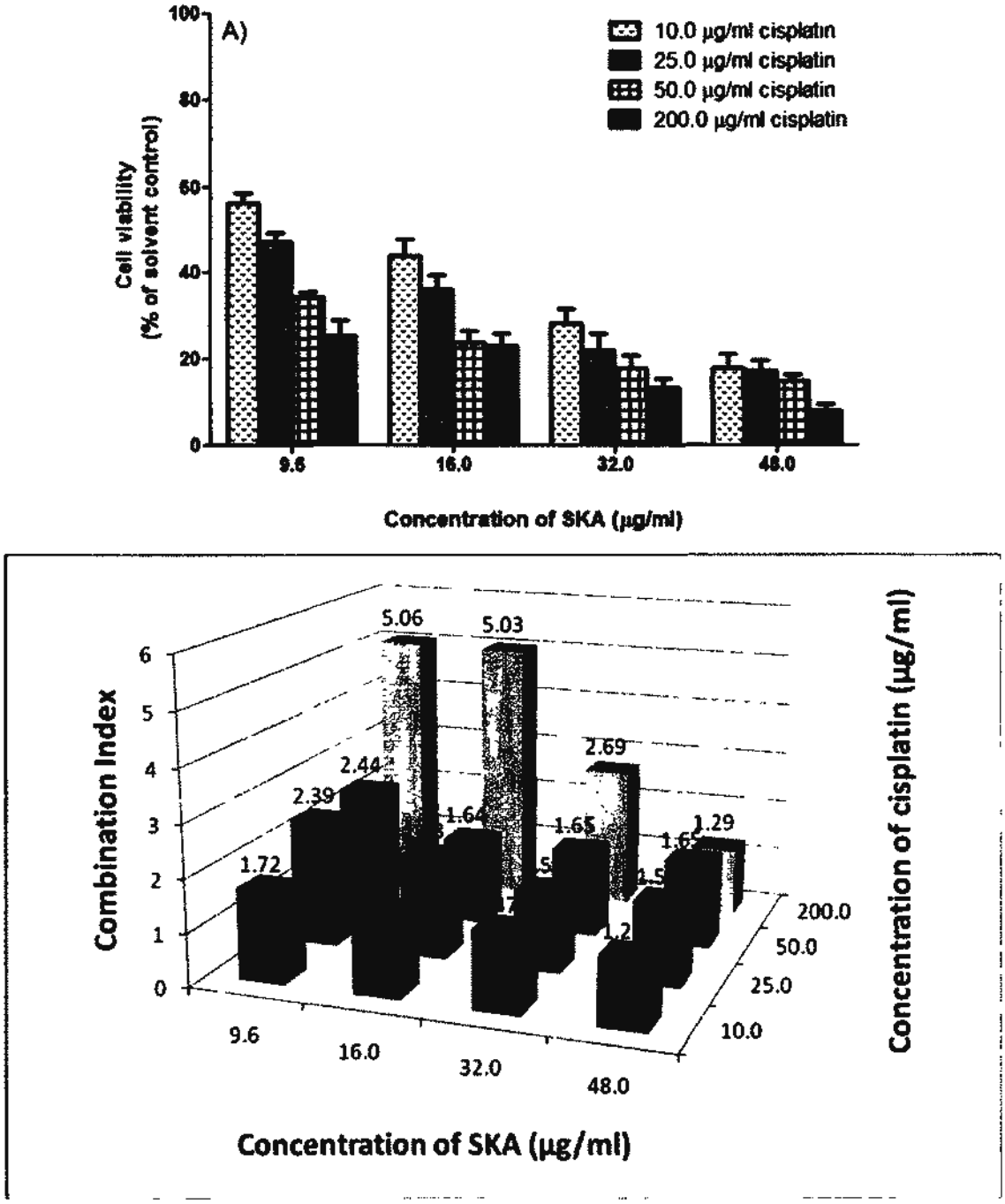

Figure 2.21 Effects of various combinations of SKA and cisplatin on the A) viability of HT-29 cells after 24 h treatment. Data are expressed as mean values ± S.E.M as a percentage of the solvent control. The solvent control was 0.01% DMSO mixed with saline, which had no effect on the viability of HT-29 cells. The experiment was performed in triplicate in three independent experiments. B) The combination index values were calculated from the mean of three independent experiments.

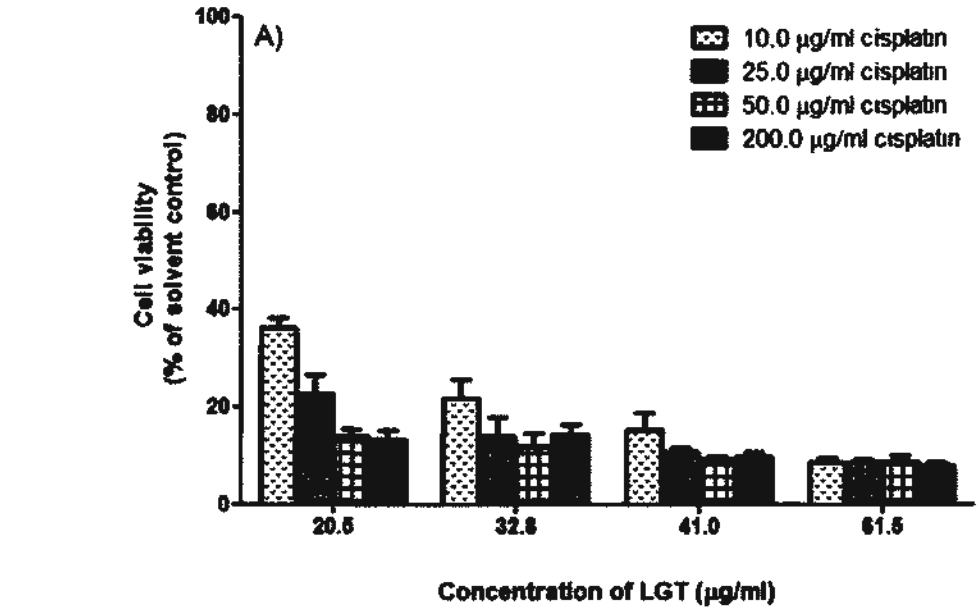

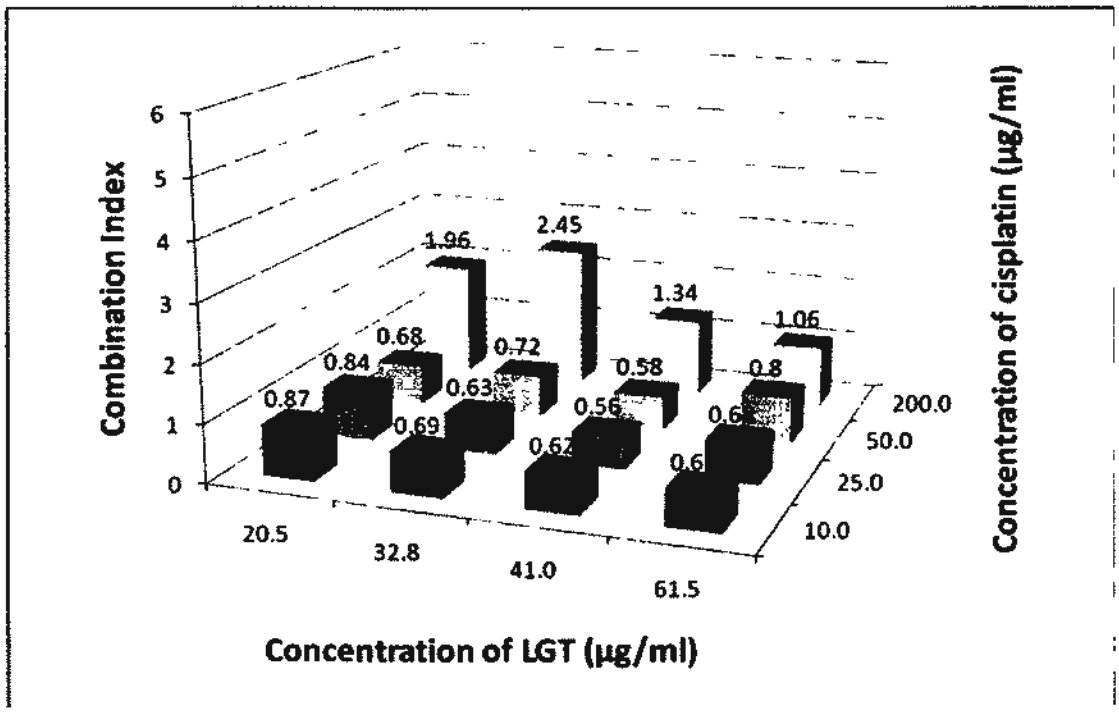

Figure 2.22 Effects of various combinations of LGT and cisplatin on the A) viability of HT-29 cells after 24 h treatment. Data are expressed as mean values ± S.E.M as a percentage of the solvent control. The solvent control was 0.01% DMSO mixed with saline, which had no effect on the viability of HT-29 cells. The experiment was performed in triplicate in three independent experiments. B) The combination index values were calculated from the mean of three independent experiments.

2.2.9 Effects of LGT on nuclear morphology of HT-29 cells

From the previous results, it showed that SKA and LGT had more potent cytotoxicity than BLP. However, SKA did not induce significant effects on sub-G_1 phase. LGT was selected for further mechanistic studies because it is the most abundant phthalide in DG extract, it showed similar activity profiles as the herbal extract and it demonstrated synergistic interactions with cisplatin. Because LGT showed an accumulation of cells in G_0/G_1 and sub-G_1 phases, DAPI staining was employed to see if any nuclear changes occurred after 12 h and 24 h LGT treatment. One of the hallmarks of apoptosis is condensed chromatin in the nucleus before the formation of and packaging of cytoplasmic contents into apoptotic bodies (Kerr *et al.*, 1972). The concentration of LGT used for this assay was 61.5 μg/ml, which is approximately 1.5-fold greater than its cytotoxicity IC_{50} value in HT-29 cells. As shown in Figure 2.23, the solvent control DMSO did not affect the nuclear morphology of HT-29 cells, which was demonstrated through the uniform, homogenous staining of the rounded cell nuclei (Figure 2.23). Treatment with 61.5 μg/ml of LGT for 12 h induced no significant changes in gross cellular morphology of adherent cells. However, LGT reduced the cell clustering and some detached cells were observed by light microscopy after 12 h (Figure 2.23). Using fluorescent microscopy, chromatin condensation on the periphery of the nucleus was observed after 61.5 μg/ml of LGT treatment, but very few cells were affected (Figure 2.23). After 24 h LGT treatment, many cells became detached and the remaining adherent cells reduced in size (Figure 2.24). Many nuclei with condensed chromatin were observed, and some cells even showed nuclear fragmentation, with loss of the rounded morphology of the nucleus (as indicated by red arrows, Figure 2.24). After 24 h, many cells adopted fragmented nuclear morphology that was characteristic of the late stages of apoptosis.

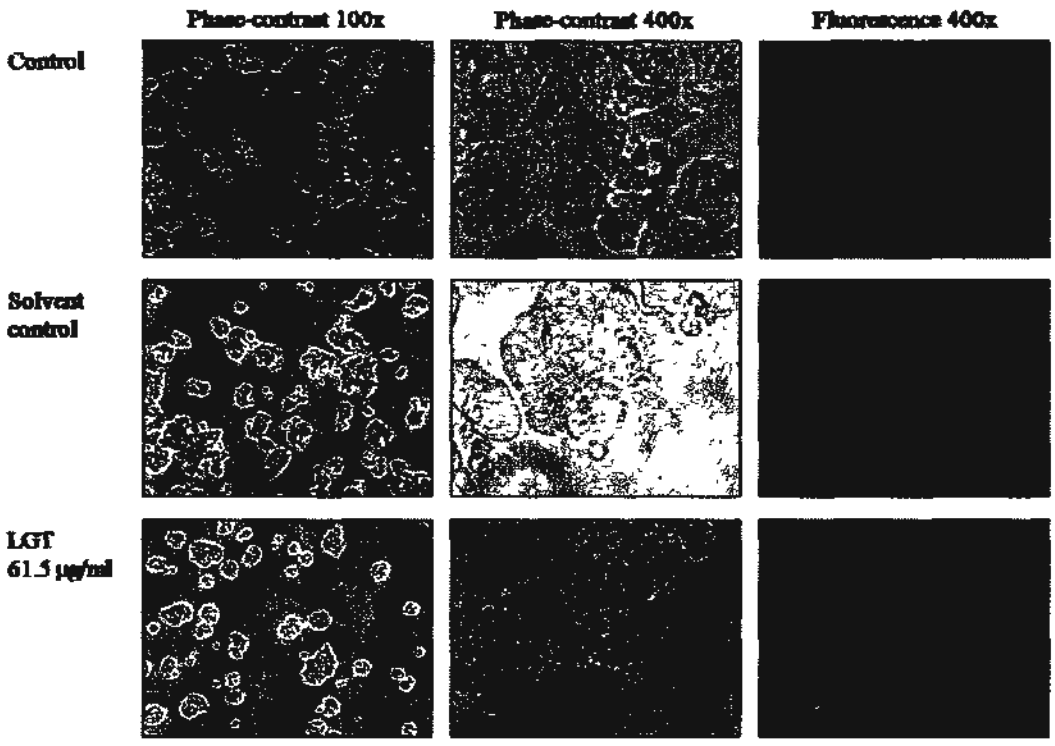

Figure 2.23 Effects of LGT on nuclear morphology of HT-29 cells after 12 h treatment. Phase-contrast microscopy at 100x and 400x magnification was used to examine the effects of LGT on general cell morphology and size and fluorescent microscopy at 400x was used to study the effects of LGT on nuclear morphology after DAPI nuclear staining. The scale bars represent 80 μM and 20 μM at 100x and 400x, respectively. The solvent control was 0.005% DMSO in culture medium. The photos are representative of results obtained from three independent experiments.

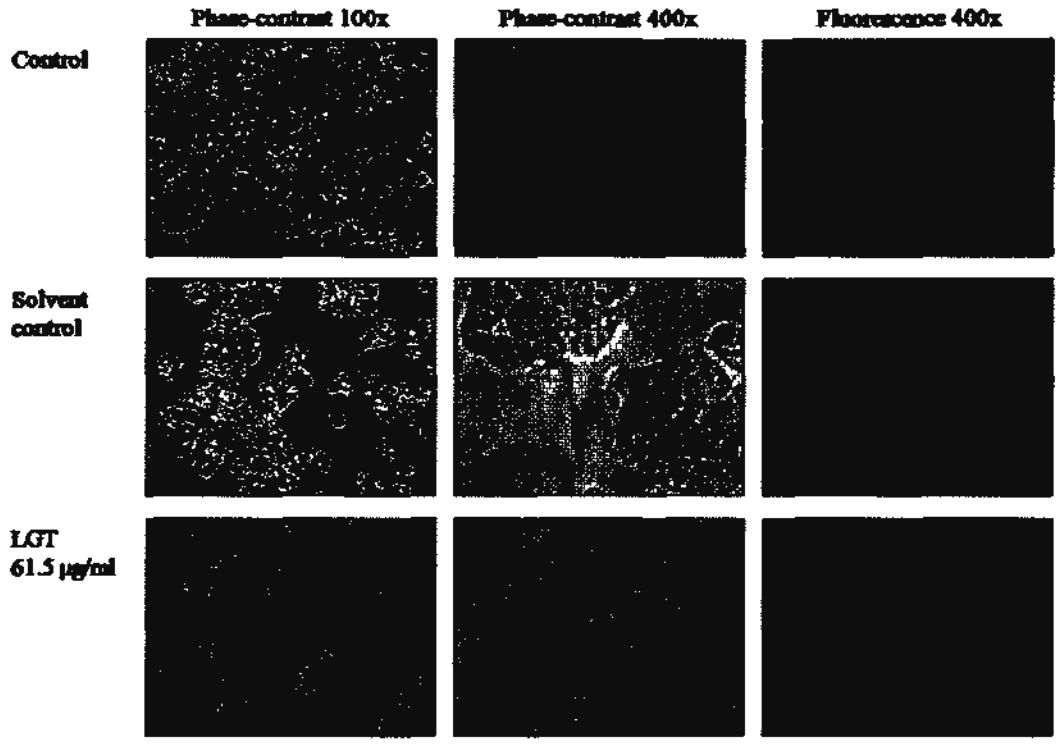

Figure 2.24 Effects of LGT on nuclear morphology of HT-29 cells after 24 h treatment. Phase-contrast microscopy at 100x and 400x magnification was used to examine the effects of LGT on general cell morphology and size and fluorescent microscopy at 400x was used to study the effects of LGT on nuclear morphology after DAPI nuclear staining. The scale bars represent 80 μM and 20 μM at 100x and 400x, respectively. The solvent control was 0.005% DMSO in culture medium. The photos are representative of results obtained from three independent experiments.

2.2.10 Effects of LGT on cleavage of PARP

One of the biochemical characteristics of apoptosis is the activation of the caspase cascade, which involves the cleavage of the zymogen executioner procaspases through activation of the extrinsic death receptor- and/or intrinsic mitochondrial-mediated pathways (Duprez *et al.,* 2009). The cleavage of pro-caspase-3 (35 kDa) into two fragments, 17 and 19 kDa, triggers activation of caspase-3, and this is an irreversible process (Huerta *et al.,* 2006). Caspase-3 cleaves various nuclear and cytosolic proteins needed for maintenance of cell structure and integrity. The effects of LGT and DG extract on the cleavage of poly(ADP-ribose)polymerase (known as PARP) were examined. PARP is a family of nuclear enzymes that recognizes and binds DNA single and double strand breaks, which allows for recruitment of base excision repair enzymes for DNA repair (Drew & Plummer, 2009; Rouleau *et al.,* 2010). PARP is a major target for activated caspase-3 and its cleavage destroys its biological function to facilitate apoptosis.

As shown in Figure 2.25A, both LGT and DG extract dose-dependently induced cleavage of PARP after 12 h treatment. The highest concentration of herbal extract tested, 75.0 μg/ml, significantly induced an 80-fold increase in the amount of cleaved caspase-3, while LGT at 82.0 μg/ml only induced an 20-fold increase ($p<0.001$, Figure 2.25B). A similar trend was demonstrated after LGT and DG treatment for 24 h in HT-29 cells. LGT and DG extract both triggered cleavage of PARP at concentrations of 61.5 and 50.0 μg/ml or higher, respectively (Figure 2.26A). Both LGT and herbal extract stimulated the cleavage of PARP in a time-dependent manner, as the cleaved PARP/intact PARP ratio was higher in the LGT and extract treatments for 24 h relative to 12 h ($p<0.05$, Figures 2.25B, 2.26B). The cleavage of PARP by LGT and DG extract is in accordance with the appearance of the apoptotic sub-G_1

peak in the flow cytometry experiments (Figures 2.16A, 2.17A) Surprisingly, after 24 h treatment, LGT at 82.0 μg/ml showed reduced amount of cleaved PARP compared to 61.5 μg/ml (Figure 2.26A). This may be due to the initiation of necrotic cell death, as almost 40% of cells showed disturbed cell membrane integrity after 82.0 μg/ml of LGT treatment for 24 h (Figure 2.8). On the other hand, SKA did not induce significant cleavage of PARP after 12 h treatment (Figure 2.27A). Only a small amount of PARP was cleaved after 24 h SKA treatment at the highest concentration tested, 64.0 μg/ml, which was around 2.5-fold higher than its IC_{50} value and consistent with the results from flow cytometry (Figures 2.15A, 2.27B). The results showed that LGT is one of the bioactive components of DG for the induction of apoptosis.

2.2.11 Effects of LGT on cleavage of pro-caspase-3

Since caspase-3 is the major executioner caspase in the apoptotic cascade, the effects of LGT on the cleavage of pro-caspase-3 were investigated. The concentration of LGT for this study was 61.5 μg/ml as this concentration induced strong cleavage of PARP after 12 h and 24 h, with minimal damage to the cell membrane integrity (Figures 2.8, 2.25, 2.26). The HT-29 cells were incubated with LGT for 3, 6, 12, 24, 36 and 48 h, followed by protein extraction for immune-blotting for intact and cleaved forms of caspase-3. As illustrated in Figure 2.28, LGT significantly provoked the cleavage of pro-caspase-3 into the active fragments as early as 12 h after treatment, which was maintained even after 48 h ($p<0.001$, Figure 2.28). This is in accordance with the results from PARP cleavage, as PARP was cleaved after 12 h and 24 h of LGT treatment (Figures 2.25, 2.26).

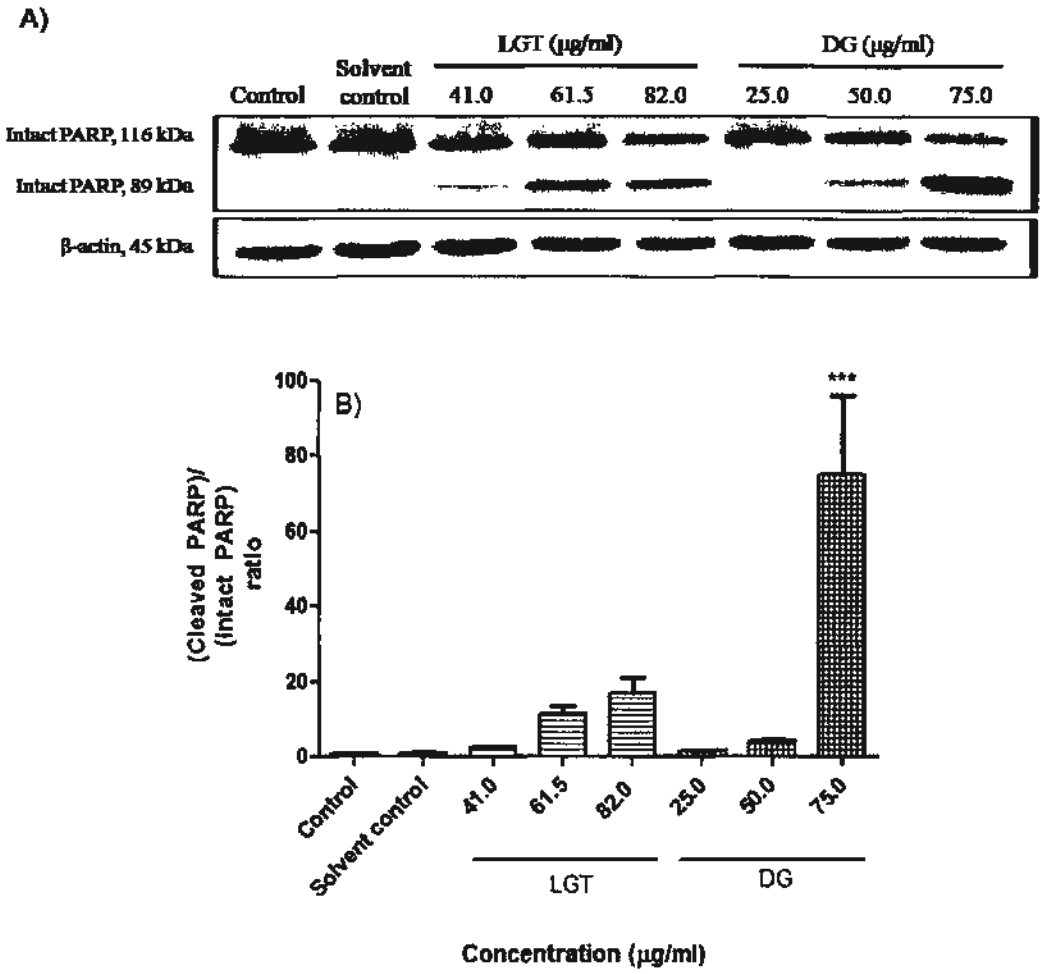

Figure 2.25 Effects of LGT and DG extract on cleavage of PARP after A) 12 h treatment. The band intensity was quantified using the Quantity One software and the B) ratio of cleaved PARP/intact PARP was calculated after intensity of each band was normalized with that of β-actin. The ratio for untreated control was considered to be one. Data are presented as mean values ± S.E.M. from three independent experiments. ***$p<0.001$ compared with solvent control (0.005% DMSO in culture medium).

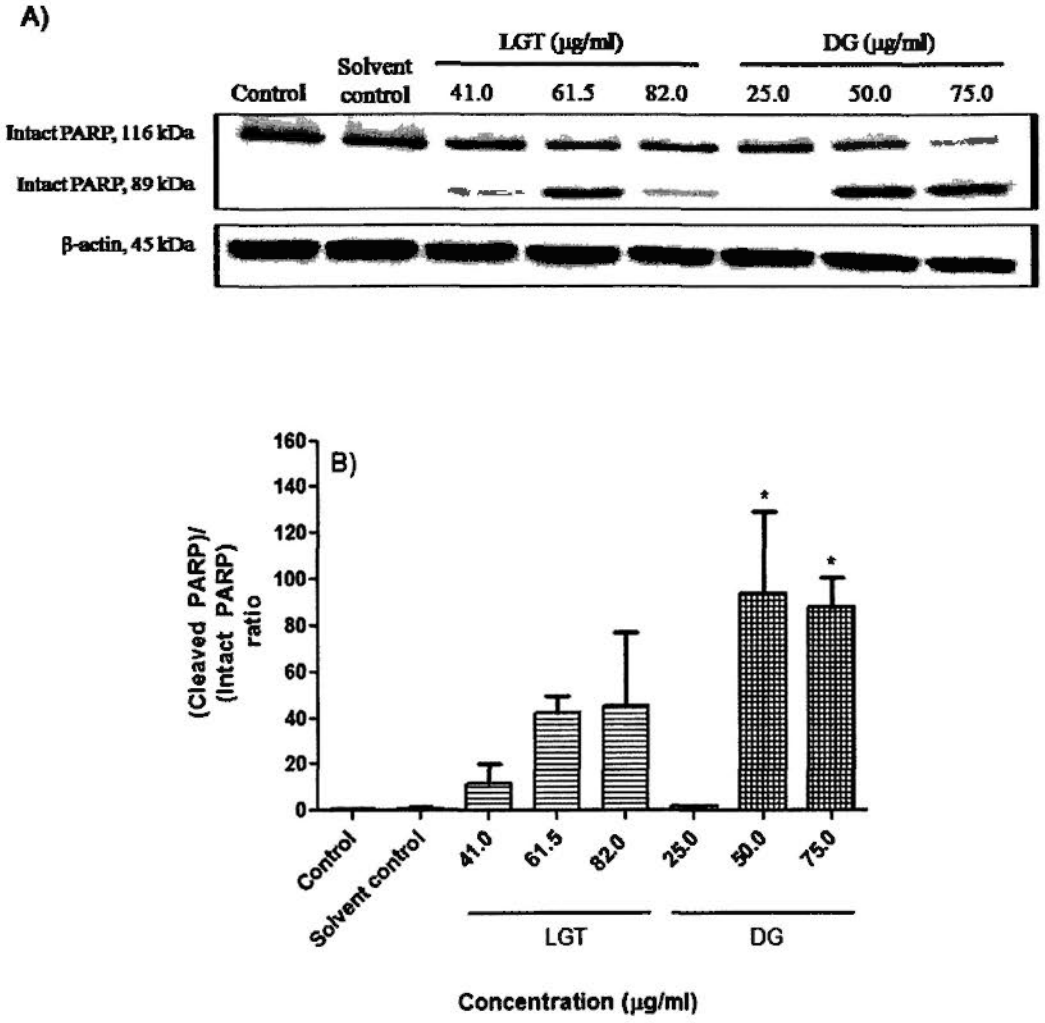

Figure 2.26 Effects of LGT and DG extract on cleavage of PARP after A) 24 h treatment. The band intensity was quantified using the Quantity One software and the B) ratio of cleaved PARP/intact PARP was calculated after intensity of each band was normalized with that of β-actin. The ratio for untreated control was considered to be one. Data are presented as mean values ± S.E.M. from three independent experiments. *$p<0.05$ compared with solvent control (0.005% DMSO in culture medium).

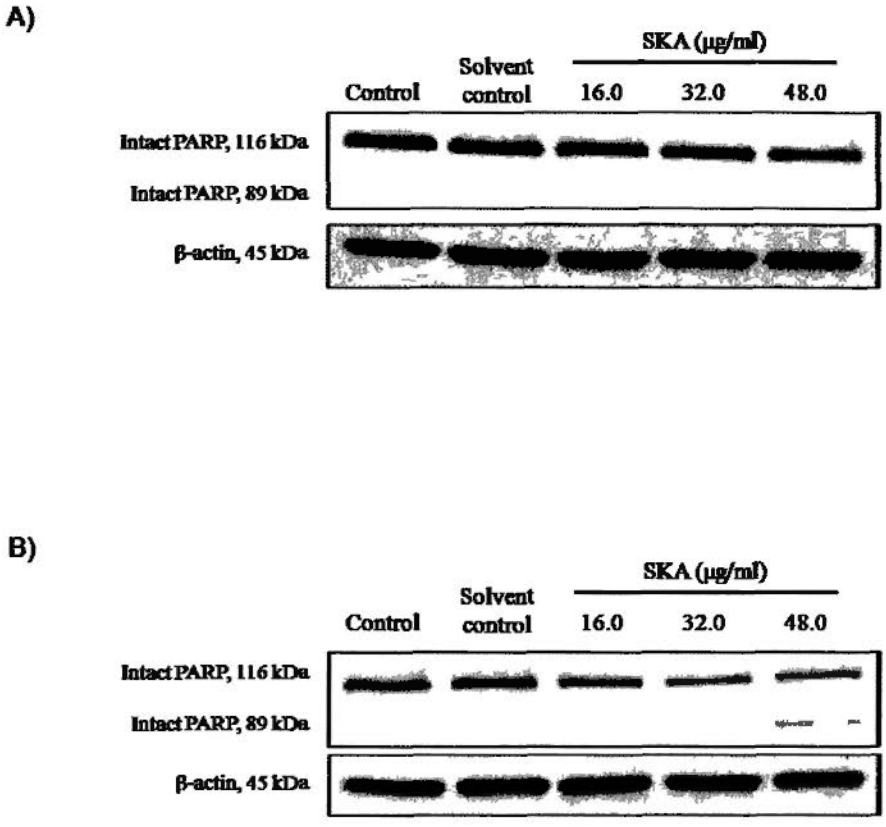

Figure 2.27 Effects of SKA on cleavage of PARP after A) 12 h and B) 24 h treatment. Data are representative of results from three independent experiments.

2.2.12 Effects of LGT on cleavage of pro-caspase-8 and -9

To determine the involvement of death receptor and mitochondrial pathways in LGT-induced apoptosis, the cleavage of pro-caspases-8 and-9 were examined, respectively. The cleaved fragment of caspase-8 (18 kDa) appeared after 24 h of LGT treatment, although the disappearance of the zymogen form (57 kDa) occurred as early as 12 h (Figure 2.29A). After 48 h, almost all of the pro-caspase-8 was absent. The ratio of cleaved caspase-8/intact caspase-8 significantly increased in a time-dependent manner, especially after 24 h ($p<0.05$, Figure 2.29B). The decrease of pro-caspase-9 (47 kDa) occurred as early as 12 h after LGT treatment and the appearance of cleaved caspase-9 (37 kDa) also occurred after 12 h (Figure 2.30A). The ratio of cleaved caspase-9/intact caspase-9 also increased in a time-dependent fashion starting after 12 h, and was significantly increased from 24-48 h ($p<0.05$, Figure 2.30B). Therefore, both pro-caspases-8 and -9 were cleaved and activated, but it appears that the appearance of the cleaved form of caspase-9 took place earlier (at 12 h) than the cleaved form of caspase-8. The cleaved form of caspase-3 also emerged after 12 h (Figure 2.28A), which suggests that caspase-9 may contribute to early apoptosis induced by LGT, and caspase-8 may contribute at a slightly later time. Ultimately, both pathways converge to activate caspase-3 to cleave cellular substrates for apoptosis.

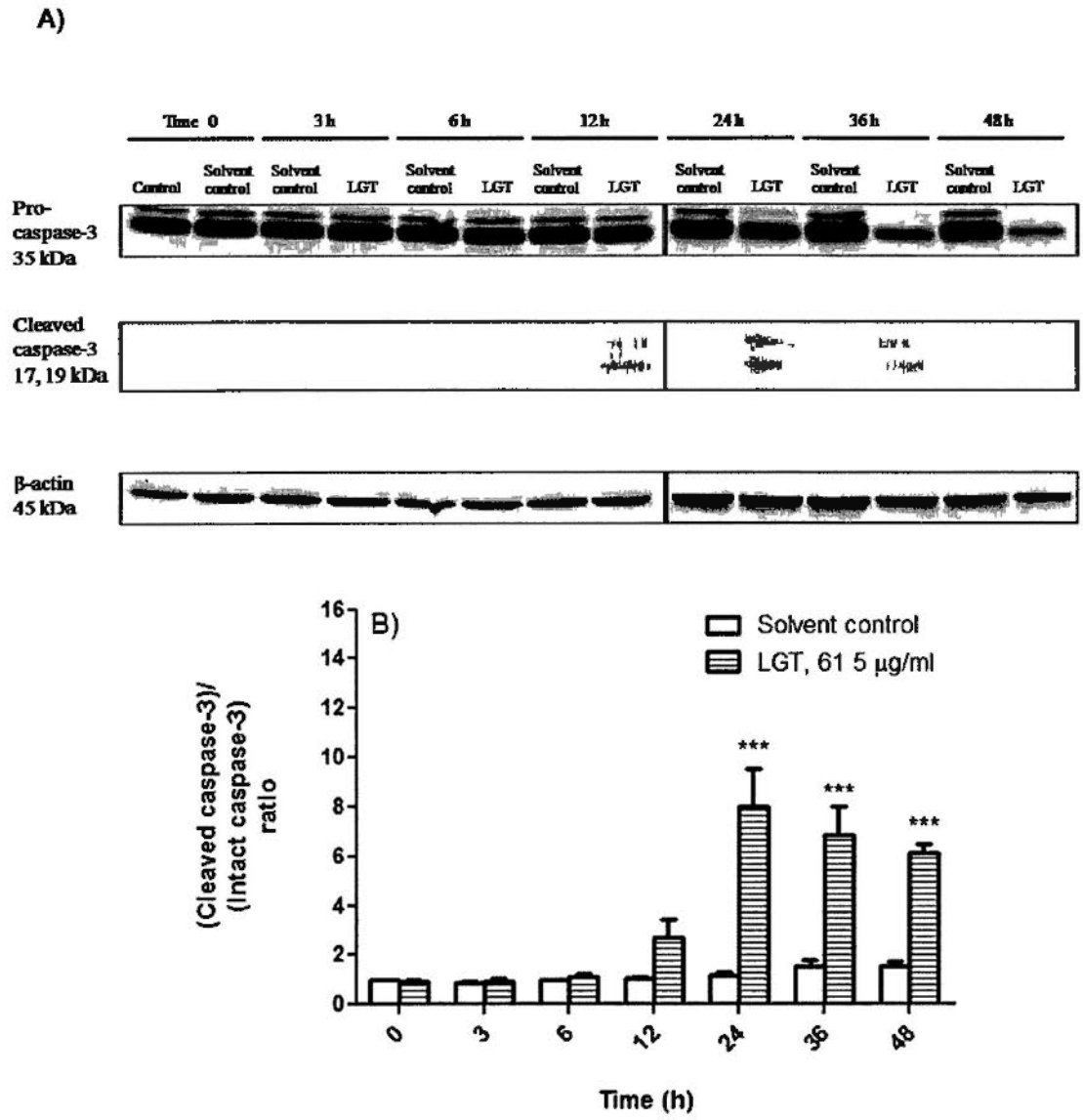

Figure 2.28 Effects of LGT on cleavage of pro-caspase-3 after A) 3, 6, 12, 24, 36 and 48 h treatment. The band intensity was quantified using the Quantity One software and the B) ratio of cleaved caspase-3/intact caspase-3 was calculated after intensity of each band was normalized with that of β-actin. The LGT treatment at time 0 corresponds to the control at time 0 in part A) and the solvent control at time 0 was considered as one. Data are presented as mean values ± S.E.M. from four independent experiments. ***$p<0.001$ compared with solvent control (0.005% DMSO in culture medium) of the respective time point.

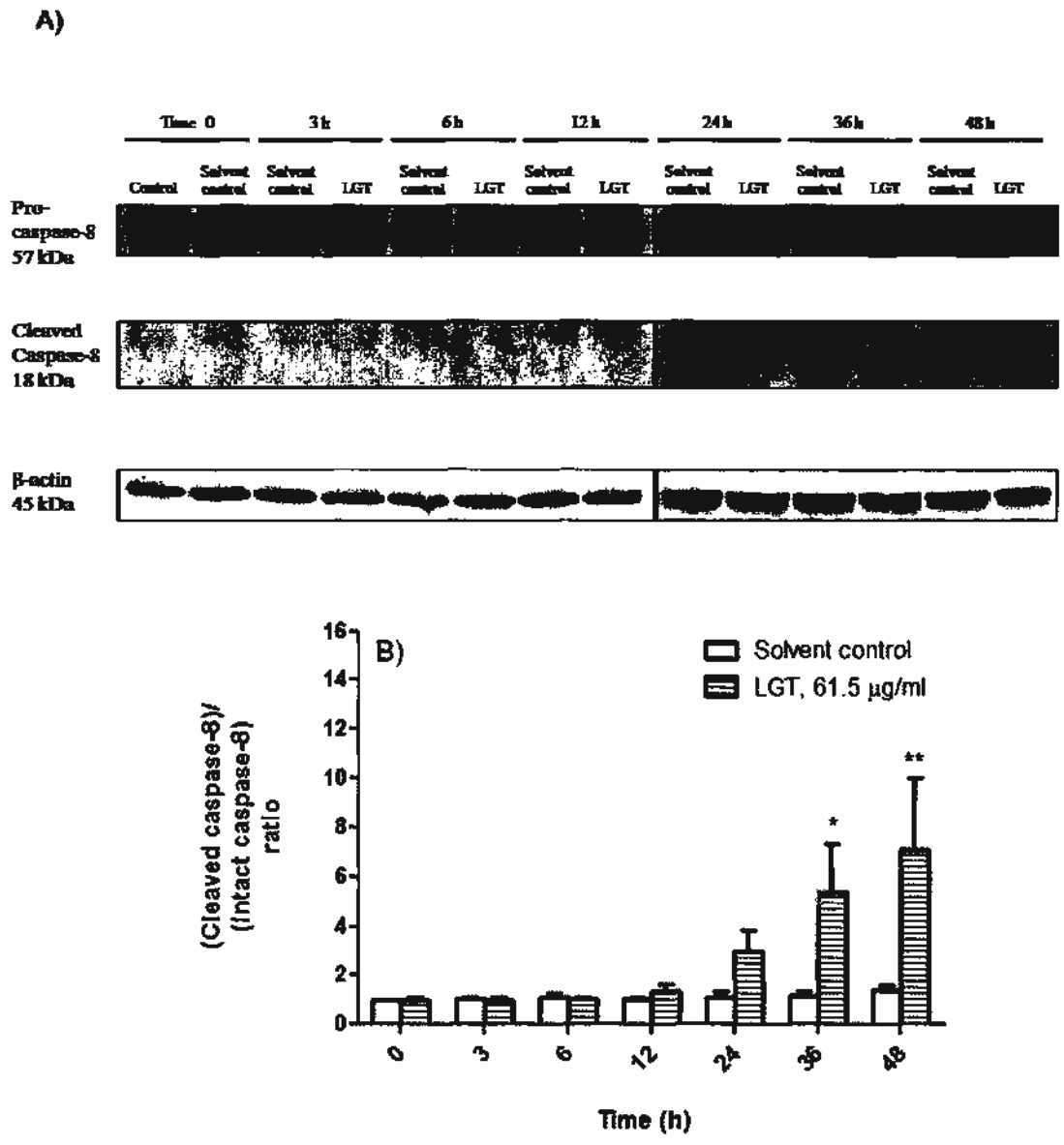

Figure 2.29 Effects of LGT on cleavage of pro-caspase-8 after A) 3, 6, 12, 24, 36 and 48 h treatment. The band intensity was quantified using the Quantity One software and the B) ratio of cleaved caspase-8/intact caspase-8 was calculated after intensity of each band was normalized with that of β-actin. The LGT treatment at time 0 corresponds to the control at time 0 in part A) and the solvent control at time 0 was considered as one. Data are presented as mean values ± S.E.M. from three independent experiments. *$p<0.05$, **$p<0.01$ compared with solvent control (0.005% DMSO in culture medium) of the respective time point.

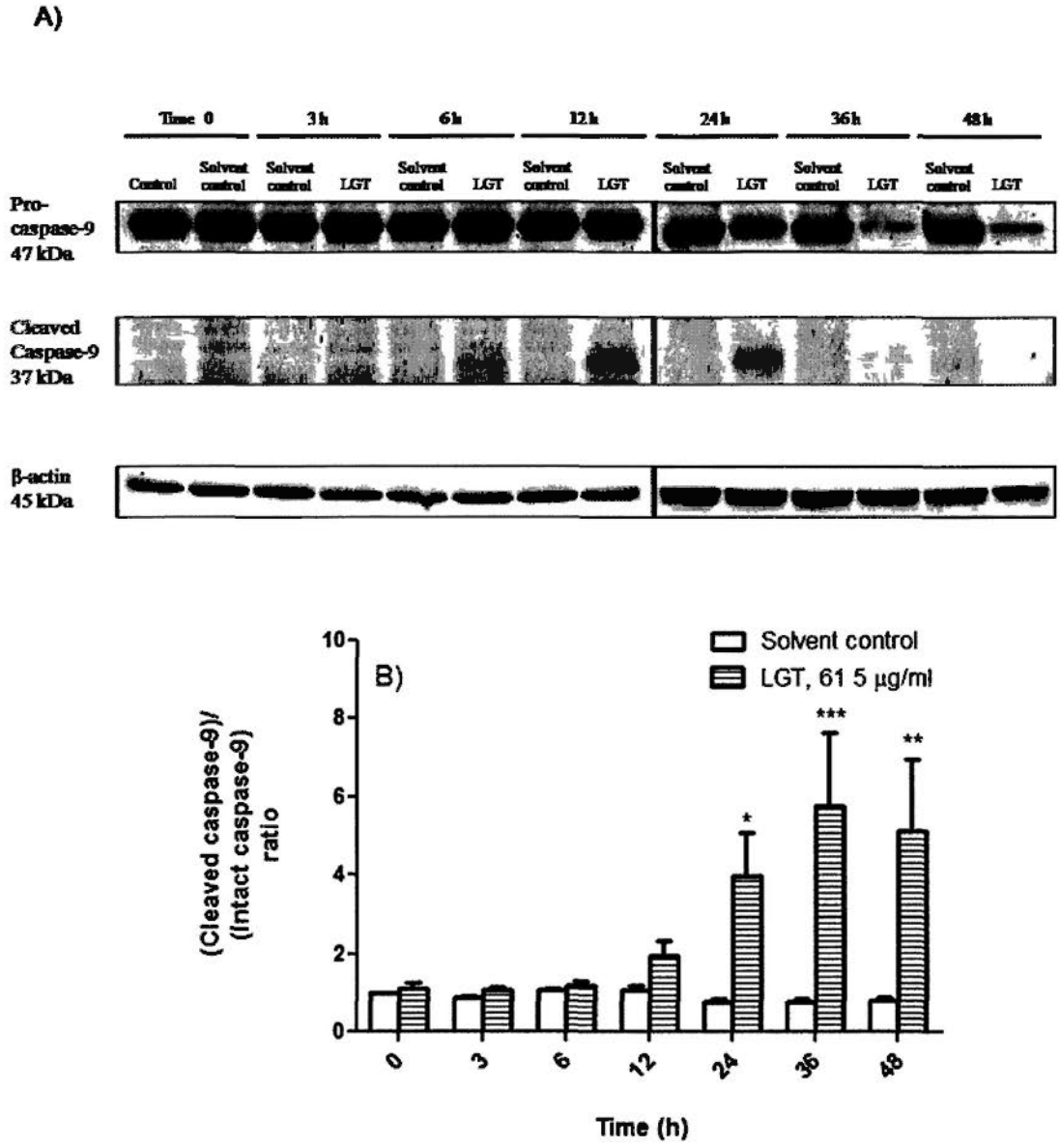

Figure 2.30 Effects of LGT on cleavage of pro-caspase-9 after A) 3, 6, 12, 24, 36 and 48 h treatment. The band intensity was quantified using the Quantity One software and the B) ratio of cleaved caspase-9/intact caspase-9 was calculated after intensity of each band was normalized with that of β-actin. The LGT treatment at time 0 corresponds to the control at time 0 in part A) and the solvent control at time 0 was considered as one. Data are presented as mean values ± S.E.M. from three independent experiments. *$p<0.05$, **$p<0.01$, ***$p<0.001$ compared with solvent control (0.005% DMSO in culture medium) of the respective time point.

2.2.13 Effects of LGT and DG extract on caspase-3 activity

A dose-dependent increase in caspase-3 activity was observed after LGT treatment, up to 82.0 μg/ml, which is in agreement with the Western blot results (Figures 2.26A, 2.28A, 2.31A). The significant rise in caspase-3 activity after treatment with 61.5 μg/ml of LGT was almost completely suppressed by a caspase-3 inhibitor, Ac-DEVD-CHO (Figure 2.31B), which implied that the LGT-induced cell death is through caspase activation and apoptosis. Likewise, the DG extract significantly increased caspase-3 activity in a dose-dependent manner ($p<0.05$, Figure 2.32A). The formation of p-nitroaniline triggered by the DG extract was significantly inhibited with Ac-DEVD-CHO ($p<0.01$, Figure 2.32B). The DG extract at 50.0 μg/ml increased caspase-3 activity to 129.9 pmol protein/min · mg protein, while 61.5 μg/ml of LGT increased caspase-3 activity to 108.1 pmol protein/min·mg protein (Figure 2.31A, 2.32A). A high concentration of BLP (120.0 μg/ml) was required to significantly increase caspase-3 activity to 115.0 pmol protein/min·mg protein ($p<0.01$, Figure 2.33). Although both LGT and DG extract activated caspase-3, a lower concentration of the extract was needed to achieve the same effect, which indicated that the three phthalides in DG may be acting together or with other bioactive components to induce apoptosis.

2.2.14 Effects of LGT on the activation of MAPK pathways

Since the MAPK pathways play a major role in cell proliferation and differentiation and cellular response to stress and apoptosis (Kim & Choi, 2010), the effects of 61.5 μg/ml of LGT on the phosphorylation and activation of ERK, JNK and p38 were studied in HT-29 cells after 3, 6 and 12 h drug treatment. At time 0, all of the MAPK showed little or no activation of MAPKs (Figures 2.34-2.36). LGT increased levels of phosphorylated ERK and p38 after 12 h (Figures 2.34, 2.36). However, as early as

3 h after LGT treatment, there was an increase in phosphorylated JNK, which continued to rise in a time-dependent manner until 12 h ($p<0.001$, Figure 2.35). Hence, the activation of JNK may be crucial to the response of HT-29 cells to LGT treatment and the subsequent signaling pathways that lead to cell death and inhibition of cell proliferation.

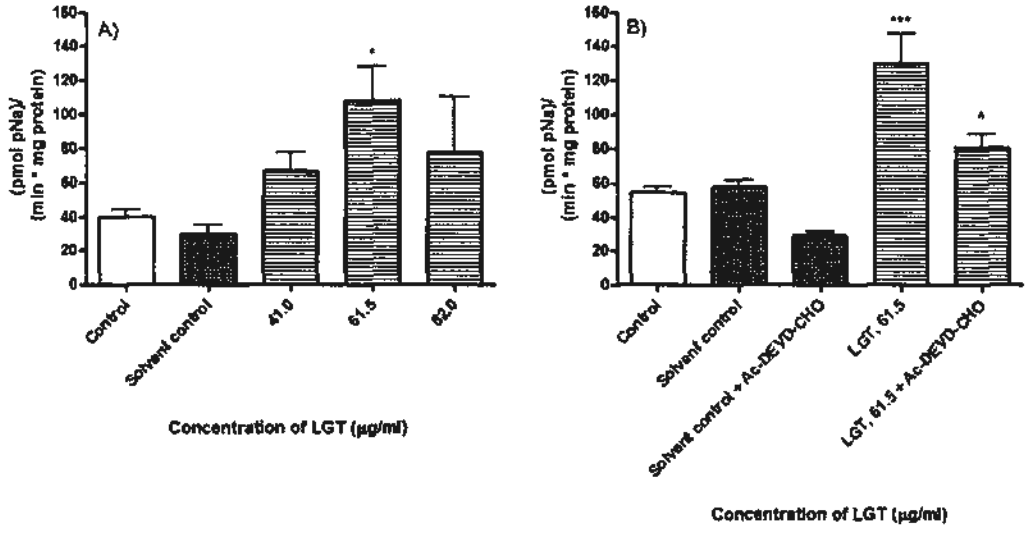

Figure 2.31 Effects of LGT on caspase-3 activity in HT-29 cells after A) 24 h incubation as determined by the rate of pNa formation. B) Caspase-3 inhibitor, Ac-DEVD-CHO, was added to cell lysates prior to LGT to determine the reversibility of LGT-induced caspase-3 activity. The experiment was conducted in duplicate and data are presented as mean values ± S.E.M. from A) three and B) four independent experiments. *$p<0.05$, ***$p<0.001$ compared with solvent control (0.002% DMSO in culture medium) and ^$p<0.05$ compared with LGT, 61.5 µg/ml.

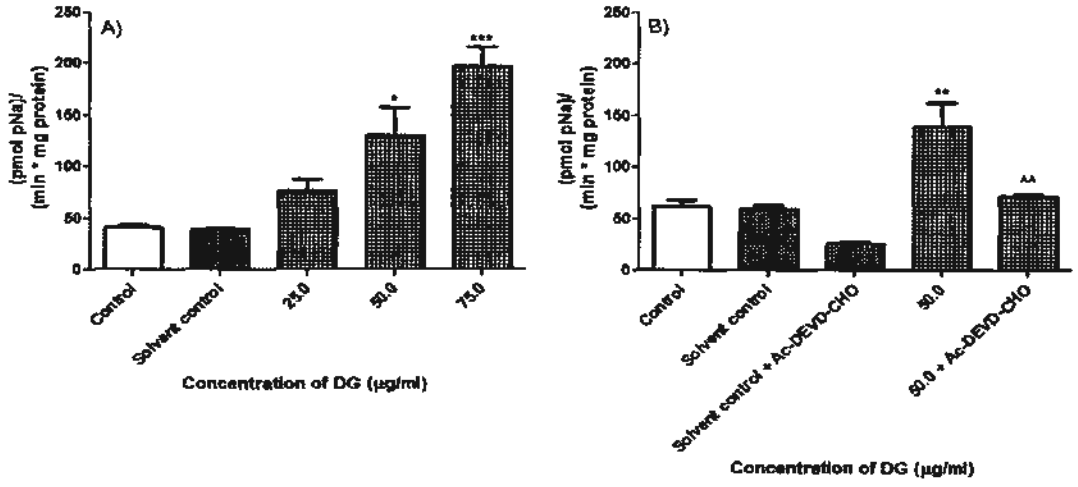

Figure 2.32 Effects of DG extract on caspase-3 activity in HT-29 cells after A) 24 h incubation as determined by the rate of pNa formation. B) Caspase-3 inhibitor, Ac-DEVD-CHO, was added to cell lysates prior to extract to determine the reversibility of LGT-induced caspase-3 activity. The experiment was conducted in duplicate and data are presented as mean values ± S.E.M. from three independent experiments. *p<0.05, **p<0.01, ***p<0.001 compared with solvent control (0.002% DMSO in culture medium), ^^p<0.01 compared with extract, 50.0 µg/ml.

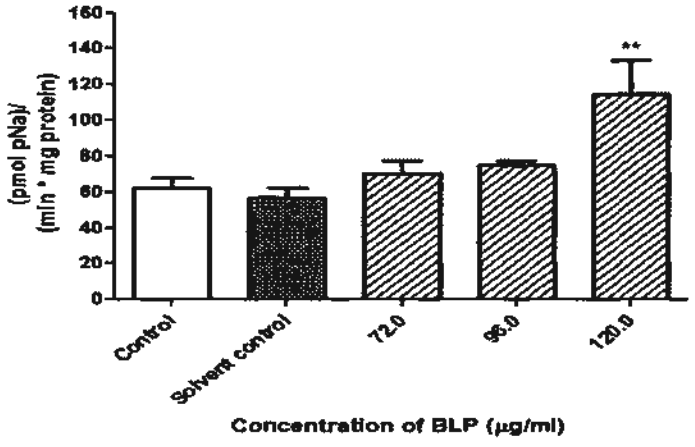

Figure 2.33 Effects of BLP on caspase-3 activity in HT-29 cells after 24 h incubation as determined by the rate of pNa formation. The experiment was conducted in duplicate and data are presented as mean values ± S.E.M. from three independent experiments. **p<0.01 compared with solvent control (0.002% DMSO in culture medium).

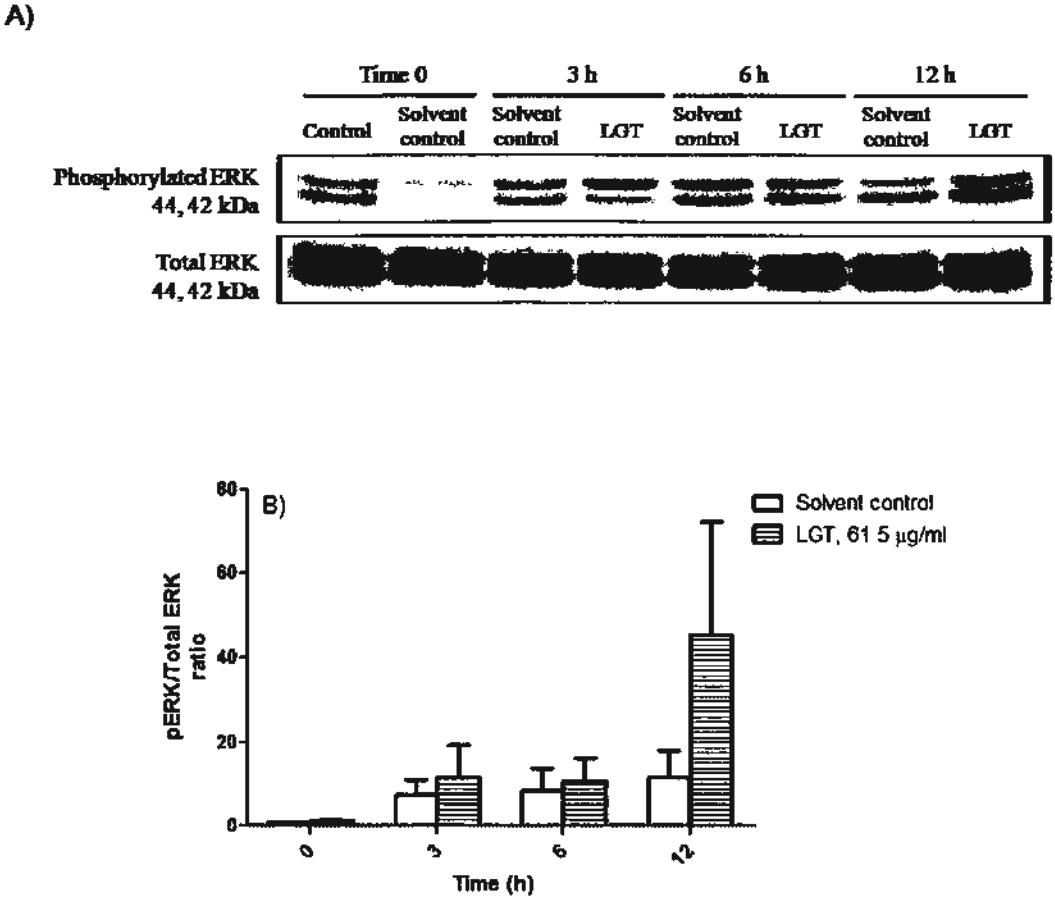

Figure 2.34 Effects of LGT (61.5 µg/ml) on phosphorylation of extracellular signal-regulated kinase-1 and -2 (ERK1/2) after A) 3, 6, and 12 h treatment in HT-29 cells. The band intensity was quantified using the Quantity One software and the B) ratio of phosphorylated ERK/total ERK was calculated using the respective band intensities. The LGT treatment at time 0 corresponds to the control at time 0 in part A) and the solvent control at time 0 was considered as one. Data are presented as mean values ± S.E.M. from four independent experiments.

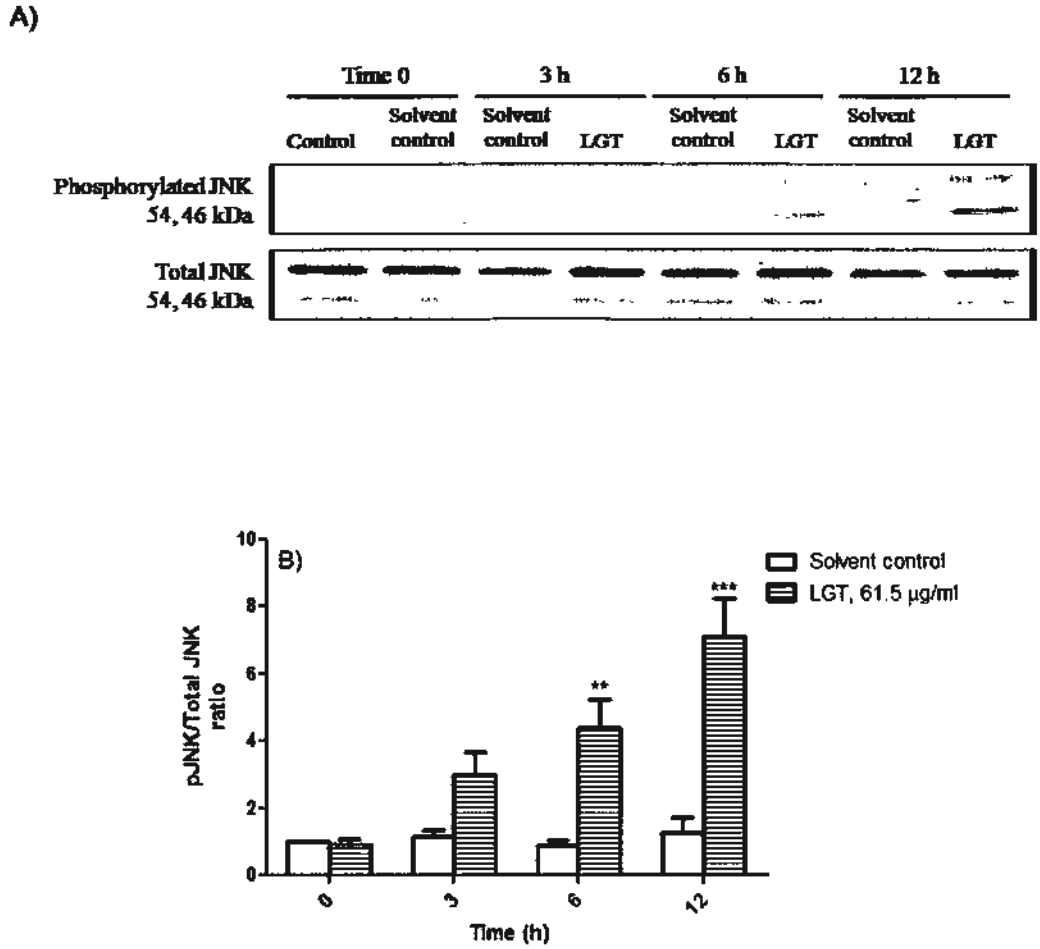

Figure 2.35 Effects of LGT (61.5 µg/ml) on phosphorylation of c-jun N-terminal kinases-1 and -2 (JNK1/2) after A) 3, 6, and 12 h treatment in HT-29 cells. The band intensity was quantified using the Quantity One software and the B) ratio of phosphorylated JNK/total JNK was calculated using the respective band intensities. The LGT treatment at time 0 in part B) corresponds to the control at time 0 in part A) and the solvent control at time 0 was considered as one. Data are presented as mean values ± S.E.M. from three independent experiments.

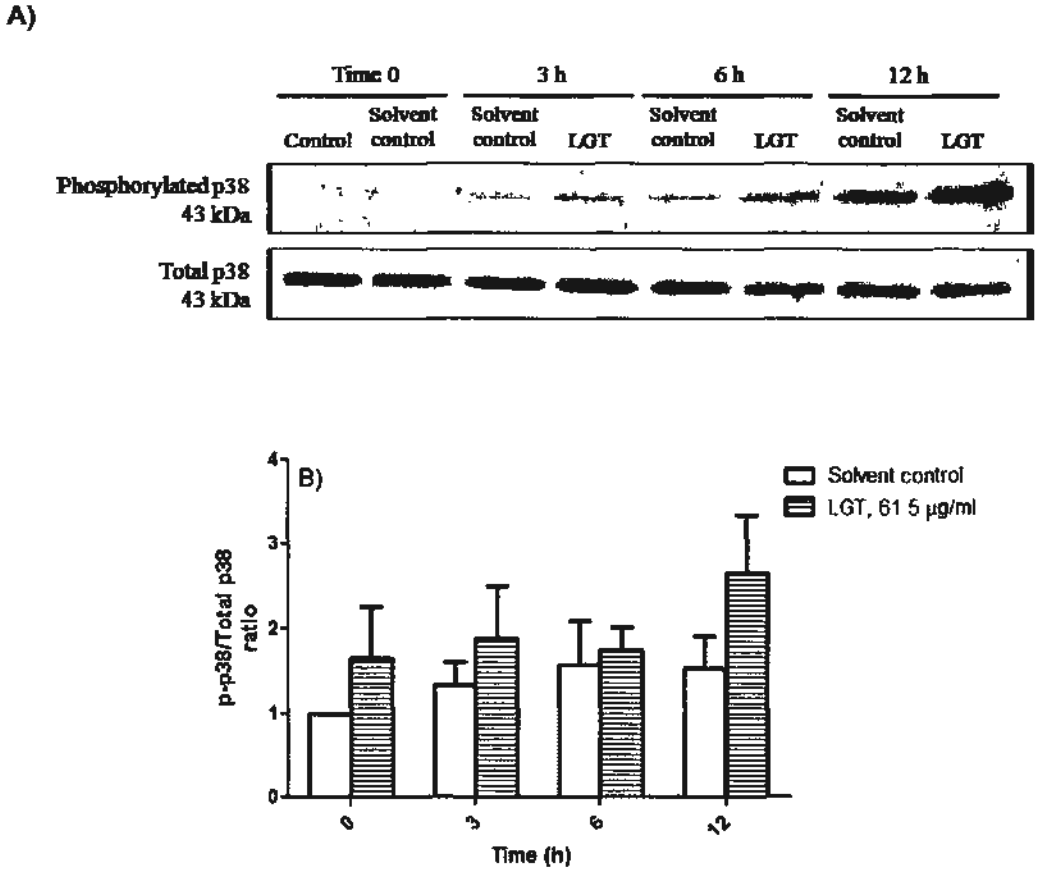

Figure 2.36 Effects of LGT (61.5 µg/ml) on phosphorylation of p38 MAPK after A) 3, 6, and 12 h treatment in HT-29 cells. The band intensity was quantified using the Quantity One software and the B) ratio of phosphorylated p38/total p38 was calculated using the respective band intensities. The LGT treatment at time 0 in part B) corresponds to the control at time 0 in part A) and the solvent control at time 0 was considered as one. Data are presented as mean values ± S.E.M. from four independent experiments.

2.2.15 Interactions between various components in DG extract and their contributions to anti-proliferative effects in HT-29 cells

From the results, the cytotoxic and anti-proliferative effects of the DG extract were more potent than the effects of the individual phthalides, BLP, SKA and LGT. In addition, the concentrations of the extract (after accounting for 41.06% of phthalides present in the extract) that induced G_0/G_1 cell cycle arrest and apoptosis were much lower than the concentrations of individual BLP, SKA and LGT that produced the same effects. Thus, this strongly suggests that there are other bioactive components in the herbal extract or there may be synergistic interactions between various compounds that lead to the higher potency of DG extract. Therefore, in the following sections, the aim of the study is to explore whether BLP, SKA and LGT act in a synergistic manner in the herbal extract to inhibit proliferation of human colon cancer cells. The sigmoidal dose-response curves for inhibition of proliferation were plotted for each of the three phthalides and the DG extract. The anti-proliferative effects of CX extract were also studied for comparison. Similar to DG, CX also contains BLP, SKA and LGT as the major active ingredients. However, the three phthalides exist in a different ratio and the total content of the three phthalides in CX is lower than that in DG (Table 2.1). Moreover, two mixtures of the three phthalides were created in the ratios as they exist in DG and CX extracts, respectively, and their anti-proliferation effects were also assessed. Analysis of multiple-drug effects were completed using the mathematical formula to calculate combination indices as indicated in section 2.1.2.11.

2.2.15.1 Effects of BLP, SKA and LGT on cell proliferation in HT-29 and CCD-18Co cells

BLP, SKA and LGT dose-dependently reduced proliferation of HT-29 cells after 24 h treatment, with anti-proliferation IC_{50} values of 44.59 ± 3.43, 10.40 ± 0.98 and 11.52 ± 1.29 μg/ml, respectively (Figure 2.37, Table 2.6). The potencies of SKA and LGT were similar, and both were approximately four times more potent than BLP, which is in accordance with the potency order of the phthalides for reduction of viability of HT-29 cells (Tables 2.5, 2.6). The same experiment was carried out in parallel in normal human colon fibroblast CCD-18Co cells to determine the selectivity of anti-proliferative effects by the three phthalides. BLP, SKA and LGT reduced [^{3}H] thymidine incorporation of CCD-18Co cells dose-dependently after 24 h incubation, with IC_{50} values of 51.22 ± 10.99, 20.95 ± 4.22 and 8.60 ± 2.19 μg/ml, respectively (Figure 2.38, Table 2.6). Both BLP and SKA showed some selectivity for decreasing the [^{3}H] thymidine incorporation of colon cancer cells, as demonstrated by their lower IC_{50} values in HT-29 cells (Table 2.6). The two IC_{50} values for LGT in both cell lines were not significantly different from each other (Table 2.6). This suggests that LGT may selectively target cell death mechanisms in colon cancer cells, as opposed to cell proliferation mechanisms.

2.2.15.2 Effects of DG extract and the mixture of phthalides on cell proliferation in HT-29 cells

To study the interactions among the three phthalides and other components in DG extract, the anti-proliferation effects of the DG and CX extracts and two mixtures of the phthalides with the same composition ratios as the two corresponding herbal extracts were analyzed in HT-29 and CCD-18Co cells.

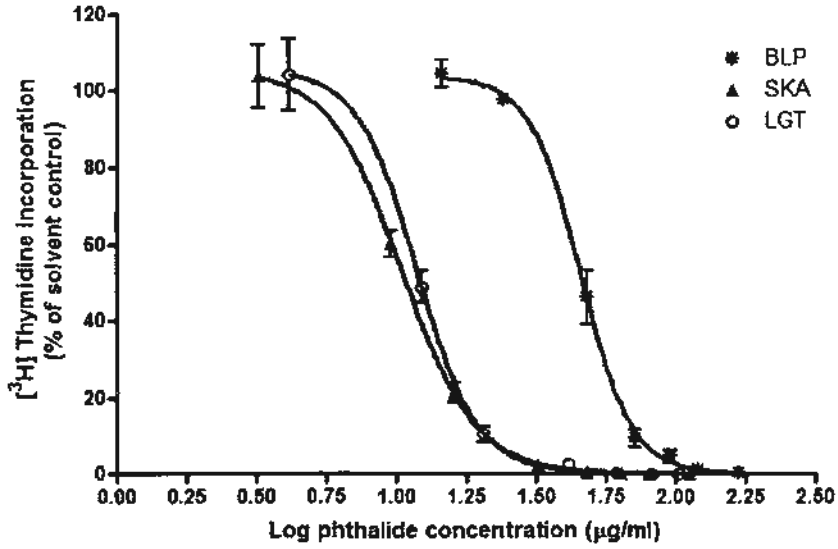

Figure 2.37 Effects of BLP, SKA and LGT on proliferation of HT-29 cells after 24 h treatment, as examined by [^{3}H] thymidine incorporation assay. Data are presented as mean values ± S.E.M. as a percentage of the solvent control from three independent experiments.

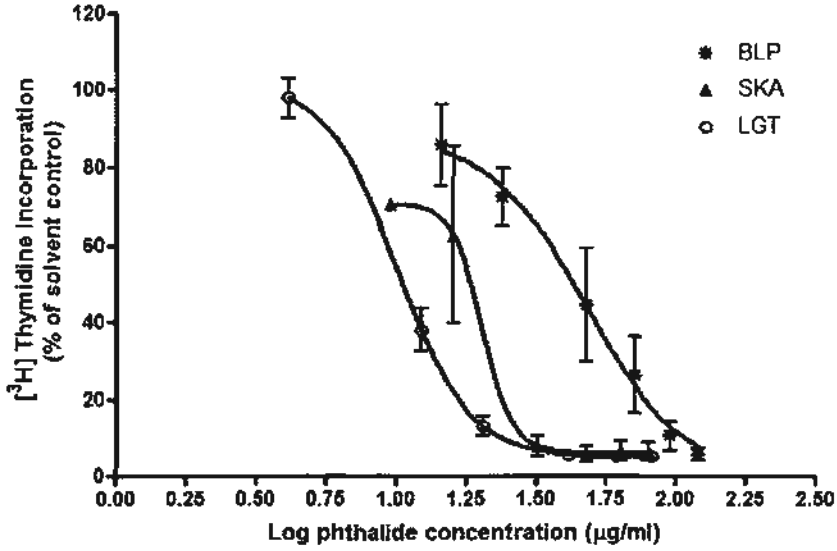

Figure 2.38 Effects of BLP, SKA and LGT on proliferation of CCD-18Co cells after 24 h treatment, as examined by [^{3}H] thymidine incorporation assay. Data are presented as mean values ± S.E.M. as a percentage of the solvent control from three independent experiments.

Table 2.6 Potency of anti-proliferative effects of BLP, SKA and LGT against HT-29 and CCD-18Co cells after 24 h treatment

Phthalide	IC_{50} in μg/ml (μM)	
	HT-29	CCD-18Co
BLP	44.59 ± 3.43	51.22 ± 10.99
	(236.90 ± 18.22)	(272.13 ± 58.39)
SKA	10.40 ± 0.98	20.95 ± 4.22
	(54.17 ± 5.10)	(109.11 ± 21.98)
LGT	11.52 ± 1.29	8.60 ± 2.19
	(60.63 ± 6.79)	(45.26 ± 11.53)

Since the percentage of total phthalides in DG and CX extracts are 41.06% and 23.99%, respectively, the concentration-response curves of the two herbal extracts were reconstructed based on this percentage (wide dash line with circles) and shifted to the left of the curves for the two herbal extracts (solid line with triangles) (Figures 2.39, 2.40). The concentration-response curves of the mixtures of the three phthalides in the same ratios as the two herbal extracts are indicated in narrow dash lines with squares (Figures 2.39, 2.40).

The DG mixture of phthalides was slightly more potent than the CX mixture of phthalides ($p<0.05$) (Table 2.7), yet the whole DG extract was approximately five-times more potent than the whole CX extract (Figures 2.39A 2.39B). The DG extract had an IC_{50} value of 14.99 ± 2.34 μg/ml, and after accounting for the fact that the phthalide content is 41.06% of the extract, the IC_{50} value was 6.14 ± 0.94 μg/ml

in HT-29 cells (Table 2.7). Likewise, the CX extract had an IC_{50} value of 78.91 ± 3.38 μg/ml, and after accounting for the fact that the phthalide content is 23.99% of the extract, the IC_{50} value was 18.93 ± 0.81 μg/ml in HT-29 cells (Table 2.7). The DG extract (calculated based on total phthalides) had a three-fold lower IC_{50} value than the CX extract (calculated based on total phthalides) ($p<0.01$). The mixture of phthalides in the ratio as they naturally exist in DG extract was less potent (IC_{50} = 16.16 ± 0.62 μg/ml) than the DG extract (IC_{50} = 6.14 ± 0.94 μg/ml) at inhibiting the proliferation of HT-29 cells ($p<0.05$) (Figure 2.39A). On the contrary, the CX extract (calculated based on total phthalides) showed similar activity as the CX mixture of phthalides as they had similar IC_{50} values and their concentration-response curves overlapped with each other (Figure 2.39B, Table 2.7).

2.2.15.3 Effects of DG extract and the mixture of phthalides on cell proliferation in CCD-18Co cells

In CCD-18Co cells, the sum of three phthalides in the DG and CX extracts demonstrated similar IC_{50} values of 5.25 ± 0.85 and 8.68 ± 1.70 μg/ml, which were significantly lower than the IC_{50} values in HT-29 cells ($p<0.05$, Table 2.7). The DG phthalide mixture also exhibited more potent anti-proliferation effects than the CX phthalide mixture. For both DG and CX, the concentration-response curves of the sum of three phthalides in the herbal extracts was shifted left of the corresponding phthalide mixtures (Figure 2.407). However, the CX phthalide mixture was less potent at inhibiting the proliferation of CCD-18Co cells than the sum of the phthalides in the CX extract (Figure 2.40B, Table 2.7).

Table 2.7 Potency of anti-proliferative effects of herbal extracts and phthalide mixtures against HT-29 and CCD-18Co cells after 24 h treatment

Extract or mixture	IC_{50} in μg/ml	
	HT-29	CCD-18Co
DG extract	14.99 ± 2.34	12.79 ± 2.06
DG extract (total phthalides)	6.14 ± 0.94	5.25 ± 0.85
DG mixture	16.16 ± 0.62	13.59 ± 1.73
CX extract	78.91 ± 3.38	35.91 ± 7.25
CX extract (total phthalides)	18.93 ± 0.81	8.68 ± 1.70
CX mixture	19.27 ± 1.21	24.30 ± 4.54

*p<0.05, **p<0.01 when compared between the two IC_{50} values

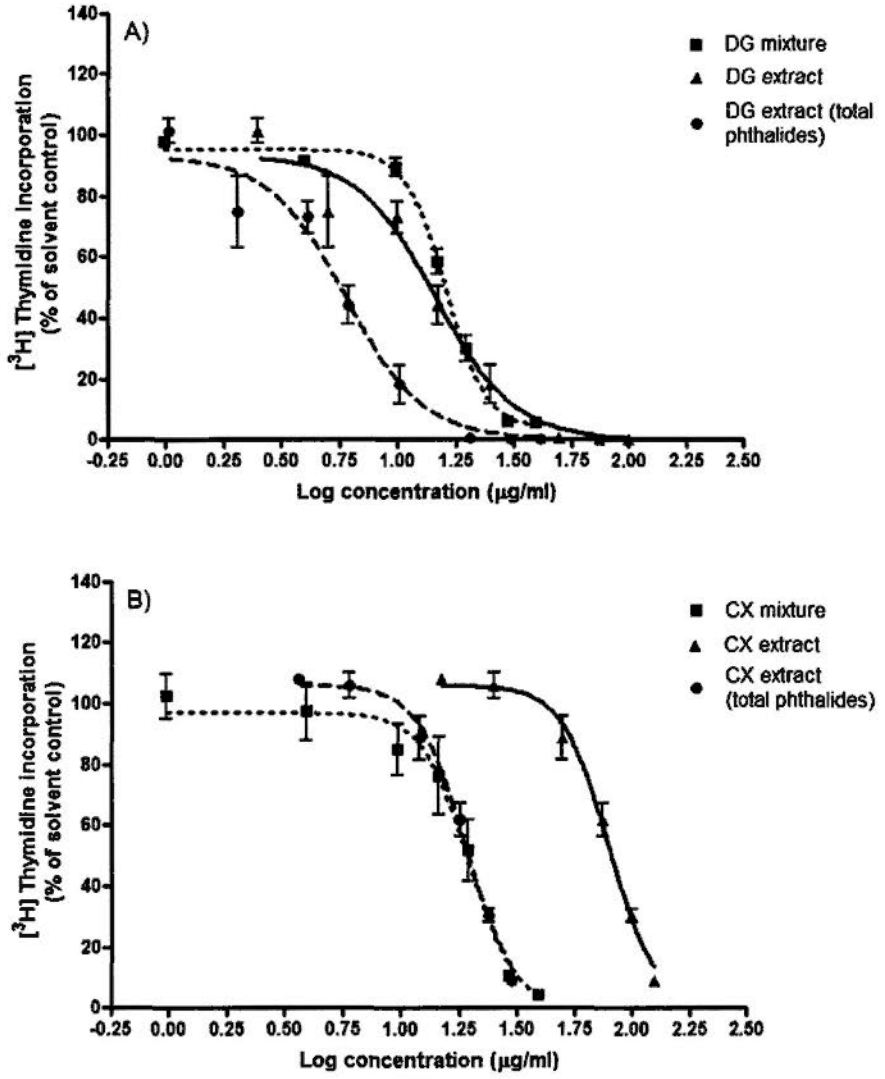

Figure 2.39 Effects of herbal extracts, total phthalides in the herbal extracts and mixtures of phthalides from A) DG and B) CX on HT-29 cells after 24 h treatment. The concentration-response curves were constructed based on concentrations of the herbal extract (solid line), the phthalide mixtures (narrow dash line) and reconstructed based on the sum of concentrations of three phthalides in the extracts (wide dash line). Data are presented as mean values ± S.E.M. as a percentage of the solvent control from three independent experiments.

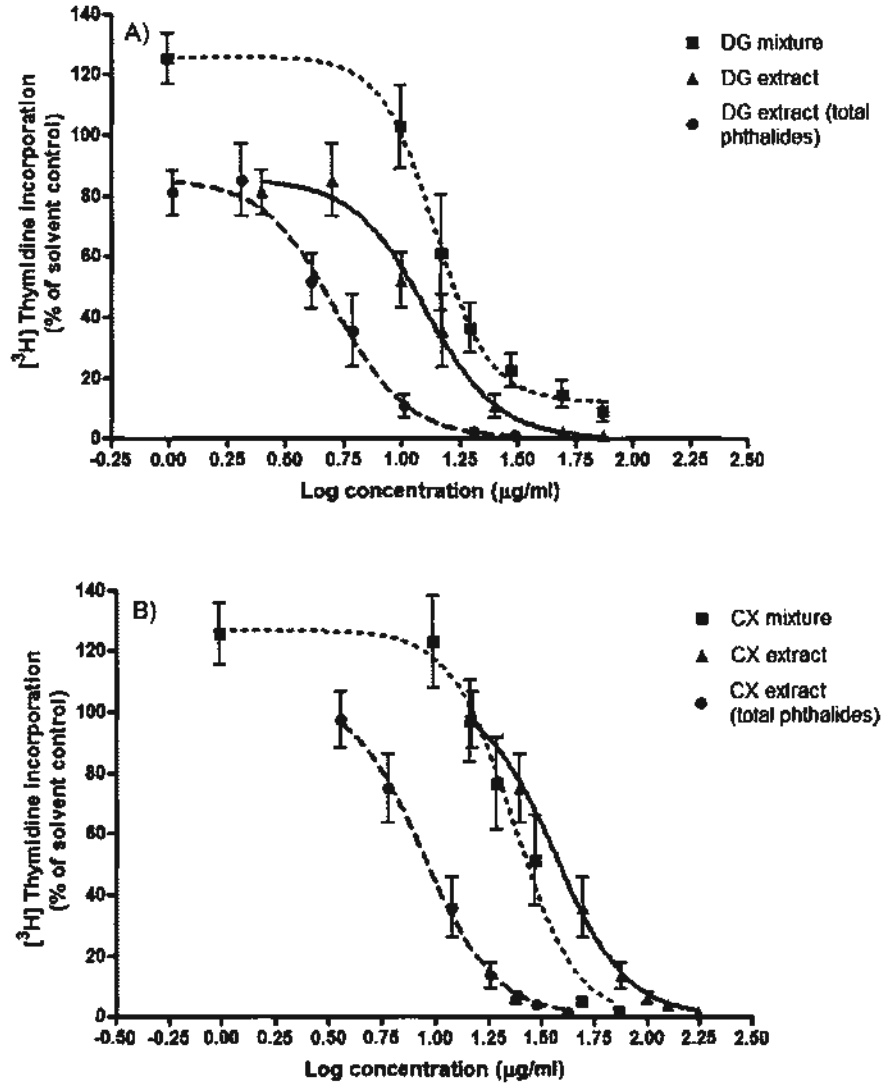

Figure 2.40 Effects of herbal extracts, total phthalides in the herbal extracts and mixtures of phthalides from A) DG and B) CX on CCD-18Co cells after 24 h treatment. The concentration-response curves were constructed based on concentrations of the herbal extract (solid line), the phthalide mixtures (narrow dash line) and reconstructed based on the sum of concentrations of three phthalides in the extracts (wide dash line). Data are presented as mean values ± S.E.M. as a percentage of the solvent control from three independent experiments.

2.2.15.4 Contribution of phthalide interactions to the anti-proliferative effects of the DG and CX extracts in HT-29 and CCD-18Co cells

Combination index values were calculated based on median-effect analysis and mathematical formula derived by Chou (2006), which is described in detail in section 2.1.2.11. From the above results, it implied that the sum of the three phthalides in the DG extract is more potent than the the artificial combination of BLP, SKA and LGT in the ratio as they exist in the extract. The potency of the three phthalides in CX extract is similar to that of the artificial combination of BLP, SKA and LGT in the ratio naturally found in the extract. The combination index values showed that BLP, SKA and LGT interacted in a synergistic manner in the DG extract to reduce proliferation of HT-29 and CCD-18Co cells (Figure 2.41). In contrast, the DG phthalide mixture displayed antagonistic interactions in HT-29 and CCD-18Co cells. Similar results were also demonstrated in flow cytometry studies in that the artificial DG mixture did not induce any significant changes in cell cycle distribution (Figure 2.42). Specifically, the DG extract significantly increased the number of cells in sub-G_1 phase at 175.0 μg/ml, which corresponded to 71.9 μg/ml of total phthalides (Figure 2.17). However, the DG mixture of only BLP, SKA and LGT failed to induce any changes in cell cycle distribution, even at the highest concentration of 175.0 μg/ml of the three phthalides (Figure 2.42). The three phthalides in CX extract interacted in an antagonistic manner to decrease [^{3}H] thymidine incorporation in HT-29 cells, but showed moderate synergistic interactions to decrease [^{3}H] thymidine incorporation in CCD-18Co cells (Figure 2.41). Correspondingly, the CX phthalide mixture interacted in an antagonistic manner to inhibit cell proliferation in both cell lines. The strongest antagonism was demonstrated by this phthalide mixture in CCD-18Co cells (Figure 2.41). Furthermore, a "blank" extract was prepared from the CX extract by removal of BLP, SKA and LGT and its effects on the viability of

HT-29 cells were studied. As shown in Figure 2.43, although the blank extract decreased the viability of HT-29 cells dose-dependently, this reduction was not significant even at the highest dose tested. The removal of BLP, SKA and LGT in the "blank"extract attenuated the cytotoxic effects of CX, which provides further support that the three phthalides were indeed the main bioactive compounds in CX (Figure 2.43).

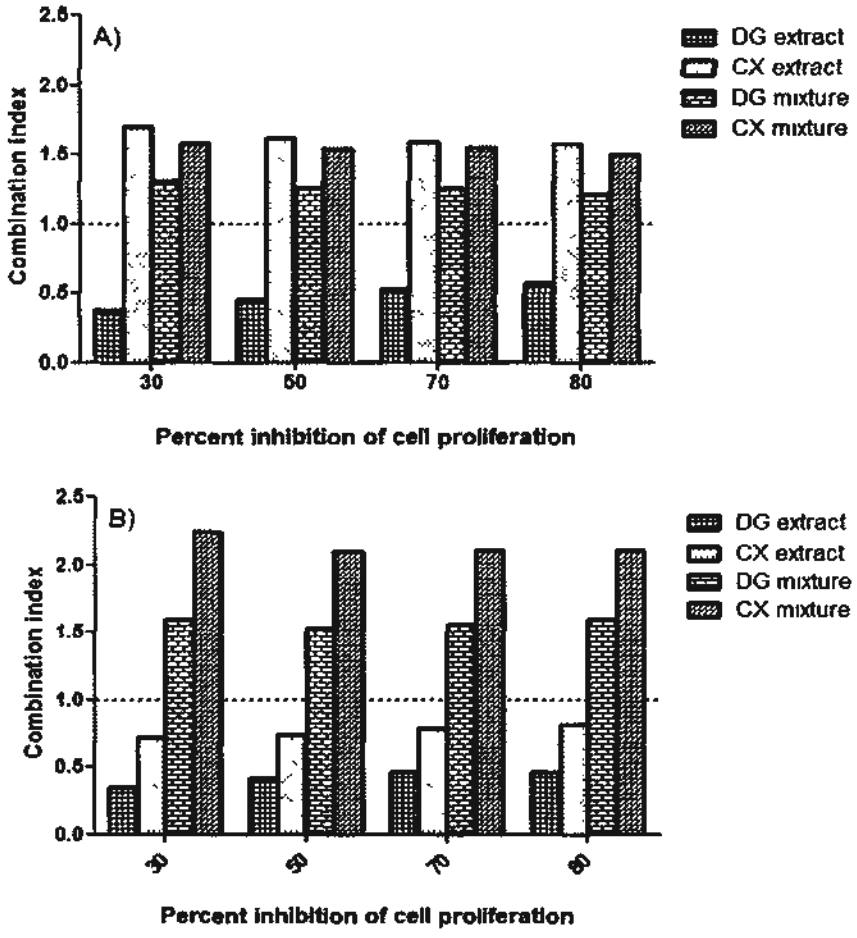

Figure 2.41 The combined effects of three phthalides in herbal extracts and phthalide mixtures on A) HT-29 and B) CCD-18Co cells. Combination index (CI) values were calculated as described in Section 2.1.2.11. CI < 1 represented synergistic effects, CI = 1 represented additive effects and CI > 1 represented antagonistic effects. Each bar is the CI value calculated from the mean of three independent experiments performed in triplicate.

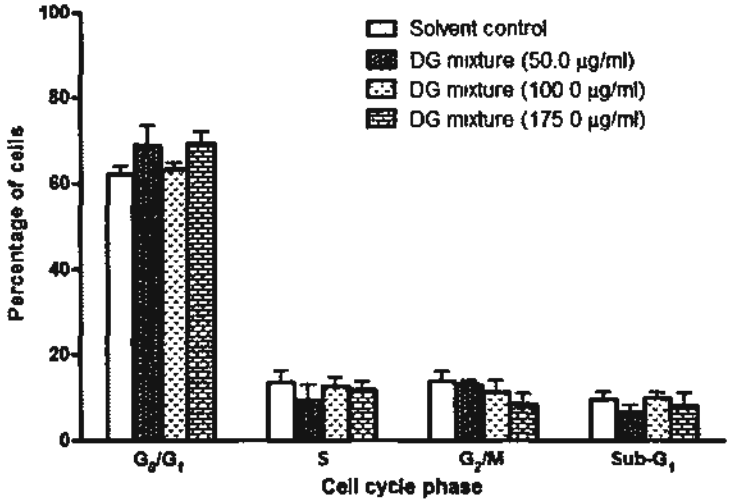

Figure 2.42 Effects of DG mixture on distribution of HT-29 cells in various phases of the cell cycle after A) 24 h treatment. The concentration of phthalides in brackets is calculated according to the phthalide content in the extract as indicated in Table 2.1. Data are presented as a percentage of control (untreated medium) as mean values ± S.E.M. from three independent experiments.

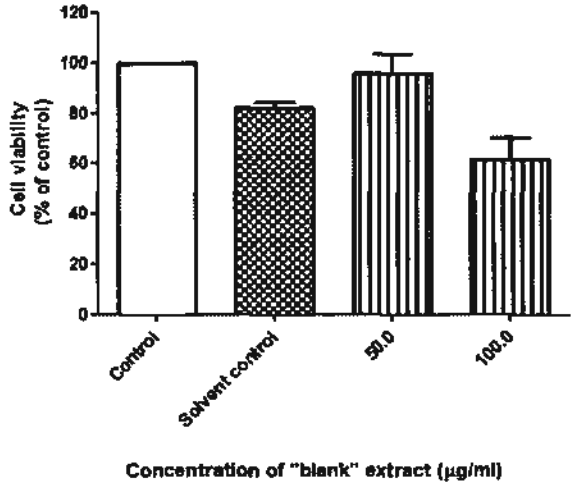

Figure 2.43 Effects of "blank" extract on the viability of HT-29 cells after 24 h treatment. The "blank" extract was prepared by the removal of BLP, SKA and LGT from the CX extract. Data are presented as a percentage of control (untreated medium) as mean values ± S.E.M. The solvent control was 0.2% DMSO. The experiment was performed in triplicate in three independent experiments.

2.3 Discussion

DG is a traditional Chinese medicinal herb that has been used to "nourish blood" and to modulate "qi," especially in menstrual disorders (Upton, 2003). The aim of the current study is to explore the potential anti-cancer effects of DG and its active components in colorectal cancer. In addition to the study of the DG extract, the rationale for choosing the phthalides, BLP, SKA and LGT, for this study is that they are the three phthalides found in the highest quantity in the essential oil of the DG extract in our study.

The results of this study showed that the DG, along with BLP, SKA and LGT reduced the viability of human colorectal HT-29 and SW1116 cell lines in a dose- and time-dependent manner and the cytotoxicity was more severe in cancer cells as opposed to normal human colon fibroblasts (Figures 2.3,-2.8, Tables 2.5-2.6). As well, all three phthalides and DG dose- and time-dependently inhibited the proliferation of HT-29 cells in a selective manner (Figures 2.10-2.11, 2.37-2.38, Table 2.6). Flow cytometry results demonstrated that the herbal extract, BLP and LGT induced G_0/G_1 cell cycle arrest with a dose-dependent accumulation of HT-29 cells in sub-G_1 apoptotic phase (Figures 2.14, 2.16-2.17). Since LGT and the DG extract showed similar cell cycle distribution profiles, LGT was chosen for further studies on cell death based on the fact that it is the most abundant phthalide in DG and it showed potent and selective cytotoxic effects on colon cancer cells. BLP did not exert effects until high dose and it naturally occurs in relatively small quantity in the extract, so the possibility that it is the bioactive ingredient is unlikely (Figure 2.14, Table 2.1). Similarly, the percentage of SKA in the extract is relatively low (less than 1%). Although MTT and [^{3}H] thymidine incorporation studies showed that SKA potently inhibited the viability and proliferation of HT-29 cells, SKA induced a

greater LDH release in CCD-18Co cells than in HT-29 cells (Figures 2.8-2.9, Tables 2.5-2.6). As well, it failed to induce an increase of cells in sub-G_1 phase, even at the highest concentration tested, which suggested that cell death may occur through non-apoptotic modes (Figure 2.15).

Phthalides are a group of compounds that are almost exclusively found in plants of the *Apiaceae* family and most of the phthalides have been isolated from DG and CX (Lin *et al.,* 1998; Dong *et al.,* 2005; Li *et al.,* 2006d; Beck & Chou, 2007; Yi *et al.,* 2009). Up to now, many studies have focused on the vasorelaxant and anti-platelet aggregation effects of BLP, SKA and LGT (Chan *et al,* 2006; Liang *et al.,* 2006; Chan *et al.,* 2007; Du *et al.,* 2007; Chan *et al.,* 2009; Zhang *et al.,* 2009). The present study is the first to show the anti-proliferative effects of the three phthalides on colon cancer and the underlying mechanisms for LGT.

Both MTT and [^{3}H] thymidine incorporation results showed that the potency order of the phthalides were SKA > LGT >> BLP for cytotoxic and anti-proliferative effects on human colon cancer cells in our study (Tables 2.5-2.6). SKA and LGT have also been reported to be more potent than BLP at inhibiting the proliferation of mouse aorta smooth muscle cells (Kobayashi *et al.,* 1992; Kobayashi *et al.,* 1993). As well, Chen *et al.* (2007) showed that LGT was potent at reducing the viability of mouse and human leukemia cell lines with IC_{50} values of 0.43 ± 0.02 μg/ml and 0.91 ± 0.03 μg/ml, respectively, after 48 h incubation. In our study, the IC_{50} values for all three phthalides were lower for anti-proliferation activity as opposed to cytotoxicity, which suggest that they may target proliferation mechanisms in colon cancer cells, as lower concentrations are required to inhibit proliferation of HT-29 cell and cell death mechanisms are activated with increasing doses of the phthalides (Tables 2.5-2.6).

For instance, the IC_{50} value for BLP is 72.51 ± 8.65 μg/ml for cytotoxicity and 44.59 ± 3.43 μg/ml for anti-proliferation, which suggests that the cell proliferation mechanisms, such as cell cycle, rather than apoptosis, are more sensitive to BLP (Li *et al.,* 2006a).

Flow cytometry results illustrated that BLP, LGT and the DG extract significantly increased the number of HT-29 cells in G_0/G_1 and sub-G_1 phases, with concomitant reduction of cells in S and G_2/M phases (Figures 2.14, 2.16-2.17). Likewise, BLP and acetone and chloroform extracts of DG were reported to induce G_0/G_1 cell cycle arrest in cancer cells, which were associated with increased protein expressions of CDK inhibitors, $p16^{INK4A}$ and $p21^{Waf1/Cip1}$, and decreased protein expressions of cyclin D1, cyclin E, cdk2, cdk4 and cdk6 (Cheng *et al.,* 2004; Tsai *et al.,* 2005; Tsai *et al.,* 2006). Increased p16 and p21 bind on to cyclins D and E and cdks 2, 4 or 6 and prevent formation of the cyclin/CDK complex, which results in decreased phosphorylation of Rb (Viglietto *et al.,* 2002; Tsai *et al.,* 2005; Tsai *et al.,* 2006). Although SKA triggered G_0/G_1 arrest, it did not induce apoptosis at all concentrations tested (Figures 2.15, 2.27). The similar effects of BLP and LGT on cell cycle may be due to their similar chemical structures. Both BLP and LGT have 3-*n*-butylidene side chains, whereas SKA has a 3-*n*-butyl side chain (Figure 1.5). Likewise, the double bond in the butylidene side chain has been proposed to be an important structure for the muscle relaxant properties of BLP and LGT (Upton, 2003). A further analysis of the three-dimensional structures of the three phthalides showed that the butylidene side chains at C3 for BLP and LGT are below the lactone surface plane, while it is above the surface plane for SKA (Figure 2.44). This suggests that BLP and LGT may be the potential active components for the cytoxic effects of the DG extract. Yet, the content of BLP is only 0.86% of the DG extract and it showed

weak apoptotic activity even at 120.0 μg/ml, which is much higher than the concentration of the extract needed for apoptosis induction (Figures 2.32-2.33). Further studies on the effects of LGT on the expressions of cyclins, cdks and tumor suppressors of the INK4 and CIP/KIP family governing the G_1/S progression would provide further insight into the molecular mechanisms of LGT-induced G_0/G_1 cell cycle arrest.

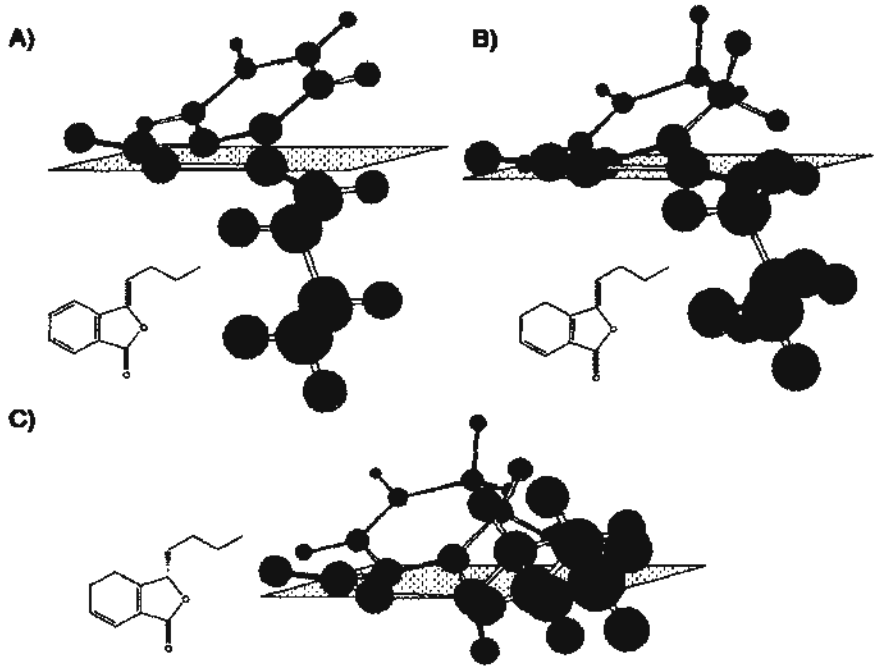

Figure 2.44 Three-dimensional structures of A) BLP, B) LGT and C) SKA with the respective chemical structures to their left.

In the present study, LGT showed synergistic interactions with cisplatin to decrease the viability of HT-29 cells at all of the tested LGT concentrations (20.5-61.5 μg/ml) and at most of the tested cisplatin concentrations (10.0-50.0 μg/ml) (Figure 2.22). However, SKA and BLP interacted in an additive or antagonistic manner with cisplatin to reduce viability of HT-29 cells (Figures 2.20, 2.21). Cisplatin (also known as *cis*-diamminedichloroplatinum) is a common drug used for the treatment of many solid tumors, such as bladder, germ cell, lung, neck and neck, ovarian,

nasopharynx and testicular tumors and lymphomas, myelomas and melanoma, as a single agent or in combination with etoposide and bleomycin (Jordan & Carmo-Fonseca, 2000; Adelstein & Rodriguez, 2008; Feldman *et al.,* 2008; Riese & Vaughn, 2009; Wheate *et al.,* 2010). Newer generation oxaliplatin and carboplatin are also in use for as adjuvant therapy of colorectal cancer and other solid tumors and satraplatin and picoplatin are currently being tested in Phase III clinical trials for hormone-refractory prostate cancer and small-cell lung cancer, respectively (Wilkes, 2005; Shah & Dizon, 2009; Dizon, 2010).

Cisplatin cross-links with DNA to form intra and interstrand adducts to inhibit DNA replication and transcription (Jordan & Carmo-Fonseca, 2000; Sedletska *et al.,* 2005). The common adducts formed are 1,2- and 1,3-intrastrand cross-links between two guanine d(GpG) or adenine/guanine d(ApG) residues or interstrand cross-links between two guanine residues (Sedletska *et al.,* 2005). The 1,2-intrastrand cross-links triggers DNA bending towards the major groove and formation of a DNA kink, which leads to the unwinding of the DNA double-helix (Takahara *et al.,* 1995; Gelasco *et al.,* 1998). The interstrand cross-links cause a larger bending of DNA towards the minor groove and unwinding of DNA (Coste *et al.,* 1999). Usually, DNA damage is repaired by the nucleotide excision, O^6-methylguanine-DNA methyltransferase, base-excision, DNA double-strand break and DNA cross-link repair pathways (Roos & Kaina, 2006). However, cisplatin-DNA adducts are poorly repaired by the nucleotide excision repair (NER) pathway due to the high affinity of high-mobility group (HMG) proteins to 1, 2-intrastrand cross links, which "shield" NER proteins from recognizing the lesion (Huang *et al.,* 1994; Zamble *et al.,* 1996). The distortion and bending of the DNA helix from the formation of cisplatin-DNA adducts may also make it physically difficult for the human excision nuclease to bind

to the lesion to initiate repair (Moggs *et al.*, 1997). In this manner, cisplatin inhibits DNA replication and it may also disrupt DNA transcription by sequestering transcription factors from their usual binding sites on RNA polymerase, such as TATA-binding protein, UBF, SRY, LEF-1 and Ixr1 (Treiber *et al.*, 1994; Love *et al.*, 1995; Werner *et al.*, 1995; McA'Nulty *et al.*, 1996; Vichi *et al.*, 1997; Jordan & Carmo-Fonseca, 2000; Sedletska *et al.*, 2005). Secondary DNA lesions and double strand breaks induced by cisplatin are recognized by ATM/ATR and activate p53 to induce cell cycle arrest (by up-regulation of p21) for repair or apoptosis in wild-type p53 cancer cells by up-regulation of Bax, PUMA and FasR and down-regulation of survivin (Lane, 1992; Hoffman *et al.*, 2002; Huerta *et al.*, 2006; Roos & Kaina, 2006). Since most cancer cells have mutated p53, DNA double strand breaks by cisplatin may directly activate c-Abl tyrosine kinase or ATM/ATR and E2F1 to stimulate p73 (Kharbanda *et al.*, 1995a; Jordan & Carmo-Fonseca, 2000; Hallstrom & Nevins, 2003). Apoptosis through the p53-dependent pathway actually requires activation for p63 and p73, but p73 can induce apoptosis by itself in p53-deficient cells (Flores *et al.*, 2002; Roos & Kaina, 2006). Through p73, an up-regulation of pro-apoptotic proteins NOXA, PUMA and Bax occurs (Roos & Kaina, 2006).

The fact that LGT acted synergistically with cisplatin to induce cytotoxic effects in HT-29 cells in the present study suggests that LGT may function through a different mechanism than cisplatin to induce apoptosis (Figure 2.22). Cisplatin prompted p53-dependent and –independent apoptosis through both mitochondrial and death receptor pathways (Brozovic *et al.*, 2004; Konstantakou *et al.*, 2009). In this study, both cisplatin and LGT induced G_0/G_1 cell cycle arrest with accumulation of HT-29 cells in sub-G_1 phase after 24 h incubation and sustained activation of JNK and p38 pathways (Figures 2.16, 2.19, 2.35. 2.36). Therefore, LGT and cisplatin may have

different mechanisms of action upstream of apoptosis, such as inducing different types of DNA damage or modulating different cell proliferation pathways like PI3K/AKT or NF-κB.

A recent study by Yu *et al.* (2010) showed that BLP reduced mRNA and protein expressions of DNA repair enzyme, O^6-methylguanine methyltransferase (MGMT), which led to increased apoptosis in hepatocellular carcinoma cells. A combination of BLP and 1,3-bis-(2-chloroethyl)-1-nitrosourea (BCNU) increased MGMT promoter CpG island hypermethylation, which led to silencing of the MGMT gene and reduced MGMT protein levels (Yu *et al.*, 2010). BLP and BCNU induced apoptosis in a synergistic manner and over-expression of MGMT led to resistance of hepatocarcinoma J5 cells to BLP. Moreover, combined treatment of BLP and BCNU to mice with hepatocellular carcinoma xenografts showed enhanced anti-tumor effects compared to each agent alone, with decreased MGMT levels (Yu *et al.*, 2010). BLP has been suggested to be an alkylating agent that directly damaged DNA to induce cell cycle arrest at G_0/G_1 (Tsai *et al.*, 2006). Since BLP and LGT have similar chemical structures, it is hypothesized that LGT may directly damage DNA or reduce the expression and activity of MGMT or other DNA repair enzymes to sensitize colon cancer cells to the effects of cisplatin.

Cisplatin binds to glutathione that is easily pumped out of the cell with an ATP-dependent export pump and it also binds to metallothionein, which is a protein that is used for the detoxification of intracellular heavy metal ions (Jordan & Carmo-Fonseca, 2000; Sedletska *et al.*, 2005). Both pathways play a role in resistance to cisplatin therapy in cancer cells. The synergistic interactions between LGT and cisplatin may be due to LGT interfering with cell resistance mechanisms by

acting as substrates of P-glycoprotein transporters and other multidrug-resistance associated protein pumps to reduce efflux of cisplatin. Since LGT is well-tolerated, the combined use of LGT and cisplatin allow cisplatin to be used at lower concentrations (Yan *et al.*, 2008). For example, cisplatin can be used at 10.0 μg/ml (four-fold lower than IC_{50} value) with a lower than IC_{50} value of LGT and still synergistically reduce cell viability (Figure 2.22). A lower concentration of cisplatin used indicates a lower possibility of adverse effects when given in a clinical setting, such as hematotoxicity, myelosuppression, ototoxicity and nephrotoxicity (Barabas *et al.*, 2008; Shah & Dizon, 2009; Tsang *et al.*, 2009; Olszewski & Hamilton, 2010). Further studies must be conducted on LGT to explore its effects on expression and activity of DNA repair enzymes. Another possibility worth exploring is whether LGT and LGT extract directly induce DNA damage. As well, the effects of the order in which LGT and cisplatin are added to the cancer cells may affect their effects on cell viability and studies for the co-administration of BLP, SKA and LGT with oxaliplatin may be more relevant for investigation of synergistic effects in colon cancer cells.

From the results, LGT induced apoptosis in HT-29 cells, as it stimulated the cleavage of PARP and pro-caspases-3, -8 and -9 and chromatin condensation and nuclear fragmentation at 61.5 μg/ml (Figures 2.23-2.26, 2.28-2.30). As well, it increased caspase-3 activity, that was significantly reduced in the presence of the caspase-3 inhibitor, Ac-DEVD-CHO, which implies that the activation of the caspase cascade is a key event in the apoptotic cell death induced by LGT (Figure 2.31). The DG extract also induced apoptosis in HT-29 cells (Figures 2.25, 2.26, 2.32), which is in accordance with previous studies in literature. An acetone extract of DG had been reported to have anti-proliferative effects in human lung, colon, brain and hepatic cancer cell lines with IC_{50} values of 35.0 ± 2.5, 40.6 ± 3.8, 45.0 ± 4.5 and 38.6 ± 4.0

μg/ml after 24 h incubation, which is similar to the IC_{50} value of the DG extract in the current study shown in Table 2.5 (Cheng *et al.,* 2004). The chloroform and acetone extracts of DG have been reported to induce apoptosis in human cancer cells, but the former extract induced cleavage of both caspase-8 and caspase-9 in brain glioblastoma and the latter induced only caspase-9 activation in lung cancer (Cheng *et al.,* 2004; Tsai *et al.,* 2005). Tsai *et al.* (2005) suggested that BLP was the bioactive ingredient responsible for the cytotoxic effects of the DG extract due to the lipid-solubility of BLP.

In the present study, LGT triggered cleavage of both caspases-8 and -9, which suggests that both the death receptor and mitochondrial-mediated pathways of apoptosis may be involved in LGT-induced cell death (Figures 2.29, 2.30). It has been shown that many anti-cancer drugs such as mitomycin and doxorubicin, upregulate FasL and other death ligands and FasR to induce apoptosis of cancer cells (Friesen *et al.,* 1996; Muller *et al.,* 1998; Fulda & Debatin, 2003). Bleomycin, cisplatin and cyclosporin A also induced FasL and FasR mRNA expression and inhibition of the interaction between FasL and FasR suppressed drug-induced apoptosis in neuroblastoma and hepatoma cells (Fulda *et al.,* 1997; Muller *et al.,* 1997). Recently, many chemopreventive agents have also been demonstrated to up-regulate death ligand and receptor expression in cancer cells. The NSAIDs, sulindac sulfide and celecoxib, triggered the increase in TRAIL-R1 and TRAIL-R2 expression in gastric, colon, prostate and lung cancer (Huang *et al.,* 2001; Jang *et al.,* 2004; Liu *et al.,* 2004). Curcumin has also been shown to up-regulate expressions of FasR and TRAIL-R1 in melanoma and prostate cancer, respectively (Bush *et al.,* 2001; Deeb *et al.,* 2004) and to induce the clustering of death receptors (FasR, TRAIL-R1 and TRAIL-R2) to facilitate the subsequent binding to adaptor proteins

(Bush *et al.,* 2001; Delmas *et al.,* 2003; Delmas *et al.,* 2004). Moreover, cisplatin has been shown to increase the migration of FADD to the death receptor and doxorubicin has been demonstrated to sensitize prostate cancer cells to TRAIL treatment by down-regulation of c-FLIP$_S$, an inhibitor of the interaction between caspase-8 and FADD (Micheau *et al,* 1999; Kelly *et al.,* 2002; de Thonel & Eriksson, 2005). Although the effects of LGT on the expression of death receptor and their respective ligands were not examined in the present study, previous studies by Tsai *et al.* (2005 & 2006) indicated that both the chloroform extract of DG at 70 μg/ml and BLP at 75 μg/ml up-regulated FasR in a time-dependent manner with no change in FasL protein expression in malignant brain tumor cells. Thus, this suggests that LGT may also alter the expression of FasR or other death receptors such as TRAIL-R1 and TRAIL-R2, which may be explored in further studies.

The dysfunction of the mitochondria is critical to the activation of the intrinsic pathway of apoptosis. Cellular stress, caused by cytotoxic drugs, induces mitochondrial outer membrane permeabilization (MOMP) and subsequent decrease in the mitochondrial membrane potential (MMP), which results in the release of pro-apoptotic factors such as cytochrome c, SMAC/DIABLO and AIF (Dias & Bailly, 2005). Normally, anti-apoptotic mediators such as Bcl-2 inhibit apoptosis by binding to and sequestering Bax, Bak and pro-apoptotic BH3-only proteins such as BAD, Bik, NOXA and PUMA (Cheng *et al.,* 2001; Nguyen & Hussain, 2007; Youle & Strasser, 2008). Upon apoptosis induction, the BH3-only proteins bind to and displace Bid/Bim or Bax/Bak from anti-apoptotic proteins (Certo *et al.,* 2006). This is in agreement with the observation that anti-apoptotic protein Bcl-2 is often up-regulated in human colon tumor specimens and the increased level correlates with resistance to chemotherapeutic drugs (Saleh *et al.,* 2000; Debatin *et al.,* 2002; Violette *et al.,*

2002). Many conventional anti-tumor drugs induce mitochondrial-mediated apoptosis by altering the ratios of Bax and Bcl-2. That is, 5-fluorouracil alone or in combination with irinotecan has been reported to reduce the ratio of Bcl-2 to Bax proteins in colon cancer cells (Nita *et al.,* 1998; Ashktorab *et al.,* 2005; Inoue *et al.,* 2006). It has been reported that the acetone extract of DG and BLP reduced Bcl-2 and increased Bax in human lung and glioblastoma cells, respectively (Cheng *et al.,* 2004; Tsai *et al.,* 2006). Thus, LGT may also induce apoptosis through modulation of the ratio between pro- and anti-apoptotic mediators. It was found in the present study that LGT induced activation of caspase-9 before caspase-8, which suggested that the mitochondrial pathway may play a major role in LGT-induced cytotoxicity, and caspase-8 may be activated through cross-talking between the two pathways of apoptosis (Figures 2.29- 2.30). Once caspase-3 is activated by caspase-9, it may cleave and activate caspases-2 and -6 (Slee *et al.,* 1999a; Huerta *et al.,* 2006). Caspase-2 promotes cytochrome c release from the mitochondria and caspase-6 is crucial in the activation of caspases-8 and -10 (Slee *et al.,* 1999b; Huerta *et al.,* 2006). It is of interest to examine whether caspase-6 is activated or not and its time course of activation by LGT to determine the amount of cross-talking between the death receptor- and mitochondrial-mediated pathways of apoptosis.

There is emerging evidence that anti-tumor drugs may directly affect other aspects of the mitochondria (Dias & Bailly, 2005). A screening of several human colorectal cancer cell lines showed that 70% of them showed somatic point mutations in mitochondrial DNA and that sensitivity to chemotherapy is strongly related to the mutation status of mitochondrial DNA (Polyak *et al.,* 1998; Singh *et al.,* 1999). Specifically, DNA intercalating agents and topoisomerase I and II inhibitors generate lesions in mitochondrial DNA and disrupt their replication (Lin *et al.,* 1991;

Okamaoto *et al.*, 2003; Dias & Bailly, 2005). Some phytochemicals such as stilbenes directly inhibit proton F_0F_1-ATP synthase of the mitochondrial respiratory chain, while some drugs initiate the opening of mitochondrial potassium-ATP channels to decrease the MMP (Breathnach, 1999; Zheng & Ramirez, 2000; Dias & Bailly, 2005). It is worth exploring whether LGT may directly induce mitochondrial damage.

Mutation or absence of the p53 tumor suppressor gene is the most common genetic abnormality in cancer (Slattery *et al.*, 2009). In cells that have mutated p53, as in the HT-29 cell line used here, DNA damage is recognized by ATM and/or ATR, which activates checkpoint kinases (CHK1 and CHK2). Then, the checkpoint kinases phosphorylate and activate E2F1, which acts as a transcription factor to up-regulate p73 (Roos & Kaina, 2006). Similar to p53, p73 stimulates the transcription of NOXA and PUMA and promotes Bax translocation to mitochondria upon activation (Melino *et al.*, 2004; Flinterman *et al.*, 2005). Since p73 is often over-expressed and almost never mutated in many cancers, chemotherapeutic drugs may still induce apoptosis even in p53-deficient cells (Melino *et al.*, 2002; Roos & Kaina, 2006). Previous studies revealed that neither the DG extract nor BLP had any effect on the expression of phosphorylated and total p53 in p53-mutated rat glioblastoma cells, but they showed increased levels of phosphorylated and total p53 in wild-type p53 glioblastoma cells (Tsai *et al.*, 2005; Tsai *et al.*, 2006). Therefore, it is speculated that LGT, along with BLP and the DG extract may induce apoptosis in HT-29 cells through a p73-dependent pathway, with stimulation of PUMA and NOXA.

The MAPK pathways, which consist of ERK, JNK/SAPK and p38, have an active role in regulation of cell proliferation, differentiation and survival and apoptosis (Fan & Chambers, 2001; Malemud, 2007). In this study, the results showed that LGT

induced activation of JNK as early as 3 h after incubation, and was maintained up to 12 h (Figure 2.35). However, ERK and p38 were not affected by LGT treatment, though there was a mild activation of ERK and p38 after 12 h of treatment (Figures 2.34, 2.36). Some studies have suggested that there is a causal link between activation of the MAPK pathways and apoptosis induction. Conventional anti-tumor drugs that are microtubule inhibitors, DNA-damaging agents, anti-metabolites and anti-hormonal agents have been demonstrated to activate JNK and induce apoptosis (Fan & Chambers, 2001). Specifically, paclitaxel activated JNK and dominant mutants of ASK1, JNKK and JNK inhibited apoptosis in leukemia and breast and ovarian cancer cells (Lee *et al.,* 1998; Shtil *et al.,* 1999; Srivastava *et al.,* 1999; Wang *et al.,* 1999; Yujiri *et al.,* 1999; Shiah *et al.,* 2001; Yagi *et al.,* 2009). The activation of JNK by microtubule inhibitors such as paclitaxel, vinblastine and vincristine in cancer cells is slow to develop and sustained for many hours (Stone & Chambers, 2000; Fan & Chambers, 2001). Similarly, in the current study, LGT induced the phosphorylation and activation of JNK in a time-dependent manner until 12 h (Figure 2.35). JNK activation has been reported to precede the onset of apoptosis. For instance, the activation of JNK by vinblastine peaked at 16 h, but the cleavage of pro-caspase-3 into its active fragement did not appear until after 36 h (Stone & Chambers, 2000). Likewise, LGT significantly increased the levels of phosphorylated JNK after 6 h, yet the cleavage of pro-caspase-3 was not significant until after 24 h (Figures 2.28, 2.35). The third common feature of JNK phosphorylation by microtubule-disrupting agents is that the increase in phosphorylated forms of JNK is only around 4 to 6 fold over the basal level and dose-dependency of the activation is weak (Wang *et al.,* 1998; Stone & Chambers, 2000; Fan & Chambers, 2001). The level of JNK activation by LGT in the present study was up to 8-fold after 12 h treatment (Figure 2.35). In addition to c-Jun,

anti-apoptotic proteins of the Bcl-2 family can also be phosphorylated by JNK. It has been hypothesized that the phosphorylation of Bcl-2 by JNK does not allow Bcl-2 to bind and sequester pro-apoptotic Bcl-2 family members, which leads to apoptosis (Haldar *et al.,* 1996; Blagosklonny *et al.,* 1997; Srivastava *et al.,* 1999; Fan & Chambers, 2001; Shiah *et al.,* 2001). JNK activation by vinblastine also led to the transcription of TNF-α, Bak and insulin-like growth factor binding protein-4, which led to the induction of apoptosis through the death receptor and mitochondrial pathways (Fan *et al.,* 2001). The activation of JNK by cisplatin, topoisomerase II inhibitor etoposide and daunorubicin, topoisomerase I inhibitor camptothecin, alkylating agent mitomycin C and anti-metabolites cytosine arabinoside and 5-fluorouracil has been well-documented and shown to lead to apoptosis and restore sensitivity of cancer cells to anti-tumor drugs (Kharbanda *et al.,* 1995a; Kharbanda *et al.,* 1995b; Nehme *et al.,* 1997; Seimiya *et al.,* 1997; Chen *et al.,* 1999; Jarvis *et al.,* 1999; Kang *et al.,* 2000; Laurent *et al.,* 2001).

Similarly, many chemotherapeutic drugs also activate the p38 MAPK pathway that may lead to apoptosis. Studies have shown that treatment of breast cancer cells with paclitaxel activated ERK and p38 prior to apoptosis and ERK and p38 inhibitors decreased the number of apoptotic cells (Bacus *et al.,* 2001). Moreover, paclitaxel in combination with subsequent treatment of ERK inhibitor PD98059, to human monocytic leukemia cells potentiated the amount of procaspase-3 cleavage, which were significantly reduced in the presence of p38 inhibitors SB203580 and SB202190 (Yu *et al.,* 2001). This suggests that the p38 and ERK pathways are crucial to the modulation of apoptosis, with possible cross-talking between the two pathways (Bacus *et al.,* 2001; Fan & Chambers, 2001; Yu *et al.,* 2001). Cisplatin activated ASK1, MKK3 and MKK4, JNK and p38 and c-Jun as early as 4 h after

treatment in human ovarian carcinoma OVCAR-3 cells, with subsequent induction of apoptosis (Chen *et al.,* 1999). 4-Hydroxytamoxifen, an antagonist of the estrogen receptor that has been used for the treatment of early breast cancer, induced both p38 activation and apoptosis induction in estrogen-receptor transfected HeLa-ER5 cells and breast cancer MCF-7 cells, which was repressed with the use of a p38 inhibitor (Zhang & Shapiro, 2000).

In the present study, it is possible that LGT triggered the JNK and p38 pathways through activation of the ASK1-MKK4/7-JNK1/2 axis (Figure 1.3), which led to apoptosis. This can be further tested by looking at the activations of ASK1 by LGT and possible inhibition by ASK1 dominant negative mutants in colon cancer cells. Although there is a slight increase in the level of phosphorylated p38 after LGT treatment for 12 h, it does not appear to be a crucial factor for apoptosis induction because p38 is usually activated within a few hours of chemotherapeutic drug treatment, and there is a time lag until the actual onset of apoptosis. For instance, p38 was activated within 4-8 h of 4-hydroxytamoxifen in HeLa-ER5 cells, but apoptosis was not detected until after 48 h of treatment (Zhang & Shapiro, 2000). The effects of p38 inhibitor and/or JNK inhibitor pretreatment on apoptosis induced by LGT must be determined to fully understand the role each MAPK pathway has in apoptosis in colon cancer cells.

There is an upregulation of epidermal growth factor receptors (EGFRs) in many cancers and the corresponding metastases, including breast, colorectal, esophageal, gastric, non-small-cell lung, prostate cancer with worse prognosis and higher recurrence rates for patients with tumors with higher EGFR expression (Itakura *et al.,* 1994; Felipe *et al.,* 1995; Cho *et al.,* 2008; Arnes *et al.,* 2009; Koumakpayi *et al.,*

2010; Watzka *et al.,* 2010; Yarom *et al.,* 2010). Upon activation by EGF or transactivation by prostaglandin EP1, EP2 and EP4 receptors, the EGFR dimerizes to induce phosphorylation and constitutive activation of the Ras-Raf-MEK-ERK pathway in cancer (Sebolt-Leopold, 2000; Wu *et al.,* 2010). Then, there is transcription of multiple immediate-early growth response genes such as c-myc, AP-1, c-Fos and c-Jun, which leads to increased cell proliferation and carcinogenesis (Wu *et al.,* 2010). Since there is a high level of activation of ERK in human tumors, it is expected that tumors are highly sensitive to treatment with drugs that inhibit this pathway.

However, there is emerging evidence that many currently-used anti-tumor drugs actually activate ERK and ERK may have a pro-apoptotic role in some cells depending on the stimulus, the intensity and duration of the stimulus, the cell type, basal ERK activity and the activation of other cell signaling pathways (Fan & Chambers, 2001). For instance, hydrogen peroxide-induced apoptosis in oligodendrocytes and camptothecin-induced apoptosis in mature mouse cortical neurons were associated with activation of ERK and apoptosis in both cases were reversed with MEK inhibitor (Bhat & Zhang, 1999; Lesuisse & Martin, 2002). The death-promoting role of ERK was also described for cisplatin- and reactive oxygen species-induced cell death in renal cell lines and primary renal proximal tubular cells (Zhuang & Schnellmann, 2006). Cisplatin triggered a dose- and time-dependent activation of ERK and both PD98059 and U0126 reduced cisplatin-induced apoptosis in human cervical carcinoma HeLa cells (Wang *et al.,* 2000). Doxorubicin induced apoptosis and activation of ERK by 17-fold in human hepatocellular carcinoma HepG2 cells, which was almost completely blocked with PD98059 and this trend was also shown for cisplatin treatment in the same cell line (Alexia *et al.,*

2004). Kim *et al.,* (2005) revealed that cisplatin produced an increase in Bax expression, mitochondrial membrane depolarization, cytochrome c release and caspase-3 activation in renal epithelial cells, which were all reversed by the MEK inhibitor. Cytochrome c release and caspase-3 activation was also repressed by MEK inhibitor in cisplatin-induced apoptosis in cervical carcinoma cells (Wang *et al.,* 2000). ERK may directly phosphorylate p53 and increase the expression of ligands and inflammatory cytokines, such as TNF-α and interleukin-1β, that bind on to death receptors to induce apoptosis (Persons *et al.,* 2000; Wang *et al.,* 2004; Jo *et al.,* 2005; Brown & Benchimol, 2006). Prolonged activation of ERK may also contribute to cell death by inhibition of the PI3K/Akt cell survival pathway (Sinha *et al.,* 2004).

Up to now, there has only been one study by Lu *et al.* (2006) that has explored the effects of LGT on the activation of MAPK pathways. LGT suppressed the proliferation of rat vascular smooth muscle cells stimulated by 10% serum with an approximate IC_{50} value of 40 μg/ml after 48 h incubation, which was accompanied with a dose-dependent decrease in the levels of phosphorylated forms of ERK, JNK and p38 (Lu *et al.,* 2006). Yet, the results from this study imply that the activation of the MAPK pathways varies greatly between cell types, normal versus malignant cells and time period for observation of phosphorylation statuses (a few minutes versus several hours) and it is difficult to compare the results of this study from the previous study on vascular smooth muscle cells. In the present study, it does not appear that the apoptosis induced by LGT is dependent on p38 nor ERK since their activation do not occur prior to onset of apoptosis (Figures 2.34, 2.36). However, to confirm this hypothesis, the effects of pre-treatment with MEK inhibitors PD98059 and U0126 on the possible potentiation or inhibition of apoptosis induced by LGT must be investigated. As well, the effects of pre-treatment with MEK inhibitors on the

expression of pro-apoptotic and anti-apoptotic proteins and death ligands and receptors such as FasL and FasR should be examined before making any solid conclusions on the contribution of ERK pathway to apoptosis.

The *in vitro* and *in vivo* anti-cancer mechanisms of BLP have been extensively studied in glioblastoma, hepatocellular carcinoma and lung cancer. Besides the induction of apoptosis, BLP has been shown to up-regulate mRNA and protein expression of orphan nuclear receptor Nur77, with IC_{50} values of 70-100 μg/ml after 24 h treatment and 25 μg/ml after 48 h treatment in glioblastoma and hepatoma cells, respectively and in tumor xenograft models (Tsai *et al.*, 2006; Chen *et al.*, 2008; Lin *et al.*, 2008). The migration of Nur77, an oncogenic survival factor, from the nucleus to the cytosol occurs at the same time as the release of cytochrome c from the mitochondria to the cytosol, after 24 h BLP treatment (Chen *et al.*, 2008; Lin *et al.*, 2008). A reduction in Nur77 through siRNA given in combination with BLP increased viability of glioblastoma cells, along with inactivation of caspase-9 and caspase-3. BLP did not activate MAPK pathways and the growth-inhibitory effects of BLP were demonstrated to be dependent on the protein kinase C (PKC) pathway in glioblastoma (Lin *et al.*, 2008). However, BLP-induced apoptosis was found to be mediated through the modulation of the PI3K/Akt and CREB pathways in hepatocellular carcinoma (Chen *et al.*, 2008). In lung cancer, BLP was cytotoxic with IC_{50} value of 62.5 μg/ml after 48 h incubation through stimulation of apoptosis and inhibition of telomerase activity and human telomerase reverse transcriptase (hTERT) expression in both A549 cells and A549 xenografts in nude mice, with involvement of the tumor suppresssor AP-2α (Wei *et al.*, 2009). MEK inhibitor PD98059 in combination with BLP synergistically reduced AP-2α and increased caspase-3 cleavage (Wei *et al.*, 2009). The above findings on BLP hint that different signaling

pathways for cell proliferation and survival are involved as PKC, ERK and AKT are involved in apoptosis induced by BLP in brain tumor, hepatocellular carcinoma and lung cancer cells, respectively. Therefore, it is tricky to hypothesize the exact mechanisms of LGT in colon cancer from the available studies in literature, despite its similar structure to BLP. Further studies must be carried out to analyze the effects of LGT on PI3K/AKT, PKC, MAPK and NF-κB pathways on apoptosis using selective inhibitors to determine which pathway mediates apoptosis to inhibit tumor growth. There is likely more than one pathway that contributes to the anti-proliferative effects of LGT and it is not surprising that one pathway may cross-talk with another one or more pathways, as demonstrated in the study by Chen *et al.* (2008) that described the involvement of PI3K/Akt and CREB pathways.

For the first time, the current study revealed the *in vitro* cytotoxic and anti-proliferative effects of LGT in colon cancer and the possible underlying mechanisms, which is summarized in Figure 2.45. Specifically, LGT induced G_0/G_1 cell cycle arrest and apoptosis that involved both the mitochondrial- and death receptor-mediated pathways of apoptosis by activation of caspases-9 and -8, respectively. The activation of JNK, ERK and p38 may be involved in LGT-induced apoptosis by up-regulation of death receptors and their respective ligands and phosphorylation and inactivation of Bcl-2, but this must be further confirmed.

The current results provide a good foundation for further studies to be conducted on the *in vivo* effects of LGT on tumor growth. Some conditions for the studies using tumor xenografts in nude mice must be carefully considered.

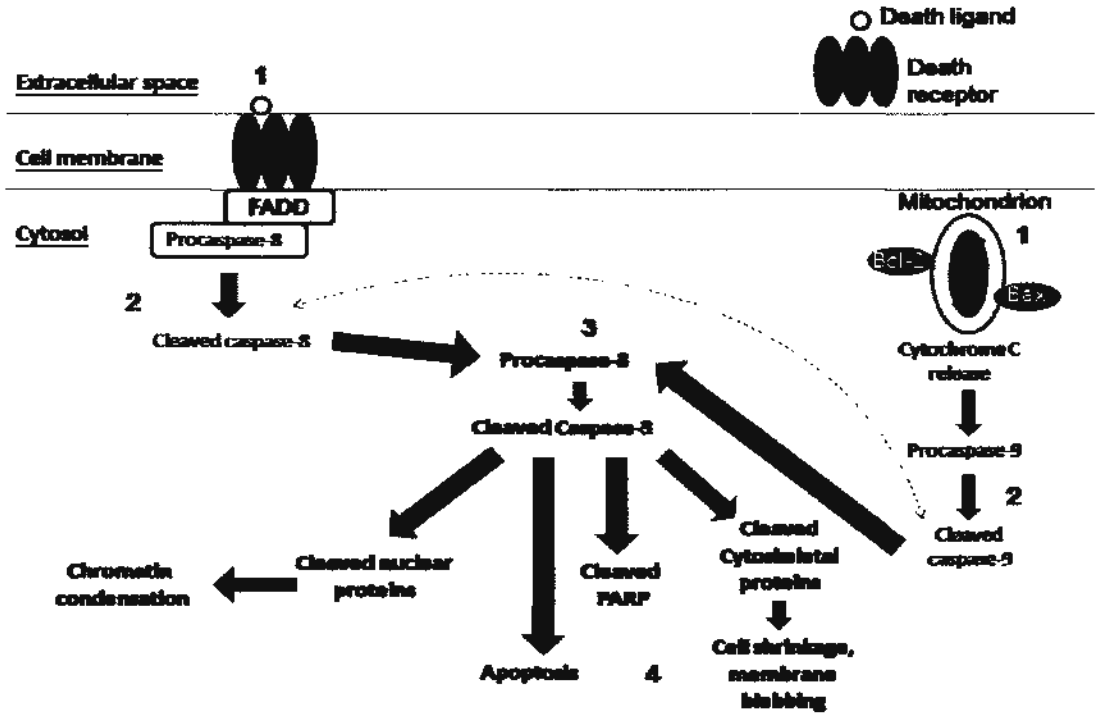

Figure 2.45 Proposed mechanism of LGT. LGT may up-regulate death receptors and their ligands to activate caspase-8 in the death receptor-mediated apoptotic pathway. LGT may also disrupt the balance between Bax and Bcl-2 in mitochondria to induce a decrease in mitochondrial membrane potential and cytochrome c release for the activation of caspase-9 in the mitochondrial-mediated apoptotic pathway. Since caspase-9 was activated before caspase-8, there may also be cross-talking between the two pathways by activation of caspase-6. The two pathways converge for the activation of caspase-3 for the typical morphological changes associated with apoptosis.

For instance, the majority of *in vivo* studies with BLP or the DG extract employed the subcutaneous route of administration once everyday or every three days for approximately a month before the mice were sacrificed (Tsai *et al.*, 2005; Tsai *et al.*, 2006; Chen *et al.*, 2008; Lin *et al.*, 2008; Wei *et al.*, 2009; Yu *et al.*, 2010). However,

one study used a daily intraperitoneal injection of the herbal extract for 30 days (Lee *et al.,* 2006). The oral bioavailability of LGT is only 2.6% due to high rates of first-pass metabolism in the liver, hence, the oral or intraperitoneal routes should be avoided (Yan *et al.,* 2008). The dosing schedule needs to be clearly determined as after intravenous administration of LGT in a rat, it was widely distributed and eliminated very quickly (Yan *et al.,* 2008). As well, LGT is very sensitive to heat and air so LGT should be kept at a temperature as low as possible to avoid photo-degradation, hydrolysis and oxidation (Upton, 2003; Cui *et al.,* 2006). As well, the treatment doses must induce no toxicity to normal tissue, yet exert anti-tumor effects. The dosing schedule and route of administration need to be well-planned to determine the anti-tumor effect of LGT in tumor xenograft mice models.

The DG extract was more potent than the three phthalides in the induction of G_0/G_1 cell cycle arrest, accumulation of cells in sub-G_1 phase and apoptosis (Figures 2.14-2.17, 2.26, 2.31, 2.32). From these results, it appears that in the DG extract: 1) there may be synergistic interactions between BLP, SKA and LGT; 2) there are other bioactive components in the extract; or 3) there may be synergistic interactions between the three phthalides and other bioactive components in the extract to account for the greater effect of the DG extract. Therefore, the interactions between different components in the DG extract were examined by studying the anti-proliferative effects of the DG and CX extracts and two mixtures of BLP, SKA and LGT, in the ratios as they naturally exist in DG and CX.

Both of the phthalide mixtures exhibited antagonistic effects in the inhibition of cell proliferation in both HT-29 and CCD-18Co cells and the antagonistic effect was stronger in the normal colon fibroblast cell line (Figure 2.41). In HT-29 cells, the

ratio of the three phthalides did not affect its anti-proliferative activity, as both DG and CX phthalide mixtures showed similar IC_{50} values (Table 2.7). However, the CX mixture showed an almost 2-fold higher IC_{50} value than the DG mixture in CCD-18Co cells (Table 2.7). Since the CX mixture had a higher IC_{50} value than the DG mixture in CCD-18Co cells, the two herbal mixtures inhibited the proliferation of colon cancer cells to the same extent. This suggests that by changing the proportion of the three phthalides the selectivity of the mixture towards cancer cells may be improved, which may reduce adverse effects on other organs when given as a therapeutic drug. From the results, it suggests that BLP, SKA and LGT are bioactive compounds since the DG and CX mixtures had similar activity in HT-29 cells, regardless of the ratios of the three phthalides. Also, the CX extract with the three phthalides removed ("blank extract"), had almost no cytotoxic activity, which provides further support that the three phthalides are bioactive ingredients (Figure 2.43).

The DG extract had stronger anti-proliferative effects in HT-29 cells than the phthalide mixture, while the *Ligusticum* extract showed similar activity as the phthalide mixture (Figure 2.39). This suggests that in addition to the three phthalides in the DG extract, there may be other compounds with bioactivity or other bioactive components that interact synergistically with the phthalides. Yet, the three phthalides are the main contributors to the anti-proliferative effects of the CX extract. Further studies revealed that in HT-29 cells, the three phthalides acted in a synergistic manner with other bioactive components in the DG extract to reduce cell proliferation, while the three phthalides acted in an antagonistic manner with other components in the CX extract to reduce cell proliferation (Figure 2.41). Both DG and CX phthalide mixtures acted in an antagonistic manner to reduce proliferation of

HT-29 cells. Although both herbal extracts contain the same three phthalides as bioactive compounds, the interactions between the phthalides and different bioactive components in each herbal extract may cause different biological effects.

The results of this study are in accordance with the theory of use of traditional Chinese medicine as an herbal formula (known as "Fu Fang" in Chinese). The herbal formula usually consists of several herbs that contain multiple bioactive compounds (Ruan *et al.*, 2006). There are four elements in an herbal formula: Jun (king or master), Chen (minister), Zuo (assistant) and Shi (servant) which act synergistically to produce beneficial medicinal effects (Dong *et al.*, 2006). The synergistic interactions among the components in the DG extract supports the idea that the phthalides are rarely used alone to treat disease. For instance, the DG extract is often prescribed together with CX in a 3:2 ratio in a herbal formula called Fo Shou San to treat atherosclerosis and hypertension in China (Hou *et al.*, 2004).

Another popular herbal formula that has been used in China since 1247 A.D. is Danggui Buxue Tang (DBT), which is a boiled decoction of *Astragali Radix* (RAS) and DG in a 5:1 ratio used to treat menstrual disorders, to raise "qi" (vital energy) and to "nourish" blood (Dong *et al.*, 2006; Mak *et al.*, 2006). Similar to the results of this study, the ratio of RAS to DG in DBT has a major effect on the therapeutic effects of the formula. For instance, Gao *et al.* (2006, 2007b) demonstrated that the 5:1 ratio of RAS to DG in DBT increased the proliferation of human T-lymphocytes, phagocytosis of macrophages and release of interleukins-2, -6 and -10, by the highest percentage relative to 1:1, 3:1, 7:1 and 10:1 ratios. As well, the two herbs alone and the combination of RAS and DG in 5:1 ratio without boiling failed to induce the phosphorylation of ERK, but DBT triggered the phosphorylation of ERK associated

with cell proliferation (Gao *et al.*, 2006). The beneficial effects of DBT in stimulating the immune system (raising "qi") were due to the stimulation of T-lymphocyte proliferation and cytokine release by activation of ERK by the polysaccharide fraction of DBT (Gao *et al.*, 2007b). After ischemia-reperfusion injury in rats, DBT reduced the amount of myocardial lactate dehydrogenase leakage and mitochondrial malondialdehyde to a greater extent than the two herbs alone or mixed together without boiling, due to increased production of glutathione and glutathione reductase in myocardial mitochondria and red blood cells (Mak *et al.*, 2006; Chiu *et al.*, 2007). The synergistic effect of DBT in enhancing the mRNA expression and release of erythropoietin, an hematopoietic growth factor specific for erythropoiesis, and in reducing platelet aggregation was also demonstrated by Dong *et al.* (2006) and Gao *et al.* (2008). Furthermore, while DBT specifically triggered activity of the estrogen-driver promoter and the phosphorylation of estrogen receptor-α and ERK1/2 without affecting proliferation of human breast cancer cells, RAS and DG alone or in combination without boiling did not affect the phosphorylation status of estrogen receptor-α and ERK (Dong *et al.*, 2006; Gao *et al.*, 2007a). These results suggest that compounds from RAS and DG act in a specific and synergistic manner to treat cardiac disease and menopausal symptoms, to regulate "qi" and to "nourish" the blood. Dong *et al.* (2006) discovered that the mixture of the two herbs in DBT in a 5:1 ratio produced the highest yield of total flavonoids, total saponins, total polysaccharides, RAS-derived astragaloside IV, calycosin and formononectin and DG-derived ferulic acid. It has been suggested that the boiling together of the two herbs in a 5:1 ratio generated new chemicals and increased the solubility of active components from both herbs (Mak *et al.*, 2006; Gao *et al.*, 2007a; Gao *et al.*, 2007b). Namely, saponins derived from RAS may improve the solubility of compounds from DG, such as ferulic acid (Dong *et al.*, 2006). The

higher amount of ferulic acid in DBT may be due to the presence of anti-oxidizing compounds in RAS that prevent the oxidation and degradation of ferulic acid in the boiling procedure (Dong *et al.*, 2006). The increased activity of DBT also implies that there may be synergistic interactions among the different components in DBT at the ratio of 5:1 (Gao *et al.*, 2007a; Gao *et al.*, 2007b). Subsequent studies demonstrated that LGT in DBT reduced the amount of astragaloside IV, calycosin, formononectin and total polysaccharides and inhibited the estrogenic activity of the formula, so DG should be processed with ethanol before combining with RAS to reduce the amount of LGT (Dong *et al.*, 2006; Zheng *et al.*, 2010). As shown from the results in the present study, the different proportion of phthalides in CX and DG resulted in different interactions among the phthalides and other compounds. The replacement of DG by CX to create Chuanxiong Buxue Tang resulted in lower yield of chemical constituents and lower biological activity when compared to the original composition of DBT (Li *et al.*, 2010c). In a similar manner, results from the present study showed that there were synergistic interactions among phthalides and other bioactive components in DG, only at the ratio of BLP, SKA and LGT as they naturally exist in DG, as opposed to in CX. Likewise, the DG extract may contain other ingredients in the essential oil that can increase the solubility of the phthalides or reduce their degradation.

Although BLP, SKA and LGT are the main phthalides in DG, other phthalides such as angelicide, butylphthalide, levistolide A, ligustilide dimers, diligustilide, angelicide, senkyuonlides D,E, F, H, I and P and sedanenolide have been isolated from DG (Lin *et al.*, 1998; Dong *et al.*, 2005; Kim *et al.*, 2006; Li *et al.*, 2006d; Beck & Chou, 2007; Yi *et al.*, 2009). Neodiligustilide has been recently shown to exert potent cytotoxic effects in mouse lymphocytic leukemia and human chronic

myelogeneous leukemia cell lines, with IC_{50} values of 5.45 ± 0.19 and 9.87 ± 0.14 μM, respectively, after 48 h incubation (Chen *et al.*, 2007). Therefore, further studies on the proportion of other phthalides in the herbal extract and their *in vitro* and *in vivo* anti-tumor effects may provide hints as to the mechanism of synergism. In addition to phthalides, the DG extract also contains ferulic acid (Lin *et al.*, 1998; Zhao *et al.*, 2003; Dong *et al.*, 2005; Li *et al.*, 2006c). However, ferulic acid probably does not contribute to anti-proliferative effects due to its low content (0.03-0.09% in extract) and it is not only found in the DG extract (Upton, 2003; Liu *et al.*, 2005b). Although the main ingredients of the essential oil of the DG extract used in this study were phthalides, the whole DG extract also contains a large percentage of polysaccharides, which has been shown to have anti-tumor effects *in vivo*. Polysaccharide fractions from DG increased the survival rates of tumor-bearing mice and reduced adhesion, migration, invasion and metastasis of hepatocellular carcinoma cells (Shang *et al.*, 2003). The anti-cancer effect of the DG extract may also be due to the stimulation of the immune system by the polysaccharide fraction by increasing the CD4+ helper-T cell population, enhancing the release of $CD4^+$-related cytokines and activating natural killer cells and macrophages (Yang *et al.*, 2006; Yang *et al.*, 2007c).

Other aromatic compounds and mono- and di-terpenes are also found in the DG extract, though they are found in very low quantity and are not widely described in literature (Upton, 2003). The CX extract also contains similar phthalides as the DG extract, such as senkyunolide H, senkyuonlide I, neocnidilide, diligustilide, levistolide A and 3-butylidenephthalide, in addition to BLP, SKA and LGT (Yan *et al.*, 2005; Lee *et al.*, 2007). However, CX also contains coniferylferulate and other ingredients, which may contribute to the antagonistic effects of the CX extract in

decreasing the proliferation of HT-29 cells (Liu *et al.*, 2005b; Yan *et al.*, 2005).

The results from this study are in accordance with the theory that CX is not traditionally associated with the treatment of cancer. It is often used for the treatment of cardiovascular diseases and hepatic fibrosis. For example, the CX extract inhibited the proliferation and viability of hepatic stellate cells by up-regulation of cell cycle inhibitors $p21^{Waf1/Cip1}$ and $p27^{Kip1}$ and induction of apoptosis (Lin *et al.*, 2006). Diligustilide and levistolide A isolated from CX extract also reduced the proliferation of hepatic stellate cells by decreasing levels of cyclins D1, D2, E, A and B1 and activating apoptosis (Lee *et al.*, 2007).

Although literature and the current studies suggest that BLP and LGT induce G_0/G_1 cell cycle arrest and apoptosis in cancer cells through the same mechanisms as the DG extract, the extract was much more potent than any of the phthalides for inducing cytoxicity and apoptosis. Further studies with median-effect analysis indicated that the DG extract contains an unique proportion of phthalides that worked in synergy with other bioactive components in the extract to exert anti-proliferative effects in human colon cancer cells. Interestingly, the results presented in this chapter are in accordance with the principles of traditional Chinese medicine, in which drugs are administered as a combination of ingredients in a specific ratio in a "fu fang" to enhance the therapeutic effects of the formula and potentiate the general health of the patient. Although LGT is a bioactive compound with cytotoxic and anti-proliferative effects in human colon cancer cells, the DG extract contains other bioactive components that induce synergistic anti-proliferative effects and it is also a stimulant of the immune system. Hence, the DG extract is a worthy candidate for further *in vivo* studies on its anti-tumor effects in colon tumor-bearing mice.

CHAPTER 3: EFFECTS OF 30-EPICAMBOGIN (EPC) AND GUTTIFERONE K (GUTK), ISOLATED FROM RESIN OF *GARCINIA HANBURYI HOOK. F.*, ON COLON CANCER

The resin of *Garcinia hanburyi* Hook. f. (藤黄, Teng Huang, TH) is derived from gamboge, the gum-resin of the trunk of the tree (Family Guttiferae/Clusiaceae). TH, along with other *Garcinia* species, have been used traditionally used for treating wounds, infections and diarrhea (Obolskiy *et al.*, 2009). Many polyprenylated xanthones and benzophenones have been isolated from the fruits, stems, twigs, and trunks of plants from the *Garcinia* genus. Currently, a xanthone isolated from TH, called gambogic acid, has been clinically used for the treatment of cancer in China since the 1970s. Many *in vitro* and *in vivo* studies support its use in leukemia and breast, gastric and hepatic carcinoma (Zhao *et al.*, 2004; Yang *et al.*, 2007d; Wang *et al.*, 2008b; Gu *et al.*, 2009). There is ongoing research to discover compounds that are structurally-related to gambogic acid with comparable potency to develop novel candidates for the treatment of colon cancer. In this chapter, several xanthones and benzophenones isolated from TH were tested for their cytotoxicity in colon cancer cells. Then, two promising candidates, 30-epicambogin (EPC) and guttiferone K (GUTK), were selected for further studies on the mechanism underlying their cytotoxic and anti-proliferative effects. The anti-tumor effects of GUTK as a single agent and in combination with 5-fluorouracil was also investigated in an *in vivo* subcutaneous tumor model using murine colon cancer cells.

3.1 Materials and Methods

3.1.1 Chemicals, Materials and Reagents

Only materials and reagents that were not mentioned previously in chapter 2 are described in detail in this section.

Drugs

Chemical/Reagent/Equipment	Product Brand	Catalog Number
5-Fluorouracil	Sigma-Aldrich®	F6627
JNK inhibitor SP600125	Calbiochem®	420128
MEK inhibitor PD98059	Calbiochem®	513001
p38 inhibitor SB203580	Calbiochem®	559398

Immuno-blotting/Western Blot

Chemical/Reagent/Equipment	Product Brand	Catalog Number
Cell cycle regulation antibody sampler kit	Cell-Signaling Technology®	9932

Serum Alanine Aminotransferase Assay/Serum Creatinine Assay Kit

Chemical/Reagent/Equipment	Product Brand	Catalog Number
DL-Alanine	Sigma-Aldrich®	A7502
Creatinine assay kit	abcam®	ab65340
1N Hydrochloric acid solution	Sigma-Aldrich®	H9892
α-Ketoglutaric acid	Sigma-Aldrich®	K1750
Sodium hydroxide	Sigma-Aldrich®	S5881
Sodium pyruvate	Sigma-Aldrich®	P8574

***In vivo* Colon-26 subcutaneous tumor model/Immunohistochemistry**

Chemical/Reagent/Equipment	Product Brand	Catalog Number
Alexa Fluor® 488 goat anti-rabbit IgG (H+L) secondary antibody	Invitrogen™	A-11034
Brightfield/fluorescence microscope	ZEISS	Axioskop2 Plus
Cleaved Caspase-3 (Asp175) (5A1E) rabbit monoclonal antibody	Cell-Signaling Technology®	9664
2-Methylbutane (isopentane)	Riedel-de Haen®	16508
Microscope cover glass (24 x 60 mm)	Deckglaser	SUPE-0101242
10% Normal goat serum	Invitrogen™	50-062Z
Paraformaldehyde	Sigma-Aldrich®	158127
Permount mounting medium	Fisher Scientific	SP15-500
Sodium chloride	Sigma-Aldrich®	S5886
Sucrose	Sigma-Aldrich®	S0389
OCT Compound	Tissue-Tek®	62550-12/4583
Slides with ground edges 90°	Superfrost® Plus	J1800AMNZ
5 ml Tube with cap	Sarstedt	60.558
Tween-80	Merck	1.06007.2500

3.1.2 Methods

3.1.2.1 Cell Lines and Cell Culture

In addition to HT-29 and CCD-18Co cell lines, mouse colon carcinoma Colon-26 cells and human colorectal carcinoma HCT 116 cell lines were used in this study. HCT116 cell line was purchased from American Type Culture Collection (Rockville, MD, USA) and Colon-26 cell line was a gift from the Cell Resource Center for

Biomedical Research, Institute of Development, Aging and Cancer at Tohoku University (Sendai, Japan). The Colon-26 and HCT 116 cell lines were grown in RPMI 1640 medium, supplemented with 10% heat-inactivated fetal bovine serum, 2.0 g/L sodium bicarbonate, 0.1 g/L streptomycin sulfate and 0.06 g/L penicillin G. Both cell lines were maintained at 37°C in a humidified atmosphere with 5% CO_2.

3.1.2.2 Extraction of bioactive compounds from TH

The resin (gamboge) of *G. hanburyi* (TH) was collected from Shanxi province and purchased from Guangzhou and the National Institute for the Control of Pharmaceutical and Biological Products (NICBP) in China (Han *et al.*, 2006a; Han *et al.*, 2006b; Han *et al.*, 2006c). The plant material was identified by staff and voucher specimens were deposited at the Herbarium of the Hong Kong Jockey Club Institute of Chinese Medicine in Hong Kong S.A.R., China. TH was dissolved in acetone and loaded on the preparative HPLC system to yield several fractions. Then, the fractions were subjected to further HPLC and eluted with acetonitrile to yield the bioactive compounds (Han *et al.*, 2006a; Han *et al.*, 2006b; Han *et al.*, 2006c). In the following experiments, all of the powdered compounds were dissolved in DMSO to produce stock concentrations of 10.0-20.0 mg/ml and further diluted with culture medium prior to use. GUTK was dissolved in DMSO to make a stock concentration of 100.0 mg/ml and further diluted with 5% Tween-80 in normal saline prior to use in *in vivo* experiments. The concentrations of DMSO in culture medium for all experiments were under 0.01% and had no effect on the viability of HT-29 cells.

3.1.2.3 3-(4,5-Dimethylthiazol-2-yl)-2,5-diphenyltetrazolium bromide (MTT) assay

The protocol is described in detail in Section 2.1.2.3.

3.1.2.4 [^{3}H]-Thymidine incorporation assay

The protocol is described in detail in Section 2.1.2.4.

3.1.2.5 Lactate dehydrogenase (LDH) activity assay

The protocol is described in detail in Section 2.1.2.5.

3.1.2.6 4'6-Diamidino-2-phenylindole (DAPI) staining assay

The protocol is described in detail in Section 2.1.2.6.

3.1.2.7 Flow cytometry assay

The protocol is described in detail in Section 2.1.2.7.

3.1.2.8 Immuno-blotting/Western Blot

The protocol is described in detail in Section 2.1.2.8. The primary antibodies used included: anti-cyclin D1, anti-cyclin D3, anti-cdk4, anti-cdk6, anti-p15 INK4B, anti-p16 INK4A, anti-p21 Waf1/Cip1, anti-p27 Kip1, anti-PARP, anti-caspase-3, anti-caspase-8, anti-caspase-9, anti-β-actin, anti-phospho-p44/p42, anti-p44/p42, anti-phospho- SAPK/JNK, anti-SAPK/JNK, anti-phospho-p48 and anti-p38 at 1/500-1/1000 dilution.

3.1.2.9 Caspase-3 activity assay

The protocol is described in detail in Section 2.1.2.9.

To determine the effects of ERK, JNK and p38 on apoptosis induced by ECA and GUTK, HT-29 cells were pre-treated with PD98059 (10.0 μM), SP600125 (20.0μM) and SB203580 (1.0 μM) for one hour before the treatment of 30-epicambogin and guttiferone K at 10.0 μM for 24 h. Then, cells were harvested by trypsinization and

lysed with lysis buffer. The lysates were assayed for protein concentration and the caspase-3 activity assay was carried out.

3.1.2.10 Animal care and housing conditions

Male BALB/c mice from age 6 to 8 weeks were provided by Laboratory Animal Services Center of The Chinese University of Hong Kong. Animals were divided into two groups with four mice in each group. All animals were maintained in a pathogen-free environment air-conditioned at 24 ± 2°C with a standard 12 h light/12 h dark cycle. Animals were allowed access to tap water and standard pellet diet *ad libitum*. Care of animals and all experimental procedures were approved by the Animal Ethics Committee of The Chinese University of Hong Kong.

3.1.2.11 Toxicity studies of GUTK in mice

GUTK was administered via intraperitoneal injection at the dose of 10.0 mg/kg every other day for two weeks. Mice in the control group were administered 5% Tween-80 in normal saline in equal volumes to that of the treatment group. The general health of the mice were monitored and the body weight were recorded every other day. On day 16, blood was collected from the mice by cardiac puncture and mice were sacrificed by cervical dislocation. The blood samples were incubated at room temperature for 30 minutes, or until clotting has occurred. Then, the blood samples were centrifuged at 1500 *g* for 20 mins to obtain the serum (supernatant). The serum samples were stored at -80°C until use for the serum ALT and creatinine assays to examine the effects of GUTK on liver and kidney function, respectively. The brain, heart, lung, stomach, small intestine, colon, kidney and liver were removed, rinsed with saline and weighed. Then, each organ was divided into two parts: one section was immediately immersed in 4% paraformaldehyde for tissue fixation and the other

half was snap-frozen in liquid nitrogen and stored at -80°C until further use.

3.1.2.12 Histopathological study

The tissue samples were incubated in 4% paraformaldehyde for 2 h with shaking on an orbital shaker at 150 rpm. Then, the tissue samples were rinsed with distilled water and incubated overnight in 30% sucrose solution with shaking on an orbital shaker at 150 rpm for cryopreservation. Tissue embedding can proceed when tissue samples sink to the bottom of the tubes when tubes are in an upright position. Tissue samples were embedded in OCT compound and immersed in 2-methylbutane cooled with liquid nitrogen. The frozen sections were stored at -80°C until sectioning with cryotome. Tissue samples were sectioned at 5 μm and incubated at room temperature for 20-30 mins for adherence to slides and then subjected to hematoxylin and eosin staining. Slides were immersed in hematoxylin for 1 min, then rinsed with tap water. Then, the slides were immersed in acidified alcohol for 1 min, followed by rinsing with tap water. After rinsing with Scott's Tap water for 10-20 seconds, the slides were viewed under brightfield microscope to check the status of nuclei staining by hematoxylin. Slides were immersed in eosin for 30 seconds, rinsed with tap water and viewed under brightfield microscope. Then, the slides were subjected to dehydration with a series of ethanol solutions (70% → 80% → 95% → 100%). After slides were immersed in 100% xylene for 3 cycles, cover slips were placed on top of slides with Permount mounting medium and histology of sections were viewed and photographed with a brightfield microscope with 100x magnification.

3.1.2.13 Serum alanine aminotransferase (ALT) assay

Serum ALT activity level is the standard clinical indicator of hepatotoxicity.

Normally, ALT catalyzes the reductive transfer of an amino group from alanine to α-ketoglutaric acid to produce α-pyruvate and L-glutamate under physiological conditions. Therefore, ALT is involved in amino acid metabolism and gluconeogenesis. There are two main isoforms of ALT: ALT1, which is mostly found in the liver and ALT2, which is found in skeletal muscle and heart (Ozer *et al.*, 2008). Hepatocytes damaged by necrosis release intracellular ALT into the circulation and is detected by increase in levels of serum ALT.

The principle of this assay is based on the reaction between α-pyruvate and 2, 4-dinitrophenylhydrazine (DNP) to stop the initial reaction between alanine and α-ketoglutaric acid. This yielded 2,4-dinitrophenylhydrazone, which reacts with sodium hydroxide to form a colored complex, whose absorbance can be measured with a microplate spectrophotometer at 505 nm. The reagents prepared for this assay are stored at 4°C and are listed in Table 3.1.

Reagent	Composition
Dulbecco's phosphate-buffered saline	Sigma-Aldrich® - Cat No. 21600-010
ALT substrate solution	0.2 M L-alanine 1.8 M α-ketoglutaric acid Dissolved in D-PBS
2,4-Dinitrophenylhydrazine (DNP) solution	1 mM DNP Dissolved in 1 M hydrochloric acid solution
0.4 M Sodium hydroxide (NaOH) solution	16 g NaOH Dissolved in 1 L distilled water

1.5 M Sodium pyruvate solution	Dissolved in D-PBS

After the sodium pyruvate solutions were prepared in 15 ml centrifuge tubes, 0.5 ml DNP solution was added to each tube. Tubes were shaken and incubated at room temperature for 20 minutes. Sodium hydroxide (5.0 ml/tube) was added to each tube and vortexed. Within 5 minutes, the absorbance of the sample was measured using a microplate spectrophotometer at 505 nm wavelength. The standard curve for sodium pyruvate was prepared according to Table 3.2 and a representative standard curve was shown in Figure 3.1.

Table 3.2 Construction of the ALT activity standard curve using sodium pyruvate

Concentration of pyruvate[a]	**0**	**1/12**	**1/6**	**1/4**	**1/3**
	Volume added (µl)				
ALT substrate solution	500	450	500	350	300
Distilled water	100	100	100	100	100
Sodium pyruvate standard	0	50	100	150	200
Total volume	600	600	600	600	600
ALT activity	0	23	50	83	125

Concentration of pyruvate[a] - The concentration of pyruvate was (total volume of sodium pyruvate standard + distilled water + ALT substrate) / (volume of sodium pyruvate standard)

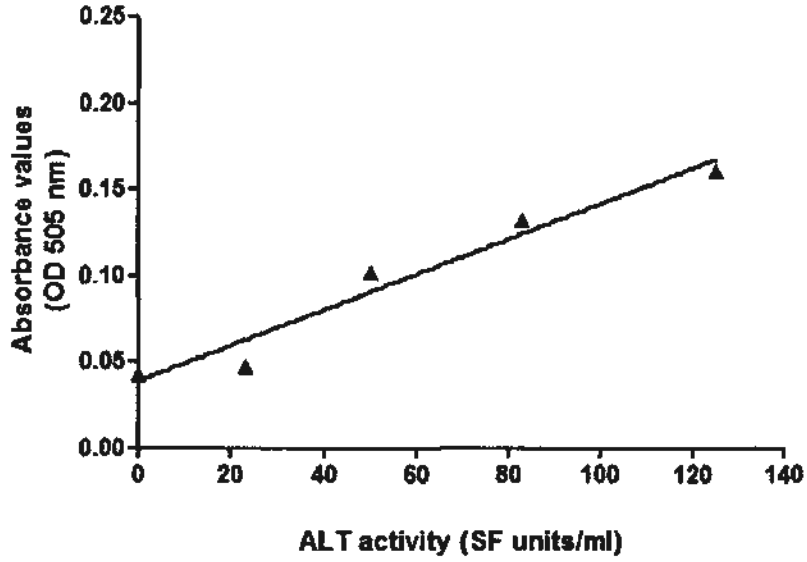

Figure 3.1 Representative standard curve for ALT activity (SF units/ml) using sodium pyruvate standard solution. The r^2 for this standard curve was 0.9539.

For the determination of ALT activity levels in serum of mice treated with vehicle and GUTK, 0.5 ml of ALT substrate solution was added to 100 µl of each serum sample in 15 ml centrifuge tubes and the tubes were incubated at 37°C for 30 minutes. Alternatively, the serum was replaced with distilled water to construct a blank control. Then, 0.5 ml of DNP solution was added to each tube and each tube was shaken and incubated at room temperature for 20 mins. Sodium hydroxide (5 ml/tube) was added to each tube and vortexed. Within 5 minutes, the absorbance of each sample was measured using a microplate spectrophotometer at 505 nm.

3.1.2.14 Serum creatinine assay kit

Serum creatinine level is a clinically-used biomarker for acute renal injury and chronic kidney disease (Rosner, 2009). Creatinine is produced as a breakdown product of creatine phosphate and it is excreted at a constant rate. The creatinine levels in serum can be used to determine glomerular filtration rate and an increase in

creatinine levels occur in the late stages of renal injury, when nephrons are significantly damaged (Rosner, 2009).

The principle of this assay is based on the conversion of creatinine into a red-colored end product with creatininase and creatinase enzymes, as describe in Figure 3.2. The creatinine assay buffer, creatinine probe, creatinine standard and the creatininase, creatinase and creatinine enzyme mix were reconstituted according to the instructions provided in the kit. The creatinine standard stock (10 µl) was added to 990 µl of assay buffer to generate 1 nmol/µl standard working solution. Then, the standard curve for creatinine was constructed according to Table 3.3 and a representative standard curve was shown in Figure 3.3.

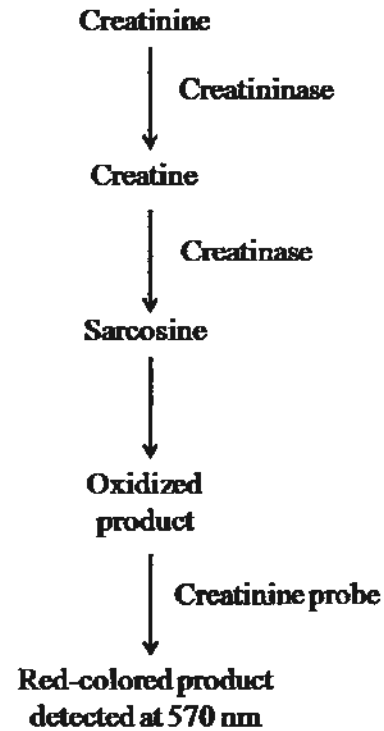

Figure 3.2 The principle of the assay for determination of serum creatinine levels using a commercially available kit

Table 3.3 Construction of the serum creatinine level standard curve using creatinine

	Volume added (µl)					
Creatinine standard working solution	0	2	4	6	8	10
Creatinine assay buffer	50	48	46	44	42	40
Total volume	50	50	50	50	50	50
Amount of creatinine (nmoles)	0	2	4	6	8	10

For each sample, 10 µl of serum was diluted with 40 µl creatinine assay buffer. Then, 50 µl of reaction mix was added to each standard and sample well, mixed thoroughly and incubated at 37°C for 1 h. For each standard or sample, the reaction mix consisted of 42 µl assay buffer, 2 µl creatinase, 2 µl creatininase, 2 µl enzyme mix and 2 µl creatinine probe. After the plate was read at 570 nm in a microplate spectrophotometer, the creatinine sample concentrations were calculated using the follow equation:

$C = Sa/Sv$ (in nmol/µl or mM)

Where Sa is the sample amount of creaitnine in nmol from the standard curve and Sv is the sample volume added to the well in µl.

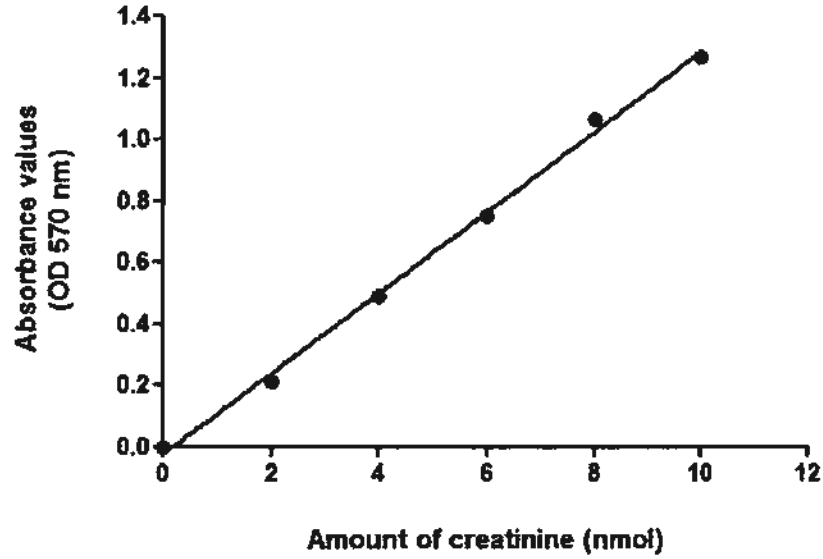

Figure 3.3 Representative standard curve for amount of creatinine (nmol) using creatinine standard solution added with reaction mix, after subtraction of reagent background absorbance value. The r^2 for this standard curve was 0.997.

3.1.2.15 Establishment of mouse Colon-26 subcutaneous tumors

Normal mice with subcutaneous Colon-26 tumor were used as a model to study the cytotoxic and anti-tumor effects of GUTK alone and in combination with 5-fluorouracil. Colon-26 mouse carcinoma cells (2.5×10^6 cells in 0.150 ml RPMI 1640 serum-free medium) were harvested by trypsinization and injected subcutaneously into the backs of BALB/c mice. When tumor dimensions reached 200-400 mm^3, the mice were randomly divided into four groups 13 days after tumor implantation. Each group consisted of four tumor-bearing mice that were tagged and monitored individually throughout the study. Group 1: vehicle control (5% Tween-80 in saline, i.p.), group 2: positive control (5-fluorouracil, 25.0 mg/kg in saline, i.p.). group 3: GUTK (5.0 mg/kg in 5% Tween-80 in saline, i.p.) and group 4: GUTK (10.0 mg/kg in 5% Tween-80 in saline, i.p.). The mice were treated 14 days after tumor

implantation and drug administration was performed once every other day for 14 days. The tumor volume and body weight of each mouse were measured every other day for 14 days before drug injection. Tumor size was measured with calipers and tumor volumes were calculated according to the formula:

Tumor volume (mm^3) = [(shortest diameter)^2 x (longest diameter)] / 2

On day 16 of drug treatment, the mice were sacrificed under anesthesia by cervical dislocation after withdrawal of blood through cardiac puncture.

In the second part of the study, the effects of a combination of 5-fluorouracil and GUTK on tumor growth were examined. BALB/c mice were implanted with Colon-26 cells to induce subcutaneous tumor and then divided into 5 groups with 5 mice each 13 days after turnor implantation. Each drug was administered to each side of the lower left or right abdomen by intraperitoneal injection. Group 1: Vehicle control (normal saline and 5% Tween-80 in saline), group 2: 5-fluorouracil in saline, 12.5 mg/kg), group 3: 5-fluorouracil in saline, 25.0 mg/kg), group 4: 5-fluorouracil, 12.5 mg/kg + GUTK, 10.0 mg/kg) and group 5: 5-fluorouracil, 25.0 mg/kg + GUTK, 10.0 mg/kg). Mice were treated every other day for 14 days. Tumor volume and body weight were monitored and recorded every other day. After 16 days of drug treatment, the mice were sacrificed under anesthesia by cervical dislocation after blood withdrawal through cardiac puncture. The tumor was removed from each mouse and divided into two parts according to section 3.1.2.11. The tumor samples were sectioned at 10 μM using the cryotome according to section 3.1.2.12 and stored at -80°C until they were used for immunohistochemical staining.

3.1.2.16 Immunohistochemistry

The cryostat sections were thawed at room temperature for 15-20 mins and washed with PBS with shaking for 15 mins. The tissues were surrounded with a hydrophobic barrier using a barrier pen. Sections were incubated with 10% normal goat serum as blocking buffer for one hour at room temperature. The cleaved caspase-3 antibody, diluted in 10% goat serum at 1:100, was added to the sectionsafter the blocking buffer was removed and incubated overnight in a humidified chamber at 4°C. The cryostat sections were washed three times with PBS for 5 mins each. The secondary antibody, diluted in 10% goat serum at 1:800, was added to the sections and slides were incubated in a humidified chamber for one hour in the dark. Slides were washed three times with PBS for 5 mins each. DAPI solution (1 μg/ml in PBS) was added to the sections and incubated in the dark for 5-10 minues. Sections were rinsed twice with PBS for 5 mins each, dehydrated with xylene and cover slips were mounted using Permount mounting medium. Sections were stored at 4°C in the dark until viewed with a fluorescent microscope.

3.1.2.17 Statistical analysis

For the *in vitro* experiments, Data are expressed as mean value ± S.E.M. from at least three independent experiments conducted in at least duplicate. The data were analyzed by one-way analysis of variance (ANOVA) followed by Bonferroni's multiple comparison post hoc test, using GraphPad Prism 5.0. For the *in vivo* experiments, repeated-measures ANOVA was used to compare tumor volumes and body weight between different treatment groups on different treatment days. Differences were considered statistically significant at $p<0.05$.

3.2 Results

3.2.1 Effects of TH extract on the viability of HT-29 cells

As shown in Figure 3.4, The TH extract significantly reduced the viability of HT-29 cells after 24 and 48 h incubation at 50.0 and 100.0 μg/ml ($p<0.001$). The cytotoxic effects of the extract were time-dependent, although there was not a large difference between the effects of 50.0 and 100.0 μg/ml extract. Since the extract induced significant cytotoxic effects, its bioactive compounds were studied in more detail.

3.2.2 Effects of various caged xanthones and their derivatives isolated from TH on the viability of HT-29 cells

The cytotoxic effects of gambogenic acid, gambogic acid, allanxanthone C, γ-mangostin and 30-epicambogin (EPC) in human colon cancer cells were studied since they are the main bioactive compounds isolated in the highest quantity from TH. All of the compounds reduced cell viability cells in a dose- and time-dependent manner when HT-29 cells were treated with the compounds for 24 and 48 h (Figures 3.5, 3.6). All of the compounds tested showed more potent cytotoxic effects than the positive controls, cisplatin and 5-fluorouracil (Table 3.4). Gambogic acid was the most potent compound, with IC_{50} values of 0.50 ± 0.03 and 0.41 ± 0.13 μM after 24 and 48 h incubation, respectively. 30-Epicambogin (EPC) had IC_{50} values of 5.11 ± 0.07 and 4.63 ± 0.43 μM after 24 and 48 h incubation, respectively (Table 3.4). After 48 h incubation, all of the compounds had potent cytotoxic effects on HT-29 cells, with IC_{50} values of less than 10 μM (Table 3.4). All of the compounds showed approximately 9-fold higher potency than 5-fluorouracil, a clinically-used drug for colon cancer.

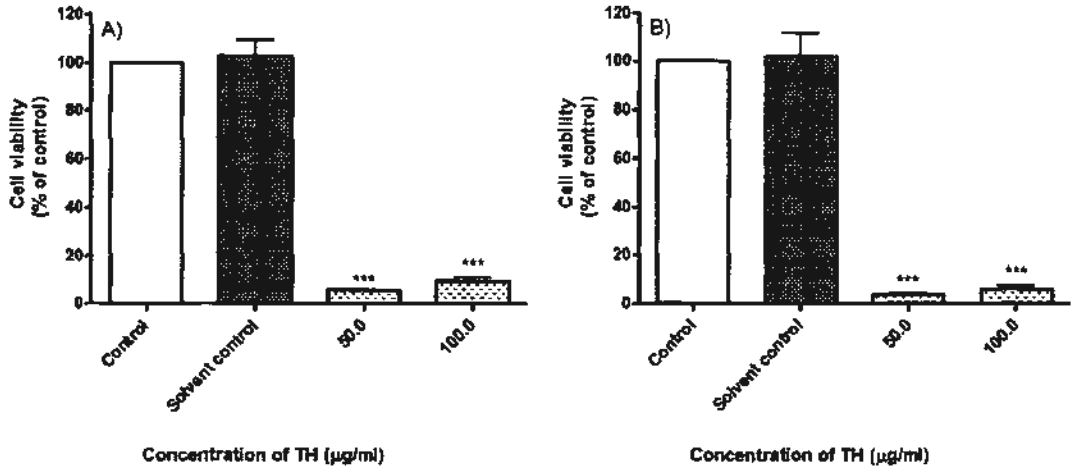

Figure 3.4 Effects of TH extract on the viability of HT-29 cells after A) 24 h and B) 48 h treatment. Data are presented as a percentage of control (untreated medium) as mean values ± S.E.M. The solvent control was 0.08% DMSO. The experiment was performed in triplicate in three independent experiments. ***$p<0.001$ compared with the solvent control.

3.2.3 Effects of various caged xanthones and their derivatives isolated from TH on the viability of CCD-18Co cells

The effects of the five isolated compounds at their IC_{50} values on the viability of CCD-18Co cells were examined after 24 and 48 h treatment (Figure 3.7). After 24 h, gambogenic acid, gambogic acid and EPC did not have any significant effects on cell viability. However, allanxanthone C and γ-mangostin increased the viability of CCD-18Co cells by approximately 25 and 28%, respectively. After 48 h, cell viability was reduced to 72.9 and 58.2% after gambogenic acid and gambogic acid treatment, respectively (Figure 3.7). Although cisplatin did not have any significant cytotoxic effects on CCD-18Co cells after 24 h, it decreased the viability of cells by 33.5% after 48 h incubation (Figure 3.7) Only EPC did not induce any change to the viability of CCD-18Co cells after both 24 and 48 h incubations.

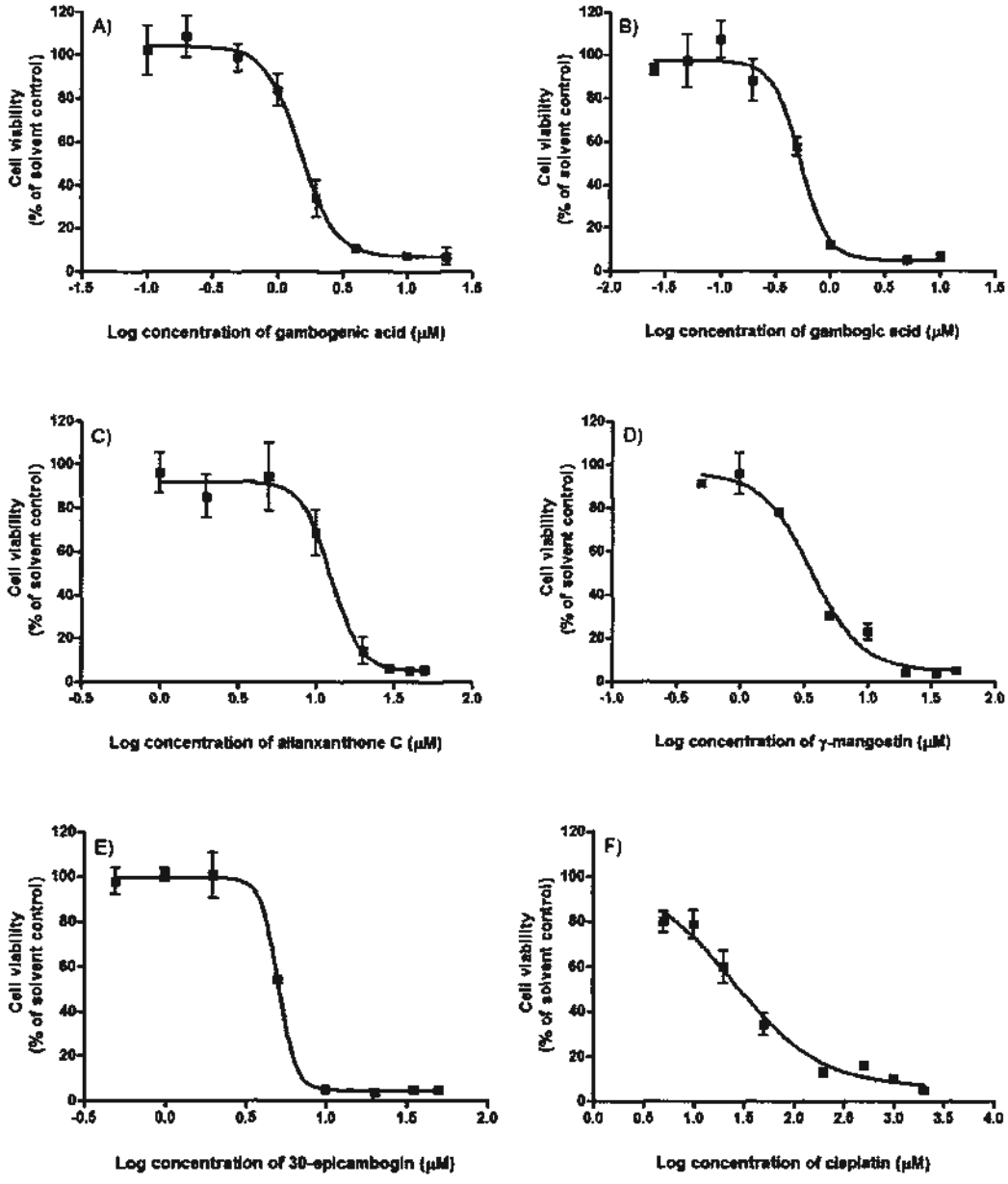

Figure 3.5 Effects of A) gambogic acid, B) gambogic acid, C) allanxanthone C, D) γ-mangostin, E) 30-epicambogin (EPC) and F) cisplatin on the viability of HT-29 cells after 24 h treatment. Data are expressed as mean values ± S.E.M as a percentage of the solvent control. The solvent control was 0.3% DMSO and 12% saline which had no effect on the viability of HT-29 cells. The experiment was performed in triplicate in three independent experiments.

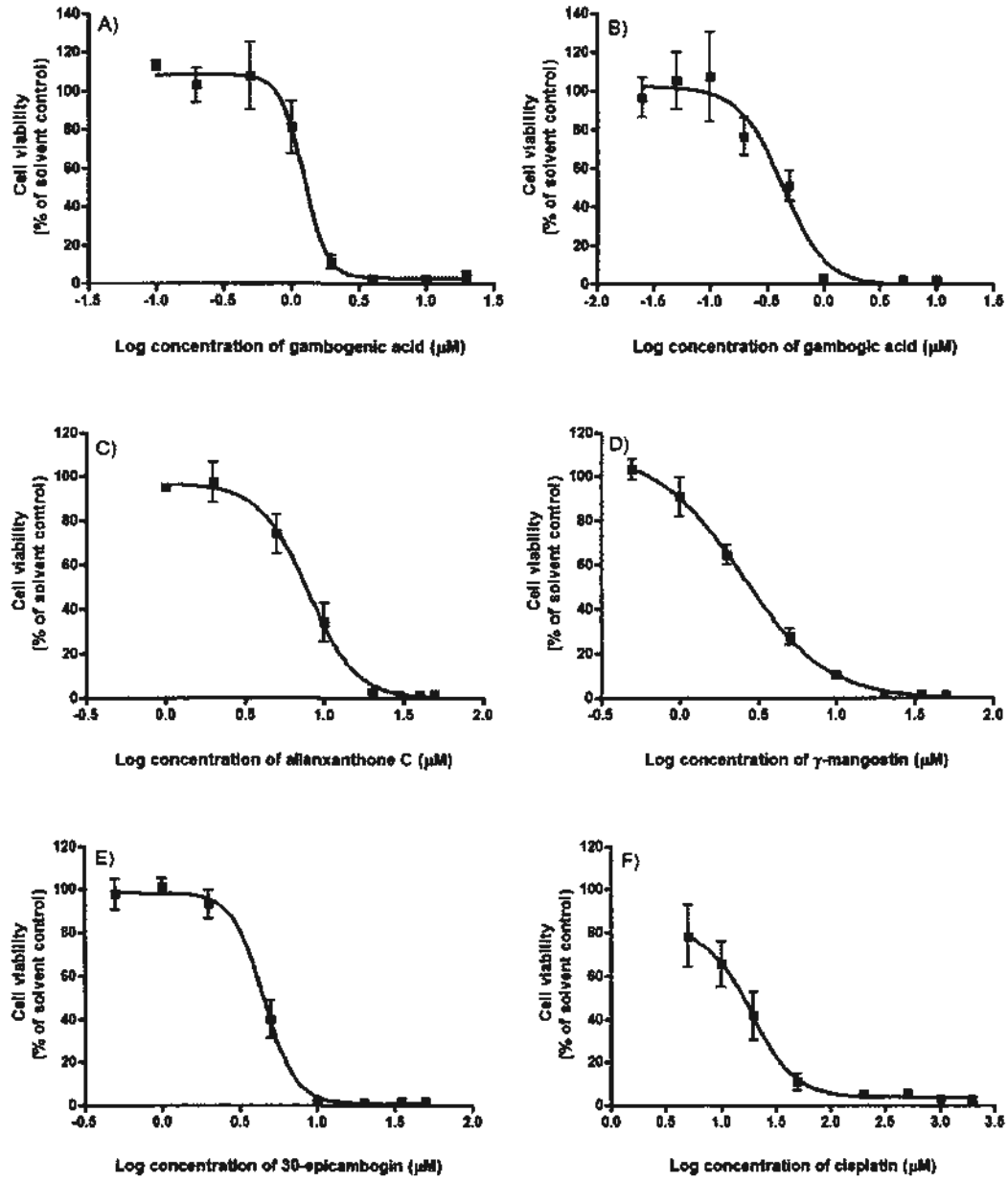

Figure 3.6 Effects of A) gambogic acid, B) gambogic acid, C) allanxanthone C, D) γ-mangostin, E) 30-epicambogin (EPC) and F) cisplatin on the viability of HT-29 cells after 48 h treatment. Data are expressed as mean values ± S.E.M as a percentage of the solvent control. The solvent control was 0.3% DMSO and 12% saline which had no effect on the viability of HT-29 cells. The experiment was performed in triplicate in three independent experiments.

Table 3.4 Cytotoxicity IC_{50} values (μM) of caged xanthones and derivatives isolated from TH on human colon cancer HT-29 cells after 24 h and 48 h treatment

Compound	24 h	48 h
Gambogenic acid	1.52 ± 0.21	1.22 ± 0.07
Gambogic acid	0.50 ± 0.03	0.41 ± 0.13
Allanxanthone C	12.44 ± 1.57	7.70 ± 1.04
γ-Mangostin	3.69 ± 0.25	2.29 ± 0.36
30-Epicambogin (EPC)	5.11 ± 0.07	4.63 ± 0.43
Cisplatin	26.69 ± 4.19	17.83 ± 1.98
5-Fluorouracil	N.D.	93.53 ± 16.09

N.D. indicates that the IC_{50} value was not determined for that time point.

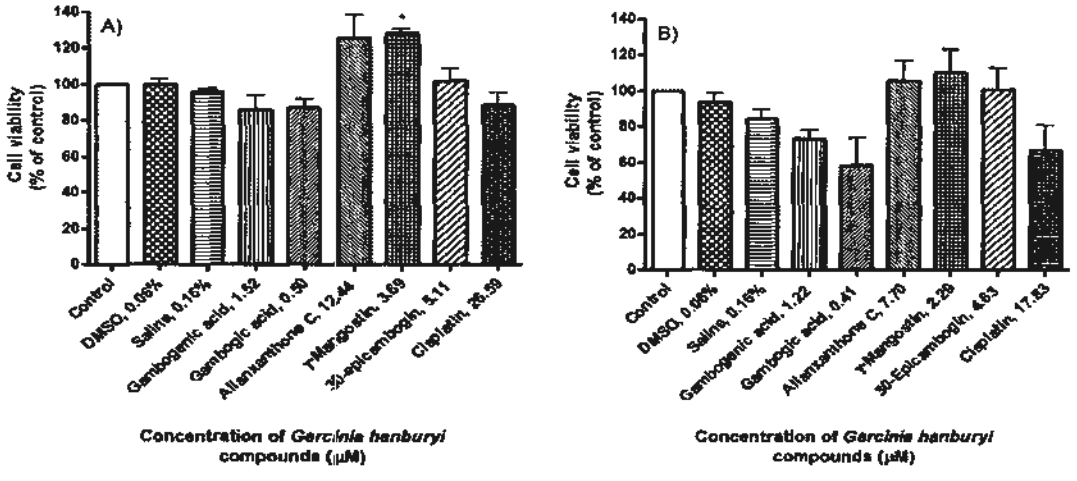

Figure 3.7 Effects of gambogic acid, gambogic acid, allanxanthone C, γ-mangostin, 30-epicambogin (EPC) and cisplatin on the viability of CCD-18Co cells after A) 24 and B) 48 h treatment. Data are expressed as mean values ± S.E.M as a percentage of the untreated control. The statistical comparisons were made between the compounds and the corresponding solvent controls. The experiment was performed in triplicate in three independent experiments. *$p<0.05$ compared with DMSO, 0.06%.

It suggests that EPC, the only benzophenone derivative from the isolated compounds, may have even better selectivity than gambogic acid for inducing cytotoxicity in colon cancer cells without affecting normal colon cells and it is worthy for further study for the development of a new chemotherapeutic drug for colon cancer.

3.2.4 Effects of various caged xanthones and their derivatives isolated from TH on the proliferation of HT-29 cells

All five compounds significantly inhibited the proliferation of HT-29 cells in a dose-dependent manner after 24 h incubation (Figure 3.8). At around each compound's IC_{50} value, cell proliferation was significantly inhibited by at least 50% ($p<0.001$). In particular, at 12.5 μM of allanxanthone C (close to its IC_{50} value), cell proliferation was significantly inhibited to 1.72% ($p<0.001$) (Figure 3.8C). Since γ-mangostin and EPC decreased the proliferation of HT-29 cells by 59.1% and 56.1% at around their IC_{50} values, they may target both cell death and cell proliferation pathways (Figures 3.8D, E). However, at its IC_{50} value, allanxanthone C almost fully suppressed cell proliferation, which suggests that it may mainly target cell proliferation pathways for its *in vitro* anti-cancer mechanism (Figure 3.8C). Out of the five isolated compounds from TH, EPC had potent cytotoxic effects on human colon cancer cells, and better selectivity towards HT-29 cells than the other four xanthones. Moreover, it potently inhibited proliferation of HT-29 cells and its biological effects have not yet been reported. Therefore, EPC was selected for further mechanistic studies for development of a novel anti-cancer drug for colon cancer.

3.2.5 Effects of other compounds structurally-related to EPC on viability of human colon cancer and normal cells

Since EPC had potent cytotoxicity in HT-29 cells, other compounds that are also benzophenone derivatives structurally similar to EPC were also isolated from TH and studied for their cytotoxicity in human colon cancer HT-29 and HCT116 cells. Due to the limited availability of the compounds, only one concentration was selected for study at each time point. The concentrations chosen for this experiment were 5.11 μM and 4.63 μM for 24 and 48 h incubations, respectively, as they were the IC_{50} values for EPC after 24 h and 48 h treatments (Table 3.4), which allowed for easy comparison between the potency of these compounds to EPC.

All of the compounds tested, with the exception of garcicowin A and B and oblongifolin D, significantly reduced the viability of HT-29 cells after 24 h treatment ($p<0.01$) (Figure 3.9A). However, only cambogin and guttiferone K (GUTK) had similar potency to EPC and reduced the viability of cells to less than 50%. After 48 h, garcicowins A and B and oblongifolin D did not have any significant effects on cell viability (Figure 3.9B). After 48 h, EPC, cambogin, guttiferone B and GUTK and oblongifolins B and C significantly decreased the viability of HT-29 cells by more than 50% ($p<0.001$). Cambogin and GUTK were the most potent compounds after 48 h incubation and decreased the viability of HT-29 cells to 23.9% and 28.9%, respectively. In HCT116 cell line, EPC, cambogin and GUTK significantly reduced the cell viability after 24 h treatment ($p<0.01$) and GUTK was the most potent and decreased the viability to 35.3% (Figure 3.10A). After 48 h, the HCT116 cells were more sensitive than HT-29 cells to the effects of the compounds. All of the compounds, except garcicowins A, B and C, exerted significant cytotoxicity to HCT116 cells in a time-dependent manner ($p<0.05$) (Figures 3.10A, B). GUTK and

cambogin at 4.63 μM were the most potent compounds and they decreased the cell viability by 88.7% and 76.5%, respectively (Figure 3.10B). None of the compounds tested showed cytotoxic effect in human normal colon CCD-18Co fibroblast cell line after 24 and 48 h treatment (Figure 3.11). From the results, GUTK and cambogin were the most potent compounds for reducing the viability of both HT-29 and HCT116 cells, without cytotoxicity to CCD-18Co cells. Due to the higher quantity of guttiferone K (GUTK) isolated, GUTK and EPC were selected for further studies on the mechanisms underlying its cytotoxic effects.

3.2.6 Effects of EPC and GUTK on viability and plasma membrane integrity of HT-29

The IC_{50} values of EPC and GUTK are summarized in Table 3.5. Although EPC and GUTK have similar IC_{50} values after 24 h, GUTK was slightly more potent after 48 h. The LDH release into extracellular environment induced by EPC and GUTK was examined to provide further evidence supporting its cytotoxicity in human colon cancer cells. Both EPC and GUTK triggered the loss of membrane integrity of HT-29 cells after 24 h incubation in a dose-dependent manner (Figure 3.10). At 5.0 μM (concentration close to their IC_{50} values) of EPC and GUTK, the percentages of LDH leakage were 18.1% and 12.9%, respectively. At 10.0 μM, EPC significantly induced 83.0% of LDH leakage, while GUTK induced 42.6% of LDH leakage (Figure 3.10). This indicates that EPC induced cell death without compromising membrane integrity over a narrow concentration range, while it took doubled the concentration of GUTK (20.0 μM) to induce the same magnitude of LDH release as EPC at 10.0 μM (Figure 3.10).

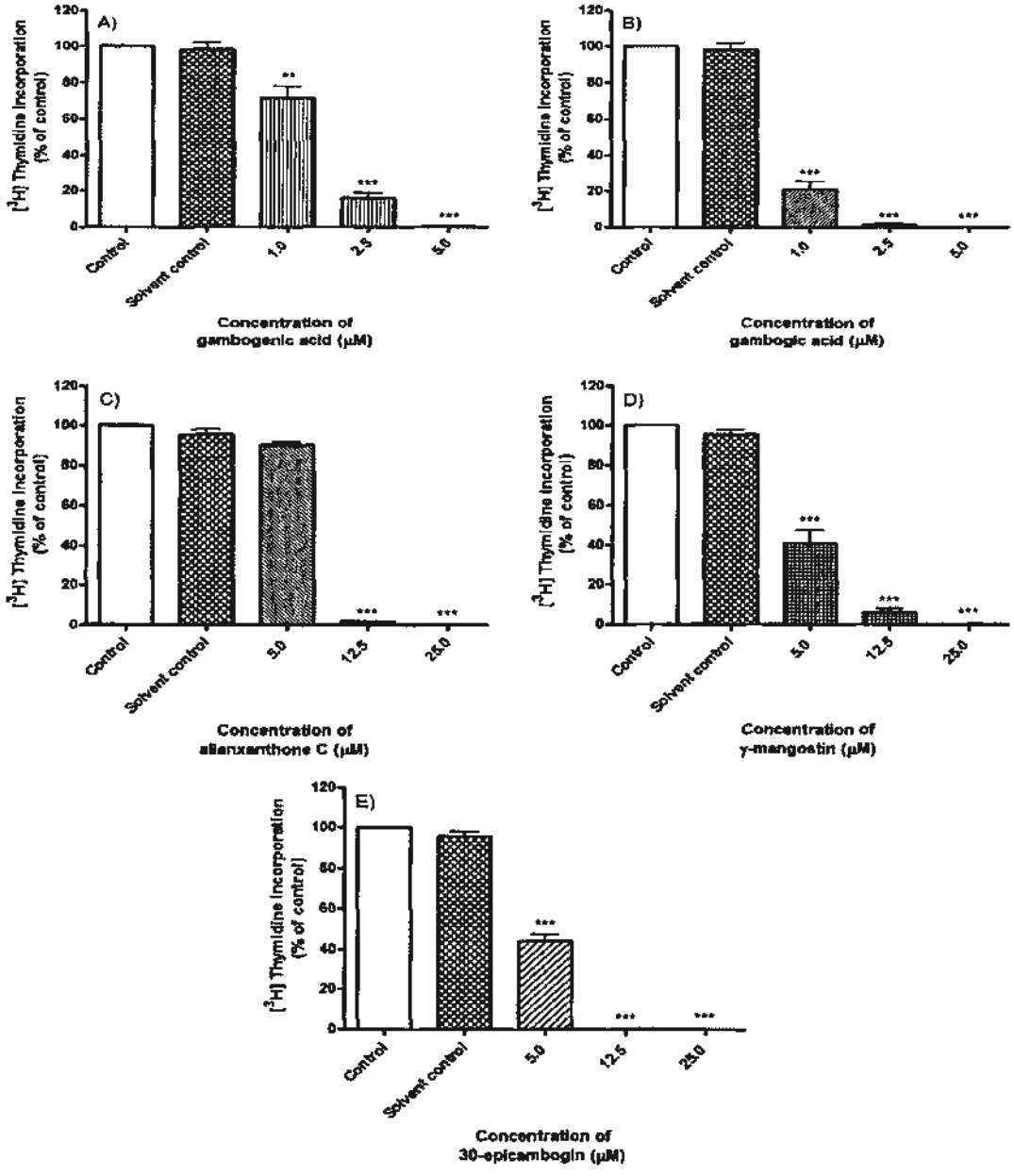

Figure 3.8 Effects of A) gambogenic acid, B) gambogic acid, C) allanxanthone C, d) γ-mangostin and e) 30-epicambogin (EPC) on the proliferation of HT-29 cells after 24 h treatment as assessed by [^{3}H] thymidine incorporation assay. Data are presented as a percentage of control (untreated medium) as mean values ± S.E.M. The solvent controls were 0.03% DMSO for A) and B) and 0.15% DMSO for C), D) and E). The experiment was performed in triplicate in three independent experiments. **$p<0.01$, ***$p<0.001$ compared with solvent control group.

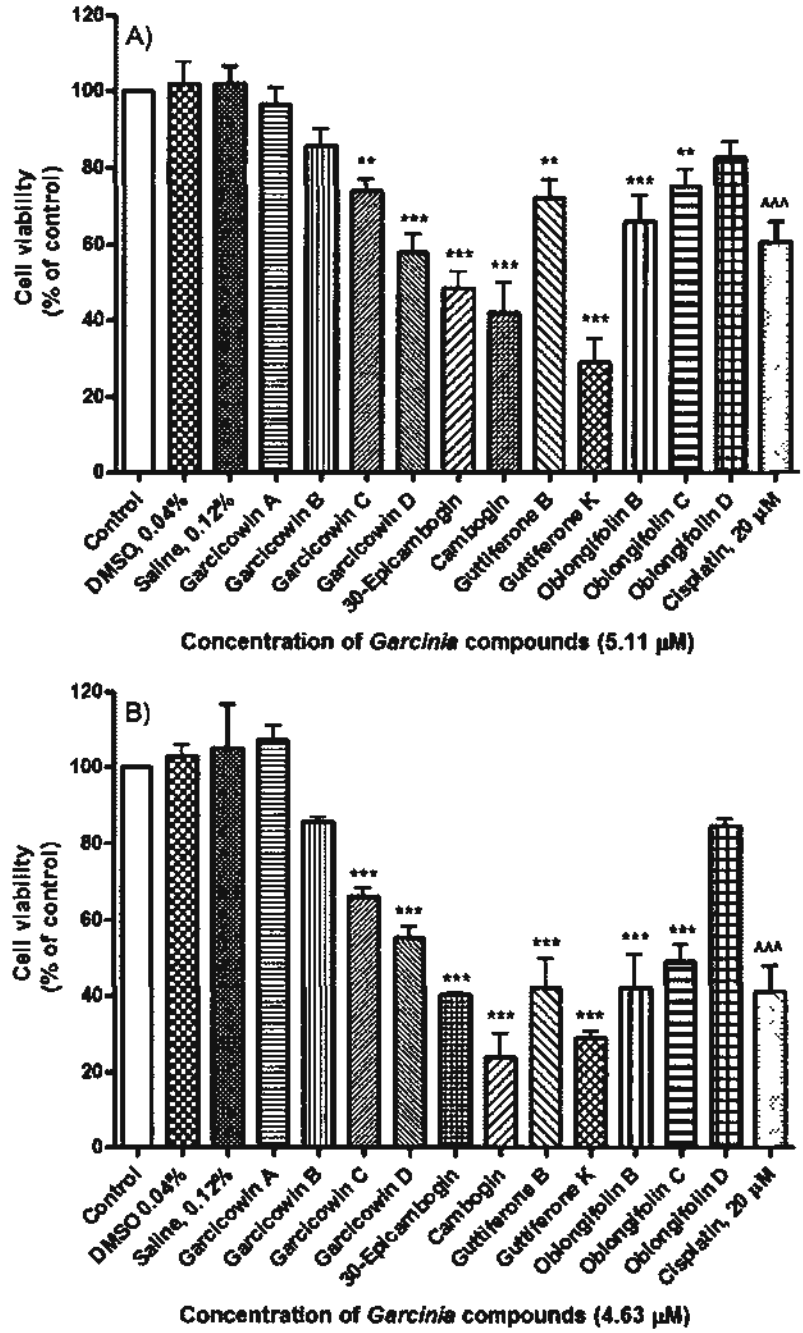

Figure 3.9 Effects of various xanthones and benzophenone derivatives from TH on the viability of HT-29 cells after A) 24 and B) 48 h treatment. Data are expressed as mean values ± S.E.M as a percentage of the untreated control. The statistical comparisons were made between the compounds and the corresponding solvent controls. The experiment was performed in triplicate in three independent experiments. **p<0.01, ***p<0.001 compared with DMSO, 0.04%; ^^^p<0.001 compared with saline, 0.12%.

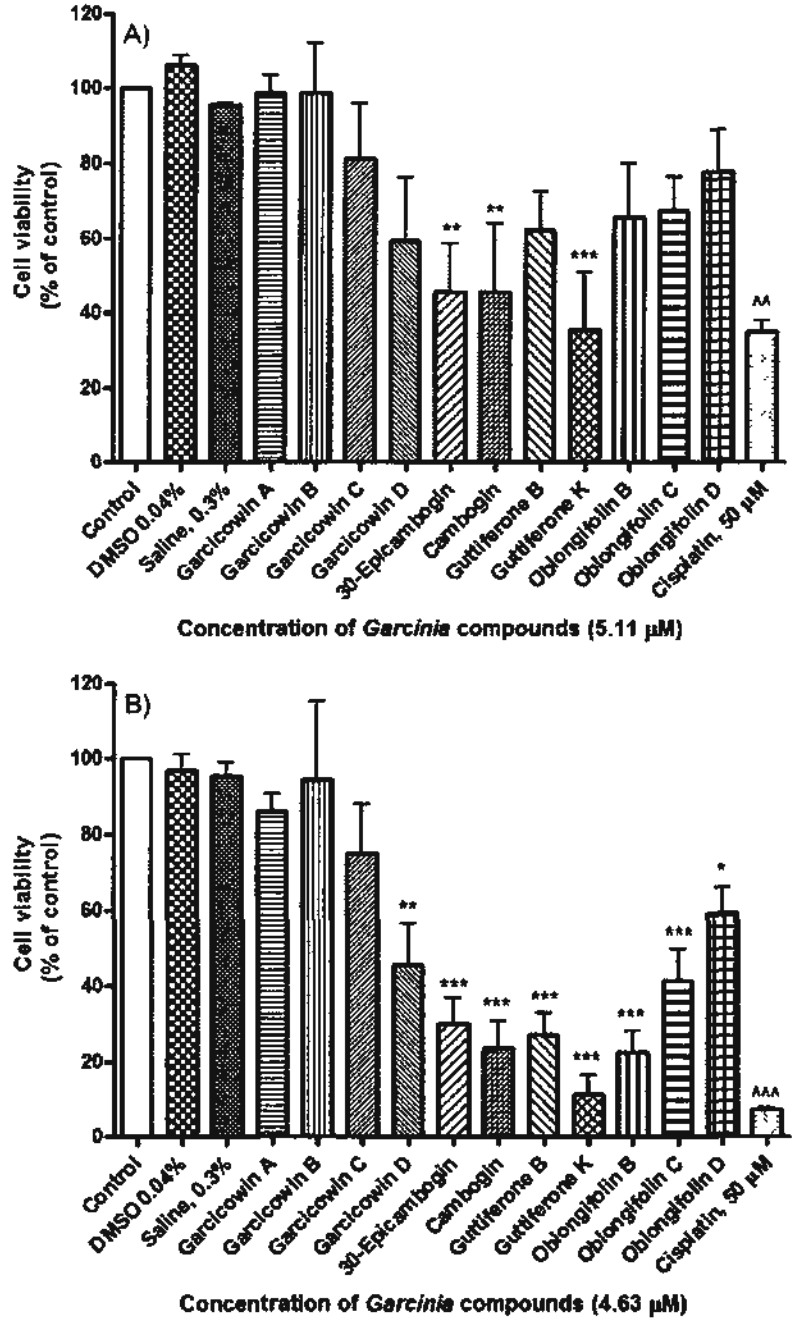

Figure 3.10 Effects of various xanthones and benzophenone derivatives from TH on the viability of HCT116 cells after A) 24 and B) 48 h treatment. Data are expressed as mean values ± S.E.M as a percentage of the untreated control. The statistical comparisons were made between the compounds and the corresponding solvent controls. The experiment was performed in triplicate in three independent experiments. *p<0.05, **p<0.01, ***p<0.001 compared with DMSO; 0.04%. ^^p<0.01, ^^^p<0.001 compared with saline, 0.3%.

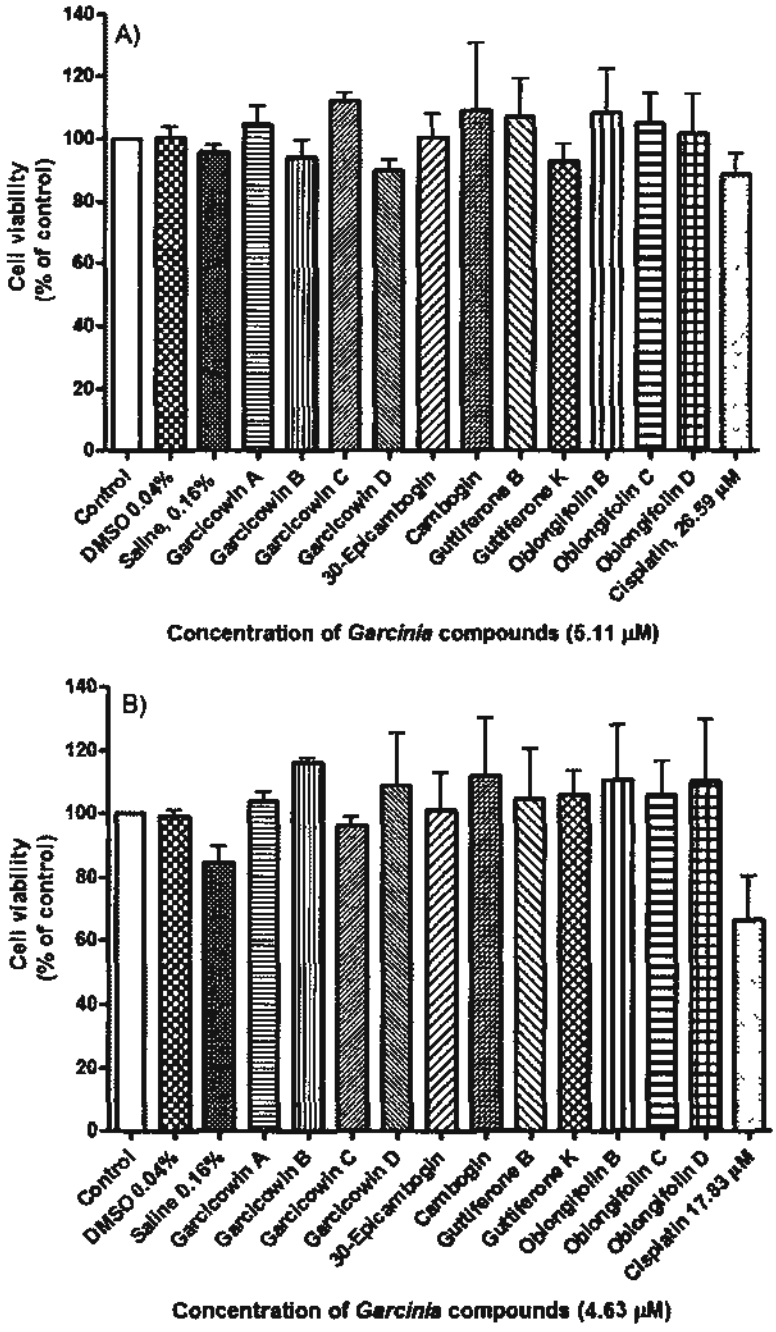

Figure 3.11 Effects of various xanthones and benzophenone derivatives from TH on the viability of CCD-18Co cells after A) 24 and B) 48 h treatment. Data are expressed as mean values ± S.E.M as a percentage of the untreated control. The statistical comparisons were made between the compounds and the corresponding solvent controls. The experiment was performed in triplicate in three independent experiments.

Table 3.5 Cytotoxicity IC_{50} values (μM) of EPC and GUTK on human colon cancer HT-29 cells after 24 h and 48 h treatment

	24 h	**48 h**
30-Epicambogin (EPC)	5.11 ± 0.07	4.63 ± 0.43
Guttiferone K (GUTK)	5.39 ± 0.22	3.29 ± 0.25

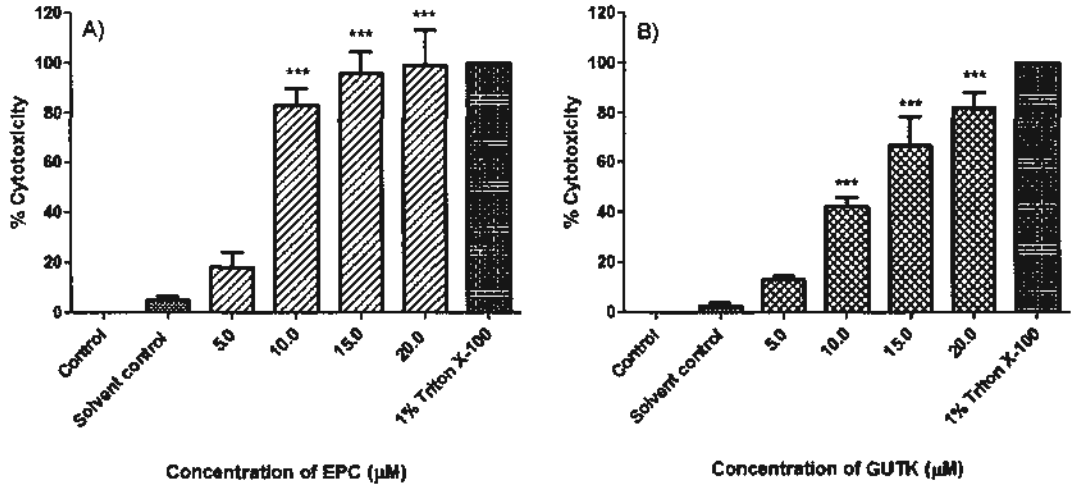

Figure 3.12 Effects of A) EPC and B) GUTK on LDH release with loss of plasma membrane integrity in HT-29 cells after 24 h treatment. Untreated control cells were normalized as 0% cytotoxicity and Triton X-100-treated positive control cells were normalized as 100% cytotoxicity. The solvent control was 0.06% DMSO. The experiment was performed in triplicate in three independent experiments and data was presented as mean values ± S.E.M. ***$p<0.001$ compared with the solvent control.

3.2.7 Effects of EPC and GUTK on the cell cycle distribution of HT-29 cells

To acquire a better understanding of the mechanisms behind the cytotoxic and anti-proliferative effects of EPC and GUTK, cell cycle analysis using propidium iodide staining was conducted (Figures 3.13, 3.14). The concentrations selected for this study were based on their IC_{50}, 2 x IC_{50}, 3 x IC_{50} and 4 x IC_{50} values after 24 h incubation. After 24 h treatment, EPC triggered a dose-dependent accumulation of cells in G_0/G_1 and sub-G_1 phases, with simultaneous reduction of cells in S and G_2/M phases (Figure 3.13A). HT-29 cells were either arrested at G_0/G_1 phase or entered sub-G_1 apoptotic phase after EPC treatment, which prevented them from migrating into the subsequent S and G_2/M phases. The effects of 10.0 μM EPC on the cell cycle were examined after 6, 12 and 24 h to track the time course of cell cycle events after treatment. No significant changes in cell cycle phases were observed after 6 h (Figure 3.13B). Yet, after 12 h, EPC increased the number of cells in G_0/G_1 phase, from 46.9% in the solvent control to 74.9% after EPC treatment (Figure 3.13C). This was accompanied with an increase from 4.4% to 13.4% of cells in sub-G_1 phase. Furthermore, the percentage of cells significant reduced from 42.7% to 9.5% in S phase, which is in accordance with the results from the [^{3}H]-thymidine incorporation studies ($p<0.001$) (Figures 3.8E, 3.13C). After 24 h, the cell cycle arrest at G_0/G_1 and inhibition of S and G_2/M phases ($p<0.05$) continued (Figure 3.13D).

While there was no significant change in the G_0/G_1 phase after GUTK treatment for 24 h in HT-29 cells, there was a dose-dependent decline in the percentage of cells in S and G_2/M phases (Figure 3.14A). In addition, a significant dose-dependent increase in sub-G_1 phase was observed after GUTK treatment ($p<0.05$). Similar to EPC, GUTK did not induce any changes in cell cycle phases after 6 h, except with a 5.3% decrease of cells in S phase (Figure 3.14B). After 12 h, GUTK induced an increase of

HT-29 cells from 6.2% to 21.7% in sub-G_1 phase and from 49.0% to 68.5% of cells in G_0/G_1 phase (Figure 3.14C). The number of cells in S phase was significantly reduced by 30.4%, which supports cytotoxic and anti-proliferative activity of GUTK in HT-29 cells ($p<0.001$). After 24 h, the G_0/G_1 arrest and inhibition of DNA synthesis in S phase were maintained, but not with the same severity as at 12 h. Many of the cells that were once accumulated in G_0/G_1 phase entered into sub-G_1 phase (Figure 3.14D). From the results, EPC and GUTK significantly affected the cell cycle distribution to lead to G_0/G_1 arrest and sub-G_1 accumulation of cells as early as after 12 h incubation.

3.2.8 Effects of EPC and GUTK on protein expression of proteins associated with G_1/S phase progression

At the G_1/S phase transition, CDK4 or CDK6 binds to Cyclin D1, D2 or D3 for activation and phosphorylation of Rb protein and downstream transcription of genes needed for the subsequent cell cycle phases (Ekholm & Reed, 2000). The activity of cyclin/cdk complexes are modulated by INK4 and CIP/KIP family of cell cycle inhibitors (Lee & Kim, 2009). Therefore, the effects of EPC and GUTK on the protein expressions of G_1/S cyclins and CDKs and INK4 and CIP/KIP families of cell cycle inhibitors were investigated after 12 h and 24 h treatment since effects of EPC and GUTK on cell cycle distribution were most prominent after these two time points. EPC reduced the protein expression of cyclin D1 and cyclin D3 in a dose- and time-dependent manner (Figure 3.15). At 10.0 μM, EPC significantly decreased cyclin D3 levels after 12 h and 24 h incubation ($p<0.001$) (Figures 3.15A, D, E). Similarly, EPC dose- and time-dependently decreased CDK4 and CDK6 levels after 12 h and 24 h incubation (Figure 3.16). GUTK also decreased protein levels of cyclin D1 and D3, and at 10.0 μM, it reduced cyclin D3 levels by more than 50% (Figures

3.17A, D, E). As well, GUTK significantly diminished the protein expression of CDK4 and CDK6 after both 12 h and 24 h time points ($p<0.01$) (Figure 3.18). The sharp increase in band intensities of cyclin D1 and cdk4 levels after 24 h incubation of EPC at 15.0 μM is due to the lower amount of total protein (as indicated by the weaker β-actin band) (Figures 3.15A and C, 3.16A and C). Generally speaking, the effects of EPC and GUTK were most severe after 12 h treatment and maintained until 24 h (Figures 3.15-3.18). The reduction of cyclin D3 and CDK4 expression by EPC and GUTK was more prominent compared to reduction cyclin D1 and CDK6, which suggests that these two compounds may decrease levels of cyclin D3 and CDK4 with higher selectivity.

3.2.9 Effects of EPC and GUTK on protein expression of CDK inhibitors

Since the INK4 and CIP/KIP family of CDK inhibitors are important negative regulators of cell cycle progression, the effects of EPC and GUTK on the protein expression of INK4 ($p15^{INK4B}$ and $p16^{INK4A}$) and CIP/KIP ($p21^{Waf1/Cip1}$ and $p27^{Kip1}$) family members were investigated. As shown in Figures 3.19A and 3.21A, there is no significant change in the expression of $p15^{INK4B}$ induced by EPC or GUTK. The decrease in $p15^{INK4B}$ band density after 15.0 μM of EPC treatment for 24 h is most likely due to the decreased number of viable cells, as indicated by the weaker β-actin band and not induced by EPC (Figure 3.19A). In HT-29 cells, no $p16^{INK4A}$ was detected, even after increasing cell density and primary and secondary antibody concentration and modifying other experimental parameters (Figures 3.19 and 3.21). It has been reported that there was a loss of $p16^{INK4A}$ expression in 84.1% of primary human colon adenomas and 61.4% of human colon adenocarcinoma specimens (Ayhan *et al.*, 2010). Hence, it is not surprising that there is no $p16^{INK4A}$ expressed in HT-29 cell line.

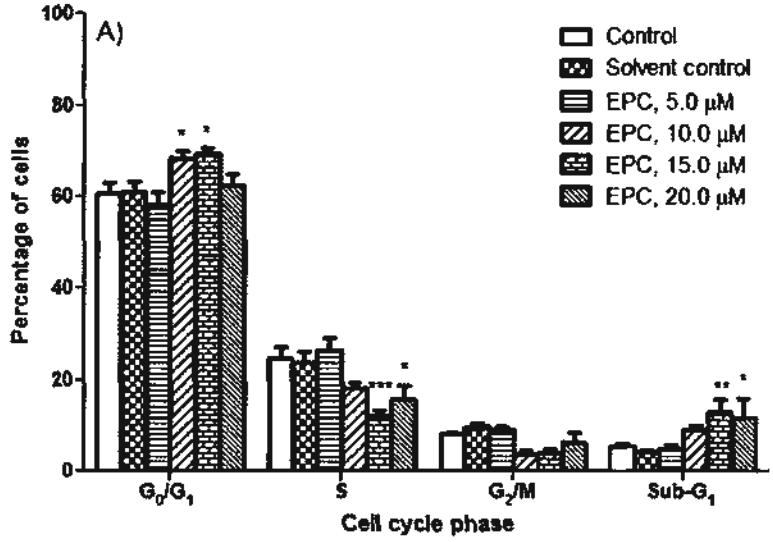
A)
Control
Solvent control
EPC, 5.0 μM
EPC, 10.0 μM
EPC, 15.0 μM
EPC, 20.0 μM
Percentage of cells
100
80
60
40
20
0
G_0/G_1
S
G_2/M
Sub-G_1
Cell cycle phase

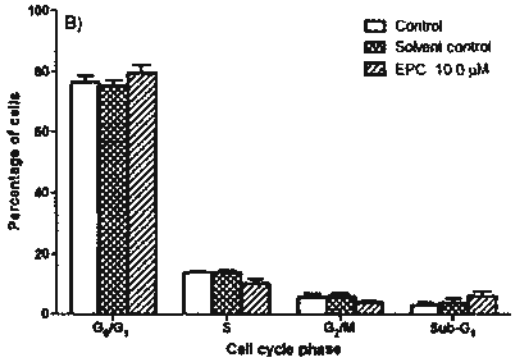
B)
Control
Solvent control
EPC 10.0 μM
Percentage of cells
Cell cycle phase

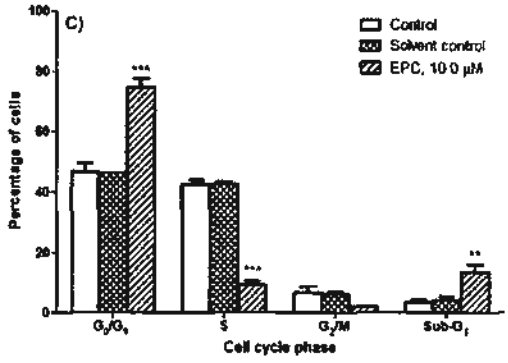
C)
Control
Solvent control
EPC, 10.0 μM
Percentage of cells
Cell cycle phase

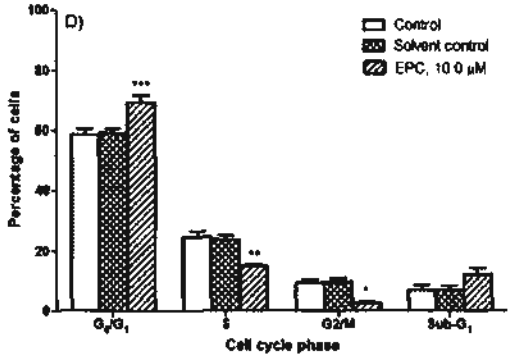
D)
Control
Solvent control
EPC, 10.0 μM
Percentage of cells
Cell cycle phase

E)

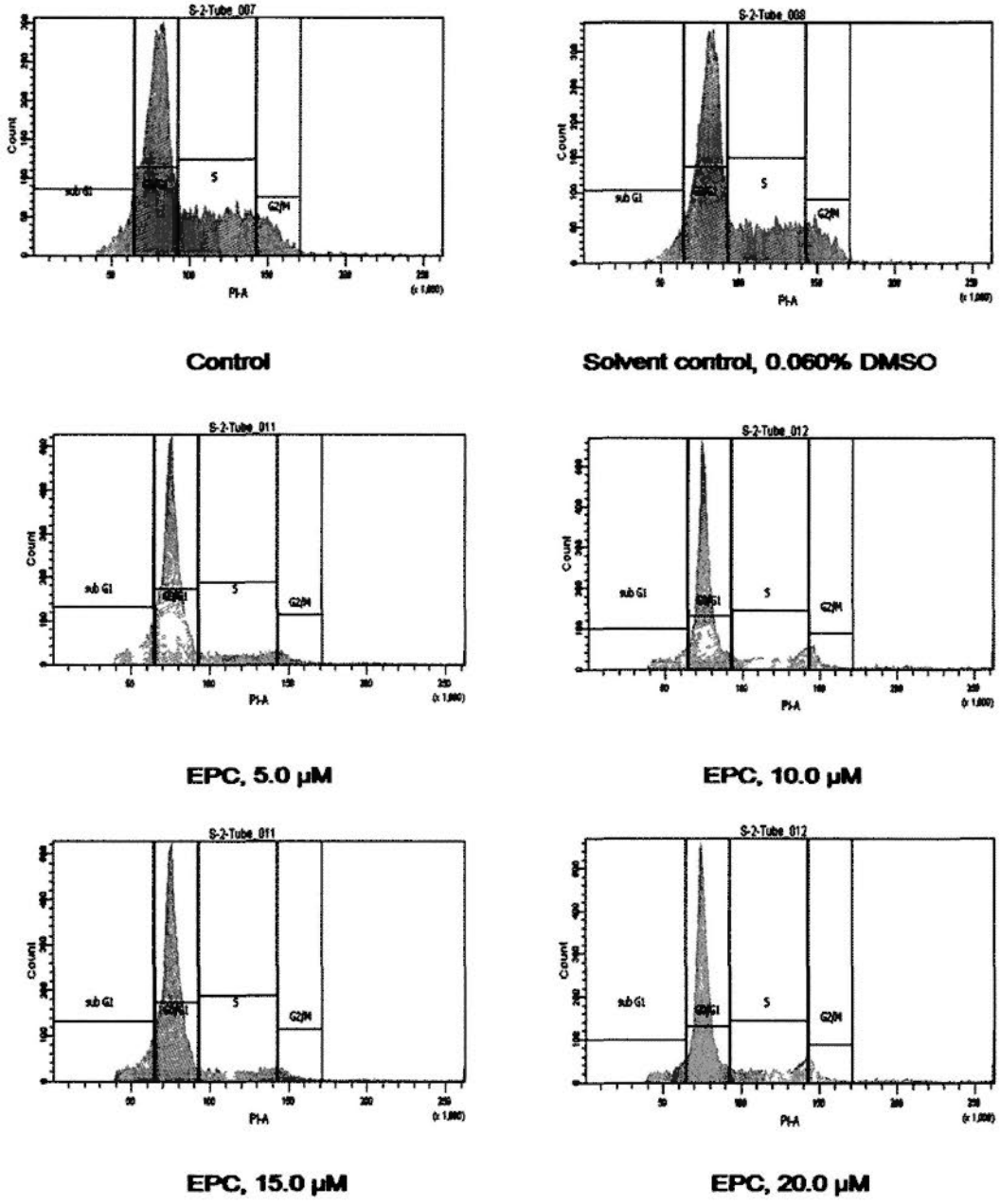

Figure 3.13 Effects of various concentrations of EPC on distribution of HT-29 cells in various phases of the cell cycle after A) 24 h treatment. The effects of EPC at 10.0 µM on cell cycle after B) 6 h, C) 12 h and D) 24 h treatment were also examined. The raw data in histogram form after 24 h EPC treatment are also shown in E). Data are presented as a percentage of control (untreated medium) as mean values ± S.E.M. from three independent experiments. *p<0.05, **p<0.01, ***p<0.001 compared with solvent control in respective phase of cell cycle.

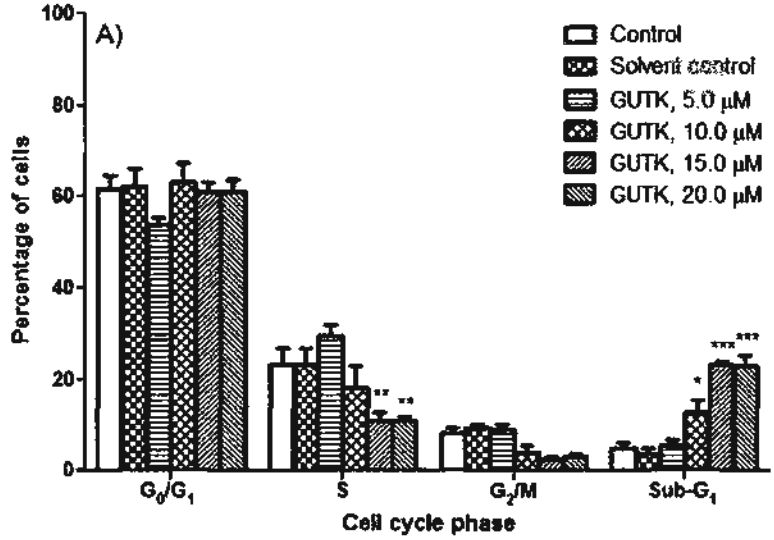
A)
Control
Solvent control
GUTK, 5.0 μM
GUTK, 10.0 μM
GUTK, 15.0 μM
GUTK, 20.0 μM
Percentage of cells
100
80
60
40
20
0
G_0/G_1
S
G_2/M
Sub-G_1
Cell cycle phase

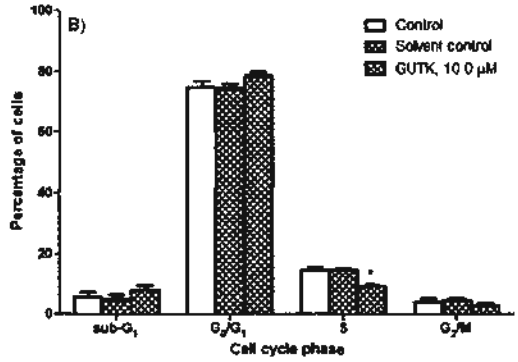
B)
Control
Solvent control
GUTK, 10.0 μM
Percentage of cells
sub-G_1
G_0/G_1
S
G_2/M
Cell cycle phase

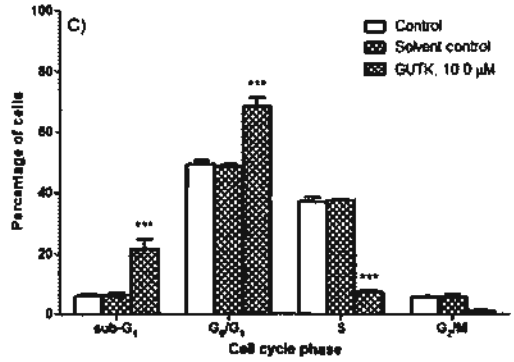
C)
Control
Solvent control
GUTK, 10.0 μM
Percentage of cells
sub-G_1
G_0/G_1
S
G_2/M
Cell cycle phase

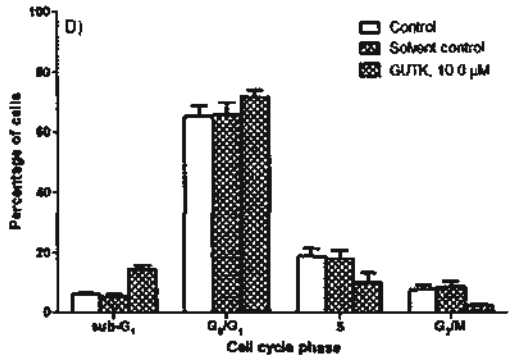
D)
Control
Solvent control
GUTK, 10.0 μM
Percentage of cells
sub-G_1
G_0/G_1
S
G_2/M
Cell cycle phase

E)

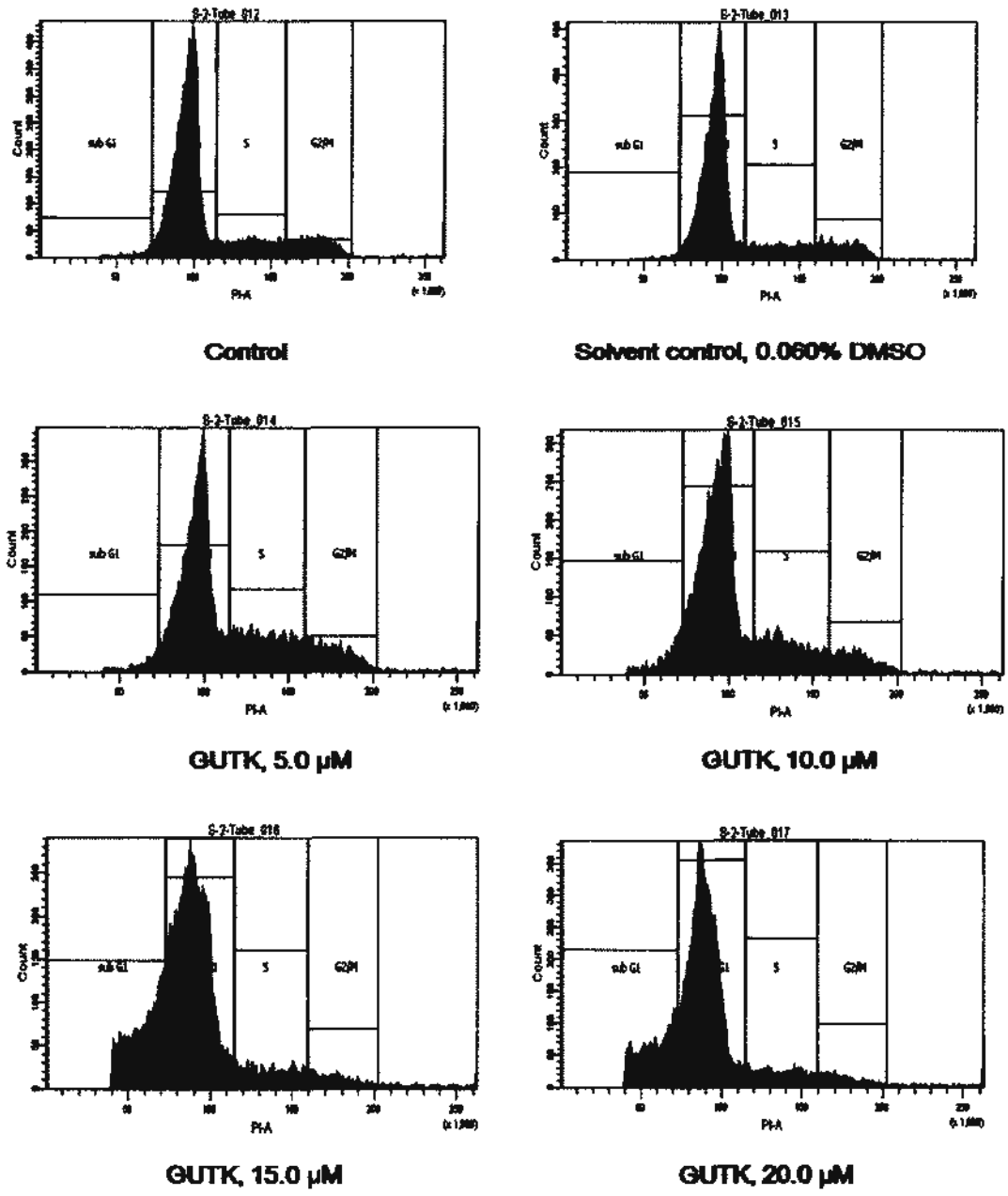

Figure 3.14 Effects of various concentrations of GUTK on distribution of HT-29 cells in various phases of the cell cycle after A) 24 h treatment. The effects of GUTK at 10.0 µM on cell cycle after B) 6 h, C) 12 h and D) 24 h treatment were also examined. The raw data in histogram form after 24 h GUTK treatment are also shown in E). Data are presented as a percentage of control (untreated medium) as mean values ± S.E.M. from three independent experiments. *p<0.05, **p<0.01, ***p<0.001 compared with solvent control in respective phase of cell cycle.

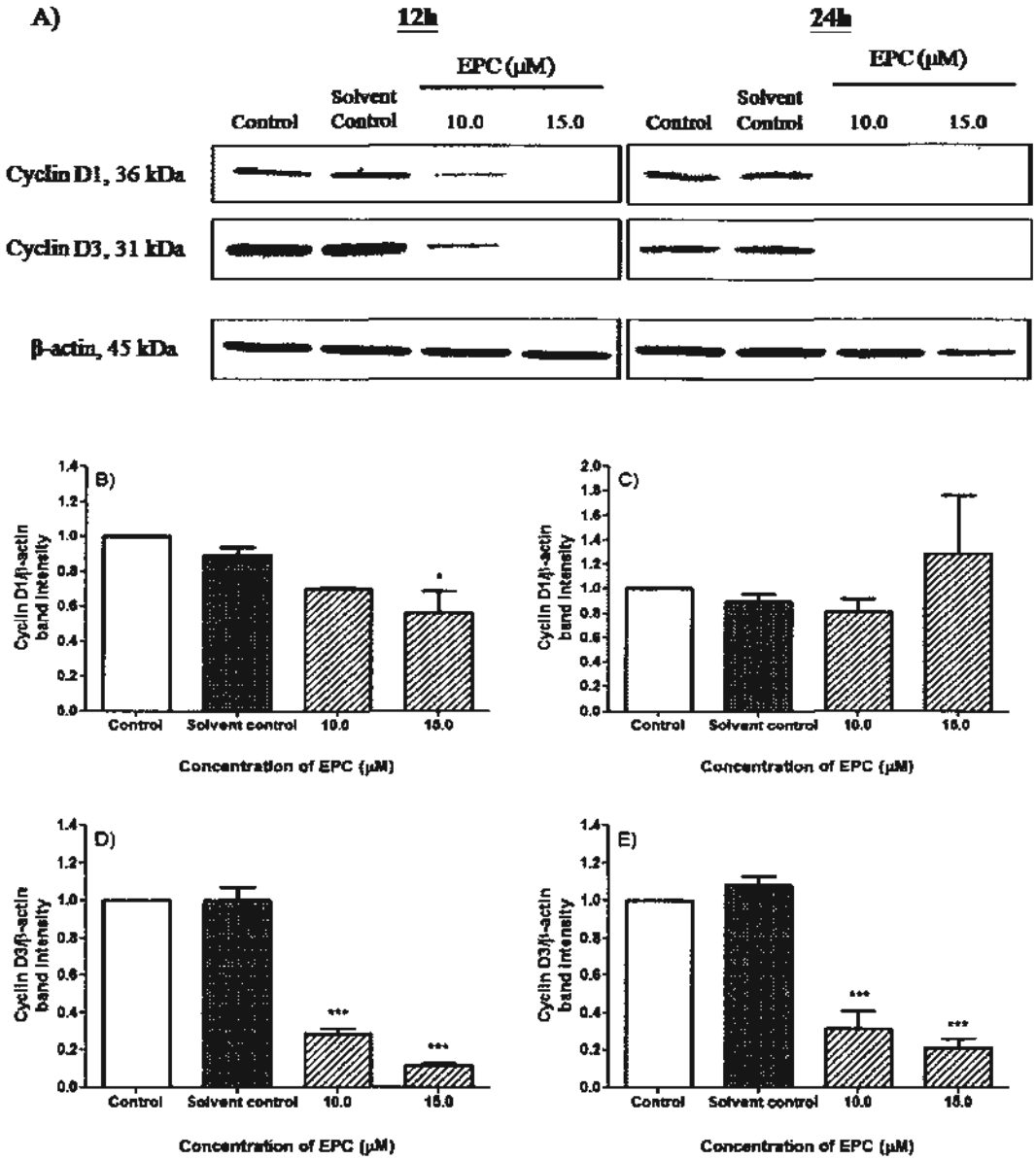

Figure 3.15 Effects of EPC on protein expression of A) cyclins D1 and D3 after 12 h and 24 h treatment in HT-29 cells. The band intensity was quantified using the Quantity One software and the band intensity of the cyclin was normalized with that of β-actin and the band intensity of untreated control was considered as one. The band intensity of cyclin D1 after EPC treatment for B) 12 h and C) 24 h and of cyclin D3 after D) 12 h and E) 24 h treatment are shown. Data are presented as mean values ± S.E.M. from three independent experiments.*$p<0.05$, ***$p<0.001$ compared with the solvent control

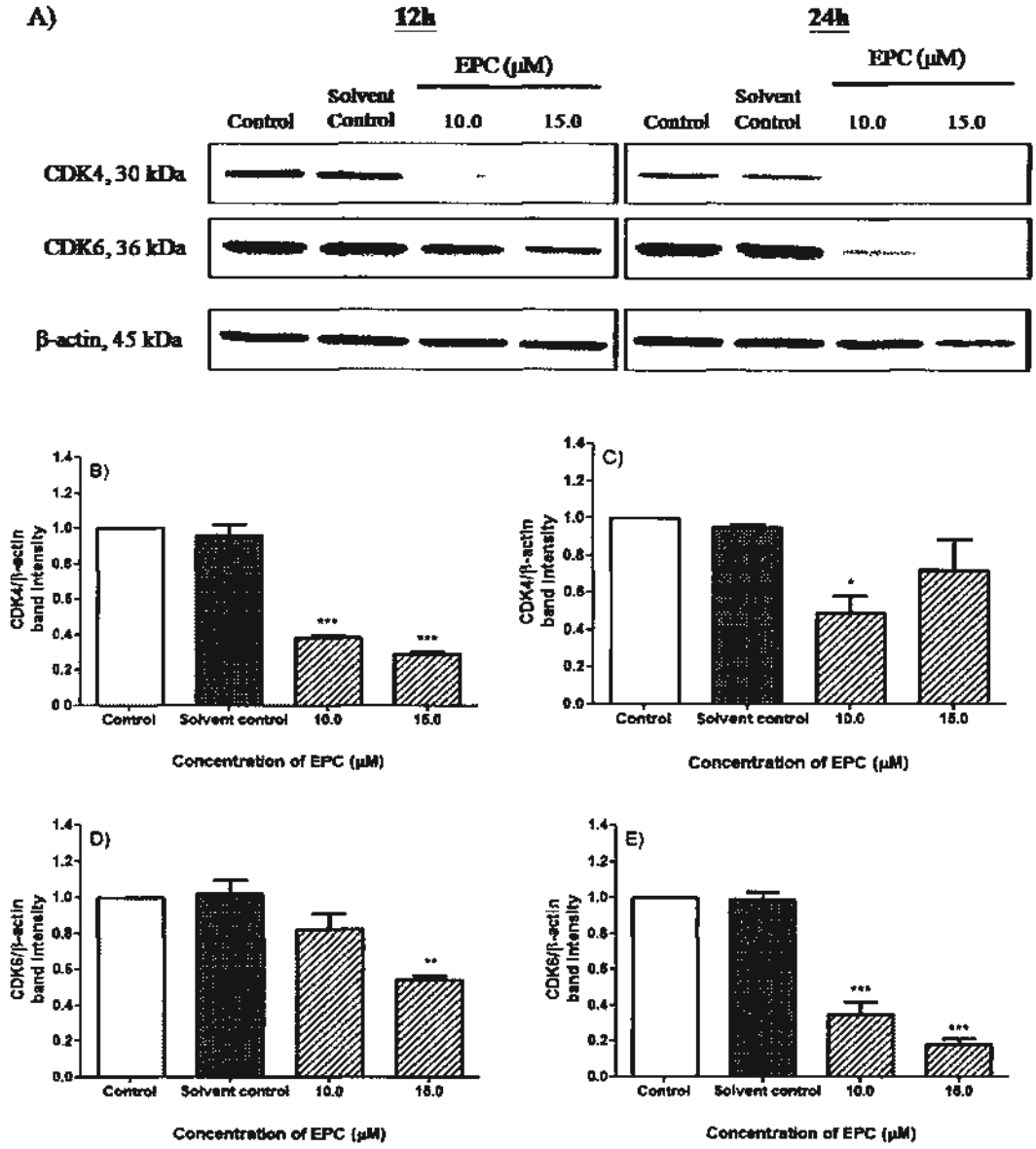

Figure 3.16 Effects of EPC on protein expression of A) CDK4 and CDK6 after 12 h and 24 h treatment in HT-29 cells. The band intensity was quantified using the Quantity One software and the band intensity of the CDK was normalized with that of β-actin and the band intensity of untreated control was considered as one. The band intensity of CDK4 after EPC treatment for B) 12 h and C) 24 h and of CDK6 for D) 12 h and E) 24 h treatment are shown. Data are presented as mean values ± S.E.M. from three independent experiments. *$p<0.05$, **$p<0.01$, ***$p<0.001$ compared with the solvent control

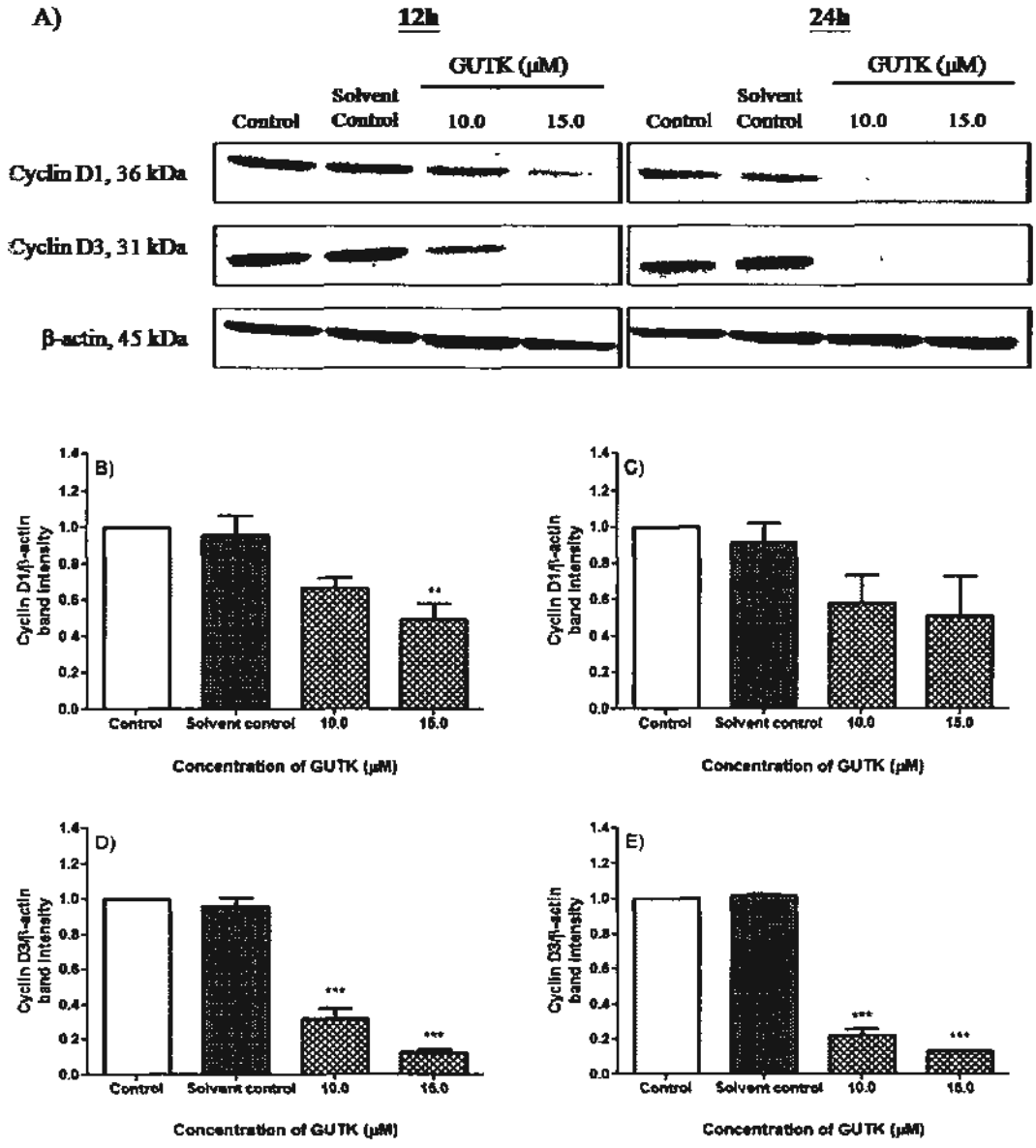

Figure 3.17 Effects of GUTK on protein expression of A) cyclins D1 and D3 after 12 h and 24 h treatment in HT-29 cells. The band intensity was quantified using the Quantity One software and the band intensity of the cyclin was normalized with that of β-actin and the band intensity of untreated control was considered as one. The band intensity of Cyclin D1 after GUTTK treatment for B) 12 h and C) 24 h and of Cyclin D3 for D) 12 h and E) 24 h treatment are shown. Data are presented as mean values ± S.E.M. from three independent experiments. **p<0.01, ***p<0.001 compared with the solvent control

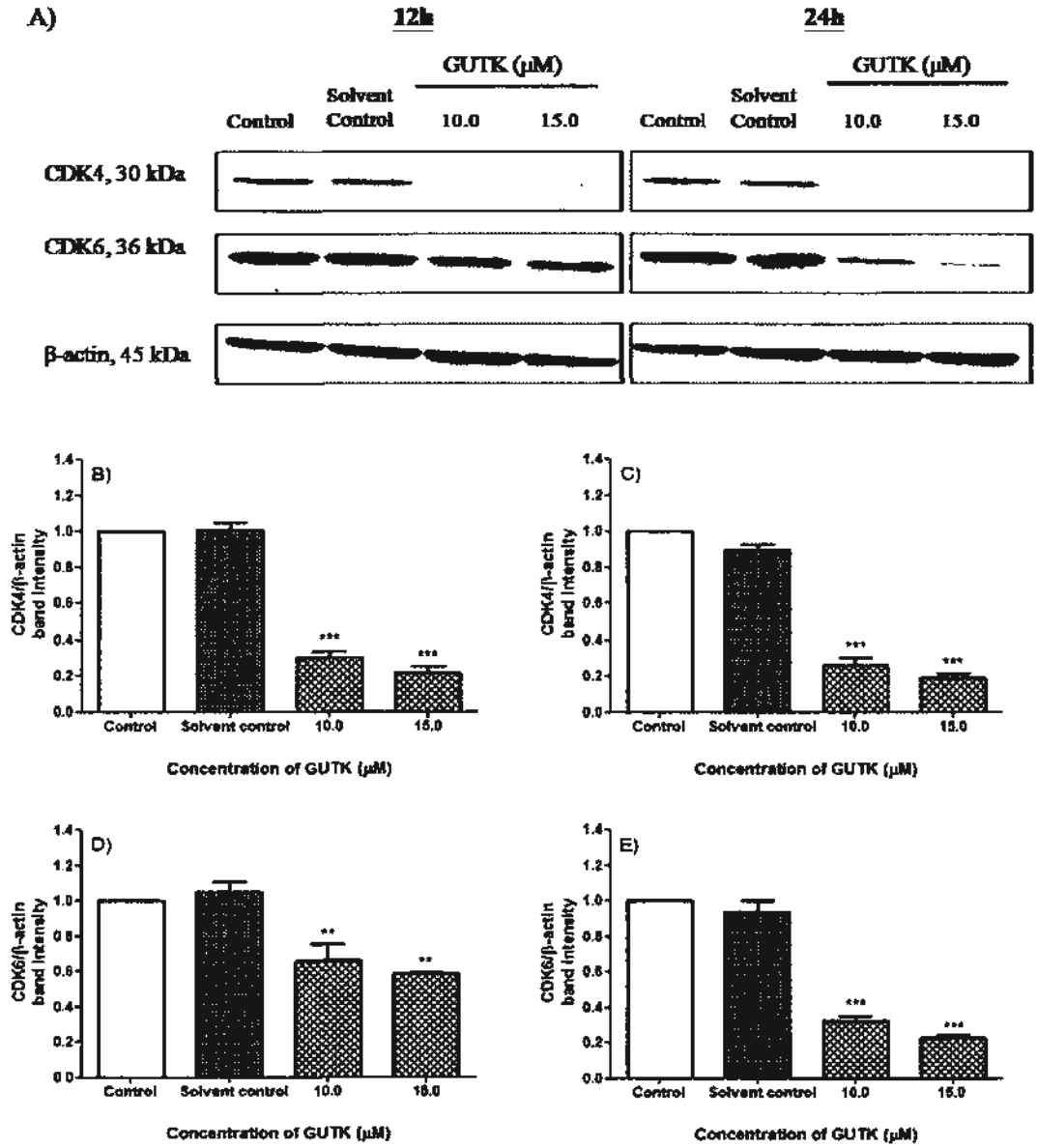

Figure 3.18 Effects of GUTK on protein expression of A) CD4 and CDK6 after 12 h and 24 h treatment in HT-29 cells. The band intensity was quantified using the Quantity One software and the band intensity of the CDK was normalized with that of β-actin and the band intensity of untreated control was considered as one. The band intensity of CDK4 after GUTK treatment for B) 12 h and C) 24 h and of CDK6 for D) 12 h and E) 24 h treatment are shown. Data are presented as mean values ± S.E.M. from three independent experiments. **p<0.01, ***p<0.001 compared with the solvent control

After 10.0 μM of EPC treatment, there was a significant increase of $p21^{Waf1/Cip1}$ and $p27^{Kip1}$ by 10.4-fold and 3.0-fold , respectively, after 12 h treatment, which was maintained until 24 h ($p<0.05$) (Figures 3.20A, B, D). After 12 h treatment, GUTK (10.0 μM) also increased $p21^{Waf1/Cip1}$ and $p27^{Kip1}$ levels by 15.4-fold and 2.0-fold, respectively, (Figures 3.22A, B, D). The increase of $p21^{Waf1/Cip1}$ protein expression was stronger than $p27^{Kip1}$ expression after both EPC and GUTK (at 10.0 and 15.0 μM) treatment, which suggested that these two compounds may target $p21^{Waf1/Cip1}$ with higher selectivity. EPC and GUTK decreased protein expression of cyclins D1 and D3 and CDK4 and CDK6 and increased protein expression of $p21^{Waf1/Cip1}$ and $p27^{Kip1}$, which led to G_0/G_1 arrest.

3.2.10 Effects of EPC and GUTK on nuclear morphology of HT-29 cells

HT-29 cells treated with medium or DMSO (0.060%) aggregated in clusters and they showed homogenous staining of rounded nuclei, as shown by DAPI staining. As observed under brightfield microscopy at 100x and 400x, there was a gradual loss of adherent cells and cell clustering with increasing concentrations of EPC and GUTK, especially after 10.0 and 15.0 μM treatment for 24 h (Figures 3.23 and 3.24). After HT-29 cells were treated with 10.0 μM of EPC or GUTK, condensed chromatin on the periphery of the nuclei and fragmented nuclei were observed (indicated by red arrows) as morphological hallmarks of apoptosis (Kerr *et al.*, 1972). The fragmented nuclei also became smaller, as the cells shrinked in size (brightfield 400x, fluorescence 400x). After 15.0 μM of EPC treatment, there were very few cells that could be stained with DAPI as most cells have detached (Figure 3.23). Treatment of cells with 15.0 μM of GUTK resulted in severe fragmentation of nuclei and formation of apoptotic bodies (Figure 3.24).

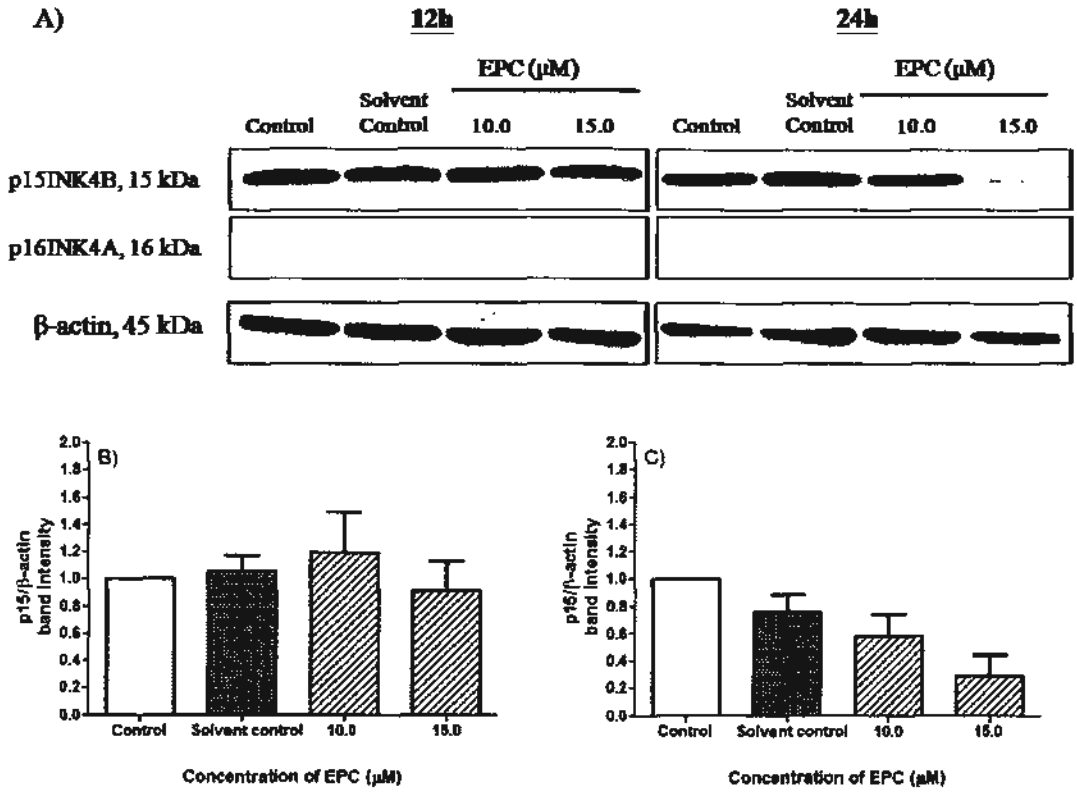

Figure 3.19 Effects of EPC on protein expression of A) $p15^{INK4B}$ and $p16^{INK4A}$ after 12 h and 24 h treatment in HT-29 cells. The band intensity was quantified using the Quantity One software and the band intensity of the INK4 family was normalized with that of β-actin and the band intensity of untreated control was considered as one. The band intensity of $p15^{INK4B}$ after EPC treatment for B) 12 h and C) 24 h are shown. The band density of $p16^{INK4A}$ was not calculated due to lack of p16 expression in HT-29 cells. Data are presented as mean values ± S.E.M. from three independent experiments.

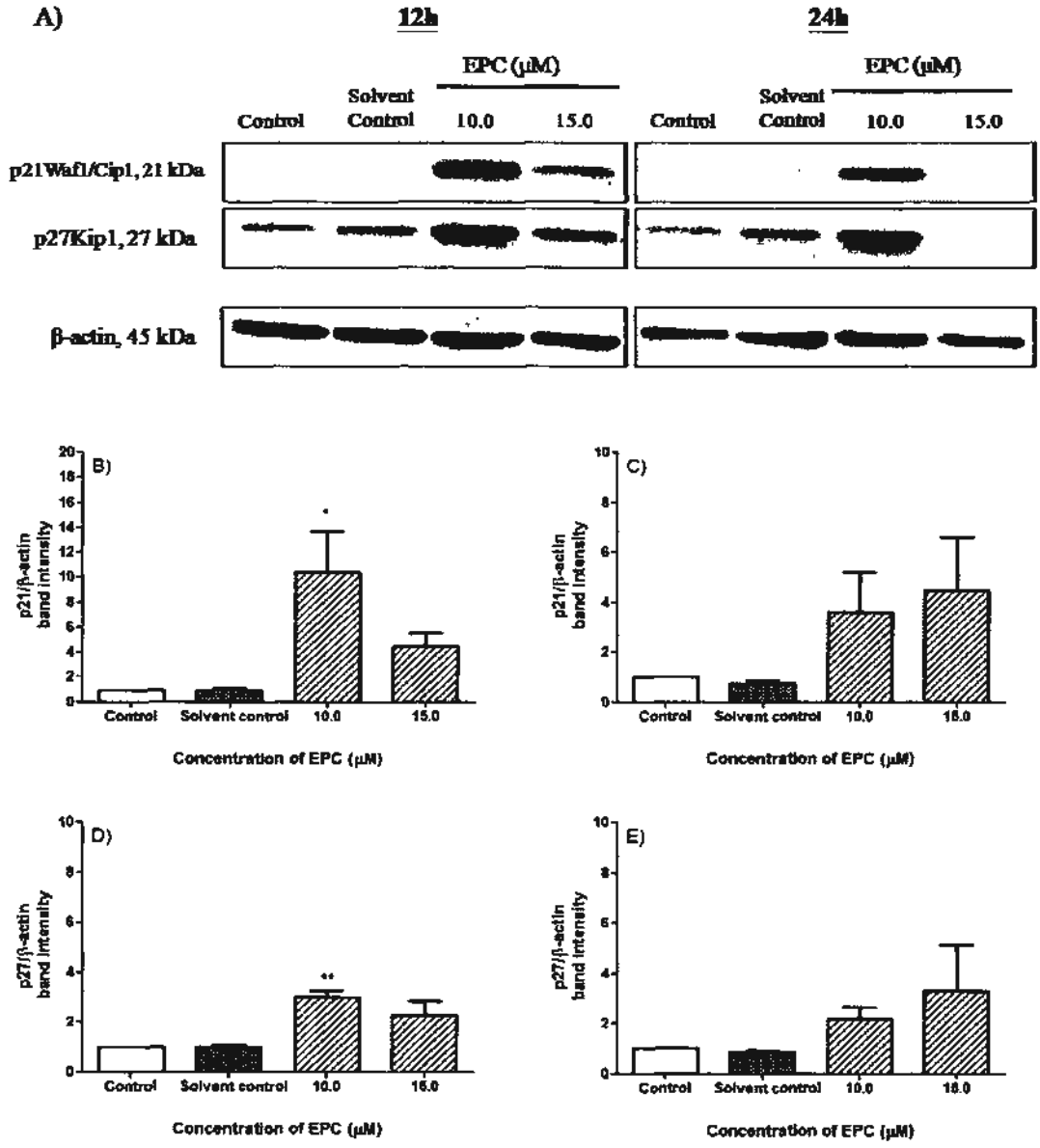

Figure 3.20 Effects of EPC on protein expression of A) $p21^{Waf1/Cip1}$ and $p27^{Kip1}$ after 12 h and 24 h treatment in HT-29 cells. The band intensity was quantified using the Quantity One software and the band intensity of the CIP/KIP family was normalized with that of β-actin and the band intensity of untreated control was considered as one. The band intensity of $p21^{Waf1/Cip1}$ after EPC treatment for B) 12 h and C) 24 h and of $p27^{Kip1}$ for D) 12 h and E) 24 h treatment are shown. Data are presented as mean values ± S.E.M. from three independent experiments. **$p<0.01$ compared with solvent control

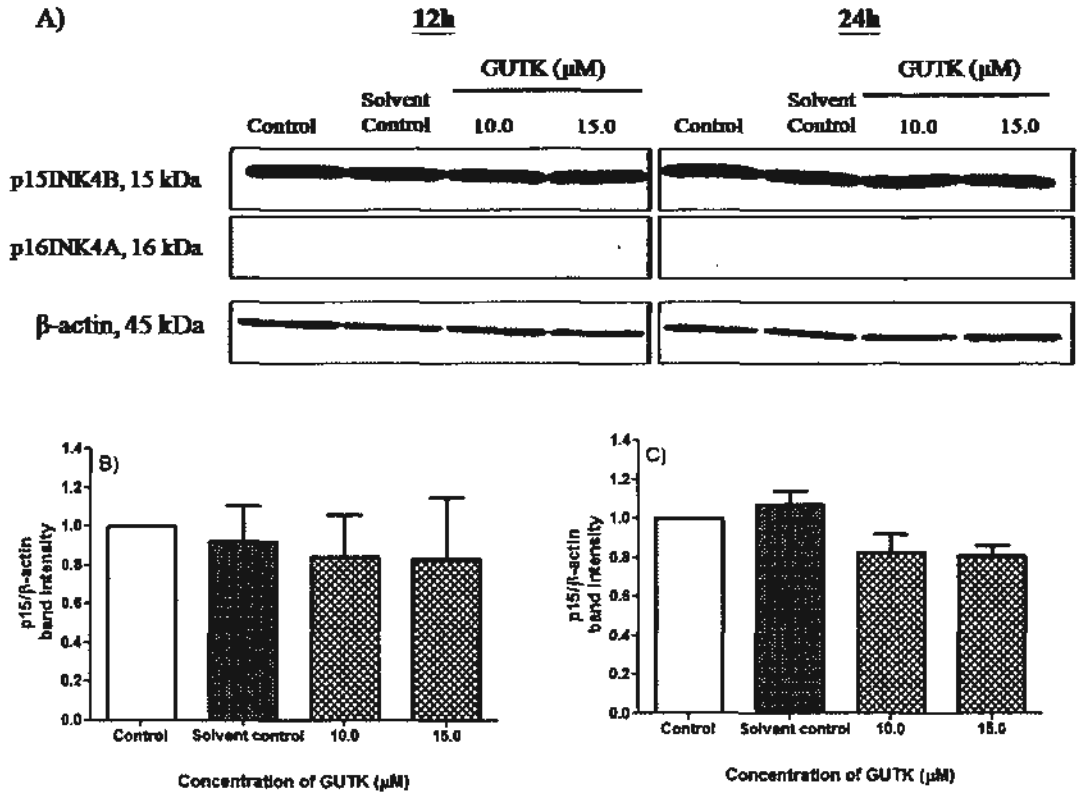

Figure 3.21 Effects of GUTK on protein expression of A) $p15^{INK4B}$ and $p16^{INK4A}$ after 12 h and 24 h treatment in HT-29 cells. The band intensity was quantified using the Quantity One software and the band intensity of the INK4 family was normalized with that of β-actin and the band intensity of untreated control was considered as one. The band intensity of $p15^{INK4B}$ after GUTK treatment for B) 12 h and C) 24 h are shown. The band density of $p16^{INK4A}$ was not calculated due to lack of $p16^{INK4A}$ expression in HT-29 cells.Data are presented as mean values ± S.E.M. from three independent experiments.

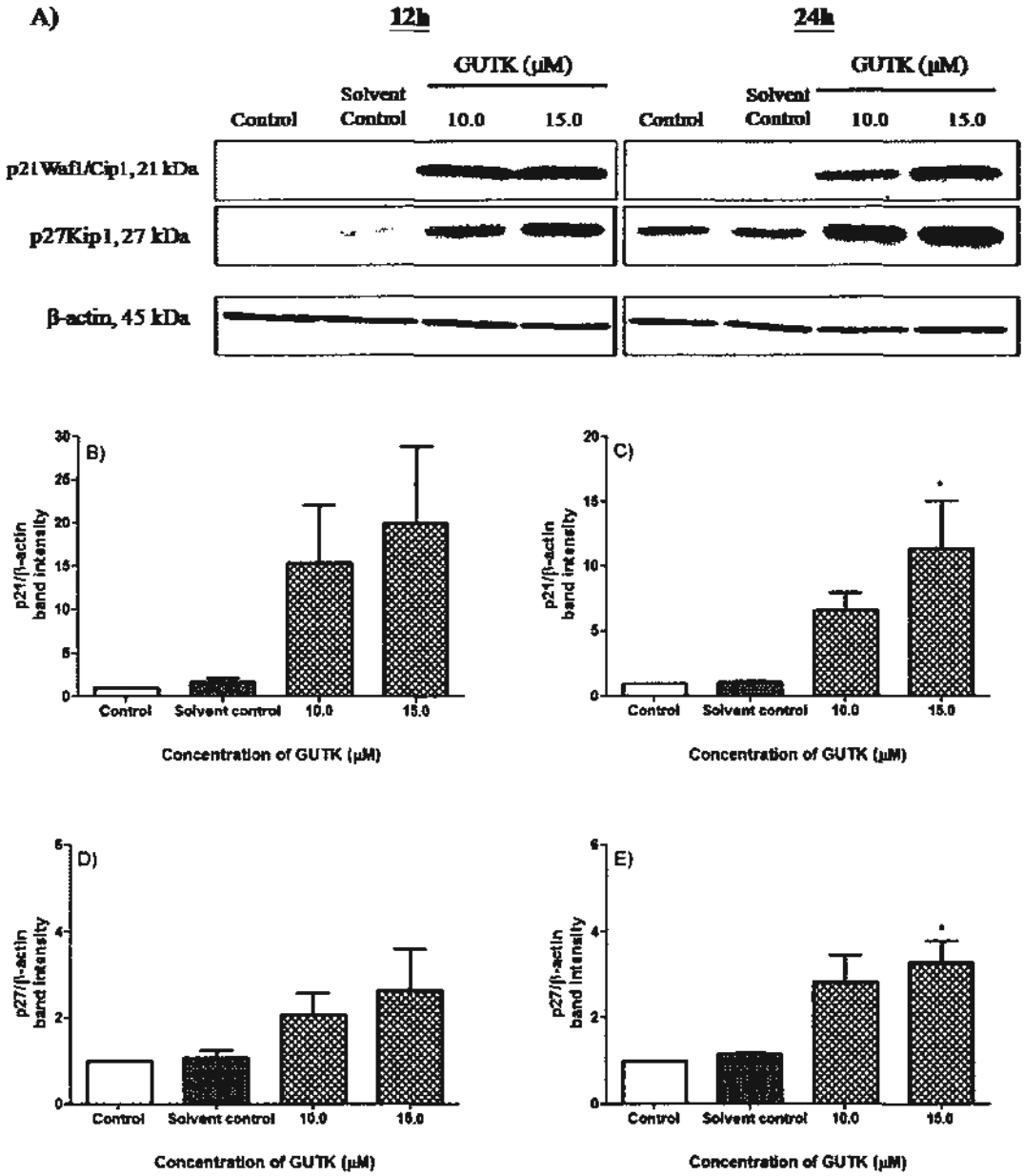

Figure 3.22 Effects of GUTK on protein expression of A) $p21^{Waf1/Cip1}$ and $p27^{Kip1}$ after 12 h and 24 h treatment in HT-29 cells. The band intensity was quantified using the Quantity One software and the band intensity of the CIP/KIP family was normalized with that of β-actin and the band intensity of untreated control was considered as one. The band intensity of $p21^{Waf1/Cip1}$ after GUTK treatment for B) 12 h and C) 24 h and of $p27^{Kip1}$ for D) 12 h and E) 24 h treatment are shown. Data are presented as mean values ± S.E.M. from three independent experiments. *$p<0.05$ compared with solvent control.

3.2.11 Effects of EPC and GUTK on the cleavage of PARP, pro-caspases-3, -8 and -9

Since flow cytometry results showed that EPC and GUTK induced an accumulation of HT-29 cells in apoptotic sub-G_1 phase, the effects of both compounds on the cleavage of pro-caspases-3, -8 and -9 and PARP (a downstream cleavage target of activated caspase-3) after 24 h treatment were studied. As indicated in Figure 3.25, EPC induced cleavage of PARP and pro-caspase-3 into its two active fragments in a dose-dependent manner, which was significant after 10.0 μM treatment ($p<0.05$). Similarly, GUTK stimulated the cleavage of PARP and pro-caspase-3 in a dose-dependent manner starting from 10.0 μM, which was significant at concentrations higher than 10.0 μM ($p<0.001$) (Figure 3.26). The ratios of cleaved to intact caspase-3 were increased by 6.1- and 7.1-fold after 10.0 μM of EPC and GUTK treatment, respectively.

After 24 h, the active, cleaved fragments of pro-caspase-8 and pro-caspase-9 appeared with 10.0 μM EPC treatment, with concomitant decrease of the intact forms (Figure 3.27A). The ratios of cleaved to intact caspases-8 and -9 increased 2.5 and 2.7-fold, respectively after EPC treatment (Figures 3.27B, C). EPC cleaved and activated caspases-8 and -9 as soon as 12 h after treatment, which activated the downstream caspase-3 to cleave PARP after 12 and 24 h (Figure 3.28). As well, GUTK (10.0 μM) induced the cleavage of pro-caspases-8 and -9 after 24 h into the active fragments by 2.9 and 3.3-fold, respectively, compared to untreated cells (Figure 3.29). Interestingly, after 20.0 μM of GUTK treatment, the ratios of cleaved to intact caspases-3, -8 and -9 were drastically reduced compared to at 10.0 μM (Figures 3.26C, 3.29C, D).

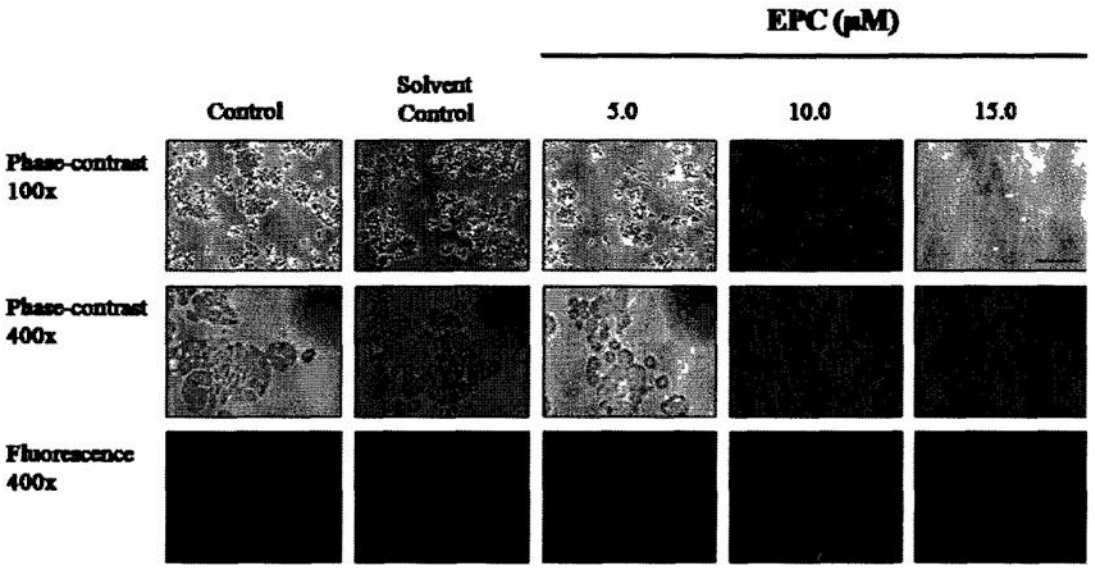

Figure 3.23 Effects of EPC on nuclear morphology of HT-29 cells after 24 h treatment. Phase-contrast microscopy at 100x and 400x magnification was used to examine the effects of EPC on general cell morphology and size and fluorescent microscopy at 400x was used to study the effects of LGT on nuclear morphology after DAPI nuclear staining. The scale bars represent 80 μM and 20 μM at 100x and 400x, respectively. The solvent control was 0.060% DMSO in culture medium. The photos are representative of results obtained from three independent experiments.

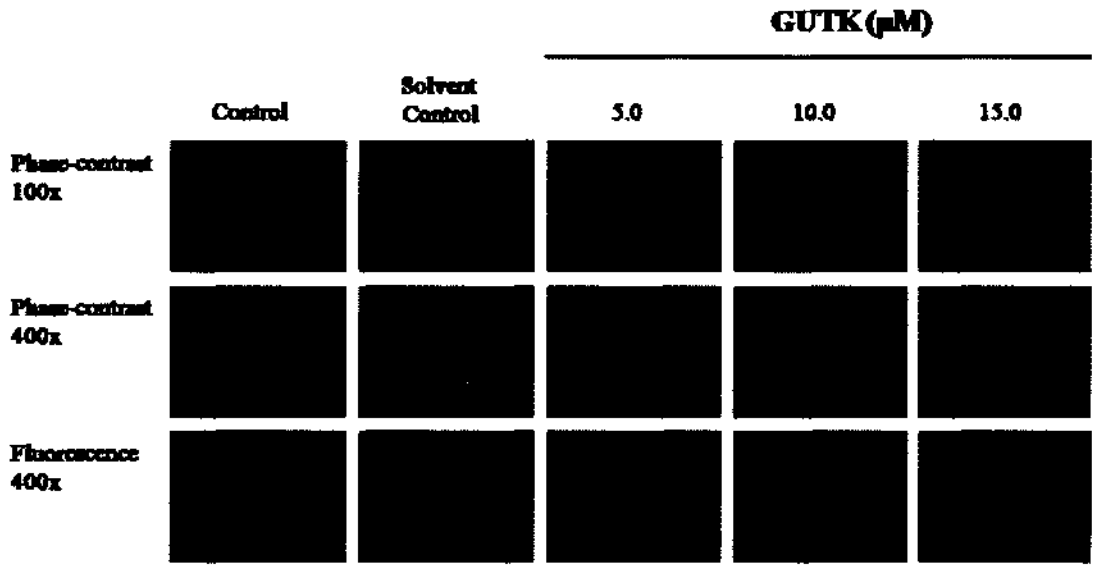

Figure 3.24 Effects of GUTK on nuclear morphology of HT-29 cells after 24 h treatment. Phase-contrast microscopy at 100x and 400x magnification was used to examine the effects of GUTK on general cell morphology and size and fluorescent microscopy at 400x was used to study the effects of LGT on nuclear morphology after DAPI nuclear staining. The scale bars represent 80 μM and 20 μM at 100x and 400x, respectively.The solvent control was 0.060% DMSO in culture medium. The photos are representative of results obtained from three independent experiments.

This may be due to the increased number of cells undergoing late stages of apoptosis, in which the viability of the cell is severely compromised due to cleavage of many cellular proteins. An increased number of cells may also be undergoing necrosis, in which there is a loss of membrane integrity due to swelling and rupturing of many cellular organelles.

3.2.12 Effects of EPC and GUTK on caspase-3 activity

Both EPC and GUTK significantly increased caspase-3 activity in a dose-dependent manner when tested at concentrations from 5.0 to 20.0 μM ($p<0.05$) (Figures 3.30A, 3.31A). After 24 h treatment of cells with 10.0 μM of EPC and GUTK, the caspase-3 activity increased from 49.7 (in the solvent control) to 187.5 pmol pNa/min·mg protein and from 37.6 (in the solvent control) to 137.6 pmol pNa/min·mg protein, respectively. From 15.0 to 20.0 μM of EPC and GUTK, the caspase-3 activity decreased, which was also seen in the Western blot results (Figure 3.29). Hence, non-apoptotic modes of cell death, such as necrosis, or secondary apoptosis may occur at high concentrations of these two compounds. Treatment with caspase-3 inhibitor, Ac-DEVD-CHO, to cell lysates that were treated with EPC or GUTK (10.0 μM), significantly suppressed most of the caspase-3 activity ($p<0.001$) (Figures 3.30B, 3.31B). However, caspase-3 activity could not be fully suppressed to the levels observed in untreated cells or cells treated with DMSO (0.12%) as a solvent control. This implied that other executioner caspases, such as caspases-6 and -7, may be involved in apoptotic cell death induced by EPC and GUTK (Figures 3.30B, 3.31B).

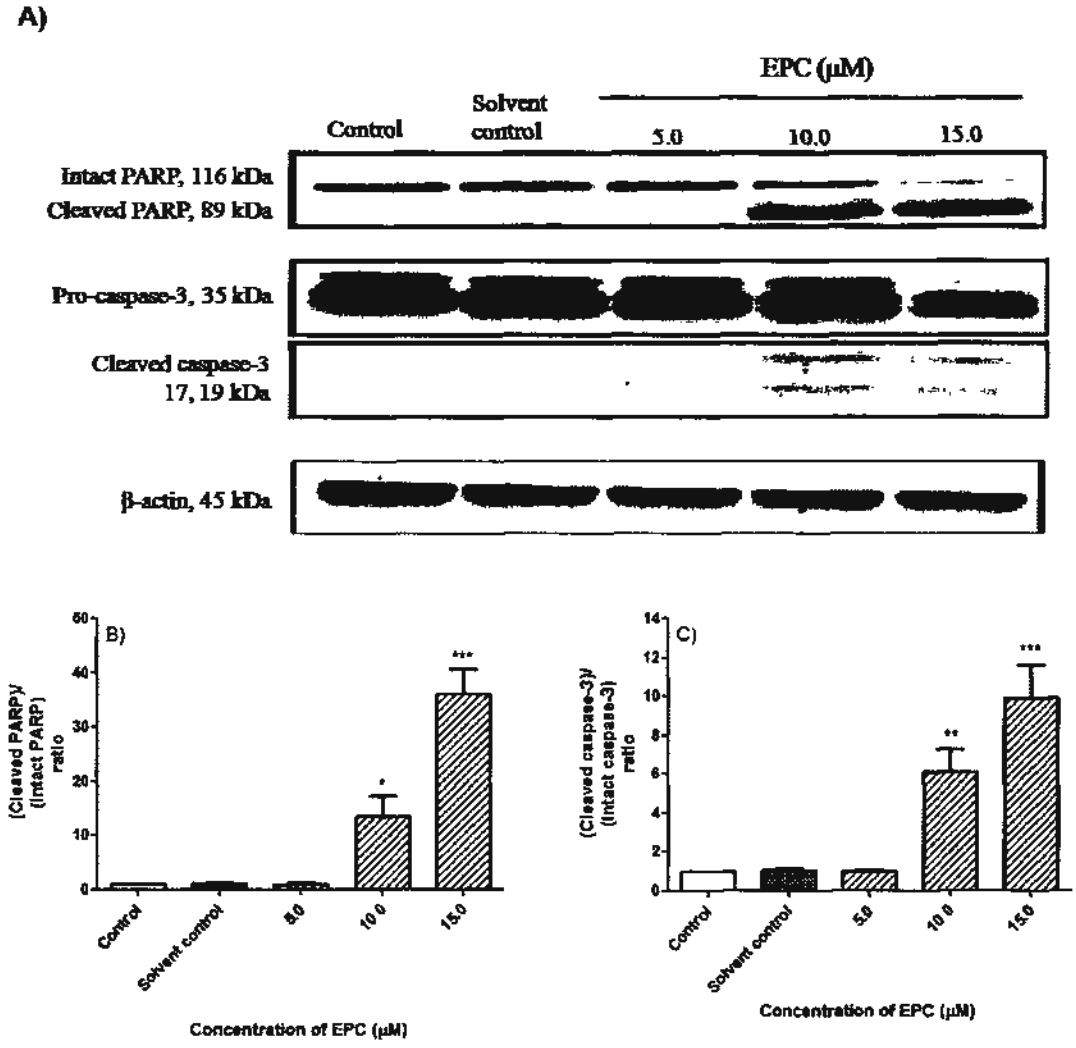

Figure 3.25 Effects of EPC on cleavage of PARP and pro-caspase-3 after A) 24 h treatment. The band intensity was quantified using the Quantity One software and the B) ratio of cleaved PARP/intact PARP and C) ratio of cleaved caspase-3/intact caspase-3 were calculated after intensity of each band was normalized with that of β-actin. Data are presented as mean values ± S.E.M. from four independent experiments. *p<0.05, **p<0.01, ***p<0.001 compared with solvent control (0.060% DMSO in culture medium).

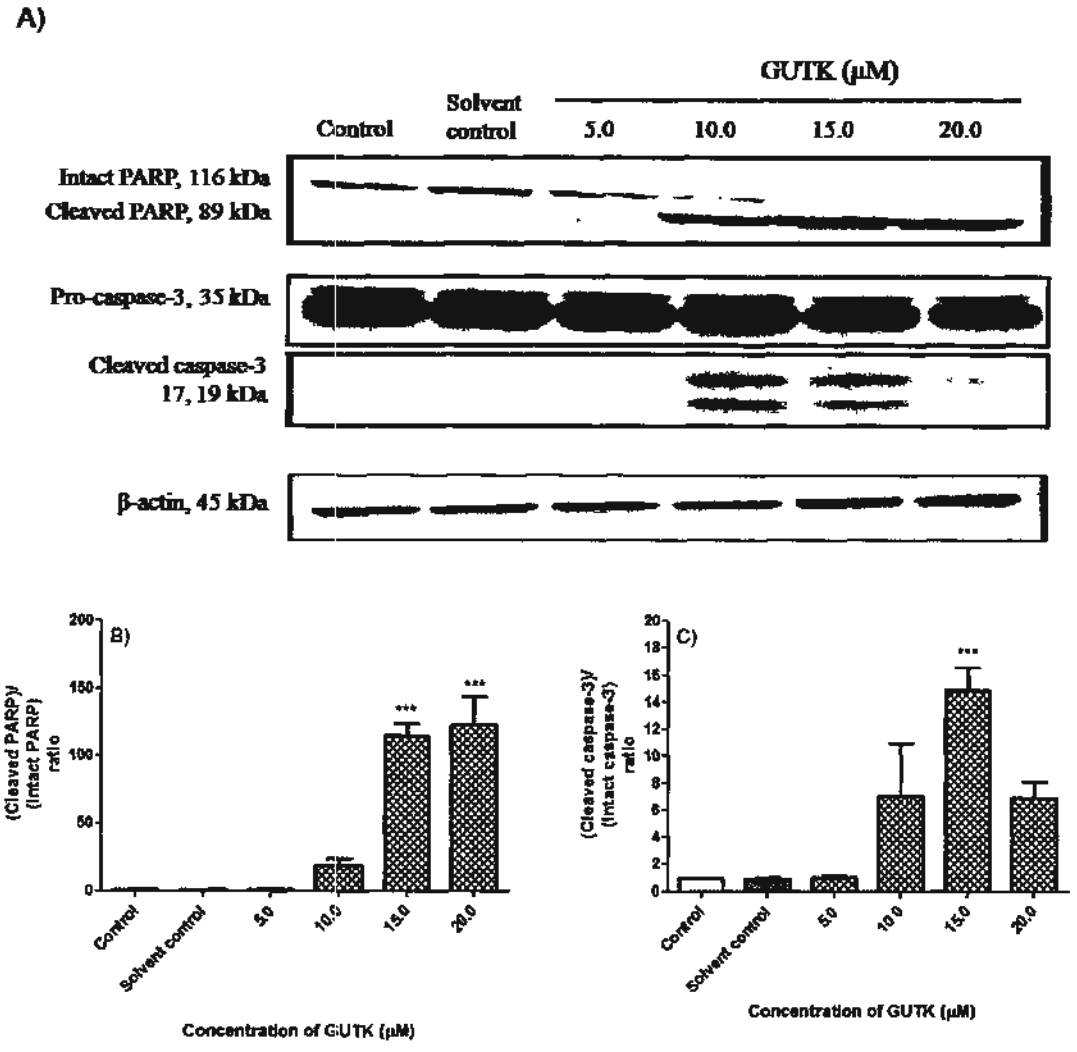

Figure 3.26 Effects of GUTK on cleavage of PARP and pro-caspase-3 after A) 24 h treatment. The band intensity was quantified using the Quantity One software and the B) ratio of cleaved PARP/intact PARP and C) ratio of cleaved caspase-3/intact caspase-3 were calculated after intensity of each band was normalized with that of β-actin. Data are presented as mean values ± S.E.M. from three independent experiments. ***$p<0.001$ compared with solvent control (0.060% DMSO in culture medium).

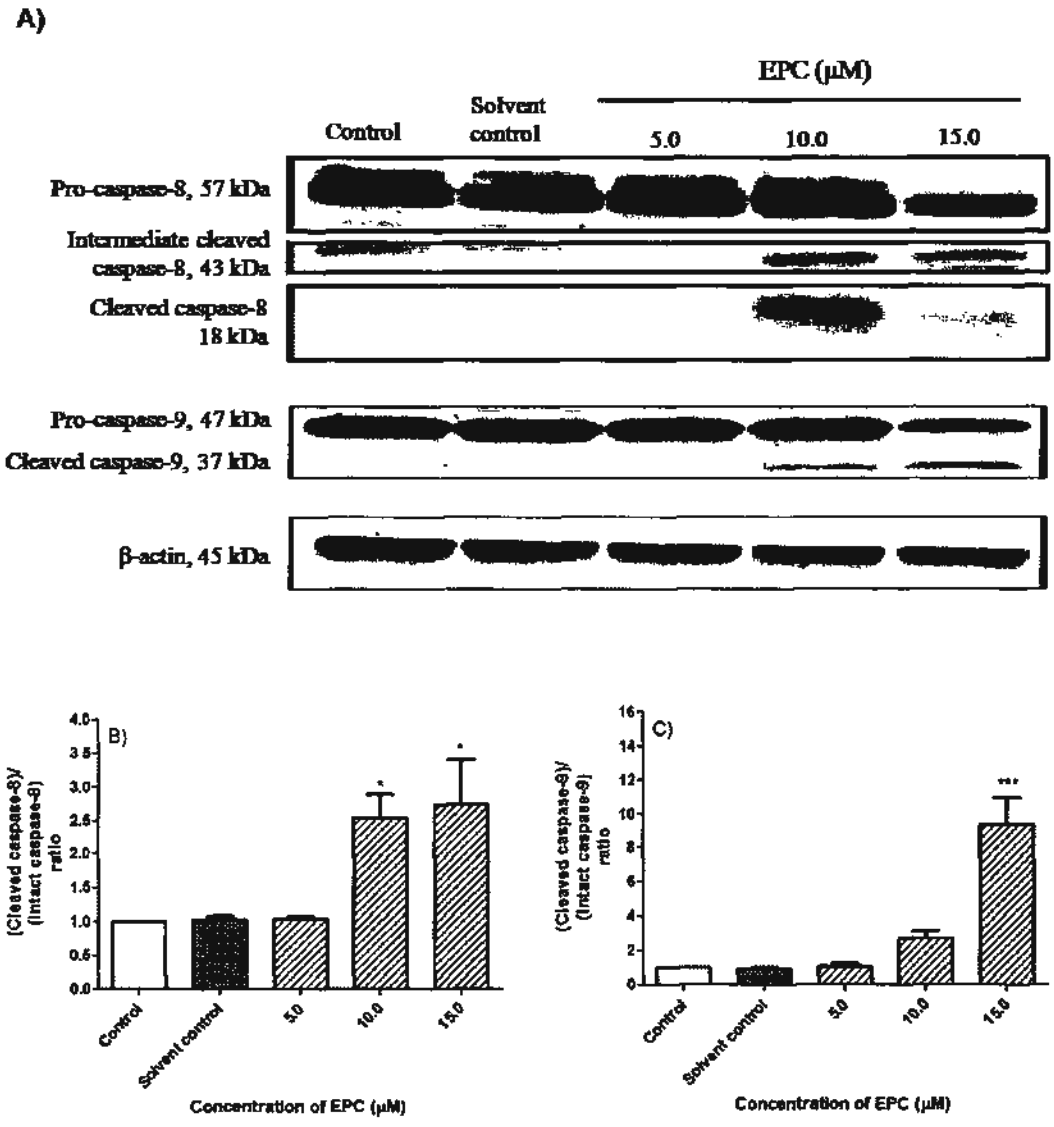

Figure 3.27 Effects of EPC on cleavage of pro-caspase-8 and pro-caspase-9 after A) 24 h treatment. The band intensity was quantified using the Quantity One software and the B) ratio of cleaved caspase-8/intact caspase-8 and C) ratio of cleaved caspase-9/intact caspase-9 were calculated after intensity of each band was normalized with that of β-actin. Data are presented as mean values ± S.E.M. from three independent experiments. *$p<0.05$, ***$p<0.001$ compared with solvent control (0.060% DMSO in culture medium).

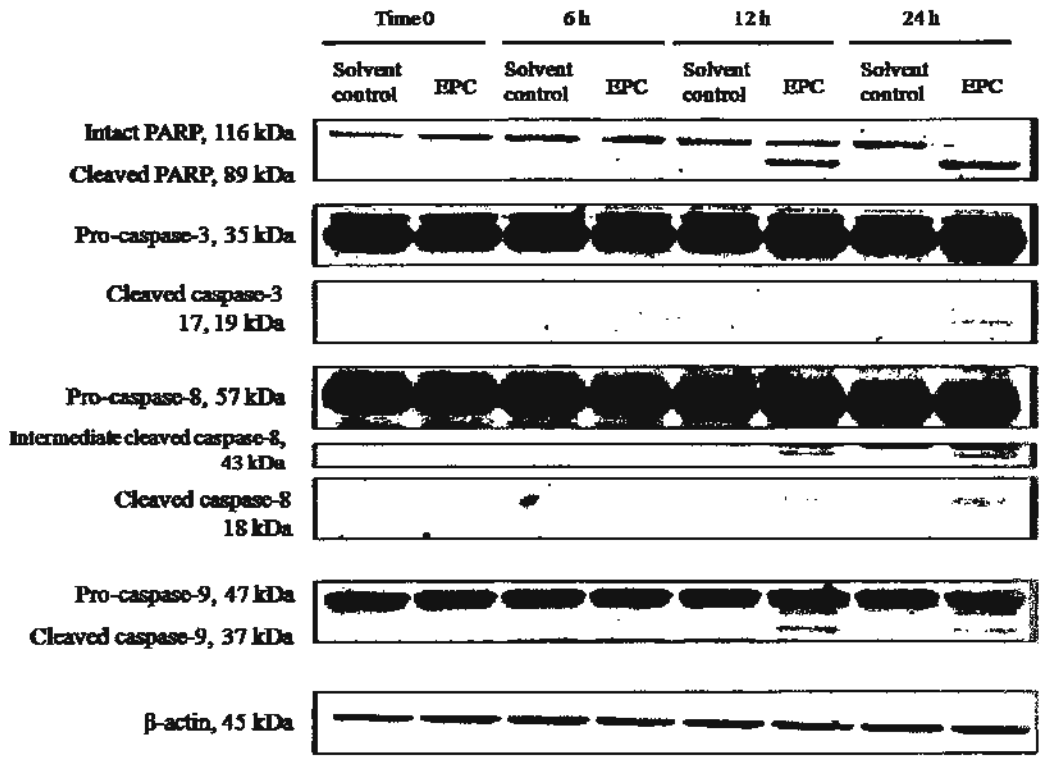

Figure 3.28 Effects of EPC on cleavage of PARP, pro-caspase-3, pro-caspase-8 and pro-caspase-9 after 6, 12, and 24 h treatment. The immunoblot is representative of data from two independent experiments. The solvent control was 0.030% DMSO in culture medium.

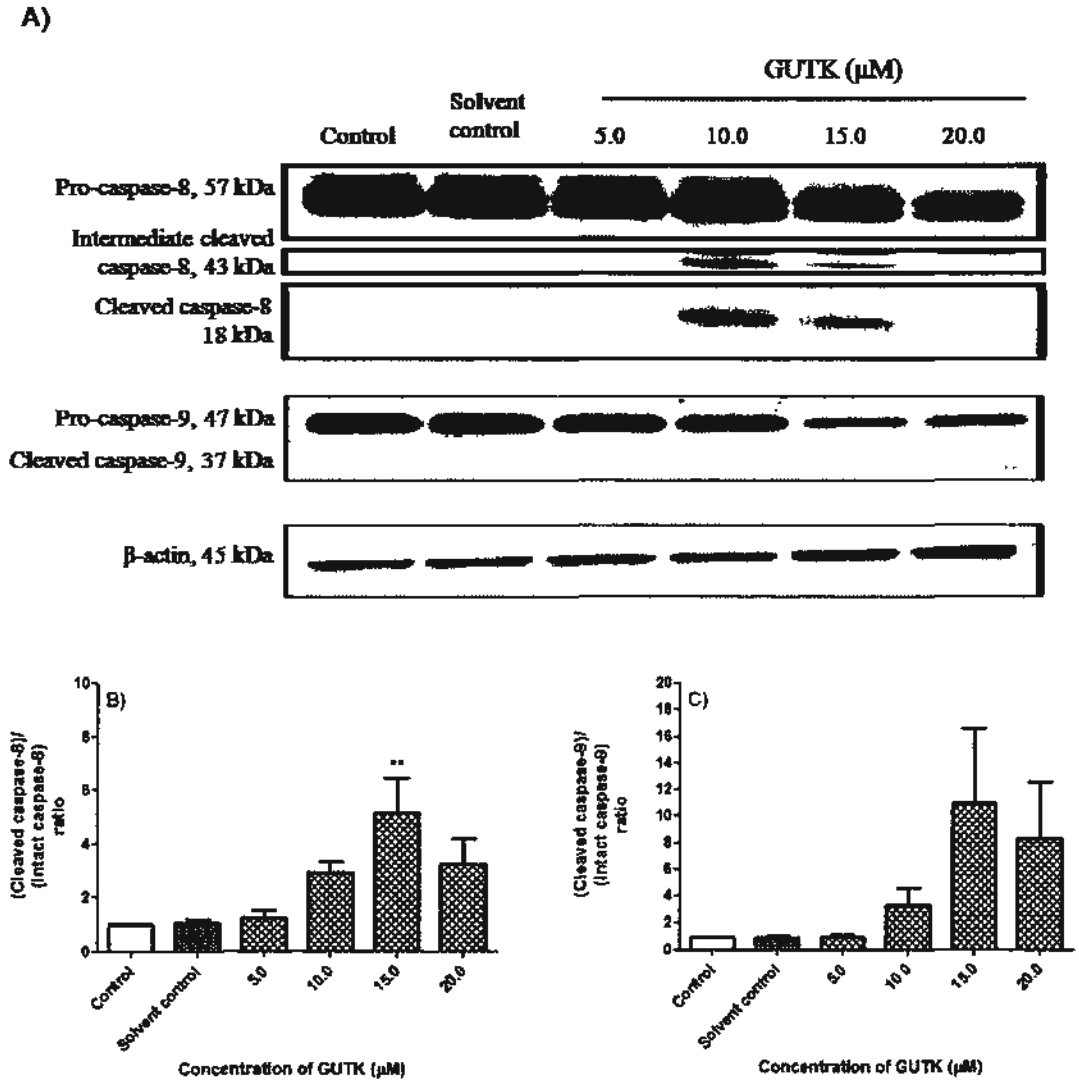

Figure 3.29 Effects of GUTK on cleavage of pro-caspase-8 and pro-caspase-9 after A) 24 h treatment. The band intensity was quantified using the Quantity One software and the B) ratio of cleaved caspase-8/intact caspase-8 and C) ratio of cleaved caspase-9/intact caspase-9 were calculated after intensity of each band was normalized with that of β-actin. Data are presented as mean values ± S.E.M. from three independent experiments. **$p<0.01$ compared with solvent control (0.060% DMSO in culture medium).

3.2.13 Effects of EPC and GUTK on the activation of MAPK pathways

The ERK, JNK and p38 members of the MAPK family have influential roles in the regulation of proliferation, differentiation and apoptosis within the cell. The effects of EPC and GUTK (at 10.0 μM) on the phosphorylation and activation of the three MAP kinases were examined after 3, 6 and 12 h in HT-29 cells since a prolonged activation of these kinases has been observed in cells treated with various anti-cancer drugs that induce apoptosis (Fan & Chambers, 2001). EPC induced phophorylation of p38 and ERK by 5.0-fold and 4.0-fold after 12 h treatment, respectively (Figures 3.32 and 3.34). However, EPC induced phosphorylation of JNK as early as 3 h after treatment and continued ever after 12 h treatment (Figure 3.33A). The increase in phosphorylated JNK was 2.6-fold higher than that of control and it was significant after 12 h ($p<0.05$) (Figure 3.33B). GUTK did not trigger any significant change in the levels of phosphorylated ERK and p38, as indicated by the constant ratios of phosphorylated ERK or p38 to intact ERK or p38 (Figures 3.35, 3.37). However, GUTK induced a time-dependent increase in the level of phosphorylated JNK, which was significantly higher than solvent control after 12 h ($p<0.05$) (Figure 3.36). Although EPC and GUTK have variable effects on the activation of ERK and p38, both triggered an activation of JNK, but it took a longer time for GUTK to phosphorylate JNK compared to EPC (Figures 3.33, 3.36).

3.2.14 Role of MAPK pathways in apoptosis induced by EPC and GUTK

Since MAPK pathways have been thought to be closely related to the apoptotic pathway, the effects of pre-treatment with specific MAPK inhibitors (SP600125 for JNK, SB203580 for p38 and PD98059 for ERK) for one hour before 24 h treatment of EPC or GUTK were investigated.

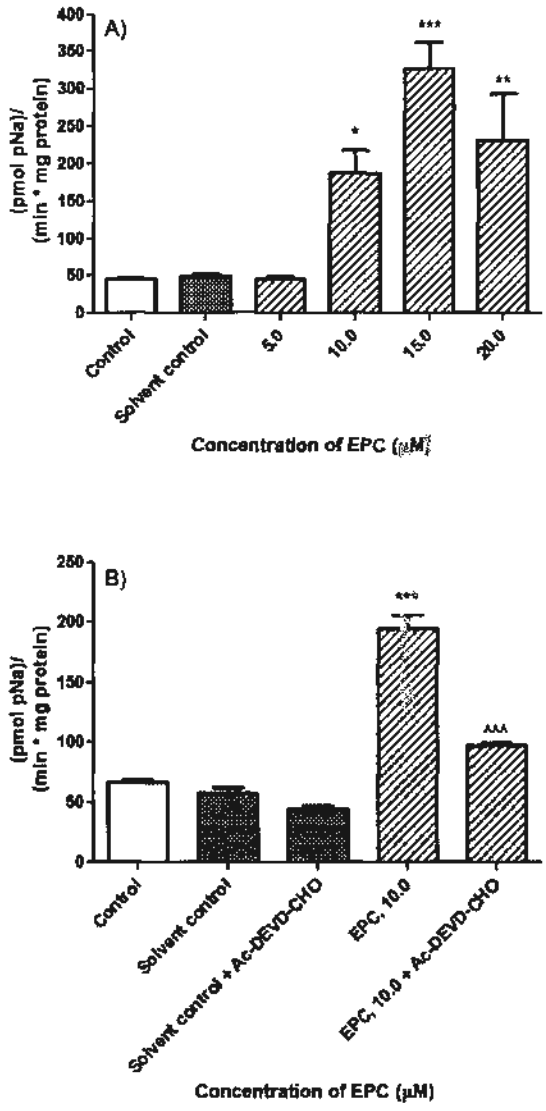

Figure 3.30 Effects of EPC on caspase-3 activity in HT-29 cells after A) 24 h incubation as determined by the rate of pNa formation. B) Caspase-3 inhibitor, Ac-DEVD-CHO, was added to cell lysates with EPC to determine the reversibility of EPC-induced caspase-3 activity. The experiment was conducted in duplicate and data are presented as mean values ± S.E.M. from three independent experiments. *$p<0.05$, **$p<0.01$, ***$p<0.001$ compared with solvent control (0.12% DMSO in culture medium) and ^^^$p<0.001$ compared with EPC, 10.0 μM.

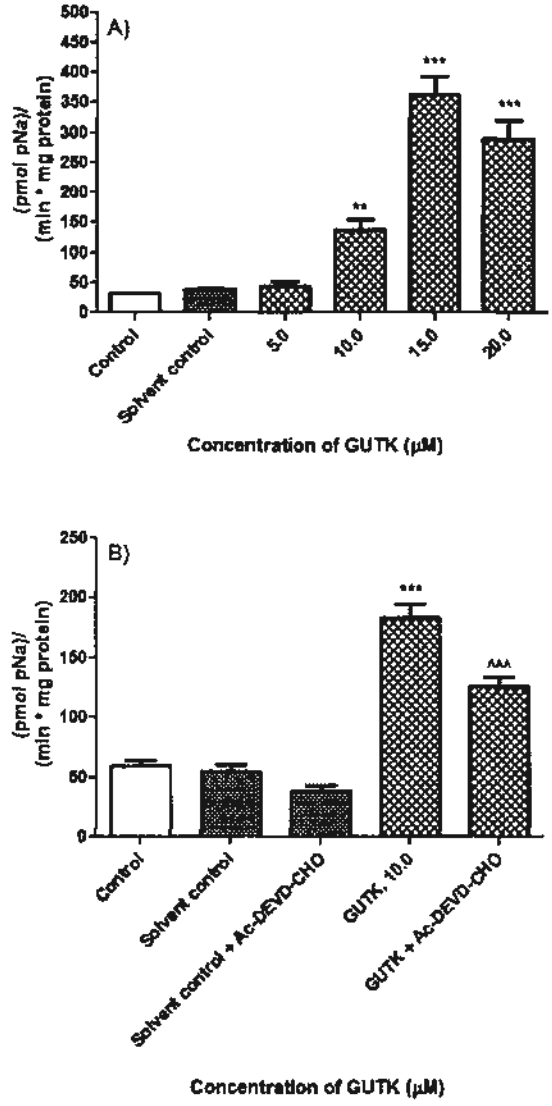

Figure 3.31 Effects of GUTK on caspase-3 activity in HT-29 cells after A) 24 h incubation as determined by the rate of pNa formation. B) Caspase-3 inhibitor, Ac-DEVD-CHO, was added to cell lysates with GUTK to determine the reversibility of GUTK-induced caspase-3 activity. The experiment was conducted in duplicate and data are presented as mean values ± S.E.M. from three independent experiments. **p<0.01, ***p<0.001 compared with solvent control (0.12% DMSO in culture medium) and ^^^p<0.001 compared with GUTK, 10.0 μM.

The solvent DMSO (0.030% in culture medium), JNK inhibitor SP600125 alone, p38 inhibitor SB203580 alone and ERK inhibitor PD98059, did not have any significant effects on caspase-3 activity (Figure 3.38A, 3.38B). EPC and GUTK, at 10.0 μM significantly increased caspase-3 activity by 3.6- and 5.1-fold, respectively, compared to the solvent control ($p<0.001$).

Pre-treatment with SP600125 significantly decreased apoptosis induced by GUTK ($p<0.001$), which suggests that the JNK pathway may have a pro-apoptotic role in HT-29 cells (Figure 3.38A). However, the JNK inhibitor did not fully inhibit caspase-3 activity induced by GUTK, which implies that other intracellular pathways may also have a role in apoptosis. Surprisingly, pre-treatment with a JNK inhibitor potentiated the apoptosis induced by EPC ($p<0.05$) (Figure 3.38A). Although both EPC and GUTK induced JNK phosphorylation as early as 3 h, it appears that EPC may not have a direct effect on JNK, while GUTK does (Figure 3.38A). The p38 inhibitor, SB203580 slightly decreased caspase-3 activity induced by EPC and GUTK, but it was not significant (Figure 3.38B). The ERK inhibitor, PD98059 slightly decreased caspase-3 activity induced by GUTK, but it potentiated EPC-induced caspase-3 activity (Figure 3.38C). The results suggest that p38 has a pro-apoptotic role in EPC- and GUTK-induced apoptosis. While JNK and ERK have pro-apoptotic roles in GUTK-induced cell death, JNK and ERK have anti-apoptotic roles in EPC-induced cell death. However, the concentrations of the ERK and p38 inhibitors and the pre-treatment period for these two inhibitors may be increased to confirm the roles of ERK and p38 in apoptosis induced by EPC and GUTK.

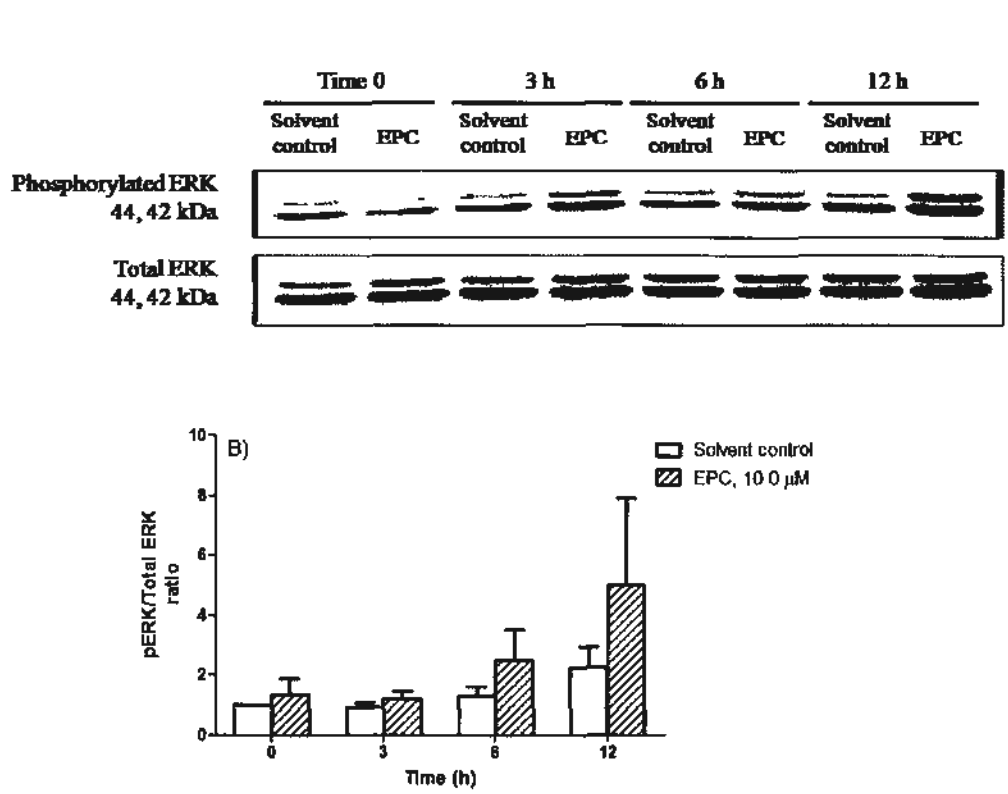

Figure 3.32 Effects of EPC (10.0 μM) on phosphorylation of extracellular signal-regulated kinase-1 and -2 (ERK1/2) after A) 3, 6, and 12 h treatment in HT-29 cells. The band intensity was quantified using the Quantity One software and the B) ratio of phosphorylated ERK/total ERK was calculated using the respective band intensities. The solvent control (0.030% DMSO in culture medium) Data are presented as mean values ± S.E.M. from three independent experiments.

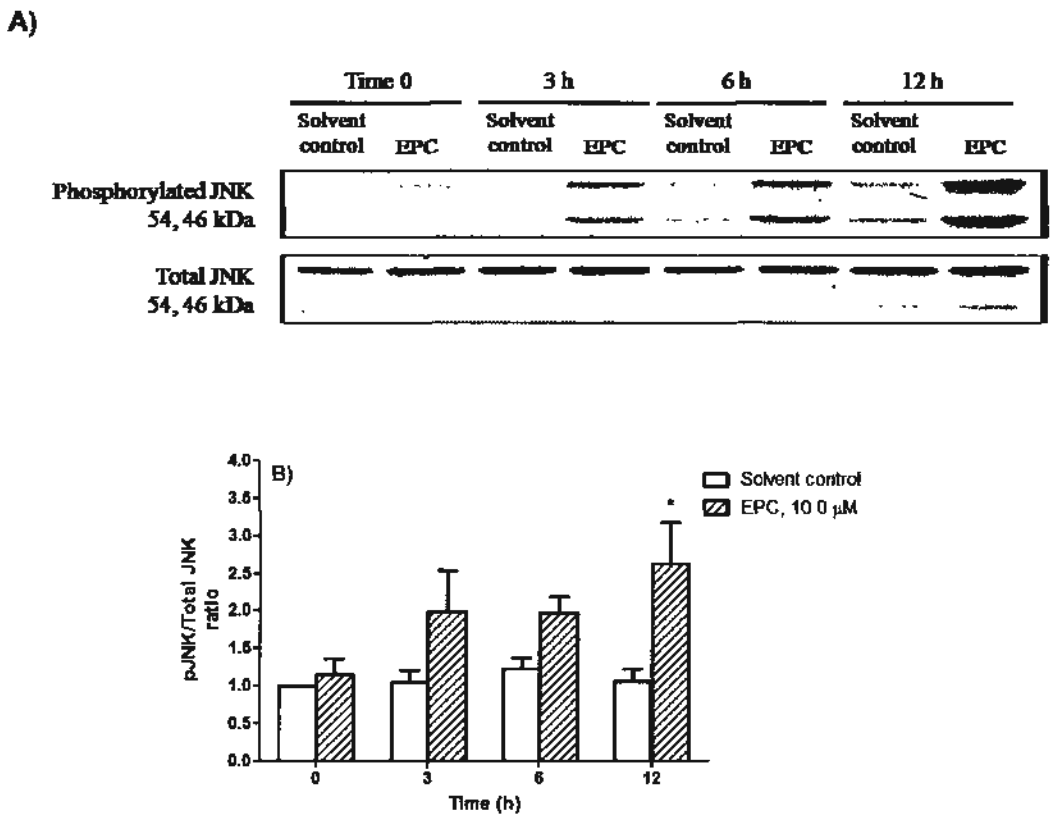

Figure 3.33 Effects of EPC (10.0 μM) on phosphorylation of c-jun N-terminal kinases-1 and -2 (JNK1/2) after A) 3, 6, and 12 h treatment in HT-29 cells. The band intensity was quantified using the Quantity One software and the B) ratio of phosphorylated JNK/total JNK was calculated using the respective band intensities. The solvent control (0.030% DMSO in culture medium) at time 0 was considered as one. Data are presented as mean values ± S.E.M. from three independent experiments. *$p<0.05$ compared with solvent control of the respective time point.

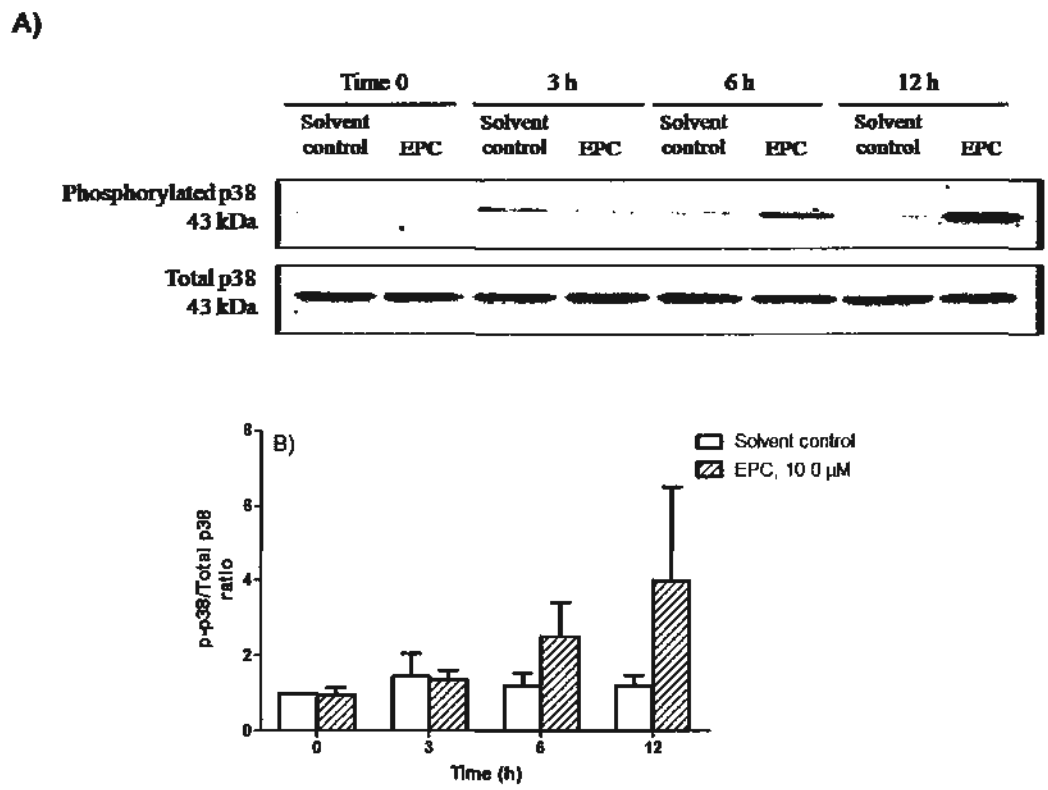

Figure 3.34 Effects of EPC (10.0 μM) on phosphorylation of p38 MAPK after A) 3, 6, and 12 h treatment in HT-29 cells. The band intensity was quantified using the Quantity One software and the B) ratio of phosphorylated p38/total p38 was calculated using the respective band intensities. The solvent control (0.030% DMSO in culture medium) at time 0 was considered as one. Data are presented as mean values ± S.E.M. from three independent experiments.

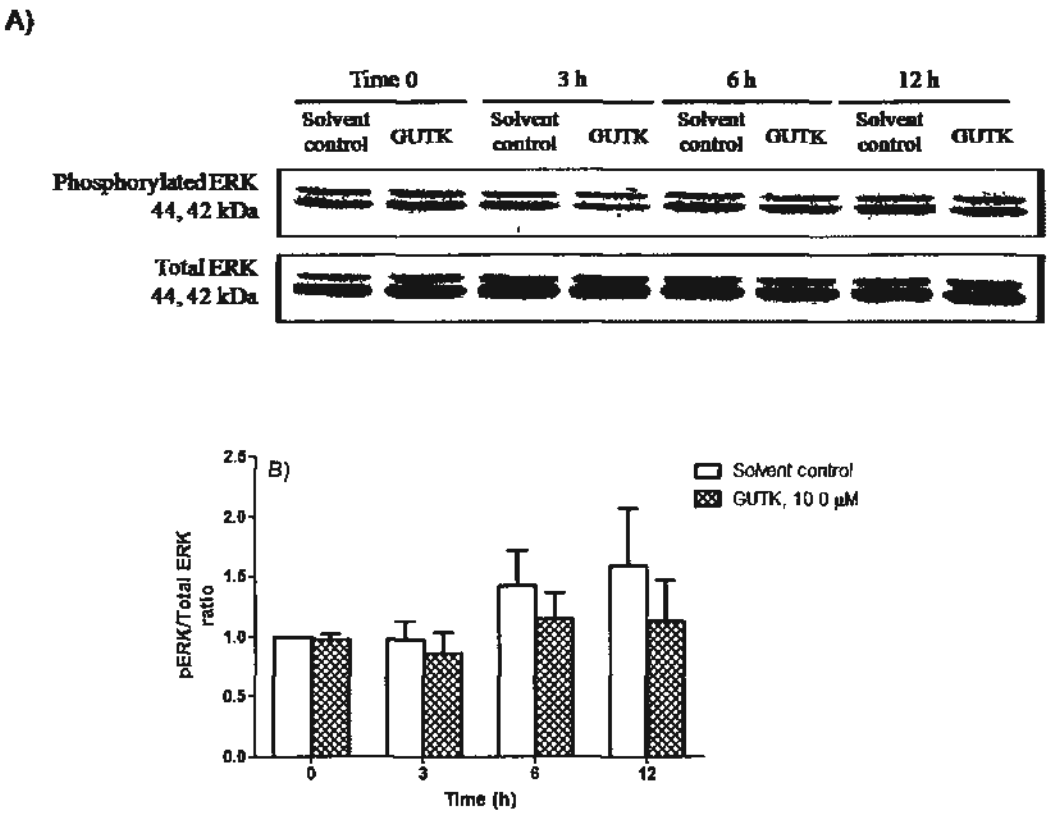

Figure 3.35 Effects of GUTK (10.0 μM) on phosphorylation of extracellular signal-regulated kinase-1 and -2 (ERK1/2) after A) 3, 6, and 12 h treatment in HT-29 cells. The band intensity was quantified using the Quantity One software and the B) ratio of phosphorylated ERK/total ERK was calculated using the respective band intensities. The solvent control (0.030% DMSO in culture medium) Data are presented as mean values ± S.E.M. from three independent experiments.

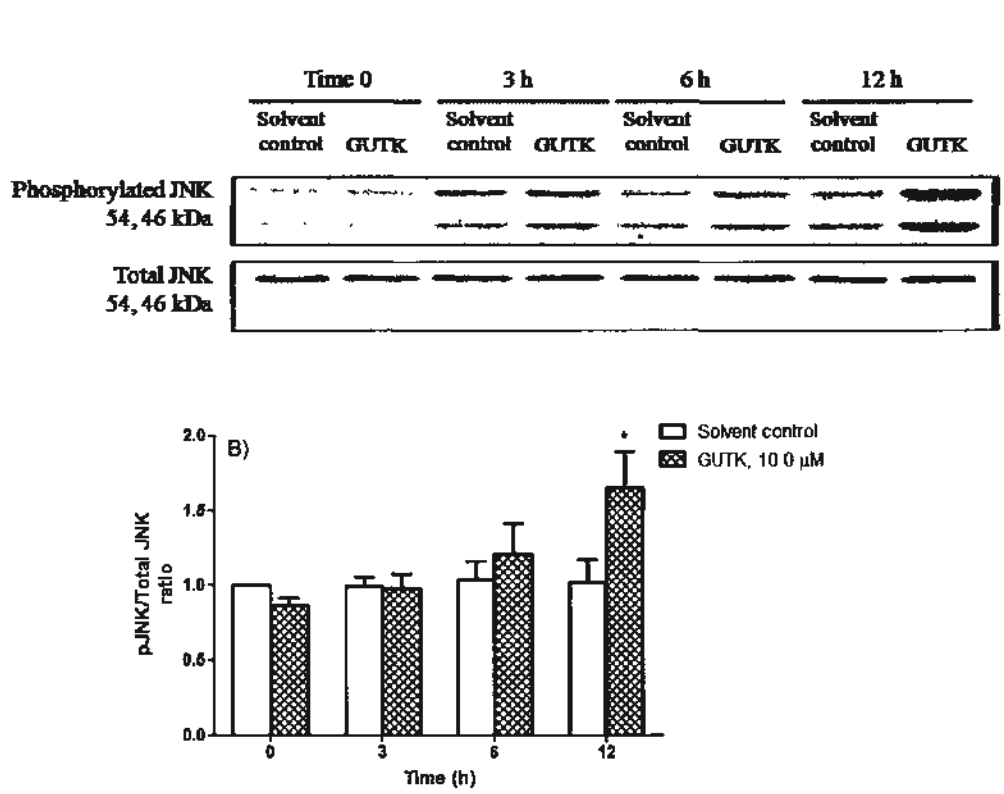

Figure 3.36 Effects of GUTK (10.0 μM) on phosphorylation of c-jun N-terminal kinases-1 and -2 (JNK1/2) after A) 3, 6, and 12 h treatment in HT-29 cells. The band intensity was quantified using the Quantity One software and the B) ratio of phosphorylated JNK/total JNK was calculated using the respective band intensities. The solvent control (0.030% DMSO in culture medium) at time 0 was considered as one. Data are presented as mean values ± S.E.M. from three independent experiments.

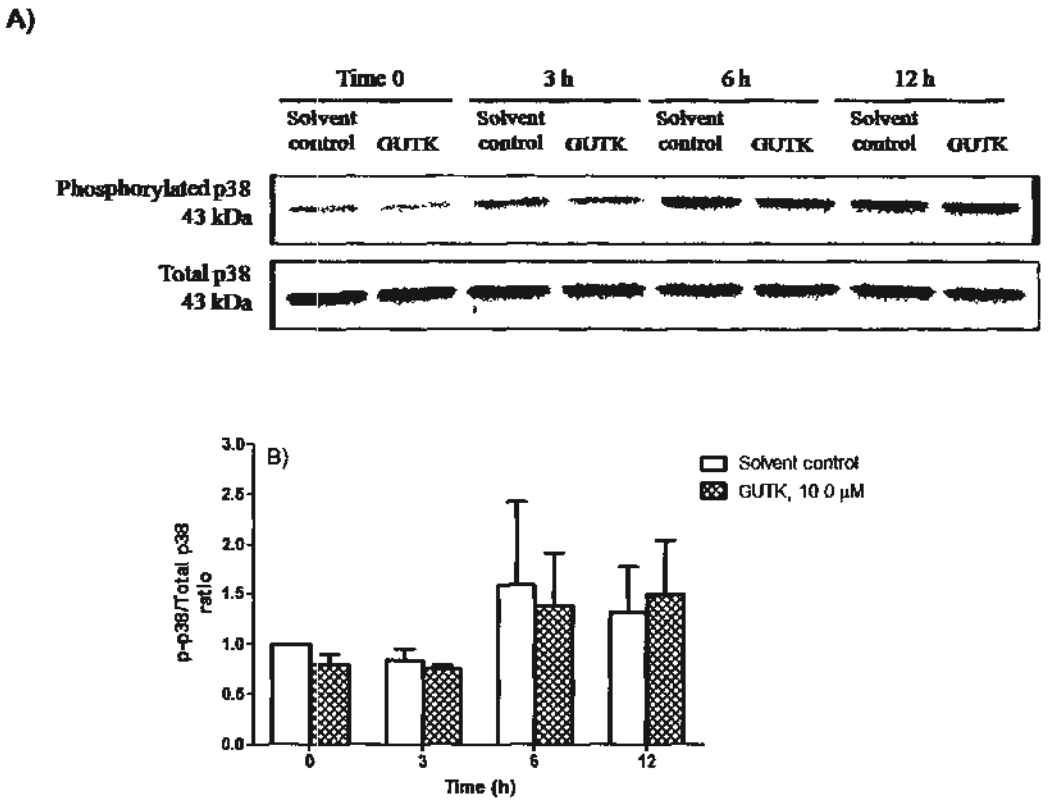

Figure 3.37 Effects of GUTK (10.0 μM) on phosphorylation of p38 MAPK after A) 3, 6, and 12 h treatment in HT-29 cells. The band intensity was quantified using the Quantity One software and the B) ratio of phosphorylated p38/total p38 was calculated using the respective band intensities. The solvent control (0.030% DMSO in culture medium) at time 0 was considered as one. Data are presented as mean values ± S.E.M. from three independent experiments.

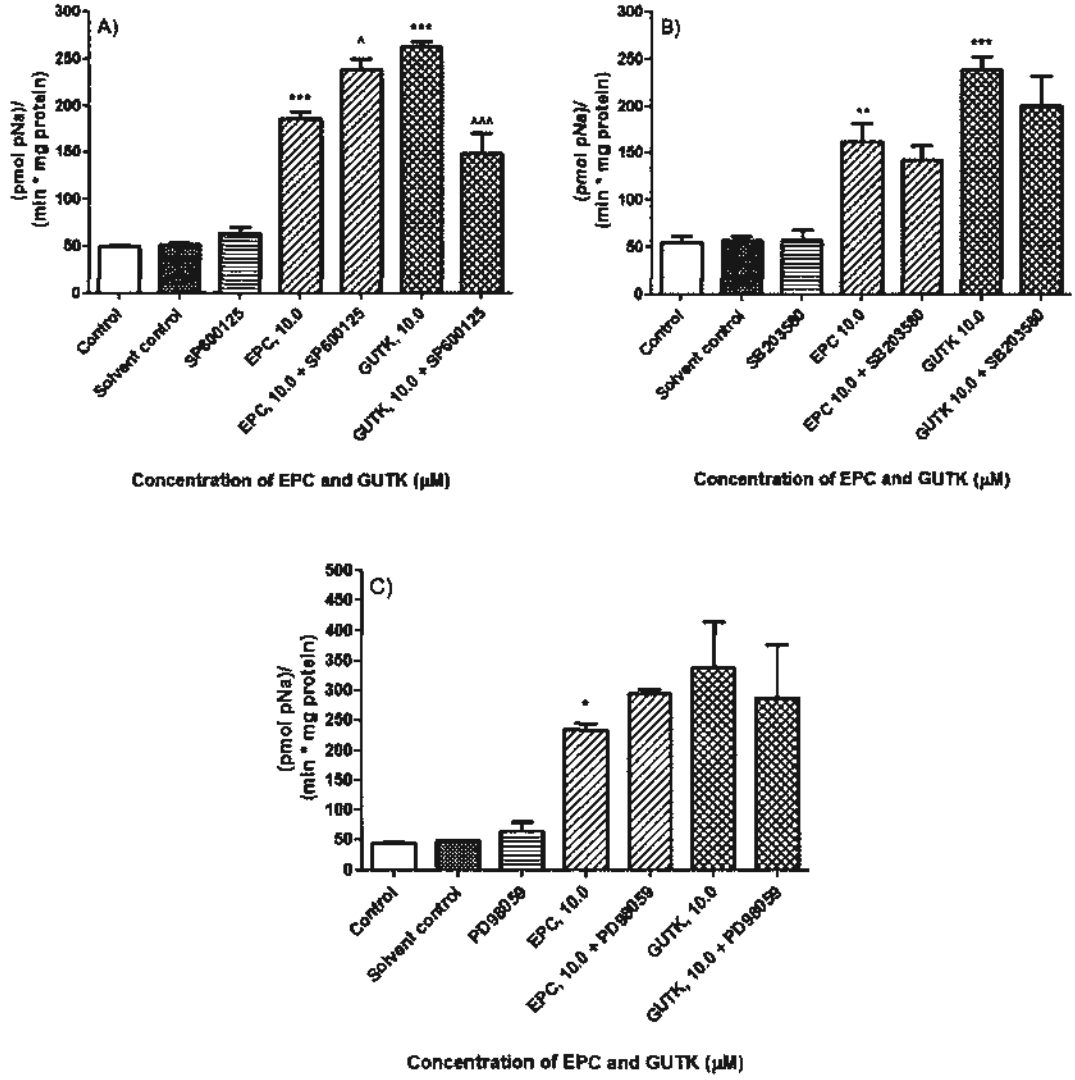

Figure 3.38 Effects of pre-treatment of MAPK inhibitors on caspase-3 activity induced by EPC and GUTK (10.0 μM) after 24 h treatment in HT-29 cells. Cells were pre-treated with A) SP600125 (JNK inhibitor – 20 μM), B) SB203580 (p38 inhibitor – 1.0 μM) or C) PD98059 (ERK inhibitor – 10 μM) for one hour before 24 incubation with EPC or GUTK (10.0 μM). Data are presented as mean values ± S.E.M. from three independent experiments. *p<0.05, **p<0.01,***p0.001 compared with solvent control; ^p<0.05, ^^^p<0.001 compared with EPC or GUTK alone.

3.2.15 Toxicity of GUTK in mice

From the *in vitro* studies, EPC and GUTK induced G_0/G_1 cell cycle arrest and apoptosis to reduce the viability and inhibit the proliferation of human colon cancer cells. Since both compounds showed promising cytotoxic effects in cells, their potential anti-tumor effects *in vivo* were examined. Due to availability of higher quanitity of GUTK, the anti-tumor effects of GUTK on colon tumor-bearing mice were studied. Since no *in vivo* work has been conducted on GUTK before, the possible toxic effects of GUTK on various body organs were studied by treating mice with 5% Tween-80 in saline as the vehicle control and 10 mg/kg (i.p.) of GUTK once every other day for 14 days and analyzing the histopathology of different organs after sacrifice.

GUTK treatment did not affect the body weights of mice and all treated animals were in good health (Figure 3.39A). After the mice were sacrificed, the brain, heart, lung, stomach, small intestine, colon, kidney and liver were fixed for hematoxylin and eosin staining for histopathological observation. There was no significant difference between the weights of most organs and the physical appearance of the organs (such as coloration or size) between vehicle and GUTK groups (Figure 3.39B). However, there was a significant decrease in the mean weight of the small intestine of GUTK-treated mice ($p<0.001$) (Figure 3.39B) but this could be due to the natural variation in length of the small intestine in mice. Organ sections stained with hematoxylin and eosin indicated that GUTK did not induce cell swelling, necrotic damage or hemorrhage in various organs (Figure 3.40).

Since it has been demonstrated that high dose gambogic acid induced toxicity in the kidney and liver after chronic administration, the effects of GUTK on serum

creatinine and ALT levels were determined by the corresponding assays (Qi *et al.*, 2008c). As shown in Figure 3.41, no significant change in serum creatinine level was observed after GUTK treatment every other day for 14 days ($p>0.05$). The serum creatinine level was 0.60 ± 0.16 mM in the vehicle control group, compared with 0.49 ± 0.07 mM in the GUTK treatment group (Figure 3.41). In addition, GUTK did not increase serum ALT levels in comparison to the vehicle control (Figure 3.42). Apparently, GUTK did not induce toxicity to various body organs using the dose of 10 mg/kg given by intraperitoneal injection every other day for 2 weeks, as verified by histopathological examination and analysis of blood biochemical parameters. Therefore, this dosage regimen of GUTK was used in subsequent studies in Colon-26 tumor-bearing mice.

3.2.16 Effects of GUTK on *in vivo* colon tumor growth

To examine the *in vivo* anti-tumor effects of GUTK, mouse colon carcinoma Colon-26 cells were injected subcutaneously on the back of the mice and tumor volume was monitored every other day until the end of the experiment (16 days). Since the *in vitro* studies of the cytotoxic activity of GUTK were in HT-29 cells, the effects of GUTK on the viability of Colon-26 cells were determined (Figure 3.43). Similar to HT-29, GUTK reduced the viability of Colon-26 cells in a dose- and time-dependent manner after 24 h and 48 h treatment. The IC_{50} values of GUTK in Colon-26 cell line were 4.9 ± 0.6 and 3.2 ± 0.2 μM after 24 h and 48 h treatment, respectively. The IC_{50} values of GUTK in HT-29 cell line was 5.4 ± 0.2 and 3.3 ± 0.3 μM after 24 h and 48 h treatment, respectively (Table 3.5). This showed that both mouse and human colon cancer cells were sensitive to the cytotoxic effects of GUTK and the IC_{50} values of GUTK in both cell lines were comparable. Thus, the effects of GUTK on immune-competent Colon-26-tumor bearing mice were studied.

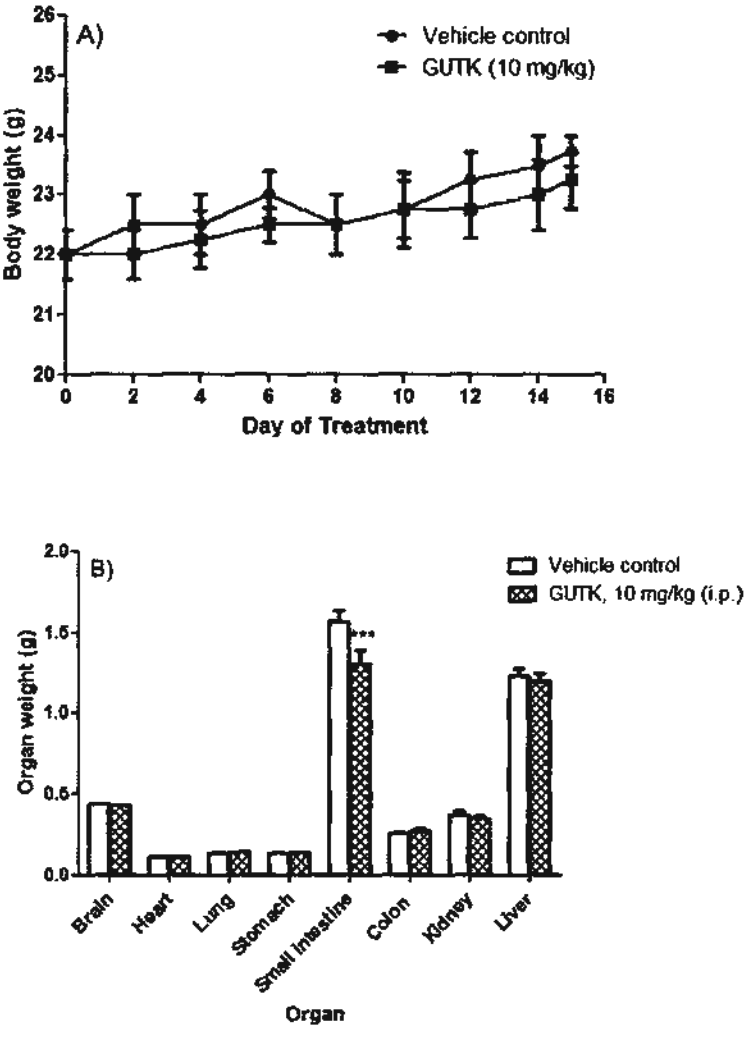

Figure 3.39 Effect of GUTK (10.0 mg/kg, i.p.) administered once every other day for 2 weeks on A) body weight and B) weight of various organs after sacrifice in male BALB/c mice. Each group contained four mice. ***$p<0.001$ compared with vehicle control.

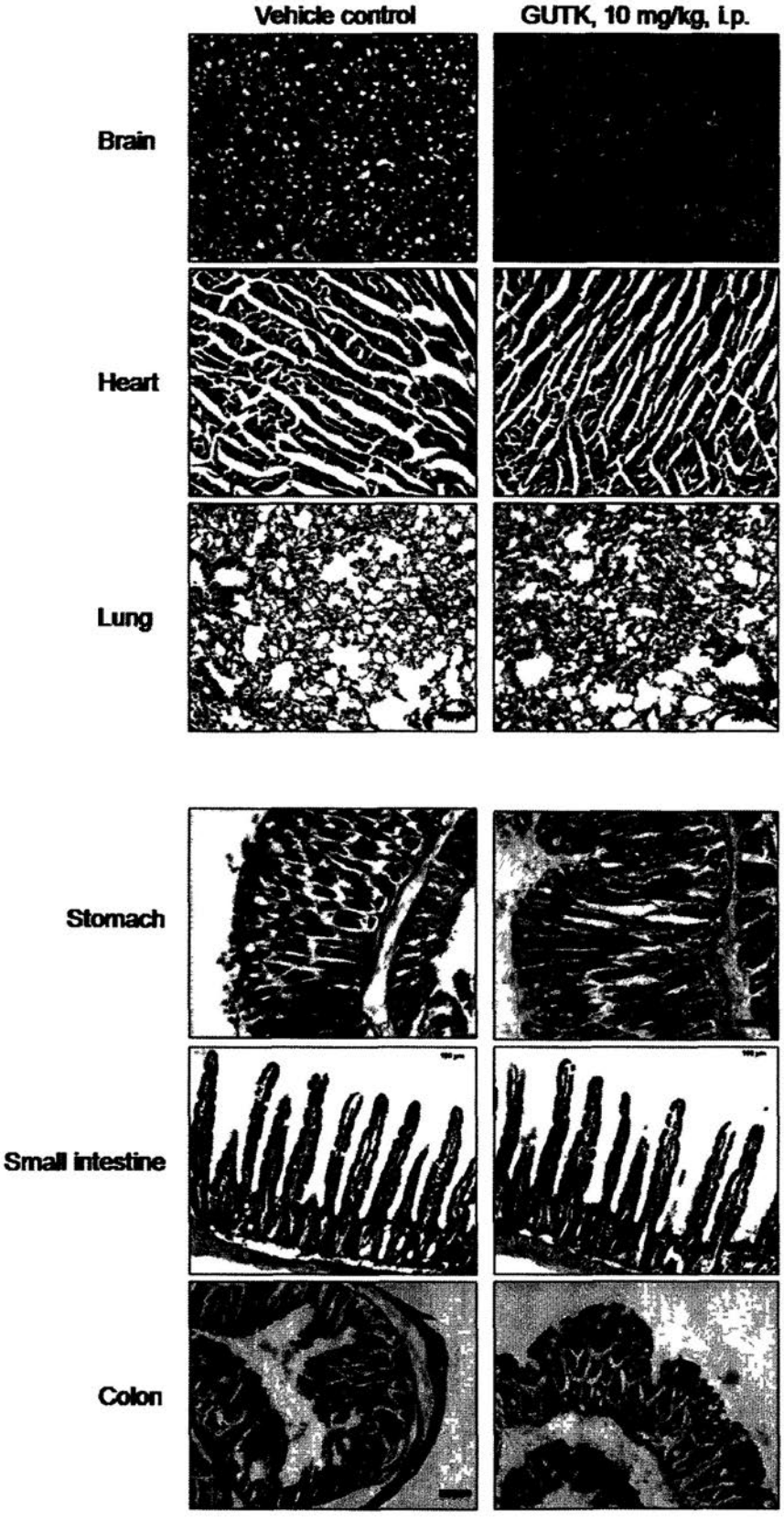
Vehicle control
GUTK, 10 mg/kg, i.p.
Brain
Heart
Lung
Stomach
Small intestine
Colon

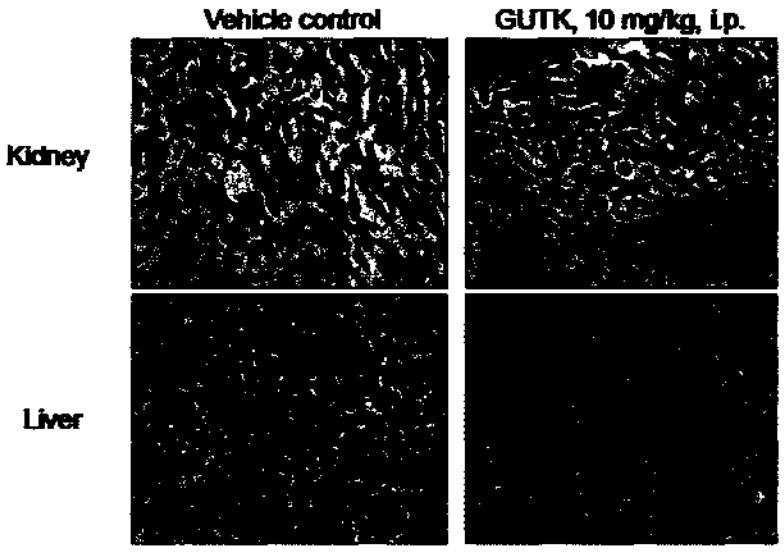

Figure 3.40 Effects of GUTK on the histological changes of the brain, heart, lung, stomach, small intestine, colon, kidney and liver after intraperitoneal injection of GUTK (10 mg/kg) once every other day for 2 weeks. Tissues were fixed by 4% paraformaldehyde and stained with hematoxylin and eosin. Images were viewed and captured using a ZEISS brightfield microscope under 100x magnification. The scale bar indicated by the black bold line refers to 100 μM. The images are representative of results from four mice for each group.

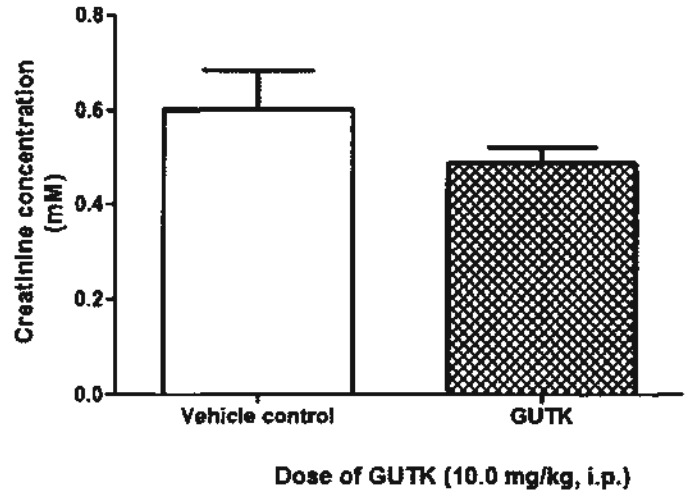

Figure 3.41 Effects of GUTK on the serum creatinine levels after intraperitoneal injection of GUTK (10 mg/kg) once every other day for 2 weeks. Blood samples were collected by cardiac puncture and serum was obtained by centrifugation at 1500 *g* for 20 mins. Data are presented as mean values ± S.E.M. from four mice per group.

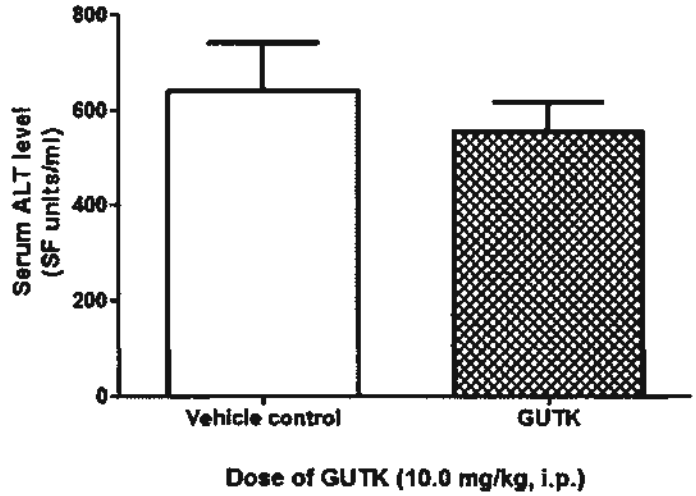

Figure 3.42 Effects of GUTK on the serum ALT levels after intraperitoneal injection of GUTK (10 mg/kg) once every other day for 2 weeks. Blood samples were collected by cardiac puncture and serum was obtained by centrifugation at 1500 *g* for 20 mins. Data are presented as mean values ± S.E.M. from four mice per group.

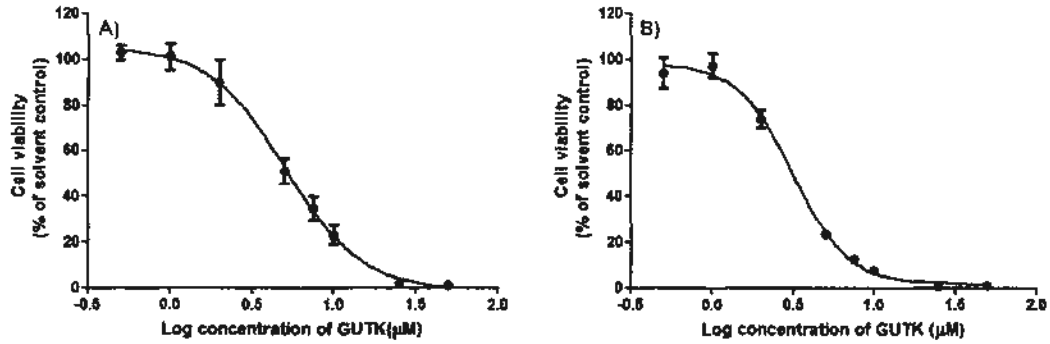

Figure 3.43 Effects of GUTK on the viability of Colon-26 cells after A) 24 h and B) 48 h treatment. Data are expressed as mean values ± S.E.M as a percentage of the solvent control. The solvent control was 0.15% DMSO which had no effect on the viability of HT-29 cells. The experiment was performed in triplicate in three independent experiments.

Body weight was monitored prior to intraperitoneal drug administration every other day for 16 days (including day of sacrifice) (Figure 3.44). Since the selection of mice for each group was based on tumor volume, the mean body weight for each treatment group varied. Hence, the change in body weight was calculated to normalize the body weights on day 0 (Figure 3.44B). While the body weights of vehicle control and GUTK treatment groups increased during the progression of the study, the mean body weight of the 5-fluorouracil group remained unchanged and was significantly different when compared to the vehicle control group on days 12-16 (Figure 3.44B).

After the 14-day treatment by intraperitoneal route, the positive control 5-fluorouracil had significant inhibitory effects on tumor growth from day 14 to day 16 when compared to the vehicle control group ($p<0.05$) (Figure 3.45A). Both GUTK treatment groups (5 mg/kg and 10 mg/kg, i.p.) slightly reduced the tumor

volume when compared with the vehicle control group, but the differences were not significant (Figure 3.45A). It appeared that there was no significant difference in effects between the GUTK 5 mg/kg group and GUTK 10 mg/kg group. Treatment with 5-fluorouracil reduced the tumor weight from 2.4 ± 0.6 g (vehicle control group) by more than 50% to 0.9 ± 0.4 g (5-FU group) (Figure 3.45B). Similar to the results from tumor volume, GUTK at 5 and 10 mg/kg only slightly decreased the tumor weight (Figure 3.45B).

3.2.17 Effects of combination of GUTK and 5-FU on *in vivo* colon tumor growth

A combination of GUTK at 10 mg/kg, i.p. with 5-FU at 12.5 mg/kg i.p. (low dose) or 25 mg/kg i.p. (high dose) was studied for its possible anti-tumor effects. Generally, the mice given the combination treatment were in good health and all the mice had increased body weights throughout the course of treatment (Figure 3.46B). On day 14, the group treated with high dose 5-FU had significantly reduced body weight while the group treated with high dose 5-FU and GUTK had decreased body weight compared to vehicle control on the day of sacrifice ($p<0.05$) (Figure 3.46B). The vehicle control group had higher body weights due to the increased tumor burden as the experiment progressed.

The 5-fluorouracil group reduced tumor volume in a dose-dependent manner throughout the 14-day treatment (Figure 3.47A). For instance, on day 16, the mean tumor volumes of vehicle control and low and high doses of 5-FU were 4757.79 mm^3, 3505.04 mm^3 and 1943.18 mm^3, respectively. 5-FU at 25 mg/kg significantly reduced the tumor volume ($p<0.01$), starting at day 12 of treatment (Figure 3.47A). GUTK at 10 mg/kg significantly reduced tumor volume to 2899.98mm^3 at the end of the treatment period ($p<0.01$) (Figure 3.47).

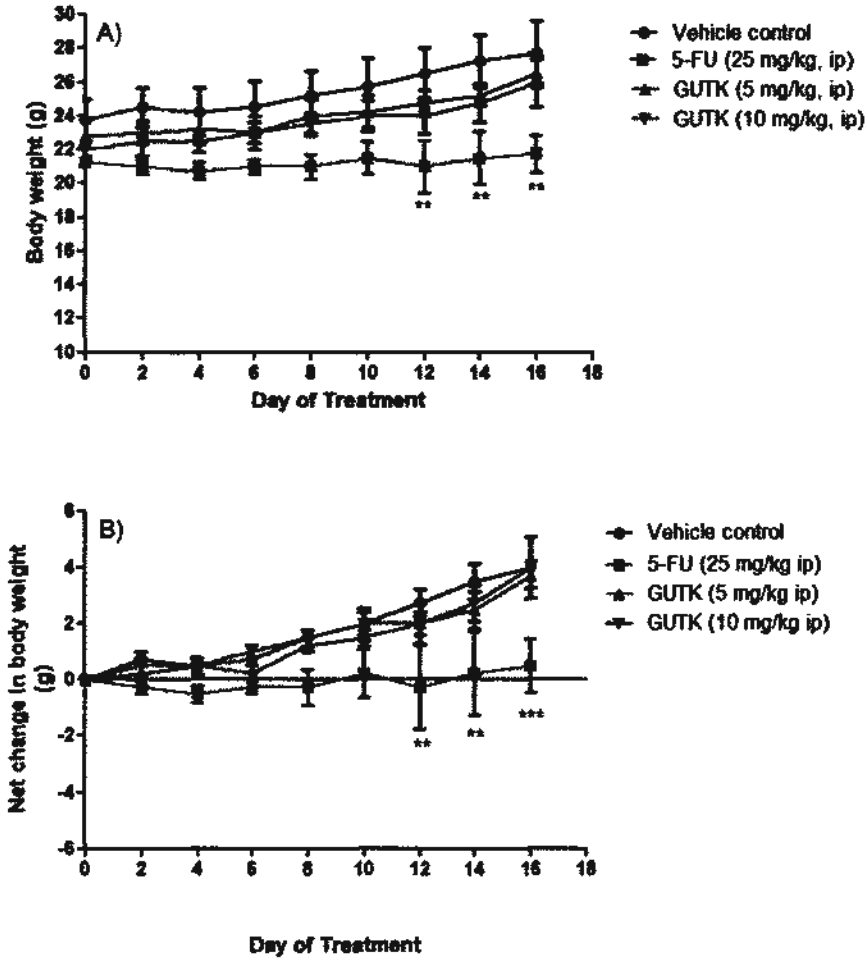

Figure 3.44 Effects of 5-fluorouracil (5-FU) and GUTK on the A) body weight and B) net change of body weight of Colon-26 tumor-bearing mice through the course of drug treatment. Body weight was measured every other day prior to drug administration for 16 days. The net change in body weight was calculated based on the mouse's weight acquired on each day of treatment relative to its weight on Day 0. Data were obtained from four mice per group and are expressed as mean values ± S.E.M. Repeated-measures two-way ANOVA was used to compare the effects between different treatment groups for each body weight measurement. **p<0.01, ***p<0.001 compared with vehicle control (equivalent volume of 5% Tween-80 in normal saline).

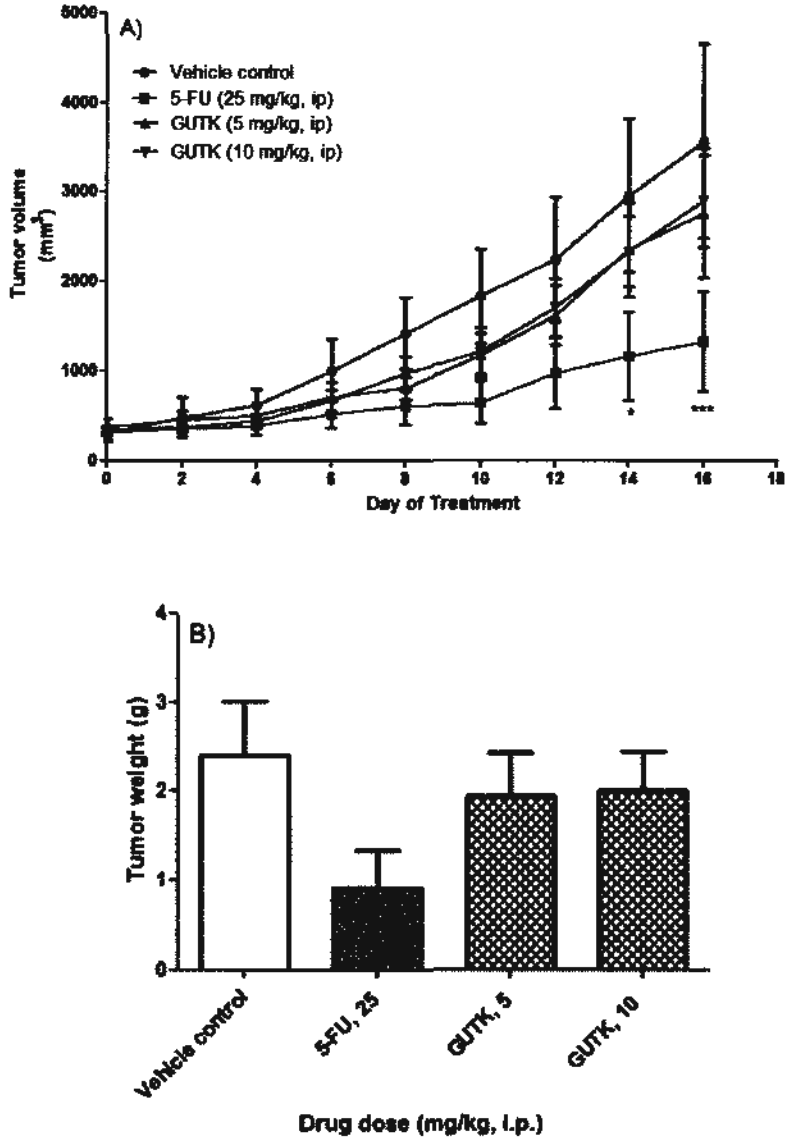

Figure 3.45 Effects of 5-fluorouracil (5-FU) and GUTK on A) tumor volume and B) tumor weight in Colon-26 tumor bearing mice. The tumor volume was measured with calipers on every other day before intraperitoneal drug administration and the tumor weight was measured on day of sacrifice after resection Data were obtained from four mice per group and are expressed as mean values ± S.E.M. Repeated-measures two-way ANOVA was used to compare the effects between different treatment groups for each tumor volume measurement. One-way ANOVA was used to compare the tumor weights between different treatment groups. *$p<0.05$, ***$p<0.001$ compared with vehicle control on the same treatment day.

The combination of GUTK at 10 mg/kg and low-dose 5-FU (12.5 mg/kg) significantly decreased tumor volume by the end of treatment ($p<0.001$) but its anti-tumor effects were only slightly better than low dose 5-FU alone. The combination of GUTK at 10 mg/kg and high dose 5-FU (25 mg/kg) also slightly increased the anti-tumor effect of high dose 5-FU alone but it was not significant. This combination treatment significantly inhibited tumor growth starting from day 10 of the treatment. The mean tumor volumes of vehicle control and GUTK combination with low and high dose 5-FU were 3747.79 mm^3, 2901.00 mm^3 and 1639.97 mm^3, respectively. 5-FU dose-dependently decreased the tumor weight. Groups treated with the combination regimens of GUTK and high or low dose 5-FU had similar tumor weights when compared to the groups treated with the respective doses of 5-FU alone (Figure 3.47B). The combination of GUTK and 5-FU at 25 mg/kg reduced the tumor weight by more than 50%, from 3.95 g in the vehicle control group to 1.44 g in the treatment group (Figure 3.47B). In addition, 5-FU induced a dose-dependent increase in the amount of cleaved caspase-3 in the tumor while GUTK at 10.0 mg/kg i.p., also showed activated caspase-3 (Figure 3.48). The combination treatments of GUTK and both doses of 5-FU induced a dose-dependent increase in the amount of cleaved caspase-3 (at two doses of 5-FU) and the amount of cleaved caspase-3 in both combination treatments were greater than 5-FU alone. Therefore, *in vivo* studies showed that GUTK induced apoptosis in the Colon-26 tumor and it is likely that the anti-tumor effects of GUTK *in vivo* are derived from a mechanism similar to the apoptotic mechanism shown by the *in vitro* studies in HT-29 cells. Furthermore, the addition of GUTK to 5-FU potentiated the apoptosis induced by 5-FU in the tumor, which suggests that GUTK may be a good candidate for combination use with 5-FU for colon cancer.

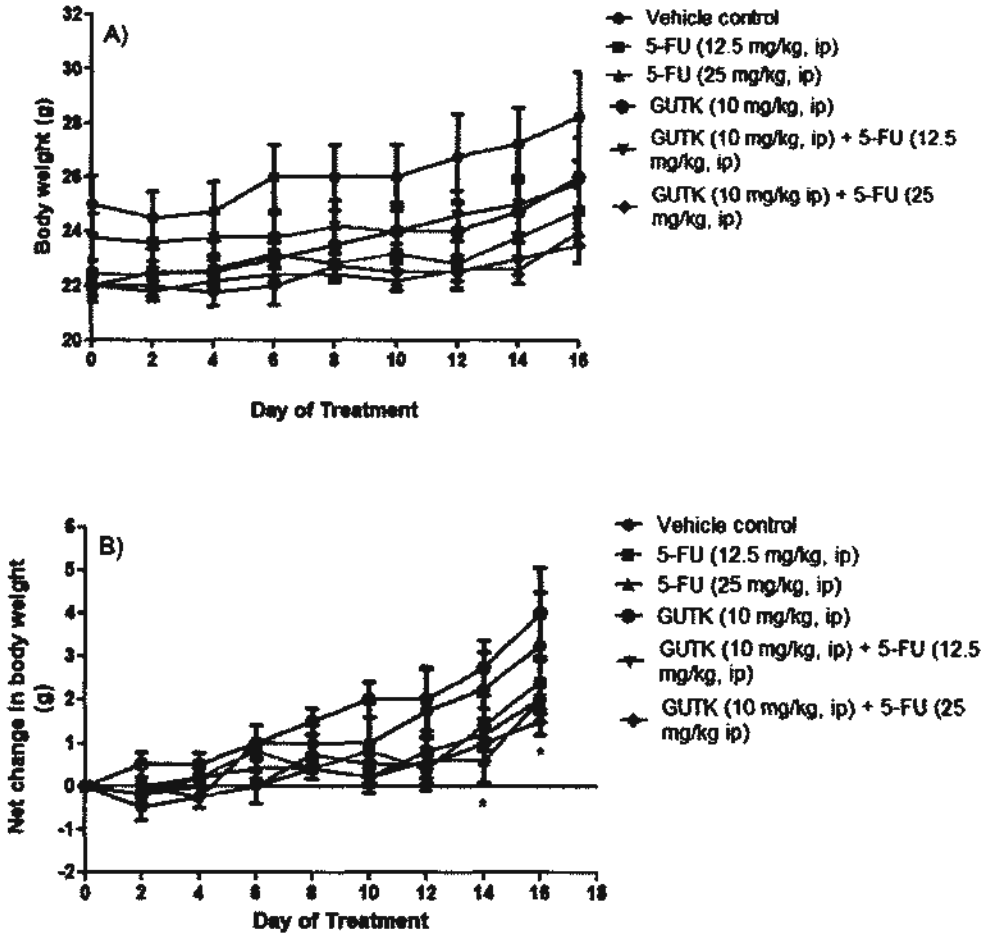

Figure 3.46 Effects of 5-FU, GUTK and combinations of 5-FU and GUTK on the A) body weight and B) net change of body weight of Colon-26 tumor-bearing mice through the course of drug treatment. Body weight was measured every other day prior to drug administration for 16 days. The net change in body weight was calculated based on the mouse's weight acquired on each day of treatment relative to its weight on Day 0. Data were obtained from five mice per group and are expressed as mean values ± S.E.M. Repeated-measures two-way ANOVA was used to compare the effects between different treatment groups for each body weight measurement. *$p<0.05$ compared with vehicle control (equivalent volume of 5% Tween-80 in normal saline).

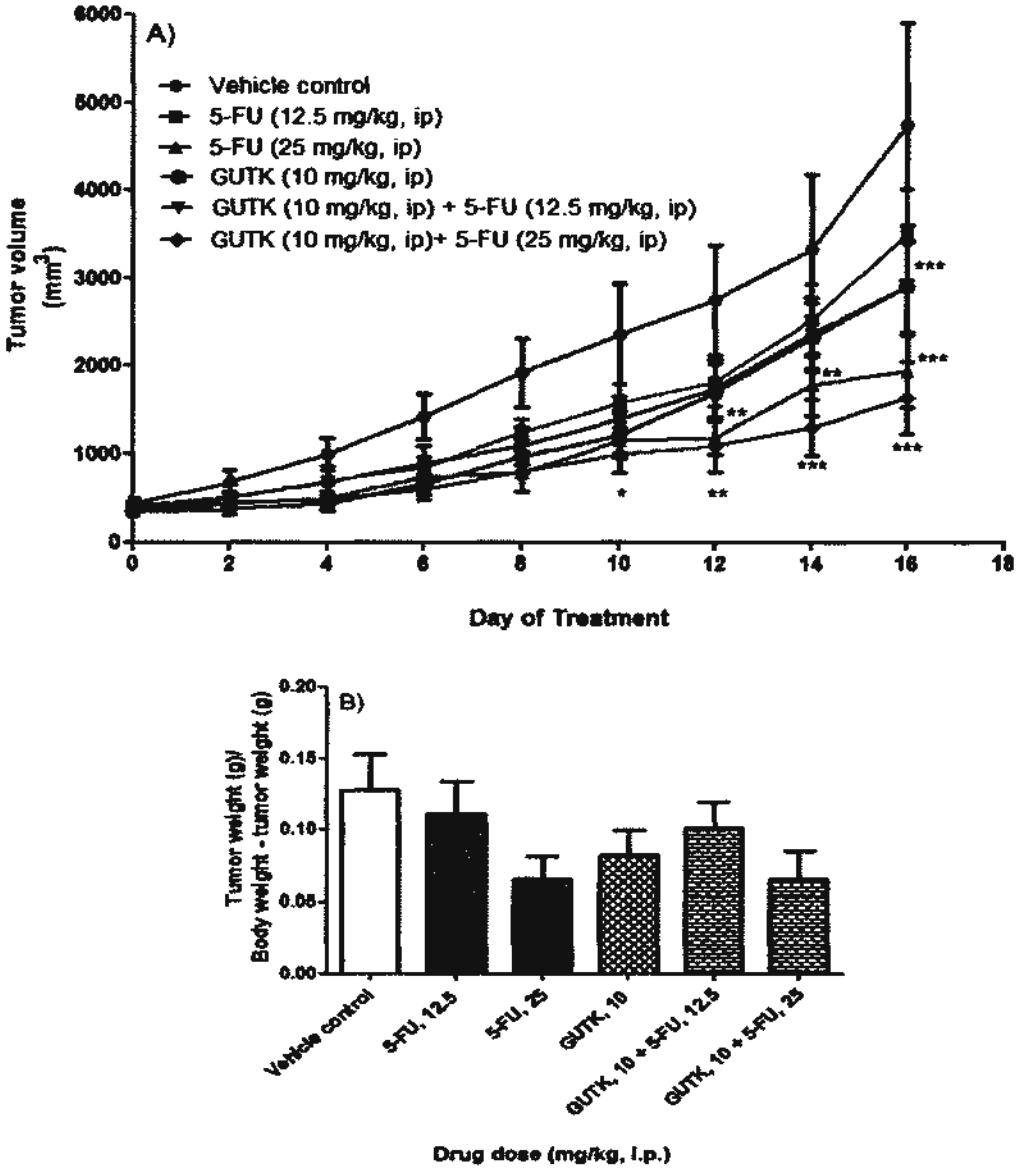

Figure 3.47 Effects of 5-FU, GUTK and combinations of 5-FU and GUTK on A) tumor volume and B) tumor weight in Colon-26 tumor bearing mice. The tumor volume was measured with calipers every other day before i.p. drug administration and the tumor weight was measured on day of sacrifice after resection Data were obtained from five mice per group and are expressed as mean values ± S.E.M. Repeated-measures two-way ANOVA was used to compare the effects between different treatment groups for each tumor volume measurement. One-way ANOVA was used to compare the tumor weights between different treatment groups. *$p<0.05$, **$p<0.01$, ***$p<0.001$ compared with vehicle control on the same treatment day.

Figure 3.48 Effects of 5-FU, GUTK and combinations of 5-FU and GUTK on A) cleaved caspase-3 expression in tumor isolated from Colon-26 tumor bearing mice using immunohistochemical staining. B) The nuclei of the tumor cells are shown by counter-staining with DAPI. Fluorescent microscopy at 200x magnification was used and the scale bars represent 100 μM at 200x. The photos are representative of results obtained from five mice per treatment group.

3.3 Discussion

TH and other *Garcinia* species are Chinese medicinal herbs traditionally used for their anti-inflammatory, wound-healing and anti-diarrheal properties (Panthong *et al.*, 2007; Pedraza-Chaverri *et al.*, 2008; Obolskiy *et al.*, 2009). Several classes of bioactive compounds from different *Garcinia* species have been discovered, such as classical and caged xanthones, benzophenones, acylphloroglucinols and terpenoids and alkaloids (Matsumoto *et al.*, 2003; Wu *et al.*, 2004b; Feng *et al.*, 2007; Wang *et al.*, 2008a; Xu *et al.*, 2008; Xu *et al.*, 2010; Zhang *et al.*, 2010b). However, the anti-cancer effects of TH have been suggested to be due to caged polyprenylated xanthones and benzophenone derivatives (Han *et al.*, 2009; Na, 2009; Xu *et al.*,

2010). In this study, the cytotoxic and anti-proliferative effects of various caged and uncaged xanthones and benzophenone derivatives were studied. Then, two novel benzophenone derivatives recently isolated by our research team from TH, EPC and GUTK, were examined for the mechanisms underlying their cytotoxicity and anti-proliferative effects in human colon cancer cells (Xu *et al.,* 2010). In addition, the *in vivo* anti-tumor effects of GUTK alone and in combination with 5-fluorouracil, first-line treatment for colon cancer, were examined.

Results from the screening of xanthones and benzophenones isolated from TH indicated that gambogic acid was the most potent in inducing cytotoxicity in HT-29 cells, followed by gambogenic acid, γ-mangostin, EPC and allanxanthone C. All of these compounds were more cytotoxic than the positive controls, cisplatin and 5-fluorouracil (Table 3.4). The above compounds also almost fully suppressed proliferation of colon cancer cells at their IC_{50} values without affecting the viability of normal human colon fibroblasts, except for gambogic acid and gambogenic acid after 48 h incubation (Figures 3.7, 3.8).

In terms of anti-cancer effects, the most well-studied xanthone of THI is gambogic acid, which has been approved for cancer use in China since the 1970s and the injectable form of the compound is currently being tested for its efficacy in phase II clinical trials (Han *et al.,* 2006a; Han & Xu, 2009). Studies have shown that gambogic acid binds reversibly on transferrin receptors to activate apoptosis in cancer cells (Kasibhatla *et al.,* 2005; Pandey *et al.,* 2007). Normal cells expressed less transferrin receptors compared to cancer cells, which allowed gambogic acid to selectively induce apoptosis in cancer cells without affecting normal cells (Kasibhatla *et al.,* 2005). As well, it has been shown that gambogic acid bind on

hepatic carcinoma SMMC-7721 cells with higher affinity than in L02 hepatocytes (Yang *et al.*, 2007d). It was widely distributed in various organs such as kidney, liver and lung after intravenous administration in tumor-bearing mice but after 4-6 h, it accumulated only in tumor tissue (Yang *et al.*, 2007d).

Studies have shown that gambogic acid and its derivatives induced G_2/M cell cycle arrest and apoptosis in glioma, leukemia and breast, gastric and skin cancer cells through mechanisms discussed in the Introduction (Zhao *et al.*, 2004; Liu *et al.*, 2005; Tao *et al.*, 2007; Qiang *et al.*, 2008; Wang *et al.*, 2008c; Zhai *et al.*, 2008; Gu *et al.*, 2009; Xie *et al.*, 2009; Xu *et al.*, 2009; Mu *et al.*, 2010). Also, gambogic acid has been reported to inhibit *in vitro* cell adhesion, migration and invasion and *in vivo* breast lung metastasis and angiogensis (Lu *et al.*, 2007; Qi *et al.*, 2008a; Qi *et al.*, 2008b). Gambogic acid reduced VEGF production in cancer cells, the phosphorylation and activation of VEGFR-2 and the downstream phosphorylation of p38 and ERK, c-Src and focal adhesion kinase in endothelial cells to suppress angiogenesis and reduce tumor volume in mice subcutaneously injected with lung and prostate cancer cells and in an orthotopic glioma model (Lu *et al.*, 2007; Qiang *et al.*, 2008; Yi *et al.*, 2008). As well, it reduced telomerase activity and the transcription of human telomerase reverse transcriptase by reducing expression of oncogene c-myc and phosphorylation of AKT, which led to inhibited tumor growth in lung, gastric and liver cancer (Guo *et al.*, 2004; Wu *et al.*, 2004; Guo *et al.*, 2006; Yu *et al.*, 2006; Zhao *et al.*, 2008). However, chronic toxicological studies using Beagle dogs injected with gambogic acid (i.p.) every other day for 13 weeks resulted in cellular damage to the kidney and the liver (Guo *et al.*, 2006). Similarly, rats fed orally with gambogic acid at 30, 60 and 120 mg/kg every other day for 13 weeks resulted in necrotic damage to the liver and kidney, decreased leucoyte count and

increased serum ALT and creatinine levels at the highest dose (Qi *et al.,* 2008c). The lack of selectivity of gambogic acid shown by the present study, along with other *in vivo* toxicity reports, suggest that more drug candidates are needed with comparable potency but better selectivity than gambogic acid.

Both allanxanthone C and γ-mangostin are considered "classical xanthones" without the 4-oxa-tricyclo[4.3.1.$0^{3,7}$]dec-8-en-2-one scaffold caged moiety (Figure 1.7) (Han & Xu, 2009). They were less potent than gambogic acid and gambogenic acid, which suggests that the scaffold for the caged structure is important for cytotoxicity in colon cancer cells. The chemical structure of gambogic acid with numbering of carbons is shown in Figure 3.49. Studies have demonstrated that caged xanthones required an intact ABC ring with a C-ring caged structure for anti-proliferative effects against leukemia cells (Chantarasriwong *et al.,* 2009).

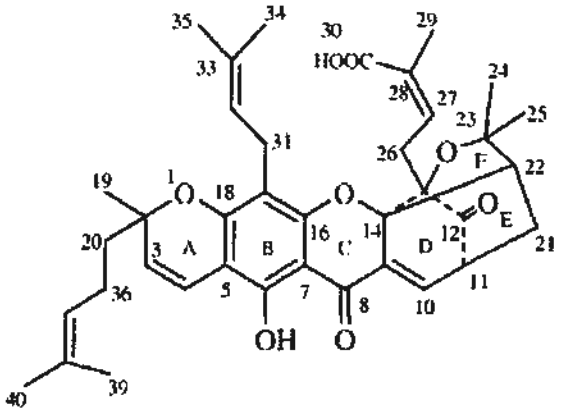

Figure 3.49 Chemical structure of gambogic acid isolated from TH

Furthermore, it has been suggested that the caged structure (of the C ring) of the xanthones is the major contributor to their cytotoxic effects in cancer cell lines, while lack of substitutions at the A ring does not affect its cytotoxicity (Batova *et al.,* 2007). The anti-proliferative effects of caged xanthones were the same in both multi-drug

resistant leukemia HL-60/ADR cell line and its parental HL-60 cell line, suggesting that the bioactivity of caged xanthones are not affected by chemoresistant mechanisms in cancer cells (Batova *et al.,* 2007; Chantarasriwong *et al.,* 2009).

The major constituents isolated from the pericarp of mangosteen, stem and root bark of *G. mangostana* are α-mangostin and γ-mangostin (Ee *et al.,* 2008; Ha *et al.,* 2009; Han *et al.,* 2009; Na *et al.,* 2009; Obolskiy *et al.,* 2009; Watanapokasin *et al.,* 2010). Other classical xanthones such as β-mangostin, garcinone D and gartanin have also been isolated from the stems and roots of *G. mangostana* (Ee *et al.,* 2008; Han *et al.,* 2009). α-Mangostin has been found to be cytotoxic in human lymphoblastoid CEM-SS and human colon cancer DLD-1 and HT-29 cells, with IC_{50} values of 11.5 μM, 12.2 μM and 1.7μM after 48 h incubation, respectively (Ee *et al.,* 2008; Ha *et al.,* 2009; Han *et al.,* 2009). The γ-mangostin tested in the present study had a similar IC_{50} value of 3.7 ± 0.3 and 2.3 ± 0.4 μM after 24 h and 48 h treatment, respectively (Table 3.4). Although α-mangostin, β-mangostin and γ-mangostin have been reported to significantly reduce the viability of human colon cancer DLD-1 cells at 20 μM, only α-mangostin and γ-mangostin induced apoptosis (Matsumoto *et al.,* 2005). In addition, intratumoral injection of a mixture of α-mangostin and γ-mangostin significantly reduced tumor volume in a mouse subcutaneous colon tumor model using COLO 205 cells, with induced apoptosis and activation of caspases-3 and -8 in the tumor tissue (Watanapokasin *et al.,* 2010). Xanthones isolated from *G. mangostana* have been found to enhance TRAIL-R2 promoter activity to up-regulate the expression of death receptors and that it re-sensitized TRAIL-resistant gastric cancer cells to TRAIL treatment (Kikuchi *et al.,* 2010). It has been postulated that the number of hydroxyl groups of classical xanthones is correlated with its anti-cancer efficacy (Matsumoto *et al.,* 2004; Matsumoto *et al.,* 2005). Since the anti-cancer effects of xanthones have been extensively studied (Na *et al.,* 2009), this study

focused on the mechanisms of G_0/G_1 cell cycle arrest and cell death induced by novel polyisoprenylated benzophenone derivatives, in particular EPC and GUTK, isolated from TH. However, EPC and GUTK are also present in *Garcinia cowa* and *Garcinia yunnanensis*.

Results showed that EPC and GUTK were very potent at reducing the viability of both HT-29 and HCT116 cells, without affecting the viability of normal human colon fibroblasts (Figures 3.9-3.11). GUTK isolated from *Rheedia calcicola* has also been reported to be cytotoxic in human ovarian cancer A2780 cell line, with an IC_{50} value of 5.98 μM (Cao *et al.*, 2007). Its potency is similar to that of EPC and GUTK in the current study, as their IC_{50} values in human colon cancer HT-29 cell line were 5.1 ± 0.1 μM and 5.4 ± 0.2 μM, respectively after 24 h incubation (Table 3.5). Interestingly, most of the tested structures had the same benzophenone backbone with or without a highly oxygenated bicyclo trione core, but the type, length and position of the geranyl or prenyl side chains have a significant effect on their bioactivities (Figure 1.7). For example, oblongifolin D had a similar chemical backbone structure to GUTK, but the shorter prenyl substitutions in GUTK produced a greater cytotoxic effect in HT-29 cells. Oblongifolin D decreased HT-29 cell viability by less than 20%, but GUTK decreased viability by almost 70% (Figure 3.9). Since the anti-cancer effects of EPC and GUTK isolated from TH have not been reported, these two polyisoprenylated benzophenone derivatives were selected for further studies on the mechanisms underlying their cytotoxic and anti-proliferative effects.

Both EPC and GUTK significantly induced G_0/G_1 cell cycle arrest (Figures 3.13C, 3,14C), which was associated with decreased protein expression of cyclins D1 and D3 and CDKs 4 and 6 (Figures 3.15-3.18). Other xanthones isolated from *G*

mangostana and polyisoprenylated benzophenones isolated from *Garcinia xanthochymus* also induced G_0/G_1 cell cycle arrest in human colon cancer cells (Matsumoto *et al.,* 2005; Protiva *et al.,* 2008). However, gambogic acid induced G_2/M cell cycle arrest as a result of microtubule disruption and depolymerization in cancer cells (Chen *et al.,* 2008). The major cyclins and CDK complexes involved in G_1/S phase transition are cyclins D1, D2 and D3 with CDK4 or 6 and cyclin E with CDK2 in the late G_1 phase (Viglietto *et al.,* 2002; Senderowicz, 2003; Fu *et al.,* 2004). The availability of cyclins is the first level of regulation of CDKs (Belletti *et al.,* 2005). Therefore, the down-regulation of cyclins D1 and D3 and CDKs4 and 6 by EPC and GUTK in the present study reduced the amount of available cyclin and CDK available in the cell. Then, less cyclins D1 and D3 and CDKs 4 and 6 bind to form the activated cyclin/CDK complex, which inhibited the downstream transcription of genes needed for G_1/S phase transition and S phase. Although the effects of EPC and GUTK on the protein expression of cyclin E and CDK2 were not examined in this study, it is expected that the two compounds also decreased the protein levels of cyclin E and CDK2 to contribute to the G_0/G_1 cell cycle arrest.

In the present study, EPC and GUTK up-regulated the protein expressions of $p21^{Waf1/Cip1}$ and $p27^{Kip1}$, without affecting the expressions of $p15^{INK4B}$ and $p16^{INK4A}$ (Figures 3.19-3.22). Both families of tumor suppressors are frequently down-regulated or de-regulated in resected human colon tumor specimens (Loda *et al.,* 1997; Ishiguro *et al.,* 2006; Mitomi *et al.,* 2010). Since the INK4 family of tumor suppressors were not affected by EPC and GUTK treatment, the two compounds most likely target the CIP/KIP family of cyclin-dependent kinase inhibitors for the induction of G_0/G_1 cell cycle arrest. The $p21^{Waf1/Cip1}$ protein is directly activated by tumor suppressor p53 binding to its promoter (Abukhdeir & Park, 2008). Since

HT-29 cells are p53-mutated, $p21^{Waf1/Cip1}$ may be up-regulated by inhibition of AKT pathway, which leads to decreased phosphorylation of $p21^{Waf1/Cip1}$ at Thr145 and decreased cytoplasmic localization of $p21^{Waf1/Cip1}$ (Zhou *et al.*, 2001). Hence, increased $p21^{Waf1/Cip1}$ remains in the nucleus to act as a cell cycle inhibitor. To confirm this finding, the effects of EPC and GUTK on the PI3K/AKT pathway and the connection between PI3K/AKT pathway and CIP/KIP family of tumor suppressors must be examined. The HT-29 cell line used in this study showed low $p21^{Waf1/Cip1}$ expression, in comparison with CCD-18Co cell line, which indicated that the up-regulation of $p21^{Waf1/Cip1}$ by EPC and GUTK may account for their selective effects on cancer cells (Figure 3.50).

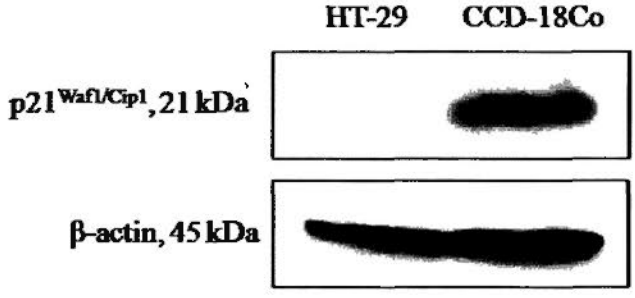

Figure 3.50 Protein expression of $p21^{Waf1/Cip1}$ in human colorectal carcinoma HT-29 cell line and human normal colon fibroblast CCD-18Co cell line.

The $p27^{Kip1}$ protein is usually de-regulated, not genetically mutated in many cancers (Chu *et al.*, 2008). The regulation of $p27^{Kip1}$ activity is through the control of its intracellular concentration, its distribution among different cyclin-CDK complexes and its sub-cellular localization (Viglietto *et al.*, 2002). The intracellular concentration of $p27^{Kip1}$ is controlled through transcriptional regulation of its promoter, translational control of mRNA translation and control of its degradation rate (Viglietto *et al.*, 2002). The most important mechanism for control of its

concentration is by its proteolysis through the ubiquitin-proteasome pathway. It has been shown that once p27 has been phosphorylated at Thr187 by cyclin E/CDK2, it is recognized by the ubiquitin ligase SCF^{Skp2}, which adds a chain of multiple ubiquitin molecules to $p27^{Kip1}$ (Pagano *et al.*, 1995; Sheaff *et al.*, 1997; Carrano *et al.*, 1999). Then, the ubiquinated- $p27^{Kip1}$ is recognized and degraded by the proteasome (Carrano *et al.*, 1999). Hence, the increase in $p27^{Kip1}$ protein levels by EPC and GUTK may be through inhibition of the proteasome degradation process. In normal cycling cells, $p27^{Kip1}$ is predominantly bound to cyclin D/CDK4, which prevents it from binding on to its main target cyclin E/CDK2, the major cyclin/CDK complex formed at the G_1/S phase transition (Sherr *et al.*, 1999). However, in cells that are undergoing G_0/G_1 cell cycle arrest, $p27^{Kip1}$ preferably binds to and inhibits cyclin E/CDK2 complex (Belletti *et al.*, 2005). The reduction of cyclin D1 and D3 levels by EPC and GUTK may prevent the binding of $p27^{Kip1}$ to the cyclin D/CDK4(6) complex, which allows it to bind and inhibit cyclin E/CDK2 complex to induce G_0/G_1 arrest. In normal cycling cells, $p27^{Kip1}$ migrates between the nucleus and cytoplasm. However, in arrested cells, $p27^{Kip1}$ is persistently present in the nucleus to inhibit the cyclin E/CDK2 complex (Viglietto *et al.*, 2002). It has been shown that $p27^{Kip1}$ can be phosphorylated by human kinase interacting stathmin on S10, which promotes its export into the cytoplasm from the nucleus (Boehm *et al.*, 2002). As well, phosphorylation of $p27^{Kip1}$ by AKT prevented the import of $p27^{Kip1}$ back into cell nuclei once it is in cytoplasm (Viglietto *et al.*, 2002). Once $p27^{Kip1}$ is exported from the cell nuclei, it cannot bind and inhibit cyclin E/CDK2 complex, which continues to phosphorylate $p27^{Kip1}$ at Thr187 to target it for proteasomal degradation. $P27^{Kip1}$ has also been shown to be phosphorylated at Thr157 to inhibit the import of $p27^{Kip1}$ into cell nuclei (Liang *et al.*, 2002). Cytoplasmic localization of $p27^{Kip1}$ has been found in 35% of human colorectal carcinoma samples (Ciaparrone *et al.*, 1998).

Therefore, EPC and GUTK may either inhibit the transcription of $p27^{Kip1}$ and/or inhibit the phosphorylation signals that target $p27^{Kip1}$ for nuclear export into the cytoplasm, which allows $p27^{Kip1}$ to remain in the nucleus and act as a cyclin E/CDK2 inhibitor.

Both EPC and GUTK were shown to induce an accumulation of cells in the apoptotic sub-G_1 phase, along with condensed chromatin and fragmented nuclei at 10 μM after 24 h treatment (Figures 3.13, 3.14, 3.23, 3.24). As well, both compounds triggered the cleavage of PARP and activation of caspase-3, caspase-8 and caspase-9 in a dose-dependent manner after 12 h (Figures 3.25-3.31). Although this study is the first to report the apoptotic activities of EPC and GUTK, several studies have focused on the anti-cancer mechanism of garcinol (also known as camboginol) isolated from *Garcinia indica* and *Garcinia cambogia*. As shown in Figure 3.51, the chemical structure of garcinol is very similar to that of GUTK.

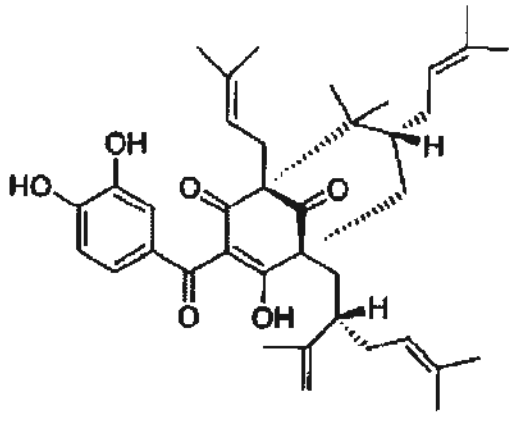

Figure 3.51 Chemical structure of garcinol isolated from *Garcinia indica*

Garcinol was cytotoxic to human leukemia cells through the induction of apoptosis by up-regulation of Bax and Bad and down-regulation of Bcl-2 and its IC_{50} value (9.42 μM) was slightly higher than that obtained from this study (Pan *et al.*, 2001).

The selectivity of garcinol for cytotoxicity in HT-29 and HCT116 cells over normal human intestine and embryonic intestine IEC-6 and INT-407 cells were demonstrated by Hong *et al.* (2007) and they demonstrated that garcinol induced apoptosis with IC_{50} values of 3.06 μM after 24 h treatment, which is similar to the IC_{50} values for EPC and GUTK obtained from this study (Table 3.5). As well, garcinol significantly potentiated TRAIL-induced apoptosis by increasing ROS (Prasad *et al.*, 2010). Garcinol induced the up-regulation of death receptors TRAIL-R1 and TRAIL-R2 in a time- and dose-dependent manner in HCT116 cells, yet there was no up-regulation of these death receptors in normal breast cells (Prasad *et al.*, 2010). Similarly, EPC and GUTK were found to activate caspase-8 in HT-29 cells in the present study and further studies should be conducted to examine the effects of these two compounds on the expression of death receptors such as FasR, TRAIL-R1 and TRAIL-2 and their effects on apoptosis. Moreover, garcinol has been reported to inhibit invasion and migration of HT-29 cells by decreasing matrix metalloproteinase-7 levels and to induce apoptosis by decreasing Bcl-2 levels and inhibiting ERK and AKT (Liao *et al.*, 2005). Guttiferone E, guttiferone H and xanthochymol, which are structurally-similar to GUTK have also been demonstrated to be cytotoxic in HCT116 and HT-29 cells with IC_{50} values of 9-15 μM after 48 h treatment (Protiva *et al.*, 2008). These three benzophenone derivatives triggered a reduction in mitochondrial membrane potential, which activated the endoplasmic reticulum stress pathway by up-regulation of ATF4 and XBP1 and the cellular energy stress pathway by up-regulation of DDIT4/REDD1 (Protiva *et al.*, 2008). The mTOR cell survival pathway was inhibited and there was increased transcription of genes needed for G_0/G_1 arrest and apoptosis. Although the current study investigated the induction of apoptosis by EPC and GUTK in HT-29 cells, the upstream cellular pathways that lead to apoptosis have not been explored. Like other benzophenone derivatives, EPC and GUTK may also activate the

endoplasmic reticulum and cellular stress pathways and the expression of genes involved in these two pathways may be explored in further studies.

The effects of EPC and GUTK on activation of MAPK pathways were examined in the present study. Both EPC and GUTK triggered the phosphorylation of JNK, but with different time courses (Figures 3.33, 3.36). Whereas EPC activated the JNK pathway early as 3 h after treatment (Figure 3.34), GUTK did not activate JNK until 12 h after treatment (Figure 3.36). Hence, the JNK pathway may not be activated by the same upstream signals after treatment with these two compounds. For instance, there are various types of MAPKKK, such as MEKK1-4, ASK1 and MLKs, and MAPKK, such as MKK4 and MKK7 (Fan & Chambers, 2001). As discussed in the previous chapter, many conventional anti-cancer drugs and chemopreventive agents, such as paclitaxel, cisplatin, etoposide and NSAIDs activate JNK-dependent apoptosis (Fan & Chambers, 2001; Kim *et al.,* 2001; Elder *et al.,* 2002). Results in the present study showed that pre-treatment with JNK inhibitor SP600125 significantly attenuated the apoptosis-induced by GUTK, which suggested that GUTK-induced apoptosis was partially mediated by the JNK pathway. In contrast, SP600125 actually enhanced the apoptosis induced by EPC, which suggests that JNK may actually have a pro-survival role in HT-29 cells treated with EPC. The pro-survival role of JNK has also been implicated in thymoquinone-induced apoptosis (El-Najjar *et al.,* 2010). Another study by Muscarella & Bloom (2008) showed that the pro-survival or pro-apoptotic role of JNK is dependent on the type and extent of cellular injury. Treatment with either chemotherapeutic drug vincristine or arsenite and hyperthermia in B-cells induced JNK activation and apoptosis, but aresenite/hyperthermia-induced apoptosis was not reversed with a JNK inhibitor, while vincristine-induced apoptosis was suppressed by a JNK inhibitor (Muscarella

& Bloom, 2008). The activation of JNK induced the phosphorylation of Bcl-2 at Thr56, which inhibited its anti-apoptotic function to stimulate apoptosis in vincristine-induced cell death, but not in arsenite/hyperthermia-induced cell death. The mechanisms of JNK-dependent and JNK-independent apoptosis induced by GUTK and EPC, respectively, may be studied further by investigation of downstream JNK phosphorylation targets in the apoptotic pathway, such as Bcl-2 and Bcl-XL .

P38, was also activated by EPC after 12 h treatment but it was not activated by GUTK (Figures 3.34, 3.37). Yet, p38 inhibitor slightly reduced the caspase-3 activity induced by EPC and GUTK (Figure 3.38B). Apoptosis mediated by activation of p38 has been reported for many chemopreventive and anti-cancer drugs in cancer cells such as indomethacin, paclitaxel, vinblastine and tamoxifen, as discussed in the previous chapter. Studies have shown that gambogic acid increased intracellular ROS, which activated JNK and p38 pathways to induce apoptosis in human hepatoma SMMC-7721 cells (Nie *et al.,* 2009). Similarly, the disruption of the microtubule cytoskeleton and depolymerization of microtubules by gambogic acid induced G_2/M arrest, associated with activation of JNK and p38 up to 12 h after gambogic acid treatment in human breast MCF-7 carcinoma cells (Chen *et al.,* 2008b). The concentration of SB203580 used in the current study was 1.0 μM pre-treatment for one hour before the addition of EPC or GUTK. However, other studies have used higher concentrations of SB203580 up to 10 μM and longer pre-treatment period up to 2 hours (Kim *et al.,* 2001; Lee *et al.,* 2010b). Therefore, the use of SB203580 at a higher concentration pre-incubated for a longer time period in HT-29 cells may be attempted to see if it has any effect on apoptosis induced by EPC and GUTK.

While EPC induced ERK phosphorylation after 12 h treatment, GUTK slightly

reduced ERK phosphorylation (Figures 3.34, 3.37, 3.38C). These results reflect the controversial role of ERK in cell survival as some studies showed that ERK has a cytoprotective role whereas other studies showed that ERK has a pro-apoptotic role, which was discussed extensively in the previous chapter (Elder *et al.,* 2002; Zhuang & Schnellmann, 2006). Similar to SB203580, the effects of PD98059 on apoptosis induced by EPC and GUTK may be examined again by increasing the concentration of PD98059 and its pre-incubation period in HT-29 cells to confirm the cytoprotective or pro-apoptotic role of ERK.

The fact that the MAPK inhibitors could not fully suppress apoptosis induced by EPC and GUTK suggests that other intracellular pathways that regulate cell proliferation, survival and death may be affected by EPC and GUTK. For instance, gambogic acid and garcinol has been demonstrated to decrease activation of the NF-κB signaling pathway in cancer cells (Pandey *et al.,* 2007; Ahmad *et al.,* 2010). The NF-κB pathway has an important role in tumorigenesis as it regulates the expression of anti-apoptotic proteins such as Bcl-2, Bcl-XL and survivin; invasion and angiogenesis proteins such as COX-2, VEGF and matrix metalloproteinase-9 (MMP-9); proliferation proteins such as cyclin D1 and c-Myc and other inflammatory cytokines and chemokines (Pandey *et al.,* 2007). Studies have revealed that gambogic acid potentiated TNF-induced apoptosis by inhibiting the expression of many anti-apoptotic, proliferation and metastasis proteins proteins induced by TNF-α, such as IAP1, IAP2, Bcl-2, cyclin D1, COX-2, MMP-9 and VEGF (Pandey *et al.,* 2007). As well, garcinol dose-dependently inhibited the DNA-binding activity of NF-κB and decreased expression of NF-κB gene products such as Bcl-2, Bcl-XL and IκBα, which were consistent with the cytotoxic and apoptotic effects of garcinol in estrogen receptor-negative human breast cancer MDA-MB-231 cells (Ahmad *et*

al., 2010). Garcinol has also been demonstrated to inhibit phosphorylation of AKT to reduce the activation of PI3K/AKT cell survival pathway in human breast cancer cells (Ahmad *et al.*, 2010). It would be interesting to see if EPC and GUTK inhibit the NF-κB pathway and how this affects regulation of MAPK and other cell survival pathways such as AKT through cross-talking.

EPC and GUTK had cytotoxic effects selectively on human colon cancer HT-29 and HCT116 cells. Both of the compounds induced G_0/G_1 arrest by down-regulation of cyclins D1 and D3 and CDKs 4 and 6 and up-regulation of tumor suppressors $p21^{Waf1/Cip1}$ and $p27^{Kip1}$. Both compounds also induced apoptosis that involved both the mitochondrial- and death receptor-mediated pathways. In addition, both EPC and GUTK induced the phosphorylation of JNK. The proposed mechanisms of EPC and GUTK are shown in Figure 3.53.

Since EPC and GUTK showed promising *in vitro* cytotoxic and anti-proliferative effects at concentrations lower than cisplatin and 5-fluorouracil, the effects of GUTK, which had relatively higher quantity, on an *in vivo* subcutaneous tumor model using Colon-26 tumor cells were investigated. The subcutaneous mouse colon carcinoma Colon-26 tumor model was used because normal BALB/c mice allowed for the analysis of anti-tumor effects in mice with an intact and healthy immune system, which mimics the clinical situation of cancer. Since no previous studies have been carried out on the pharmacokinetics of GUTK in mice or rats, the doses of GUTK used and the dosage regimen in this study were selected based on published work on gambogic acid used in similar *in vivo* subcutaneous tumor models and nude mice tumor xenografts for lung, gastric and hepatic cancer (Guo *et al.*, 2004; Liu *et al.*, 2005; Yang *et al.*, 2007; Rong *et al.*, 2009). In these studies, gambogic acid was

administered at various doses from 2.0-8.0 mg/kg three times a week or every other day for 2-3 weeks through intravenous or intraperitoneal administration (Guo *et al.*, 2004; Wu *et al.*, 2004; Liu *et al.*, 2005; Rong *et al.*, 2009).

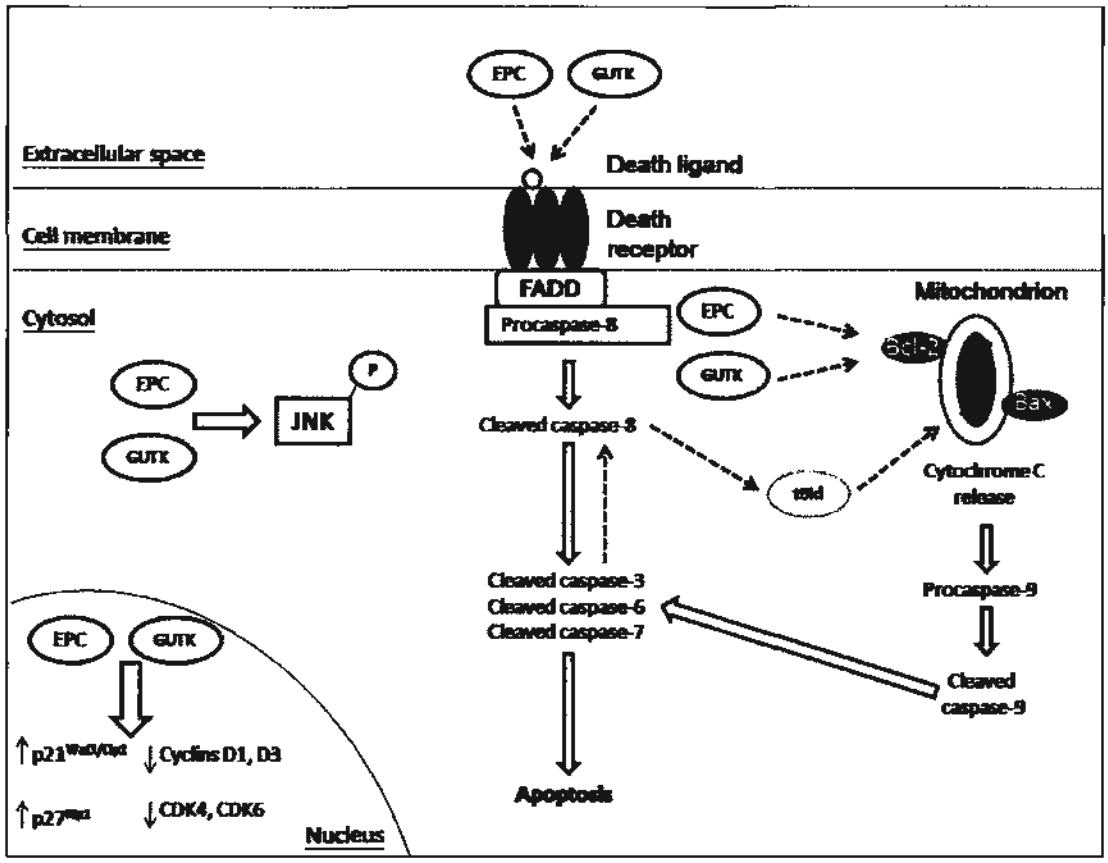

Figure 3.53 Proposed mechanism of EPC and GUTK. EPC and GUTK may up-regulate death receptors and their ligands to activate caspase-8 in the death receptor-mediated apoptotic pathway. EPC and LGT may also disrupt the balance between Bax and Bcl-2 in mitochondria to induce a decrease in mitochondrial membrane potential and cytochrome c release for the activation of caspase-9 in the mitochondrial-mediated apoptotic pathway. Cross-talking between the two pathways may occur by activation of caspase-8 by caspase-6 and by truncated Bid. The two pathways converge for the activation of caspase-3 for the typical morphological changes associated with apoptosis. Dashed arrows indicate possible mechanisms.

A minimum dose of 4 mg/kg of gambogic acid significantly reduced tumor volume in mice injected with human lung H1299 cells, human gastric BGC-823 and human hepatoma SMMC-7721 cells (Guo *et al.,* 2004; Liu *et al.,* 2005 Rong *et al.,* 2009). As well, at the doses used in the xenograft studies, gambogic acid did not induce significant changes in body weight, organ weight, white cell count in blood and karyote count in bone marrow (Zhao *et al.,* 2004; Guo *et al.,* 2006). The LD_{50} of mice injected intraperitoneally with gambogic acid for 14 days was 45-96 mg/kg (Guo *et al.,* 2006). Therefore, two doses of GUTK were selected for the tumor study: 5.0 mg/kg and 10.0 mg/kg through intraperitoneal injection every other day for two weeks, which is consistent with the dosage regimen of gambogic acid used clinically in China for treatment of various cancers (Han *et al.,* 2006a; Qi *et al.,* 2008; Han & Xu, 2009). In the present study, at 10 mg/kg i.p., GUTK did not induce any toxicity to the brain, heart, lung, stomach, small intestine, colon, kidney and liver, as assessed by body weight measurements, histopathological observation and serum creatinine and ALT levels (Figures 3.39-3.42).

GUTK at 5.0 and 10.0 mg/kg reduced the tumor weight and tumor volume starting from day 8 of treatment but the reduction was not as significant as that of the positive control, 5-fluorouracil at 25.0 mg/kg i.p. (Figure 3.45). Recently, a study by Wang *et al.* (2008) demonstrated that a combination of gambogic acid and 5-fluorouracil had synergistic cytotoxic effects in human gastric carcinoma BGC-823 cells through the reduction of thymidine synthetase and dihydropyrimidine dehydrogenase mRNA levels by gambogic acid. Furthermore, the combination of 8 mg/kg gambogic acid with 10 mg/kg 5-fluorouracil in gastric tumor-bearing mice further reduced the tumor volume when compared with either agent alone (Wang *et al.,* 2009). Similarly, a combination of 5-fluorouracil and GUTK at 10.0 mg/kg i.p. was administered to

tumor-bearing mice, which mimics the clinical situation of combination chemotherapy. Mice treated with GUTK (10.0 mg/kg) combined with 5-fluorouracil (12.5 mg/kg or 25.0 mg/kg) further reduced tumor volumes compared to the mice treated with 5-fluorouracil alone at 12.5 mg/kg or 25.0 mg/kg (Figure 3.47). The combination treatment of 10 mg/kg GUTK and 25.0 mg/kg 5-fluorouracil significantly reduced the tumor volume when compared with the vehicle control ($p<0.05$) (Figure 3.47). However, the effect of such combination was not significantly different from 5-fluorouracil alone at both doses. The potentiation of 5-FU's anti-tumor effect by GUTK appear to be due to enhanced apoptosis in the tumor, as increased cleaved caspase-3 was detected after combination treatment as opposed to 5-5U alone Figure 3.48). A higher dose of GUTK and/or a longer dosage regimen may be needed to further potentiate the anti-tumor effects of 5-fluorouracil, provided that a higher dose of GUTK does not increase toxicity to other organs. As well, most of the administration routes for gambogic acid used in animal tumor models were through intravenous injection (Guo *et al.,* 2004; Liu *et al.,* 2005), which allows gambogic acid to avoid first-pass metabolism as it directly enters the systemic circulation for distribution into various organs. Hence, the bioavailability of GUTK may be enhanced. The pharmacokinetics of GUTK has not been studied before and further studies in this area will aid in the determination of the appropriate dose, dosing schedule and administration route for *in vivo* anti-tumor studies. It is also worthwhile to examine the effects of GUTK in a nude mice xenograft model using HT-29 cells as it is more relevant to the *in vitro* studies carried out in the current study. As well, the effects of the combination of GUTK and 5-FU on apoptosis, proliferation and angiogensis may be further examined by immunohistochemical staining of tumor tissue for proliferation marker Ki-67 and microvessel density marker CD31 to further support the possible potentiating anti-tumor effect of GUTK

and its mechanism *in vivo* relative to *in vitro* results from HT-29 cells. Since the major adverse effects of 5-FU are nausea and vomiting and mucositis, it would be interesting to investigate whether GUTK can reduce the adverse effects of 5-FU when given in combination.

Both EPC and GUTK showed potent *in vitro* cytotoxic activity towards human colon cancer cells by G_0/G_1 cell cycle arrest and apoptosis. Both compounds were more potent than clinically used chemotherapeutic drugs, 5-FU and cisplatin (Tables 3.4 and 3.5) and had selectivity towards cancer cells better than gambogic acid (Figures 3.7 and 3.11). In addition, GUTK showed anti-tumor properties by itself and in combination with 5-FU in Colon-26 tumor-bearing mice by apoptosis induction. However, further studies using higher doses of GUTK and mice xenograft HT-29 tumor model need to be carried out to support the anti-cancer potential of GUTK.

CHAPTER 4: FINAL DISCUSSION AND CONCLUSIONS

Colorectal cancer is a serious disease that is currently treated by surgical resection followed by combination chemotherapy as adjuvant therapy to reduce reccurence rates. However, despite the use of chemotherapy, the disease has high recurrence rates, as 60% of stage III patients experience a relapse (Chau & Cunningham, 2006; Kosmider & Lipton, 2007). The tumor response rate to single agents is low and patients may have an inherent or developed resistance to anti-tumor drugs (Longley *et al.,* 2003; Noordhuis *et al.,* 2004). In addition, all chemotherapeutic drugs have poor selectivity towards their tumor targets and induce adverse effects such as gastrotoxicity, hematotoxicity and neurotoxicity (Wilkes, 2005; Kosmider & Lipton, 2007). Thus, there is a high demand for new anti-cancer drug candidates that can selectively target the tumor site with high efficiency.

Recently, there is increasing interest in the use of complementary and alternative medicine (CAM) to treat cancer, such as natural products (including TCM), mind-body medicine (including acupuncture) and body-based practices (including massage therapy). It has been reported that 63% of cancer patients used CAM, which reduced symptoms such as discomfort from the disease and chemotherapy, depression and anxiety and helped them cope with stress and increased their quality of life (Sparber *et al.,* 2000). Many cancer patients also use TCM to enhance general health, to enhance immunity, to reduce adverse effects from conventional chemotherapy, to individualize treatment and to gain sense of control over the disease (Chiu *et al.,* 2009).

The use of TCM is based on numerous theories about the interdependence of different organs in the body. Health and treatment is based on the balance of the yin and yang and the circulation of "qi" through meridians in the body. As well, the diagnosis and treatment of the disease is based on the individual's characteristics: cold/heat, interior/exterior, excess/deficiency, yin/yang and fire/earth/metal/water/wood, which correspond to various organs or regions in the body (Ruan *et al.,* 2006; Gao *et al.,* 2007b; Chiu *et al.,* 2009).

The biological effects of Chinese medicine may be studied by: 1) using an herbal extract or combination of herbal extracts or 2) using a single compound isolated from an herbal extract. The objective of the present study was to examine the anti-cancer effects of different TCM herbs through both approaches, by studying a single compound or a mixture of ingredients, for the development of novel chemotherapeutic drug candidates for colon cancer. The traditional use of Chinese medicine is a combination of ingredients, often herbs, in a formula known as "fu fang." The composition of the formula and the dosage of each ingredient are tailored for each individual according to his yin/yang, "qi," state of each body organ and general health of the body (Ruan *et al.,* 2006). Alternatively, individual compounds may also be isolated from herbal extracts and studied for their biological effects, which is similar to the principles of Western medicine.

Given the link between inflammation and colon cancer, the DG and TH extracts were selected for this study based on their traditional use to treat inflammation and gastrointestinal injury. The polysaccharide fraction of DG has been shown to be effective for the treatment of gastric ulcer, ulcerative colitis and immunological colon injury (Cho *et al.,* 2000; Ye *et al.,* 2001a; Ye *et al.,* 2001b; Ye *et al.,* 2001c; Liu *et al.,*

2003b; Ye *et al.,* 2003; Wong *et al.,* 2008). As well, a mixture of extracts that contained DG reduced urate crystal-induced inflammation by decreasing the levels of pro-inflammatory cytokines and increasing the level of anti-inflammatory prostaglandin D_2 (Jung *et al.,* 2007). TH has been traditionally used as herbal medicine for treating wounds, inflammation and skin infections (Pedraza-Chaverri *et al.,* 2008; Han & Xu, 2009; Obolskiy *et al.,* 2009). Recent evidence has shown that TH extract inhibited chemically-induced inflammation by reduction of the synthesis and/or release of inflammatory mediators (Panthong *et al.,* 2007). It is well-established that chronic inflammation is a predisposing factor for the promotion, invasion and metastasis of colon cancer and cyclooxygenase-2 promotes angiogenesis and tumorigenesis (Kim *et al.,* 2001; Sinicrope & Gill, 2004; Dalgleish & O'Byrne, 2006; Sinicrope, 2006; Kashfi, 2009). Patients with ulcerative colitis, Crohn's disease and other gastrointestinal inflammatory diseases are at higher risk for developing colon cancer (Itzkowitz & Yio, 2004). The anti-cancer effects of DG extract was studied as a mixture of ingredients since it is always used as a whole extract or in combination with other extracts for the treatment of diseases in practice. However, the anti-cancer effects of TH was studied as single, isolated compounds since gambogic acid, a caged xanthone isolated from TH, has been prescribed for the treatment of cancer in China since the 1970s (Han & Xu, 2009). Therefore, the present study aimed to investigate the potential anti-tumor effects of DG and TH on colon cancer, according to their traditional, empirical use as a whole extract and as a single compound, respectively. The present study examined the anti-tumor effects of various TCM herbs on colon cancer by using both approaches to study TCM: as a mixture of components and as a single compound.

This study is the first to demonstrate that *n*-butylidenephthalide (BLP), senkyunolide

A (SKA) and *z*-ligustilide (LGT) are three bioactive ingredients in DG extract that induced cytotoxicity and anti-proliferative effects in human colon cancer HT-29 cells, without significant effects in normal human colon CCD-18Co fibroblasts, using MTT and [^{3}H] thymidine incorporation assays. The combination of the three phthalides in different ratios also induced anti-proliferative effects in HT-29 cells (Table 2.7). In addition, removal of BLP, SKA and LGT from the CX extract abrogated the cytotoxic effects of the herbal extract (Figure 2.43). The results suggested that the phthalides, in particular BLP, SKA and LGT, are the main bioactive ingredients for the anti-proliferative effects of the DG and CX extracts. Previous studies by other research groups have only focused on the anti-cancer effects of BLP alone, which is present in less than 1% in the DG extract (Tsai *et al.*, 2006; Chen *et al.*, 2008a; Yu *et al.*, 2010). Hence, the present study identified SKA and LGT as other bioactive compounds in DG extract that may contribute to its anti-tumor effects.

For the first time, the mechanism underlying the cytotoxic effects of LGT, the most abundant phthalide in DG, on human colon cancer cells was examined (Figure 2.45). Using flow cytometry, Western blot and caspase-3 activity assays, LGT was shown to induce cytotoxic and anti-proliferative effects in human colon cancer cells by G_0/G_1 cell cycle arrest and apoptosis that involved both mitochondrial- and death receptor-mediated pathways by activation of caspases-3, -8 and -9 (Figures 2.28-2.31) and cleavage of PARP (Figures 2.25, 2.26) after 24 h treatment. The proposed mechanism of LGT is summarized in Figure 2.45. Other morphological changes associated with apoptosis such as chromatin condensation, DNA fragmentation and formation of apoptotic bodies, were observed after treatment with LGT in HT-29 cells using DAPI and propidium iodide staining (Figures 2.16, 2.23, 2.24). As well,

the present study showed that LGT induced the early activation of JNK and slow and sustained activation of ERK and p38 in HT-29 cells. The effects of LGT on the MAPK pathways have not been examined before and this study is the first to suggest the possible involvement of JNK in LGT-induced apoptosis. Previous studies by other research groups have identified BLP as the main bioactive ingredient of DG extract accounting for the anti-cancer effects of the extract (Tsai *et al.,* 2005; Tsai *et al.,* 2006). However, the present study showed that LGT is also a major bioactive component of the DG extract present in higher proportion than BLP (Table 2.1), and the cytotoxic and apoptotic effects of LGT are almost twice as potent as BLP (Figures 2.14, 2.16, 2.31, 2.33, Table 2.5).

Subsequently, BLP, SKA and LGT were each combined with cisplatin, a commonly used chemotherapeutic drug for solid tumors, and their cytotoxic effects on HT-29 cells were examined. By using median-effect analysis, the current study demonstrated that both BLP and SKA interacted in an antagonistic manner with cisplatin, especially at high concentrations of cisplatin, to exert cytotoxic effects in HT-29 cells (Figures 2.20, 2.21). However, LGT interacted in a synergistic manner with cisplatin to reduce the viability of HT-29 cells after 24 h incubation at all of the concentrations of LGT tested and most of the concentrations of cisplatin tested (Figure 2.22). This implies that LGT is a good candidate for further study as adjuvant chemotherapy in combination with other conventional anti-tumor drugs for colon cancer. The results also showed that lower than IC_{50} values of both LGT and cisplatin can be used, which suggests that adverse effects and dose-limiting toxicities, such as ototoxicity and neurotoxicity, are less likely to occur. The synergistic effects of LGT in combination with other conventional anti-cancer drugs have not been demonstrated prior to the present study, although BLP has been shown to interact

synergistically with BCNU to reduce viability of human hepatocellular carcinoma cells (Yu *et al.*, 2010). The phthalides appear to be good candidates for combined use with standard chemotherapeutic drugs, with LGT being the most potent, and this is a solid foundation for further studies of combinations of LGT with other drugs currently used for colon cancer, such as 5-FU and oxaliplatin.

In the present study, the results showed that the DG extract also decreased the viability and proliferation of HT-29 cells by G_0/G_1 cell cycle arrest and apoptosis through a mechanism similar to that of LGT, but at concentrations much lower than that of any of the three phthalides (Figures 2.16, 2.17, 2.25, 2.26, 2.31, 2.32). Hence, it was hypothesized that 1) there may be other bioactive ingredients in the extract, 2) synergistic interactions between the phthalides or 3) synergistic interactions between phthalides and other bioactive ingredients in the herbal extract. Therefore, the anti-proliferative effects of DG and CX, an herbal extract that also contained BLP, SKA and LGT as the three major phthalides, but in a different proportion ratio from that in DG (Table 2.1), were examined. Two mixtures only containing the three phthalides were also prepared, in the same ratios as they naturally exist in the two herbal extracts and their anti-proliferative effects were examined in comparison to the effects of the two herbal extracts. While both mixtures of the three phthalides (DG and CX mixture of phthalides) had anti-proliferative effects in HT-29 cells, the DG mixture was significantly more potent than the CX mixture ($p<0.05$) in HT-29 cells (Table 2.7). However, the CX mixture had a higher IC_{50} value than the DG mixture in normal human colon fibroblast cells (Table 2.7). This suggests that different ratios of the three phthalides had different cytotoxic potencies in colon cancer and normal cells. Specifically, the ratio of the three phthalides may be altered to create a mixture with cytotoxic potency in colon cancer cells, but little effect in

normal colon cells. The results from the present study imply that variations in the proportion ratios of the three phthalides as they exist naturally may have drastic effects on the efficacy of the mixture. Therefore, strict quality control of all of the bioactive ingredients in the mixture or extract must be applied and each batch must be checked for consistency in the content and ratio of bioactive ingredients to ensure that TCM will produce similar biological effects and have reproducible outcomes among batches.

While the DG extract was more potent than the DG mixture of phthalides, the CX extract had similar anti-proliferative potency to the CX mixture of phthalides in HT-29 cells (Figure 2.39, Table 2.7). Moreover, median-effect analysis indicated that the three phthalides in the DG extract showed synergistic interactions with other bioactive components in the extract to contribute to the greater anti-proliferative effects of the extract. However, the three phthalides in the CX extract had antagonistic interactions with other bioactive components in the extract (Figure 2.41). As well, the phthalides in the DG and CX phthalide mixtures interacted in an antagonistic manner with each other to exert anti-proliferative effects in HT-29 cells (Figure 2.41). Interestingly, although BLP, SKA and LGT are the main bioactive ingredients in both the DG and CX extracts, the different proportions of the three phthalides in both extracts caused the phthalides to interact synergistically with other bioactive components in the DG extract while the phthalides interacted antagonistically with other bioactive components in the CX extract. The present study is the first to demonstrate the synergistic or antagonistic interactions in DG and CX extracts, respectively, and their effects on bioactivity through an objective, mathematical approach using median-effect analysis. Since the content and proportion of each bioactive compound can be accurately determined, this

mathematical formula is an easy way to determine the different types of interactions between different ingredients in the formula and it can be used to modify ratios of bioactive ingredients to create a formula with the highest efficacy.

The present study employed a modern, scientific, mathematical approach to demonstrate the synergistic effects of the DG extract, which provides support for the traditional use of combination of ingredients in a TCM formula. The beauty of TCM lies in the synergistic interactions between different components in the mixture that can further enhance the therapeutic effects by targeting the general health and various organs in the body and reduce the adverse effects of other components in the mixture (Chang, 2002; Vickers, 2002; Ruan *et al.,* 2006). Specifically, the phthalides in DG extract are never prescribed alone for the treatment of diseases. DG is always prescribed as a whole extract or in combination with other herbal extracts or drugs for the treatment of disease, due to the synergistic interactions of various components in the DG extract. The DG extract is always used in combination with other herbs in various formulas, such as DBT to "nourish the blood," Danggui-Shaoyao-San to treat gynecological disorders and with CX to treat cardiovascular diseases (Hou *et al.,* 2005; Gao *et al.,* 2008; Chen *et al.,* 2009). DG has also been demonstrated to reduce the gastrointestinal toxicity and cardiotoxicity induced by cyclophosphamide and doxorubicin, respectively, when given in combination (Hui *et al.,* 2006; Xin *et al.,* 2007). On the contrary, the antagonistic interactions between the phthalides and other bioactive components in the CX extract support the fact that CX is not used for in cancer therapy, but it is often prescribed alone or in combination with other herbal extracts for the treatment of cardiovascular diseases and hepatic fibrosis (Hou *et al.,* 2004; Hou *et al.,* 2005; Lin *et al.,* 2006). As well, the phthalides in the CX extract interacted synergistically with other bioactive components in the extract to have

detrimental cytotoxic effects on normal colon fibroblasts (Figures 2.40, 2.41), which would adversely affect the selectivity of the extract on colon cancer cells. Therefore, it is crucial to select the appropriate herb, with the right proportion of phthalides or bioactive ingredients, for the best therapeutic effects in certain diseases.

Our results support the use of DG whole extract, instead of the individual phthalides for the possible treatment of cancer. Results from the present study are in good agreement with previously-reported findings in that both the acetone and chloroform extracts of DG have been shown to be more potent than BLP for the inhibition of *in vitro* and *in vivo* growth of human glioblastoma multiforme and lung cancer (Cheng *et al.,* 2004; Tsai *et al.,* 2005; Tsai *et al.,* 2006). It has also been reported that the DG extract was more potent than BLP in inhibiting the *in vitro* and *in vivo* growth of brain astrocytoma and in reducing the microvessel growth within the tumor (Lee *et al.,* 2006). Although the current study showed that DG extract was more potent than LGT at triggering cytotoxicity by apoptosis and anti-proliferative effects by G_0/G_1 cell cycle arrest, further studies to examine the *in vivo* anti-tumor effects of DG extract on HT-29 tumor xenograft mice model would confirm the synergistic effects of the extract with better efficacy than the use of a single compound. The present study revealed for the first time that the use of DG extract, rather than the individual phthalides, may be beneficial in the treatment of colon cancer in combination therapy with conventional anti-cancer drugs and can be further explored by *in vivo* tumor studies.

In the second part of the present study, 15 bioactive compounds were isolated from TH and investigated for their anti-cancer effects in colon cancer as a single agent *in vitro* and *in vivo*. Gambogic acid isolated from TH has been clinically used for its

anti-cancer effects of various types of cancers in China since the 1970s (Han & Xu, 2009). However, previous studies have shown that gambogic acid induced toxicity to the liver and kidney after chronic treatment in mice and dogs, at the same doses that are used for *in vivo* tumor studies (Guo *et al.*, 2006b; Qi *et al.*, 2008c). As well, it reduced the viability of both HT-29 and CCD-18Co cells to the same extent at the same dose in the present study (Figure 3.7, Table 3.4). Therefore, the present study focused on the discovery of single compounds from TH that has cytotoxcity in colon cancer comparable to that of gambogic acid, but with less effect in normal human colon fibroblasts. The anti-cancer effects of individual compounds from TH were examined, rather than the TH extract, according to the empirical use of this herb. Firstly, several xanthones, which are structurally-related to gambogic acid, were screened for their effects on the viability of human colon cancer cell lines. Among them, EPC was selected based on its selective potency in HT-29 cells. Then, numerous compounds structurally-related to EPC were screened for their effects on the viability of HT-29 cells and CCD-18Co cells. GUTK was selected since it had the highest selectivity towards colon cancer cells, among all of the compounds tested. Although EPC and GUTK were not as potent as gambogic acid, a caged xanthone, in reducing the viability of human colon cancer cells, both compounds were the most potent compounds out of the benzophenone class of compounds isolated from TH, with IC_{50} values much lower than 5-FU and cisplatin, and had better selectivity than gambogic acid on HT-29 and HCT116 cells than CCD-18Co cells. As well, benzophenones isolated from TH have not been studied extensively for their anti-cancer effects except for garcinol (Pan *et al.*, 2001; Hong *et al.*, 2007; Prasad *et al.*, 2010).

Subsequent mechanistic studies demonstrated that EPC had anti-proliferative effects

in HT-29 cells by induction of G_0/G_1 cell cycle arrest, which was associated with down-regulation of cyclins D1, D3 and CDK4 and CDK6 and up-regulation of tumor suppressor proteins, $p21^{Waf1/Cip1}$ and $p27^{Kip1}$. Part of the selectivity of EPC may arise from the up-regulation of $p21^{Waf1/Cip1}$, which is absent in HT-29 cells, but abundant in CCD-18Co cells (Figure 3.49). As shown by Western blot, at concentrations as low as 10.0 μM, EPC induced the cleavage of PARP and procaspases-3, -8 and -9 as early as 12 h after treatment, which was maintained until 24 h (Figure 3.26-3.28). After 24 h, EPC induced activation of caspase-3, cell shrinkage and nuclear changes such as chromatin condensation and nuclear fragmentation, as shown by caspase-3 activity assay, DAPI staining and flow cytometry (Figures 3.13, 3.23). EPC induced G_0/G_1 cell cycle arrest after 12 h, which was followed by caspase-dependent apoptosis after 24 h that involved both the death receptor and mitochondrial pathways. In addition, EPC induced early activation of JNK followed by slow activation of p38 and ERK, yet pre-treatment with JNK, p38 and ERK inhibitors did not have any significant effect on apoptosis induced by EPC (Figure 3.38).

Similarly, GUTK induced cytotoxic effects on HT-29 and HCT116 cells by initiation of G_0/G_1 cell cycle arrest after 12 h and apoptosis after 24 h (Figure 3.14). The G_0/G_1 cell cycle arrest induced by GUTK was mediated by the down-regulation of cyclins D1 and D3 and CDK4 and CDK6 and up-regulation of tumor suppressor proteins, $p21^{Waf1/Cip1}$ and $p27^{Kip1}$, with no effects on $p15^{INK4B}$ and $p16^{INK4A}$ (Figures 3.17, 3.18, 3.21, 3.22). Similar to EPC, GUTK may be cytotoxic to HT-29 cells in a selective manner due to its ability to up-regulate $p21^{Waf1/Cip1}$, which is absent in HT-29 cells (Figure 3.49). GUTK triggered the cleavage of PARP and pro-caspases-3, -8 and -9 after 24 h (Figures 3.26, 3.29), which was accompanied with chromatin condensation and increase of cells in the sub-G_1 phase of the cell cycle, as demonstrated by flow

cytometry (Figures 3.14, 3.24). GUTK-induced apoptosis was caspase-3-dependent and involved both the death receptor and mitochondrial pathways, similar to EPC. However, GUTK only activated JNK after 12 h, with no effect on p38 and ERK (Figures 3.35-3.37). Pre-treatment of HT-29 cells with SP600125, a JNK inhibitior, partially attenuated the caspase-3 activity induced by GUTK, which suggested that GUTK-induced apoptosis is partially mediated by JNK.

The proposed mechanism for EPC and GUTK is summarized in Figure 3.53. It is speculated that in addition to the up-regulation of $p21^{Waf1/Cip1}$ and $p27^{Kip1}$, EPC and GUTK may directly up-regulate the expression of death ligands and/or death receptors to activate caspase-8 and the death receptor pathway of apoptosis. EPC and GUTK may also directly alter the ratio of Bcl-2 to Bax to increase the permeability of the mitochondrial outer membrane, which allows for the leakage of cytochrome c and activation of caspase-9. Both pathways converge to cleave and activate caspase-3 for the cleavage of downstream cellular protein targets for the late stages of apoptosis. There may also be cross-talking between both pathways of apoptosis by the possible cleavage of Bid by EPC and GUTK. GUTK-induced activation of JNK may interact with different pro- and anti-apoptotic proteins in the apoptotic pathway and render them active or inactive by phosphorylation. The mechanisms of EPC and GUTK are similar to gambogic acid in that they all activate both death receptor and mitochondrial pathways of apoptosis (Liu *et al.,* 2005; Xie *et al.,* 2009; Mu *et al.,* 2010). Specifically, gambogic acid has been shown to bind directly to the transferrin receptor on the cell surface to initiate apoptosis and to up-regulate the ratio of Bax to Bcl-2 to increase mitochondrial outer membrane permeability (Zhao *et al.,* 2004; Kasibhatla *et al.,* 2005; Liu *et al.,* 2005; Pandey *et al.,* 2005). However, whereas EPC and GUTK induced G_0/G_1 cell cycle arrest, gambogic acid induced G_2/M cell cycle

arrest in human breast and gastric cancer cells (Yu *et al.*, 2007; Chen *et al.*, 2008b; Wang *et al.*, 2008c). Gambogic acid has been reported to be a cytoskeleton-disrupting agent by promoting microtubule depolymerization and studies have also shown that it can directly down-regulate CDK7 mRNA and protein expression, thereby reducing its activity and triggering G_2/M arrest (Yu *et al.*, 2007; Chen *et al.*, 2008b). Hence, we revealed that EPC and GUTK, both benzophenone derivatives had distinct effects on the cell cycle, that were in good agreement with the effects of xanthochymol, another benzophenone isolated from *G. xanthochymus*, but different from the effects of gambogic acid, a caged xanthone (Protiva *et al.*, 2008).

We were the first research group to isolate and identify EPC and GUTK as bioactive compounds from TH, that had cytotoxic and anti-proliferative effects. As well, we have revealed the *in vitro* mechanisms underlying the cytotoxic and anti-proliferative effects of two novel benzophenone derivatives, in particular EPC and GUTK on colon cancer. Up to now, most studies have been conducted on caged xanthones such as gambogic acid and one benzophenone derivative, garcinol, but none of these studies focused on their effects on colon cancer. The present study suggests that benzophenone derivatives with similar structures to EPC and GUTK are worthy drug candidates for further study and development as novel colon cancer chemotherapeutic drugs.

Since the *in vivo* anti-tumor effects of benzophenone derivatives have never been studied before and there was a relatively higher quantity of GUTK available, GUTK was selected for further studies *in vivo*. Firstly, the toxic effects of GUTK on various body organs in normal BALB/c mice after 10 mg/kg i.p. treatment every other day

for 14 days were examined using creatinine and serum ALT assays and histopathological analysis. GUTK (at 10 mg/kg i.p.) did not induce toxicity to the brain, heart, lung, stomach, small intestine, colon, kidney and liver and serum creatinine and ALT levels remained similar to those in vehicle control after treatment for 14 days (Figures 3.40-3.42). This study is the first to examine the biological effects and potential toxicity of GUTK in an animal model. No studies have been carried out prior to this one on the toxicity of benzophenone derivatives isolated from TH on rodent models. Since the dose of GUTK at 10 mg/kg did not induce toxicity in the mice, this dosing regimen was used in the subsequent *in vivo* animal tumor model studies, which is similar to the dosing regimen used for human clinical trials (Han & Xu, 2009). BALB/c mice were subcutaneously inoculated with Colon-26 murine colon cancer cells on their backs and drug treatment began 14 days post-inoculation. GUTK, administered at 5 mg/kg i.p. or 10 mg/kg i.p., every other day for 14 days slightly decreased tumor volume, while 5-FU (at 25.0 mg/kg i.p.) significantly reduced tumor volume (Figure 3.45). The present study showed that GUTK at 10 mg/kg i.p. potentiated the anti-tumor effects of 5-FU administered at both 12.5 mg/kg i.p. and 25 mg/kg i.p (Figure 3.47). GUTK induced apoptosis through activation of caspase-3 in the tumors and it further enhanced the amount of cleaved caspase-3 when given in combination with 5-FU (Figure 3.48). The results demonstrated that although GUTK had anti-tumor activity by itself, higher efficacy can be achieved if it is used in combination with 5-FU or other chemotherapeutic drugs. This study is the first to demonstrate the *in vivo* anti-cancer activity of GUTK, as a single agent and in combination with 5-FU, the first-line chemotherapeutic drug for colon cancer. As well, the results revealed the potential mechanism underlying the *in vivo* anti-tumor effects of GUTK, which are in agreement with the mechanistic studies conducted *in vitro*. Previous studies have only focued on the *in vivo*

anti-tumor activity of gambogic acid and other caged xanthone derivatives, but never on benzophenones isolated from TH. We have demonstrated that GUTK is a worthy candidate for further study as a new chemotherapeutic drug candidate in combination with 5-FU for colon cancer. Although more evidence is needed to support the *in vivo* anti-tumor potential of GUTK for the development as a novel chemotherapeutic drug candidate for colon cancer, this study provides a solid foundation for future work to be based on. The present study provides promising results of GUTK as a novel anti-cancer drug candidate that may be developed as a single compound for adjuvant chemotherapy, which is similar to the Western medicine approach of drug discovery.

It is difficult to say whether it is better to study TCM as a mixture of different herbs and components or as a single bioactive compound since there are advantages and disadvantages associated with both approaches. A mixture of ingredients in a "fu fang" may lead to synergistic therapeutic effects and reduced adverse effects, while providing individualized therapy for the patient. However, lack of standardization and unknown herb-drug interactions and exact mechanisms of action of TCM formulas lead to safety concerns. The study of a single compound allows for the easy determination of the specific anti-cancer mechanisms, pharmacokinetics, and safety profiles. Many people tend to study the biological effects of TCM by using either one of the approaches, but the traditional and empirical usage and the properties of the compound/formula must be considered before deciding on whether to study a mixture of ingredients or a single compound. For instance, if a single compound has high potency and is available in high quantity and purity, it may be developed as a drug. On the other hand, if the components in an extract act in synergism to have a therapeutic effect, a mixture may be developed as a drug. We have shown that both approaches can be used, as long as the properties of the extract or compound and its

traditional and empirical use are considered carefully.

In conclusion, the present study employed DG and TH to demonstrate the two approaches to study their anti-tumor effects on colon cancer, either as a mixture of ingredients in an herbal extract or as an individual compound. By studying DG as a whole extract, we have revealed the bioactivities of each of the three main phthalides, BLP, SKA and LGT, by themselves and in combination with each other in human colon cancer cells. The anti-proliferative effects of the DG extract were more potent than each of the three phthalides and the three phthalides in combination as the three phthalides acted in a synergistic manner with other bioactive components in the DG extract to exert anti-proliferative effects in human colon cancer cells. The interactions were unique and specific to DG as the three phthalides in a different proportion had antagonistic interactions in CX extract. Due to synergistic interactions in the DG extract, the extract containing the three phthalides is worthy of further study for its anti-tumor effects *in vivo*. On the other hand, EPC and GUTK are benzophenone derivatives isolated from TH that are promising candidates for further *in vivo* studies to justify their potential to be developed as single chemical entities for combination use with 5-fluorouracil to treat colon cancer. The present study demonstrated the significance of using both approaches to study the anti-tumor effects of DG and TH for development as drug candidates for colon cancer, either as whole herbal extract or as individual compounds.

REFERENCES

Abukhdeir, A.M., & Park, B.H. (2008). P21 and p27: roles in carcinogenesis and drug resistance. *Expert Reviews in Molecular Medicine, 10,* e19.

Adelstein, D.J., & Rodriguez, C.P. (2008). Current and emerging standards of concomitant chemoradiotherapy. *Seminars in Oncology, 35,* 211-220.

Ahmad, A., Wang, Z., Ali, R., Maitah, M.Y., Kong, D., Banerjee, S., Padhye, S., & Sarkar, F.H. (2010). Apoptosis-inducing effect of garcinol is mediated by NF-κB signaling in breast cancer cells. *Journal of Cellular Biochemistry, 109,* 1134-1141.

Alexia, C., Fallot, G., Lasfer, M., Schweizer-Groyer, G., & Groyer, A. (2004). An evaluation of the role of insulin-like growth factors (IGF) and of type-I IGF receptor signaling in hepatocarcinogenesis and in the resistance of hepatocarcinoma cells against drug-induced apoptosis. *Biochemical Pharmacology, 68,* 1003-1015.

Antí, M., Armuzzi, A., Morini, S., Iascone, E., Pignataro, G., Coco, C., Lorenzetti, R., Paolucci, M., Covino, M., Gasbarrini, A., Vecchio, F., & Gasbarrini, G. (2001). Severe imbalance of cell proliferation and apoptosis in the left colon and in the rectosigmoid tract in subjects with a history of large adenomas. *Gut, 48,* 238-246.

Armstrong, T., Cohen, M.Z., Hess, K.R., Manning, R., Lee, E.L., Tamayo, G., Baumgartner, K., Min, S.J., Yung, A., & Gilbert, M. (2006). Complementary and alternative medicine use and quality of life in patients with primary brain tumors. *Journal of Pain and Symptom Management, 32,* 148-154.

Armstrong, T.S. (2008). Use of complementary and alternative medical therapy by patients with primary brain tumors. *Current Neurology and Neuroscience Reports, 8,* 264-268.

Armstrong, T.S., & Gilbert, M.R. (2008). Use of complementary and alternative medical therapy by patients with primary brain tumors. *Current Neurology and Neuroscience Reports, 8,* 264-268.

Arnes, J.B., Begin, L.R., Stefansson, I., Brunet, J.S., Nielsen, T.O., Foulkes, W.D., & Akslen, L.A. (2009). Expression of epidermal growth factor receptor in relation to BRCA1 status, basal-like markers and prognosis in breast cancer. *Journal of Clinical Pathology, 62,* 139-146.

Artandi, S.E., & DePinho, R.A. (2010). Telomeres and telomerase in cancer. *Carcinogenesis, 31,* 9-18.

Asano, J., Chiba, K., Tada, M., & Yoshii, T. (1996). Cytotoxic xanthones from *Garcinia hanburyi*. *Phytochemistry, 41,* 815-820.

Ashkenazi, A., & Dixit, V.M. (1998). Death receptors: signaling and modulation. *Science, 281,* 1305-1308.

Ashktorab, H., Dawkins, F.W., Mohamed, R., Larbi, D., & Smoot, D.T. (2005). Apoptosis induced by aspirin and 5-fluorouracil in human colonic adenocarcinoma cells. *Digestive Diseases and Sciences, 50,* 1025-1032.

Ayhan, S., Isisag, A., Saruc, M., Nese, N., Demir, M.A., & Kucukmetin, N.T. (2010). The role of pRB, p16 and cyclin D1 in colonic carcinogenesis. *Hepatogastroenterology, 57,* 251-256.

Bacus, S.S., Gudkov, A.V., Lowe, M., Lyass, L., Yung, Y., Komarov, A.P., Keyomarsi, K., Yarden, Y., & Seger, R. (2001). Taxol-induced apoptosis depends on MAP kinase pathways (ERK and p38) and is independent of p53. *Oncogene, 20,* 147-155.

Balmanno, K., & Cook, S.J. (2009). Tumor cell survival signaling by the ERK1/2 pathway. *Cell Death and Differentiation, 16,* 368-377.

Barabas, K., Milner, R., Lurie, D., & Adin, C. (2008). Cisplatin: a review of toxicities and therapeutic applications. *Veterinary and Comparative Oncology, 6,* 1-18.

Batova, A., Lam, T., Waschołowski, V., Yu, A.L., Giannis, A., & Theodorakis, E.A. (2007). Synthesis and evaluation of caged *Garcinia xanthones*. *Organic & Biomolecular Medicine, 5,* 494-500.

Beck, J.J., & Chou, S.C. (2007). The structural diversity of phthalides from the Apiaceae. *Journal of Natural Products, 70,* 891-900.

Bedi, A., Pasricha, P.J., Akhtar, A.J., Barber, J.P., Bedi, G.C., Giardiello, F.M., Zehnbauer, B.A., Hamilton, S.R., & Jones, R.J. (1995). Inhibition of apoptosis during development of colorectal cancer. *Cancer Research, 55,* 1811-1816.

Belletti, B., Nicoloso, M.S., Schiappacassi, M., Chimienti, E., Berton, S., Lovat, F., Colombatti, A., & Baldassarre, G. (2005). $p27^{kip1}$ Functional regulation in human cancer: a potential target for therapeutic designs. *Current Medicinal Chemistry, 12,* 1589-1605.

Bennett, M., & Lengacher, C. (1999). Use of complementary therapies in a rural cancer population.

Oncology Nursing Forum, 26, 1287-1294.

Bhat, N.R., & Zhang, P. (1999). Hydrogen peroxide activation of multiple mitogen-activated protein kinases in an oligodendrocyte cell line: role of extracellular signal-regulated kinase in hydrogen peroxide-induced cell death. *Journal of Neurochemistry, 72,* 112-119.

Blagosklonny, M.V., Giannakakou, P., el-Deiry, W.S., Kingston, D.G., Higgs, P.I., Neckers, L., & Fojo, T. (1997). Raf-1/bcl-2 phosphorylation: a step from microtubule damage to cell death. *Cancer Research, 57,* 130-135.

Boehm, M., Yoshimoto, T., Crook, M.F., Nallamshetty, S., True, A., Nabel, G.J., & Nabel, E.G. (2002). A growth factor-dependent nuclear kinase phosphorylates p27(Kip1) and regulates cell cycle progression. *The EMBO Journal, 21,* 3390-3401.

Brancho, D., Tanaka, N., Jaeschke, A., Ventura, J.J., Kelkar, N., Tanaka, Y., Kyuuma, M., Takeshita, T., Flavell, R.A., & Davis, R.J. (2003). Mechanism of p38 MAP kinase activation *in vivo. Genes & Development, 17,* 1969-1978.

Breathnach, A.S. (1999). Azelaic acid: potential as a general antitumoural agent. *Medical Hypotheses, 52,* 221-226.

Broker, L.E., Kruyt, F.A., & Giaccone, G. (2005). Cell death independent of caspases: a review. *Clinical Cancer Research, 11,* 3155-3162.

Brown, L., & Benchimol, S. (2006). The involvement of MAPK signaling pathways in determining the cellular response to p53 activation: cell cycle arrest or apoptosis. *The Journal of Biological Chemistry, 281,* 3832-3840.

Brozovic, A., Fritz, G., Christmann, M., Zisowsky, J., Jaehde, U., Osmak, M., & Kaina, B. (2004). Long-term activation of SAPK/JNK, p38 kinase and fas-L expression by cisplatin is attenuated in human carcinoma cells that acquired drug resistance. *International Journal of Cancer, 112,* 974-985.

Bush, J.A., Cheung, K.J. Jr., Li, G. (2001). Curcumin induces apoptosis in human melanoma cells through a Fas receptor/caspase-8 pathway independent of p53. *Experimental Cell Research, 271,* 305-314.

Cai, Y., Luo, Q., Sun, M., & Corke, H. (2004). Antioxidant activity and phenolic compounds of 112 traditional Chinese medicinal plants associated with anticancer. *Life Sciences, 74,* 2157-2184.

Cai, Y.Z., Sun, M., Xing, J., Luo, Q., & Corke, H. (2006). Structure-radical scavenging activity relationships of phenolic compounds from traditional Chinese medicinal plants. *Life Sciences, 74,* 2872-2888.

Cardone, M.H., Roy, N., Stennicke, H.R., Salvesen, G.S., Franke, T.F., Stanbridge, E., Frisch, S., & Reed, J.C. (1998). Regulation of cell death protease caspase-9 by phosphorylation. *Science, 282,* 1318-1321.

Carrano, A.C., Eytan, E., Hershko, A., & Pagano, M. (1999). SKP2 is required for ubiquitin-mediated degradation of the CDK inhibitor p27. *Nature Cell Biology, 1,* 193-199.

Certo, M., Del Gaizo Moore, V., Nishino, M., Wei, G., Korsmeyer, S., Armstrong, S.A., & Letai, A. (2006). Mitochondria primed by death signals determine cellular addiction to antiapoptotic BCL-2 family members. *Cancer Cell, 9,* 351-365.

Chan, S.S., Choi, A.O., Jones, R.L., & Lin, G. (2006). Mechanisms underlying the vasorelaxing effects of butylidenephthalide, an active constituent of *Ligusticum chuanxiong,* in rat isolated aorta. *European Journal of Pharmacology, 537,* 111-117.

Chan, S.S., Cheng, T.Y., & Lin, G. (2007). Relaxation effects of ligustilide and senkyunolide A, two main constituents of *Ligusticum chuanxiong*, in rat isolated aorta. *Journal of Ethnopharmacology, 111,* 677-680.

Chan, S.S., Jones, R.L., & Lin, G. (2009). Synergistic interactions between the *Ligusticum chuanxiong* constituent butylidenephthalide and the nitric oxide donor sodium nitroprusside in relaxing rat isolated aorta. *Journal of Ethnopharmacology, 122,* 308-312.

Chang, R. (2002). Bioactive polysaccharides from traditional Chinese medicine herbs as anticancer adjuvants. *The Journal of Alternative and Complementary Medicine, 8,* 559-565.

Chantarasriwong, O., Cho, W.C., Batova, A., Chavasiri, W., Moore, C., Rheingold, A.L., Theodorakis, E.A. (2009). Evaluation of the pharmacophoric motif of the caged *Garcinia* xanthones. *Organic & Biomolecular Medicine, 7,* 4886-4894.

Chau, I., & Cunningham, D. (2006). Adjuvant therapy in colon cancer – what, when and how? *Annals of Oncology, 17,* 1347-1359.

Chen, Z., Seimiya, H., Naito, M., Mashima, T., Kizaki, A., Dan, S., Imaizumi, M., Ichijo, H.,

Miyazono, K., & Tsuruo, T. (1999). ASK1 mediates apoptotic cell death induced by genotoxic stress. *Oncogene, 18,* 173-180.

Chen, X., Chen, J., Zhang, P., & Du, J. (2006). *Angelica* stimulates proliferation of murine bone marrow mononuclear cells by the MAPK pathway. *Blood Cells, Molecules, and Diseases, 36,* 402-405.

Chen, Q.C., Lee, J., Jin, W., Youn, U., Kim, H., Lee, I.S., Zhang, X., Song, K., Seong, Y., & Bae, K. (2007). Cytotoxic constituents from *Angelicae sinensis* radix. *Archives of Pharmacal Research, 30,* 565-569.

Chen, Y.L., Jian, M.H., Lin, C.C., Kang, J.C., Chen, S.P., Lin, P.C., Hung, P.J., Chen, J.R., Chang, W.L., Lin, S.Z., & Harn, H.J. (2008a). The induction of orphan nuclear receptor Nur77 expression by *n*-butylidenephthalide as pharmaceuticals on hepatocellular carcinoma cell therapy. *Molecular Pharmacology, 74,* 1046-1058.

Chen, J., Gu, H.Y., Lu, N., Yang, Y., Liu, W., Qi, Q., Rong, J.J., Wang, X.T., You, Q.D., & Guo, Q.L. (2008b). Microtubule depolymerization and phosphorylation of c-Jun-N-terminal kinase-1 and p38 were involved in gambogic acid induced cell cycle arrest and apoptosis in human breast carcinoma cells. *Life Sciences, 83,* 103-109.

Chen, L., Qi, J., Chang, Y.X., Zhu, D., & Yu, B. (2009). Identification and determination of the major constituents in Traditional Chinese Medicinal formula Danggui-Shaoyao-San by HPLC-DAD-ESI-MS/MS. *Journal of Pharmaceutical and Biomedical Analysis, 50,* 127-137.

Cheng, E.H., Wei, M.C., Weiler, S., Flavell, R.A., Mak, T.W., Lindsten, T., & Korsmeyer, S.J. (2001). BCL:-2, BCL-X(L) sequester BH3 domain-only molecules preventing BAX- and BAK-mediated mitochondrial apoptosis. *Molecular Cell, 8,* 705-711.

Cheng, Y.L., Chang, W.L., Lee, S.C., Liu, Y.G., Chen, C.J., Lin, S.Z., Tsai, N.M., Yu, D.S., Yen, C.Y., & Harn, H.J. (2004). Acetone extract of *Angelica sinensis* inhibits proliferation of human cancer cells via inducing cell cycle arrest and apoptosis. *Life Sciences, 75,* 1579-1594.

Chipuk, J.E., Bouchier-Hayes, L., & Green, D.R. (2006). Mitochondrial outer membrane permeabilization during apoptosis: the innocent bystander scenario. *Cell Death and Differentiation, 13,* 1396-1402.

Chiu, P.Y., Leung, H.Y., Siu, A.H., Poon, M.K., Dong, T.T., Tsim, K.W., & Ko, K.M. (2007).

Dang-Gui Buxue Tang protects against oxidant injury by enhancing cellular glutathione in H9c2 cells: role of glutathione synthesis and regeneration. *Planta Medica, 73,* 134-141.

Chiu, J., Yau, T., & Epstein, R.J. (2009). Complications of traditional Chinese/herbal medicines (TCM) – a guide for perplexed oncologists and other cancer caregivers. *Support Care in Cancer, 17,* 231-240.

Cho, S.K., Abd El-Aty, A.M., Choi, J.H., Kim, M.R., & Shim, J.H. (2007). Optimized conditions for the extraction of secondary volatile metabolites in *Angelica* roots by accelerated solvent extraction. *Journal of Pharmaceutical and Biomedical Analysis, 44,* 1154-1158.

Cho, E.Y., Han, J.J., Choi, Y.L., Kim, K.M., & Oh, Y.L. (2008). Comparison of Her-2, EGFR and cyclin D1 in primary breast cancer and paired metastatic lymph nodes: an immunohistochemical and chromogenic in situ hybridization study. *Journal of Korean Medical Science, 23,* 1053-1061.

Chou, T.C. (2006). Theoretical basis, experimental design, and computerized simulation of synergism and antagonism in drug combination studies. *Pharmacological Reviews, 58,* 621-681.

Chu, I.M., Hengst, L., & Slingerland, J.M. (2008). The Cdk inhibitior p27 in human cancer: prognostic potential and relevance to anticancer therapy. *Nature Reviews. Cancer, 8,* 253-267.

Ciaparrone, M., Yamamoto, H., Yao, Y., Sgambato, A., Cattoretti, G., Tomita, N., Monden, T., Rotterdam, H., & Weinstein, I.B. (1998). Localization and expression of p27KIP1 in multistage colorectal carcinogenesis. *Cancer Research, 58,* 114-122.

Circosta, C., Pasquale, R.D., Palumbo, D.R., Samperi, S., & Occhiuto, F. Estrogenic activity of standardized extract of *Angelica sinensis. Phytotherapy Research, 20,* 665-669.

Colorectal Cancer (2010, January 4). Retrieved from http://www.chp.gov.hk/en/content/9/25/51.html

Coste, F., Malinge, J.M., Serre, L., Shepard, W., Roth, M., Leng, M., & Zelwer, C. (1999). Crystal structure of a double-stranded DNA containing a cisplatin interstrand cross-link at 1.63 A resolution: hydration of the platinated site. *Nucleic Acids Research, 27,* 1837-1846.

Cowling, V., & Downward, J. (2002). Caspase-6 is the direct activator of caspase-8 in the cytochrome c-induced apoptosis pathway: absolute requirement for removal of caspase-6 prodomain. *Cell Death and Differentiation, 9,* 1046-1056.

Cui, F., Feng, L., & Hu, J. (2006). Factors affecting stability of z-ligustilide in the volatile oil of Radix Angelicae sinensis and Ligusticum chuanxiong and its stability prediction. *Drug Development and Industrial Pharmacy*, 32, 747-755.

Cutsem, E.V., & Oliveira, J. (2009). Primary colon cancer: ESMO clinical recommendations for diagnosis, adjuvant treatment and follow-up. *Annals of Oncology, 20,* iv 49-50.

Dalgleish, A.G., & O'Byrne, K. (2006). Inflammation and cancer: the role of the immune response and angiogenesis. *Cancer Treatment Research, 130,* 1-38.

Datta, S.R., Dudek, H., Tao, X., Masters, S., Fu, H., Gotoh, Y., & Greenberg, M.E. (1997). Akt phosphorylation of BAD couples survival signals to the cell-intrinsic death machinery. *Cell, 91,* 231-241.

Davis, R.J. (2000). Signal transduction by the JNK group of MAP kinases. *Cell, 103,* 239-252.

Debatin, K.M., Poncet, D., & Kroemer, G. (2002). Chemotherapy: targeting the mitochondrial cell death pathway. *Oncogene, 21,* 8786-8803.

Deeb, D., Jiang, H., Gao, X., Hafner, M.S., Wong, H., Divine, G., Chapman, R.A., Dulchavsky, S.A., & Gautam, S.C. (2004). Curcumin sensitizes prostate cancer cells to tumor necrosis factor-related apoptosis-inducing ligand/Apo2L by inhibiting nuclear factor-kappaB through suppression of IkappaBalpha phosphorylation. *Molecular Cancer Therapeutics, 3,* 803-812.

de la Taille, A., Buttyan, R., Hayek, O., Bagiella, E., Shabsigh, A., Burchardt, M., Chopin, D.K., & Katz, A.E. (2000). Herbal therapy PC-SPES: *in vitro* effects and evaluation of its efficacy in 69 patients with prostate cancer. *Journal of Urology, 164,* 1229-1234.

Delmas, D., Rebe, C., Lacour, S., Filomenko, R., Athias, A., Gambert, P., Cherkaoui-Malki, M., Jannin, B., Dubrez-Daloz, L., Latruffe, N., & Solary, E. (2003). Resveratrol-induced apoptosis is associated with Fas redistribution in the rafts and the formation of a death-inducing signaling complex in colon cancer cells. *The Journal of Biological Chemistry, 278,* 41482-41490.

Delmas, D., Rebe, C., Micheau, O., Athias, A., Gambert, P., Grazide, S., Laurent, G., Latruffe, N., & Solary, E. (2004). Redistribution of CD95, DR4 and DR5 in rafts accounts for the synergistic toxicity of resveratrol and death receptor ligands in colon carcinoma cells. *Oncogene, 23,* 8979-8986.

Detailed Guide: Colon and Rectum Cancer – What are the Key Statistics for Colorectal Cancer? In

American Cancer Society. Retrieved May 4, 2010, from http://www.cancer.org/docroot/cri/content/cri_2_4_1x_what_are_the_key_statistics_for_colon_and_rectum_cancer.asp

de Thonel, A. & Eriksson, J.E. (2005). Regulation of death receptors – relevance in cancer therapies. *Toxicology and Applied Pharmacology, 207,* S123-S132.

Dhillon, A.S., Hagan, S., Rath, O., & Kolch, W. (2007). MAP kinase signaling pathways in cancer. *Oncogene, 26,* 3279-3290.

Dias, N. & Bailly, C. (2005). Drugs targeting mitochondrial functions to control tumor cell growth. *Biochemical Pharmacology, 70,* 1-12.

Dietz, B.M., Liu, D., Hagos, G.K., Yao, P., Schinkovitz, A., Pro, S.M., Deng, S., Farnsworth, N.R., Pauli, G.F., van Breemen, R.B., & Bolton, J.L. (2008). *Angelica sinensis* and its alkylphthalides induce the detoxification enzyme NAD(P)H: quinine oxidoreductase 1 by alkylating Keap1. *Chemical Research in Toxicology, 21,* 1939-1948.

Dizon, D.S. (2010). Treatment options for advanced endometrial carcinoma. *Gynecologic Oncology, 117,* 373-381.

Dong, Z.B., Li, S.P., Hong, M., & Zhu, Q. (2005). Hypothesis of potential active components in *Angelica sinensis* by using biomembrane extraction and high performance liquid chromatography. *Journal of Pharmaceutical and Biomedical Analysis, 38,* 664-669.

Dong, T.T., Zhao, K.J., Gao, Q.T., Ji, Z.N., Zhu, T.T., Li, J., Duan, R., Cheung, A.W., & Tsim, K.W. (2006). Chemical and biological assessment of a Chinese herbal decoction containing Radix *Astragali* and *Radix Angelicae sinensis*: determination of drug ratio in having optimized properties. *Journal of Agricultural and Food Chemistry, 54,* 2767-2774.

Drew, Y., & Plummer, R. (2009). PARP inhibitors in cancer therapy: two modes of attack on the cancer cell widening the clinical applications. *Drug Resistance Updates, 12,* 153-156.

Droge, W. (2002). Free radicals in the physiological control of cell function. *Physiological Reviews, 82,* 47-95.

Du, C., Fang., M., Li, Y., Li., L., & Wang, X. (2000). Smac, a mitochondrial protein that promotes cytochrome c-dependent caspase activation by eliminating IAP inhibition. *Cell, 102,* 33-42.

Du, J.R., Yu, Y., Yao, Y., Bai, B., Zong, X., Lei, Y., Wang, C.Y., & Qian, Z.M. (2007). Ligustilide reduces phenylephrine induced-aorta tension *in vitro* but has no effect on systolic pressure in spontaneously hypertensive rats. *The American Journal of Chinese Medicine, 35,* 487-496.

Duprez, L., Wirawan, E., Berghe, T.V., & Vandenabeele, P. (2009). Major cell death pathways at a glance. *Microbes and Infection, 11,* 1050-1062.

Ee., G.C., Daud, S., Izzaddin, S.A., & Rahmani, M. (2008). *Garcinia mangostana:* a source of potential anti-cancer lead compounds against CEM-SS cell line. *Journal of Asian Natural Products Research, 10,* 481-485.

Ekholm, S.V., & Reed, S.I. (2000). Regulation of G1 cyclin-dependent kinases in the mammalian cell cycle. *Current Opinion in Cell Biology, 12,* 676-684.

Elmore, S. (2007). Apoptosis: a review of programmed cell death. *Toxicologic Pathology, 35,* 495-516.

El-Najjar, N., Chatila, M., Moukadem, H., Vuorela, H., Ocker, M., Gandesiri, M., Schneider-Stock, R., & Gali-Muhtasib, H. (2010). Reactive oxygen species mediate thymoquinone-induced apoptosis and activate ERK and JNK signaling. *Apoptosis, 15,* 183-195.

Enari, M., Sakahira, H., Yokoyama, H., Okawa, K., Iwamatsu, A., & Nagata, S. (1998). A caspase-activated DNase that degrades DNA during apoptosis, and its inhibitor ICAD. *Nature, 391,* 43-50.

Endo, H., Hosono, K., Fujisawa, T., Takahashi, H., Sugiyama, M., Yoneda, K., Nozaki, Y., Fujita, K., Yoneda, M., Inamori, M., Wada, K., Nakagama, H., & Nakajima, A. (2009). Involvement of JNK pathway in the promotion of the early stage of colorectal carcinogenesis under high-fat dietary conditions. *Gut, 58,* 1637-1643.

Ernst, E. The role of complementary and alternative medicine in cancer. The *Lancet Oncology, 1,* 176-180.

Fadok, V.A., de Cathelineau, A., Daleke, D.L., Henson, P.M., & Bratton, D.L. (2001). Loss of phospholipid asymmetry and surface exposure of phosphatidylserine is required for phagocytosis of apoptotic cells by macrophages and fibroblasts. *The Journal of Biological Chemistry, 276,* 1071-1077.

Fan, M., & Chamber, T.C. (2001). Role of mitogen-activated protein kinases in the reponse of tumor cells to chemotherapy. *Drug Resistance Updates, 5,* 253-267.

Fan, M., Goodwin, M.E., Birrer, M.J., & Chambers, T.C. (2001). The c-Jun NH(2)-terminal protein kinase/AP-1 pathways is required for efficient apoptosis induced by vinblastine. *Cancer Research, 61,* 4450-4458.

Farrell, M.P., & Kummar, S. (2003). Phase I/IIA randomized study of PHY906, a novel herbal agent, as a modulator of chemotherapy in patients with advanced colorectal cancer. *Clinical Colorectal Cancer, 2,* 253-256.

Feagins, L.A., Souza, R.F., & Spechler, S.J. (2009). Carcinogenesis in IBD: potential targets for the prevention of colorectal cancer. *Nature Reviews. Gastroenterology and Hepatology, 6,* 297-305.

Feldman, D.R., Bosl, G.J., Sheinfeld, J., & Motzer, R.J. (2008). Medical treatment of advanced testicular cancer. *The Journal of the American Medical Association, 299,* 672-684.

Feng, F., Liu, W.Y., Chen, Y.S., Guo, Q.L., & You, Q.D. (2007). Five novel prenylated xanthones from *Resina Garciniae. Journal of Asian Natural Products Research, 9,* 735-741.

Filipe, M.I., Osborn, M., Linehan, J., Sanidas, E., Brito, M.J., & Jankowski, J. (1995). Expression of transforming growth factor alpha, epidermal growth factor receptor and epidermal growth factor in precurson lesions to gastric carcinoma. *British Journal of Cancer, 71,* 30-36.

Flinterman, M., Guelen, L., Ezzati-Nik, S., Killick, R., Melino, G., Tominaga, K., Mymryk, J.S., Gaken, J., & Tavassoli, M. (2005). E1A activates the transcription of p73 and Noxa to induce apoptosis. *The Journal of Biological Chemistry, 280,* 5945-5959.

Flores, E.R., Tsai, K.Y., Crowley, D., Sengupta, S., Yang, A., McKeon, F., & Jacks, T. (2002). p63 and p73 are required for p53-dependent apoptosis in response to DNA damage. *Nature, 416,* 560-564.

Fredersdorf, S., Burns, J., Milne, A.M., Packham, G., Fallis, L., Gillett, C.E., Royds, J.A., Peston, D., Hall, P.A., Hanby, A.M., Barnes, D.M., Shousha, S., O'Hare, M.J., & Lu, X. (1997). High level expression of $p27^{kpl}$ and cyclin D1 in some human breast cancer cells: Inverse correlation between the expression of $p27^{kpl}$ and degree of malignancy in human breast and colorectal cancers. *Proceedings of the National Academy of Science of the United States of America, 94,* 6380-6385.

Friesen, C., Herr, I., Krammer, P.H., & Debatin, K.M. (1996). Involvement of the CD95 (APO-1/FAS)

receptor/ligand system in drug-induced apoptosis in leukemia cells. *Nature Medicine, 2,* 574-577.

Fu, M., Wang, C., Li, Z., Sakamaki, T., & Pestell, R.G. (2004). Mini-review: cyclin D1: normal and abnormal functions. *Endocrinology, 145,* 5439-5447.

Fuertes, M.A., Castilla, J., Alonso, C., & Perez, J.M. (2003). Cisplatin biochemical mechanism of action: from cytotoxicity to induction of cell death through interconnections between apoptotic and necrotic pathways. *Current Medicinal Chemistry, 10,* 257-266.

Fugh-Berman, A. (2000). Herb-drug interactions. *Lancet, 355,* 134-138.

Fulda, S., Sieverts, H., Friesen, C., Herr, I., & Debatin, K.M. (1997). The CD95 (APO-1/Fas) system mediates drug-induced apoptosis in neuroblastoma cells. *Cancer Research, 57,* 3823-3829.

Fulda, S., & Debatin, K.M. (2003). Death receptor signaling in cancer therapy. *Current Medicinal Chemistry. Anticancer Agents, 3,* 253-262.

Galluzzi, L., Larochette, N., Zamzami, N., & Kroemer, G. (2006). Mitochondria as therapeutic targets for cancer chemotherapy. *Oncogene, 25,* 4812-4830.

Gao, Q.T., Cheung, J.K., Li, J., Chu, G.K., Duan, R., Cheung, A.W., Zhao, K.J., Dong, T.T., & Tsim, K.W. (2006). A Chinese herbal decoction, Danggui Buxue Tang, prepared from *Radix Astragali* and *Radix Angelicae sinensis* stimulates the immune responses. *Planta Medica, 72,* 1227-1231.

Gao, Q.T., Choi, R.C., Cheung, A.W., Zhu, J.T., Li, J., Chu, G.K., Duan, R., Cheung, J.K., Jiang, Z.Y., Dong, X.B., Zhao, K.J., Dong, T.T., & Tsim, K.W. (2007a). Danggui Buxue Tang – a Chinese herbal decoction activates the phosphorylations of extracellular signal-regulated kinase and estrogen receptor α in cultured MCF-7 cells. *FEBS Letters, 581,* 233-240.

Gao, Q.T., Cheung, J.K., Li, J., Jiang, Z.Y., Chu, G.K., Duan, R., Cheung, A.W., Zhao, K.J., Choi, R.C., Dong, T.T., & Tsim, K.W. (2007b). A Chinese herbal decoction, Danggui Buxue Tang, activates extracellular signal-regulated kinase in cultured T-lymphocytes. *FEBS Letters, 581,* 5087-5093.

Gao, Q., Li, J., Cheung, J.K., Duan, J., Ding, A., Cheung, A.W., Zhao, K., Li, W.Z., Dong, T.T., & Tsim, K.W. (2007c). Verification of the formulation and efficacy of Danggui Buxue Tang (a decoction of *Radix Astragali* and *Radix Angelicae Sinensis*): an exemplifying systematic approach to revealing the complexity of Chinese herbal medicine formulae. *Chinese Medicine, 29,* 2-12.

Gao, Q.T., Cheung, J.K., Choi, R.C., Cheung, A.W., Li, J., Jiang, Z.Y., Duan, R., Zhao, K.J., Ding, A.W., Dong, T.T., & Tsim, K.W. (2008). A Chinese herbal decoction prepared from *Radix Astragali* and *Radix Angelicae sinensis* induces the expression of erythropoietin in cultured Hep3B cells. *Planta Medica, 74,* 392-395.

Gelasco, A., & Lippard, S.J. (1998). NMR solution structure of a DNA dodecamer duplex containing a cis-diammineplatinum(II) d(GpG) intrastrand cross-link, the major adduct of the anticancer drug cisplatin. *Biochemistry, 37,* 9230-9239.

Gerber, B., Scholz, C., Reimer, T., Briese, V., & Janni, W. (2006). Complementary and alternative therapeutic approaches in patients with early breast cancer: a systematic review. *Breast Cancer Research and Treatment, 95,* 199-209.

Green, D.R., & Kroemer, G. (2004). The pathophysiology of mitochondrial cell death. *Science, 305,* 626-629.

Gu, H., Wang, X., Rao, S., Wang, J., Zhao, J., Ren, F.L., Mu, R., Yang, Y., Qi, Q., Liu, W., Lu, N., Ling, H., You, Q., & Guo, Q. (2008). Gambogic acid mediates apoptosis as a p53 inducer through down-regulation of mdm2 in wild-type p53-expressing cancer cells. *Molecular Cancer Therapeutics, 7,* 3298-3305.

Gu, H., Rao, S., Zhao, J., Wang, J., Mu, R., Rong, J., Tao, L., Qi, Q., You, Q., & Guo, Q. (2009). Gambogic acid reduced bcl-2 expression via p53 in human breast MCF-7 cancer cells. *Journal of Cancer Research and Clinical Oncology, 135,* 1777-1782.

Guo, Q.L., You, Q.D., Wu, Z.Q., Yuan, S.T., Zhao, L. (2004). General gambogic acids inhibited growth of human hepatoma SMMC-7721 cells *in vitro* and in nude mice. *Acta Pharmacologica Sinica, 25,* 769-774.

Guo, Q.L., Lin, S.S., You, Q.D., Gu, H.Y., Yu, J., Zhao, L., Qi, Q., Liang, F., Tan, Z., & Wang, X. (2006a). Inhibition of human telomerase reverse transcriptase gene expression by gambogic acid in human hepatoma SMMC-7721 cells. *Life Sciences, 78,* 1238-1245.

Guo, Q., Qi, Q., You, Q., Gu, H., Zhao, L., & Wu, Z. (2006b). Toxicological studies of gambogic acid and its potential targets in experimental animals. *Basic & Clinical Pharmacology & Toxicology, 99,* 178-184.

Guyot, F., Faivre, J., Manfredi, S., Meny, B., Bonithon-Kopp, C., & Bouvier, A.M. (2005). Time

trends in the treatment and survival of recurrences from colorectal cancer. *Annals of Oncology, 16,* 756-761.

Ha, L.D., Hansen, P.E., Vang, O., Duus, F., Pham, H.D., & Nguyen, L.H. (2009). Cytotoxic geranylated xanthones and *o*-alkylated derivatives of α-mangostin. *Chemical & Pharmaceutical Bulletin, 57,* 830-834.

Haines, C.J., Lam, P.M., Chung, T.K., Cheng, K.F., & Leung, P.C. (2008). A randomized, double-blind, placebo-controlled study of the effect of a Chinese herbal medicine preparation (Dang Gui Buxue Tang) on menopausal symptoms in Hong Kong Chinese women. *Climacteric, 11,* 244-251.

Haldar, S., Chintapalli, J., & Croce, C.M. (1996). Taxol induces bcl-2 phosphorylation and death of prostate cancer cells. *Cancer Research, 56,* 1253-1255.

Hallstrom, T.C., & Nevins, J.R. (2003). Specificity in the activation and control of transcription factor E2F-dependent apoptosis. *Proceedings of the National Academy of Sciences of the United States of America, 100,* 10848-10853.

Han, Q., Yang, L., Liu, Y., Wang, Y., Qiao, C., Song, J., Xu, L., Yang, D., Chen, S., & Xu, H. (2006a). Gambogic acid and epigambogic acid, C-2 epimers with novel anticancer effects from *Garcinia hanburyi. Planta Medica, 72,* 281-284.

Han, Q.B., Wang, Y.L., Yang, L., Tso, T.F., Qiao, C.F., Song, J.Z., Xu, L.J., Chen, S.L., Yang, D.J., & Xu, H.X. (2006b). Cytotoxic polyprenylated xanthones from the resin of *Garcinia hanburyi. Chemical & Pharmaceutical Bulletin, 54,* 265-267.

Han, Q.B., Yang, L., Wang, Y.L., Qiao, C.F., Song, J.Z., Sun, H.D., & Xu, H.X. (2006c). A pair of novel cytotoxic polyprenylated xanthone epimers from gamboges. *Chemistry & Biodiversity, 3,* 101-105.

Han, Q.B., & Xu, H.X. (2009). Caged *Garcinia* xanthones: development since 1937. *Current Medicinal Chemistry, 16,* 3775-3796.

Han, A.R., Kim, J.A., Lantvit, D.D., Kardono, L.B., Riswan, S., Chai, H., Carcache de Blanco, E.J., Farnsworth, N.R., Swanson, S.M., & Kinghorn, A.D. (2009). Cytotoxic xanthone constituents of the stem bark of *Garcinia mangostana* (mangosteen). *Journal of Natural Products, 72,* 2028-2031.

Hengartner, M.O. (2000). The biochemistry of apoptosis. *Nature, 407,* 770-776.

Hirata, J.D., Swiersz, L.M., Zell, B., Small, R., & Ettinger, B. (1997). Does dong quai have estrogenic effects in postmenopausal women? A double-blind, placebo-controlled trial. *Fertility and Sterility, 68,* 981-986.

Hoffman, W.H., Biade, S., Zilfou, J.T., Chen, J., & Murphy, M. (2002). Transcriptional repression of the anti-apoptotic survivin gene by wild type p53. *The Journal of Biological Chemistry, 277,* 3247-3257.

Hong, J., Kwon, S.J., Sang, S., Ju, J., Zhou, J., Ho, C.T., Huang, M.T., & Yang, C.S. (2007). Effects of garcinol and its derivatives on intestinal cell growth: inhibitory effects and autoxidation-dependent growth-stimulatory effects. *Free Radical Biology & Medicine, 42,* 1211-1221.

Hou, Y.Z., Zhao, G.R., Yang, J., Yuan, Y.J., Zhu, G.G., & Hiltunen, R. (2004). Protective effect of *Ligusticum chuanxiong* and *Angelica sinensis* on endothelial cell damage induced by hydrogen peroxide. *Life Sciences, 75,* 1775-1786.

Hou, Y.Z., Zhao, G.R., Yuan, Y.J., Zhu, G.G., & Hiltunen, R. (2005). Inhibition of rat vascular smooth muscle cell proliferation by extract of *Ligusticum chuanxiong* and *Angelica sinensis. Journal of Ethnopharmacology, 100,* 140-144.

Huang, J.C., Zamble, D.B., Reardon, J.T., Lippard, S.J., & Sancar, A. (1994). HMG-domain proteins specifically inhibit the repair of the major DNA adduct of the anticancer drug cisplatin by human excision nuclease. *Proceedings of the National Academy of Sciences of the United States of America, 91,* 10394-10398.

Huang, Y., He, Q., Hillman, M.J., Rong, R., & Sheikh, M.S. (2001). Sulindac sulfide-induced apoptosis involves death receptor 5 and the caspase-8 dependent pathway in human colon and prostate cancer cells. *Cancer Research, 61,* 6918-6924.

Huang, L.F., Li, B.Y., Liang, Y.Z., Guo, F.Q., & Wang, Y.L. (2004). Application of combined approach to analyze the constituents of essential oil from Dong quai. *Analytical and Bioanalytical Chemistry, 378,* 510-517.

Huang, S.H., Lin, C.M., & Chiang, B.H. (2008). Protective effects of *Angelica sinensis* extract on amyloid beta-peptide-induced neurotoxicity. *Phytomedicine, 15,* 710-721.

Huang, S.X., Feng, C., Zhou, Y., Xu, G., Han, Q.B., Qiao, C.F., Chang, D.C., Luo, K.Q., & Xu, H.X. (2009). Bioassay-guided isolation of xanthones and polycyclic prenylated acylphloroglucinols from

Garcinia oblongifolia, 72, 130-135.

Huerta, S., Arteaga, J.R., Irwin, R.W., Ikezoe, T., Heber, D., & Koeffler, H.P. (2002). PC-SPES inhibits colon cancer growth *in vitro* and *in vivo*. *Cancer Research, 62,* 5204-5209.

Huerta, S., Goulet, E.J., & Livingston, E.H. (2006). Colon cancer and apoptosis. *The American Journal of Surgery, 191,* 517-526.

Huerta, S., Goulet, E.J., Huerta-Yepez, S., & Livingston, E.H. (2007). Screening and detection of apoptosis. *Journal of Surgical Research, 139,* 143-156.

Hui, M.K., Wu, W.K., Shin, V.Y., So, W.H., & Cho, C.H. (2006). Polysaccharides from the root of *Angelica sinensis* protect bone marrow and gastrointestinal tissues against the cytotoxicity of cyclophosphamide in mice. *International Journal of Medical Sciences, 3,* 1-6.

Hutadilok-Towatana, N., Kongkachuay, S., & Mahabusarakam, W. (2007). Inhibition of human lipoprotein oxidation by morelloflavone and camboginol from *Garcinia dulcis. Natural Product Research, 21,* 655-662.

Inoue, Y., Tanaka, K., Hiro, J., Yoshiyama, S., Toiyama, Y., Eguchi, T., Miki, C., & Kusunoki, M. (2006). *In vitro* synergistic antitumor activity of a combination of 5-fluorouracil and irinotecan in human colon cancer. *International Journal of Oncology, 28,* 479-486.

Ip, Y.T., & Davis, R.J. (1998). Signal transduction by the c-Jun N-terminal kinase (JNK) – from inflammation to development. *Current Opinion in Cell Biology, 10,* 205-219.

Ishiguro, A., Takahata, T., Saito, M., Yoshiya, G., Tamura, Y., Sasaki, M., & Munakata, A. (2006). Influence of methylated p15 and p16 genes on clinicopathological features in colorectal cancer. *Journal of Gastroenterology and Hepatology, 21,* 1334-1339.

Itakura, Y., Sasano, H., Shiga, C., Furukawa, Y., Shiga, K., Mori, S., & Nagura, H. (1994). Epidermal growth factor receptor overexpression in esophageal carcinoma. An immunohistochemical study correlated with clinicopathologic findings and DNA amplification. *Cancer, 74,* 795-804.

Jang, T.J., Kang, H.J., Kim, J.R., & Yang, C.H. (2004). Non-steroidal inflammatory drug activated gene (NAG-1) expression is closely related to death receptor-4 and -5 induction, which may explain sulindac sulfide induced gastric cancer cell apoptosis. *Carcinogenesis, 25,* 1853-1858.

Jang, S.W., Okada, M., Sayeed, I., Xiao, G., Stein, D., Jin, P., & Ye, K. (2007). Gambogic amide, a selective agonist for TrkA receptor that possesses robust neurotrophic activity, prevents neuronal cell death. *Proceedings of the National Academy of Sciences of the United States of America, 104,* 16329-163.

Jia, R.R., Gou, Y.L., Ho, L.S., Ng, C.P., Tan, N.H., & Chan, H.C. (2005). Anti-apoptotic activity of *Bak Foong Pills* and its ingredients on 6-hydroxydopamine-induced neurotoxicity in PC12 cells. *Cell Biology International, 29,* 835-842.

Jarvis, W.D., Johnson, C.R., Fornari, F.A., Park, J.S., Dent, P., & Grant, S. (1999). Evidence that the apoptotic actions of etoposide are independent of c-Jun/activating protein-1-mediated transregulation. *The Journal of Pharmacology and Experimental Therapeutics, 290,* 1384-1392.

Jo, S.K., Cho, W.Y., Sung, S.A., Kim, H.K., & Won, N.H. (2005). MEK inhibitor, U0126, attenuates cisplatin-induced renal injury by decreasing inflammation and apoptosis. *Kidney International, 67,* 458-466.

Julien, L.A., & Thorson, A.G. (2010). Current neoadjuvant strategies in rectal cancer. *Journal of Surgical Oncology, 101,* 321-326.

Jordan, P., & Carmo-Fonseca, M. (2000). Molecular mechanisms involved in cisplatin cytotoxicity. *Cellular and Molecular Life Sciences, 57,* 1229-1235.

Jung, S.M., Schumacher, H.R., Kim, H., Kim, M., Lee, S.H., & Pessler, F. (2007). Reduction of urate crystal-induced inflammation by root extracts from traditional oriental medicinal plants: elevatin of prostaglandin D2 levels. *Arthritis Research & Therapy, 9,* R64.

Kan, W.L., Cho, C.H., Rudd, J.A., & Lin, G. (2008). Study of the anti-proliferative effects and synergy of phthalides from *Angelica sinensis* on colon cancer cells. *Journal of Ethnopharmacology, 120,* 36-43.

Kane, L.P., Shapiro, V.S., Stokoe, D., & Weiss, A. (1999). Induction of NF-kappaB by the Akt/PKB kinase. *Current Biology, 9,* 601-604.

Kang, C.D., Ahn, B.K., Jeong, C.S., Kim, K.W., Lee, H.J., Yoo, S.D., Chung, B.S., & Kim, S.H. (2000). Downregulation of JNK/SAPK activity is associated with the cross-resistance to P-glycoprotein-unrelated drugs in multidrug-resistant FM3A/M cells overexpressing P-glycoprotein. *Experimental Cell Research, 256,* 300-307.

Kashfi, K. (2009). Anti-inflammatory agents as cancer therapeutics. *Advances in Pharmacology, 57,* 31-89.

Kasibhatla, S., Jessen, K.A., Maliartchouk, S., Wang, J.Y., English, N.M., Drewe, J., Qiu, L., Archer, S.P., Ponce, A.E., Sirisoma, N., Jiang, S., Zhang, H.Z., Gehlsen, K.R., Cai, S.X., Green, D.R., & Tseng, B. (2005). A role for transferrin receptor in triggering apoptosis when targeted with gambogic acid. *Proceedings of the National Academy of Sciences of the United States of America, 102,* 12095-12100.

Kawasaki, H., Altieri, D.C., Lu, C.D., Toyoda, M., Tenjo, T., & Tanigawa, N. (1998). Inhibition of apoptosis by surviving predicts shorter survival rates in colorectal cancer. *Cancer Research, 58,* 5071-5074.

Keku, T.O., Amin, A., Galanko, J., Martin, C., Schliebe, B., Sandler, R.S. (2008). Apoptosis in normal rectal mucosa, baseline adenoma characteristics, and risk of future adenomas. *Cancer Epidemiology, Biomarkers & Prevention, 17,* 306-310.

Kelly, M.M., Hoel, B.D., & Voelkel-Johnson, C. (2002). Doxorubicin pretreatment sensitizes prostate cancer cell lines to TRAIL induced apoptosis which correlates with the loss of c-FLIP expression. *Cancer Biology & Therapy, 1,* 520-527.

Kerr, J.F., Wyllie, A.H., & Currie, A.R. (1972). Apoptosis: a basic biological phenomenon with wide-ranging implications in tissue kinetics. *British Journal of Cancer, 26,* 239-257.

Kharbanda, S., Ren, R., Pandey, P., Shafman, T.D., Feller, S.M., Weichselbaum, R.R., & Kufe, D.W. (1995a). Activation of the c-Abl tyrosine kinase in the stress response to DNA-damaging agents. *Nature, 376,* 785-788.

Kharbanda, S., Pandey, P., Ren, R., Mayer, B., Zon, L., & Kufe, D. (1995b). c-Abl activation regulates induction of the SEK1/stress-activated protein kinase pathway in the cellular response to 1-beta-D-arabinofuranosylcytosine. *The Journal of Biological Chemistry, 270,* 30278-30281.

Kikuchi, H., Ohtsuki, T., Koyano, T., Kowithayakorn, T., Sakai, T., & Ishibashi, M. (2010). Activity of mangosteen xanthones and teleocidin A-2 in death receptor expression enhancement and tumor necrosis factor related apoptosis-inducing ligand assays. *Journal of Natural Products, 73,* 452-455.

Kim, T.I., Jin, S.H., Kim, W.H., Kang, E.H., Choi, K.Y., Kim, H.J., Shin, S.K., & Kang, J.K. (2001). Prolonged activation of mitogen-activated protein kinases during NSAID-induced apoptosis in HT-29

colon cancer cells. *International Journal of Colorectal Disease, 16,* 167-173.

Kim, R., Tanabe, K., Uchida, Y., Emi, M., Inoue, H., & Toge, T. (2002). Current status of the molecular mechanisms of anticancer drug-induced apoptosis. The contribution of molecular level analysis to cancer chemotherapy. *Cancer Chemotherapy and Pharmacology, 50,* 343-352.

Kim, B.N., Yamamoto, H., Ikeda, K., Damdinsuren, B., Sugita, Y., Ngan, C.Y., Fujie, Y., Ogawa, M., Hata, T., Ikeda, M., Ohue, M., Sekimoto, M., Monden, T., Matsuura, N., & Monden, M. (2005a). Methylation and expression of p16INK4 tumor suppressor gene in primary colorectal cancer tissues. *International Journal of Oncology, 26,* 1217-1226.

Kim, Y.K., Kim, H.J., Kwon, C.H., Kim, J.H., Woo, J.S., Jung, J.S., & Kim, J.M. (2005b). Role of ERK activation in cisplatin-induced apoptosis in OK renal epithelial cells. *Journal of Applied Toxicology, 25,* 374-382.

Kim, M.R., Abd El-Aty, A.M., Choi, J.H., Lee, K.B., Shim, J.H. (2006). Identification of volatile components in *Angelica* species using supercritical-CO2 fluid extraction and solid phase microextraction coupled to gas chromatography-mass spectrometry. *Biomedical Chromatography, 20,* 1267-1273.

Kim, J.H., Jung, C.H., Jang, B.H., Go, H.Y., Park, J.H., Choi, Y.K., Hong, S.I., Shin, Y.C., & Ko, S.G. (2009). Selective cytotoxic effects on human cancer cell lines of phenolic-rich ethyl-acetate fraction from *Rhus verniciflua* Stokes. *The American Journal of Chinese Medicine, 37,* 609-620.

Kim, E.K., & Choi, E.J. (2010). Pathological roles of MAPK signaling pathways in human diseases. *Biochimica et Biophysica Acta, 1802,* 396-405.

Kim, S.M., Kim, J.S., Kim, J.H., Yun, C.O., Kim, E.M., Solca, F., Choi, S.Y., & Cho, B.C. (2010). Acquired resistance to cetuximab is mediated by increased PTEN instability and leads cross-resistance to gefitinib in HCC827 NSCLC cells. *Cancer Letters,* doi:10.1016/j.canlet.2010.04.006.

Kobayashi, S., Mimura, Y., Notoya, K., Kimura, I., & Kimura, M. (1992). Antiproliferative effects of the traditional Chinese medicine *Shimotsu-To,* its component Cnidium rhizome and derived compounds on primary cultures of mouse aorta smooth muscle cells. *The Japanese Journal of Pharmacology, 60,* 397-401.

Kobayashi, S., Mimura, Y., Naitoh, T., Kimura, I., & Kimura, M. (1993). Chemical structure-activity of Cnidium rhizome-derived phthalides for the competence inhibition of proliferation in primary

cultures of mouse aorta smooth muscle cells. *The Japanese Journal of Pharmacology, 63,* 353-359.

Kohne, C.H., & Lenz, H.J. (2009). Chemotherapy with targeted agents for the treatment of metastatic colorectal cancer. *The Oncologist, 14,* 478-488.

Kondo, M., Zhang, L., Ji, H., Kou, Y., & Ou, B. (2009). Bioavailability and antioxidant effects of a xanthone-rich mangosteen (*Garcinia mangostana*) product in humans. *Journal of Agricultural and Food Chemistry, 57,* 8788-8792.

Konstantakou, E.G., Voutsinas, G.E., Karkoulis, P.K., Aravantinos, G., Margaritis, L.H., & Stravopodis, D.J. (2009). Human bladder cancer cells undergo cisplatin-induced apoptosis that is associated with p53-dependent and p53-independent responses. *International Journal of Oncology, 35,* 401-416.

Kosmider, S. & Lipton, L. (2007). Adjuvant therapies for colorectal cancer. *World Journal of Gastroenterology, 13,* 3799-3805.

Kothakota, S., Azuma, T., Reinhard, C., Klippel, A., Tang, J., Chu, K., McGarry, T.J., Kirschner, M.W., Koths, K., Kwiatkowski, D.J., & Williams, L.T. (1997). Caspase-3-generated fragment of gelsolin: effector of morphological change in apoptosis. *Science, 278,* 294-298.

Koumakpayi, I.H., Le Page, C., Mes-Masson, A.M., & Saad, F. (2010). Hierarchical clustering of immunohistochemical analysis of the activated ErbB/PI3K/Akt/NF-kappaB signaling pathway and prognostic significance in prostate cancer. *British Journal of Cancer, 102,* 1163-1173.

Kroemer, G., Dallaporta, B., & Resche-Rigon, M. (1998). The mitochondrial death/life regulator in apoptosis and necrosis. *Annual Review of Physiology, 60,* 619-642.

Kuang, X., Yao, Y., Du, J.R., Liu, Y.X., Wang, C.Y., & Qian, Z.M. (2006). Neuroprotective role of *z*-ligustilide against forebrain ischemic injury in ICR mice. *Brain Research, 1102,* 145-153.

Kuang, X., Du, J.R., Liu, Y.X., Zhang, G.Y., & Peng, H.Y. (2008). Postischemic administration of *z*-ligustilide ameliorates cognitive dysfunction and brain damage induced by permanent forebrain ischemia in rats. *Pharmacology, Biochemistry and Behavior, 88,* 213-221.

Kuang, X., Du, J.R., Chen, Y.S., Wang, J., & Wang, Y.N. (2009). Protective effect of *z*-ligustilide against amyloid beta-induced neurotoxicity is associated with decreased pro-inflammatory markers in rat brains. *Pharmacology, Biochemistry and Behavior, 92,* 635-641.

Kubota, T., Hisatake, J., Hisatake, Y., Said, J.W., Chen, S.S., Holden, S., Taguchi, H., & Koeffler, H.P.

(2000). PC-SPES: a unique inhibitor of proliferation of prostate cancer cells *in vitro* and *in vivo*. *Prostate, 42,* 163-171.

Lane, D.P. (1992). Cancer. p53, guardian of the genome. *Nature, 358,* 15-16.

Lau, C.B., Ho, T.C., Chan, T.W., & Kim, S.C. (2005). Use of dong quai (*Angelica sinensis*) to treat peri- or postmenopausal symptoms in women with breast cancer: is it appropriate? *Menopause, 12,* 734-740.

Laurent, G., & Jaffrezou, J.P. (2001). Signaling pathways activated by daunorubicin. *Blood, 98,* 913-924.

Lee, L.F., Li, G., Templeton, D.J., & Ting, J.P. (1998). Paclitaxel (Taxol)-induced gene expression and cell death are both mediated by the activation of c-Jun NH2-terminal kinase (JNK/SAPK). *The Journal of Biological Chemistry, 273,* 28253-28260.

Lee, E.J., Park, H.G., Kang, H.S. (2003). Sodium salicylate induces apoptosis in HCT116 colorectal cancer cells through activation of p38MAPK. *International Journal of Oncology, 23,* 503-508.

Lee, W.H., Jin, J.S., Tsai, W.C., Chen, Y.T., Chang, W.L., Yao, C.W., Sheu, L.F. & Chen, A. (2006). Biological inhibitory effects of the Chinese herb Danggui on brain astrocytoma. *Pathobiology, 73,* 141-148.

Lee, T.F., Lin, Y.L., & Huang, Y.T. (2007). Studies on antiproliferative effects of phthalides from *Ligusticum chuanxiong* in hepatic stellate cells. *Planta Medica, 73,* 527-534.

Lee, J., & Kim, S.S. (2009). The function of $p27^{KIP1}$ during tumor development. *Experimental and Molecular Medicine, 41,* 765-771.

Lee, Y.C., Lin, H.H., Hsu, C.H., Wang, C.J., Chiang, T.A., & Chen, J.H. (2010a). Inhibitory effects of andrographolide on migration and invasion in human non-small cell lung cancer A549 cells via down-regulation of PI3K/Akt signaling pathway. *European Journal of Pharmacology, 632,* 23-32.

Lee, Y.K., Hwang, J.T., Kwon, D.Y., Surh, Y.J., & Park, O.J. (2010b). Induction of apoptosis by quercetin is mediated through AMPKα/ASK1/p38 pathway. *Cancer Letters, 292,* 228-236.

Lesuisse, C., & Martin, L.J. (2002). Immature and mature cortical neurons engage different apoptotic mechanisms involving caspase-3 and the mitogen-activated protein kinase pathway. *Journal of*

Cerebral Blood Flow and Metabolism, 22, 935-950.

Letai, A. (2005). Pharmacological manipulation of Bcl-2 family members to control cell death. *The Journal of Clinical Investigation, 115,* 2648-2655.

Li, J.Q., Miki, H., Wu, F., Saoo, K., Nishioka, M., Ohmori, M., & Imaida, K. (2002). Cyclin A correlates with carcinogenesis and metastasis, and $p27^{kip1}$ correlates with lymphatic invasion, in colorectal neoplasms. *Human Pathology, 33,* 1006-1015.

Li, S.L., Chan, S.S., Lin, G., Ling, L., Yan, R., Chung, H.S., & Tam, Y.K. (2003). Simultaneous analysis of seventeen chemical ingredients of *Ligusticum chuanxiong* by on-line high performance liquid chromatography-diode array detector-mass spectrometry. *Planta Medica, 69,* 445-451.

Li, S.L., Lin, G., Chung, H.S., & Tam, Y.K. (2004). Study on fingerprint of *Rhizoma chuanxiong* by HPLC-DAD-MS. *Yao Xue Xue Bao, 39,* 621-626.

Li, W., Lam, M.S., Birkeland, A., Riffel, A., Montana, L., Sullivan, M.E., & Post, J.M. (2006a). Cell-based assays for profiling activity and safety properties of cancer drugs. *Journal of Pharmacological and Toxicological Methods, 54,* 313-319.

Li, W., Lam, M., Choy, D., Birkeland, A., Sullivan, M.E., & Post, J.M. (2006b). Human primary renal cells as a model for toxicity assessment of chemo-therapeutic drugs. *Toxicology in Vitro, 20,* 669-676.

Li, P., Li, S.P., Lao, S.C., Fu, C.M., Kan, K.K., Wang, Y.T. (2006c). Optimization of pressurized liquid extraction for *z*-ligustilide, *z*-butylidenephthalide and ferulic acid in *Angelica sinensis*. *Journal of Pharmaceutical and Biomedical Analysis, 40,* 1073-1079.

Li, S.L., Li, P., Sheng, L.H., Li, R.Y., Qi, L.W., Zhang, L.Y. (2006d). Live cell extraction and HPLC-MS analysis for predicting bioactive components of traditional Chinese medicines. *Journal of Pharmaceutical and Biomedical Analysis, 41,* 576-581.

Li, S.L., Lin, G., & Tam, Y.K. (2006e). Time-course accumulation of main bioactive components in the rhizome of *Ligusticum chuanxiong, 72,* 278-280.

Li, S.Y., Yu, Y., & Li, S.P. (2007). Identification of antioxidants in essential oil of Radix *Angelicae sinensis* using HPLC coupled with DAD-MS and ABTS-based assay. *Journal of Agricultural and Food Chemistry, 55,* 3358-3362.

Li, S.L., Yan, R., Tam, Y.K., & Lin, G. (2007b). Post-harvest alteration of the main chemical

ingredients in *Ligusticum chuanxiong* Hort. (*Rhizoma Chuanxiong*). *Chemical & Pharmaceutical Bulletin, 55,* 140-144.

Li, X.L., Wang, C.Z., Mehendale, S.R., Sun, S., Wang, Q., & Yuan, C.S. (2009). Panaxadiol, a purified ginseng component, enhances the anti-cancer effects of 5-fluorouracil in human colorectal cancer cells. *Cancer Chemotherapy and Pharmacology, 64,* 1097-1104.

Li, J., Hou, N., Faried, N., Tsutsumi, S., & Kuwano, H. (2010a). Inhibition of autophagy augments 5-fluorouracil chemotherapy in human colon cancer in vitro and in vivo model. *European Journal of Cancer, doi: 10.1016/j.ejca.2010.02.021.*

Li, Q., Cheng, H., Zhu, G., Yang, L., Zhou, A., Wang, X., Fang, N., Xia, L., Su, J., Wang, M., Peng, D., & Xu, Q. (2010b). Gambogenic acid inhibits proliferation of A549 cells through apoptosis-inducing and cell cycle arresting. *Biological and Pharmaceutical Bulletin, 33,* 415-420.

Li, W.Z., Li, J., Bi, C.W., Cheung, A.W., Huang, W., Duan, R., Choi, R.C., Chen, I.S., Zhao, K.J., Dong, T.T., Duan, J.A., & Tsim, K.W. (2010c). Can *Rhizoma Chuanxiong* replace *Radix Angelica sinensis* in the traditional Chinese herbal decoction Danggui Buxue Tang? *Planta Medica, 75,* 602-606.

Liang, J., Zubovitz, J., Petrocelli, T., Kotchetkov, R., Connor, M.K., Han, K., Lee, J.H., Ciarallo, S., Catzavelos, C., Beniston, R., Franssen, E., & Slingerland, J.M. (2002). PKB/Akt phosphorylates p27, impairs nuclear import of p27 and opposes p27-mediated G1 arrest. *Nature Medicine, 8,* 1153-1160.

Liang, M.J., & He, L.C. (2006). Inhibitory effects of ligustilide and butylidenephthalide on bFGF-stimulated proliferation of rat smooth muscle cells. *Acta Pharmaceutica Sinica, 41,* 161-165.

Liao, C.H., Sang, S., Ho, C.T., & Lin, J.K. (2005). Garcinol modulates tyrosine phosphorylation of FAK and subsequently induces apopotsis through down-regulation of Src, ERK and Akt survival signaling in human colon cancer cells. *Journal of Cellular Biochemistry, 99,* 155-169.

Lin, J.H., & Castora, F.J. (1991). DNA topoisomerase II from mammalian mitochondria is inhibited by the antitumor drugs, m-AMSA and VM-26. *Biochemical and Biophysical Research Communications, 176,* 690-697.

Lin, L.Z., He, X.G, Lian, L.Z., King, W., & Elliot, J. (1998). Liquid-chromatographic-electrospray mass spectrometric study of the phthalides of *Angelica sinensis* and chemical changes of *z*-ligustilide. *Journal of Chromatography A, 810,* 71-79.

Lin, Y.L., Lee, T.F., Huang, Y.J., & Huang, Y.T. (2006). Inhibitory effects of *Ligusticum chuanxiong* on the proliferation of rat hepatic stellate cells. *Journal of Gastroenterology and Hepatology, 21,* 1257-1265.

Lin, P.C., Chen, Y.L., Chiu, S.C., Yu, Y.L., Chen, S.P., Chien, M.H., Chen, K.Y., Chang, W.L., Lin, S.Z., Chiou, T.W., & Harn, H.J. (2008). Orphan nuclear receptor, Nurr-77 was a possible target gene of butylidenephthalide chemotherapy on glioblastoma multiform brain tumor. *Journal of Neurochemistry, 106,* 1017-1026.

Liu, J., Burdette, J.E., Xu, H., Gu, C., van Breemen, R.B., Bhat, K.P., Booth, N., Constantinou, A.I., Pezzuto, J.M., Fong, H.H., Farnsworth, N.R., & Bolton, J.L. (2001). Evaluation of estrogenic activity of plant extracts for the potential treatment of menopausal symptoms. *Journal of Agricultural and Food Chemistry, 49,* 2472-2479.

Liu, F.T., Newland, A.C., Jia, L. (2003a). Bax conformational change is a crucial step for PUMA-mediated apoptosis in human leukemia. *Biochemical and Biophysical Research Communications, 310,* 956-962.

Liu, S.P., Dong, W.G., Wu, D.F., Luo, H.S., & Yu, J.P. (2003b). Protective effects of Angelica sinensis polysaccharide on experimental immunological colon injury in rats. *World Journal of Gastroenterology, 9,* 2786-2790.

Liu, X., Yue, P., Zhou, Z., Khuri, F.R., & Sun, S.Y. (2004). Death receptor regulation and celecoxib-induced apoptosis in human lung cancer cells. *Journal of the National Cancer Institute, 96,* 1769-1780.

Liu, W., Guo, Q.L., You, Q.D., Zhao, L., Gu, H.Y., & Yuan, S.T. (2005a). Anticancer effect and apoptosis induction of gambogic acid in human gastric cancer line BGC-823. *World Journal of Gastroenterology, 11,* 3655-3659.

Liu, L., Ning, Z.Q., Shan, S., Zhang, K., Deng, T., Lu, X.P., & Cheng, Y.Y. (2005b). Phthalide lactones from *Ligusticum chuanxiong* inhibit lipopolysaccharide-induced TNF-alpha production and TNF-alpha-mediated NF-kappaB activation. *Planta Medica, 71,* 808-813.

Liu, X., Lazenby, A.J., & Siegal, G.P. (2006). Signal transduction cross-talk during colorectal tumorigenesis. *Advances in Anatomic Pathology, 13,* 270-274.

Liu, X., Bian, C., Ren, K., Jin, H., Li, B., & Shao, R.G. (2007). Lidamycin induces marked G2 cell

cycle arrest in human colon carcinoma HT-29 cells through activation of p38 MAPK pathway. *Oncology Reports, 17,* 597-603.

Loda, M., Cukor, B., Tam, S.W., Lavin, P., Fiorentino, M., Draetta, G.F., Jessup, J.M., & Pagano, M. (1997). Increased proteasome-dependent degradation of the cyclin-dependent kinase inhibitor p27 in aggressive colorectal carcinomas. *Nature Medicine, 3,* 231-234.

Longley, D.B., Harkin, D.P., & Johnston, P.G. (2003). 5-Fluorouracil: Mechanisms of action and clinical strategies. *Nature Reviews. Cancer 3,* 330-338.

Longley, D.B., Wilson, T.R., McEwan, M., Allen, W.L., McDermott, U., Galligan, L., & Johnston, P.G. (2006). c-FLIP inhibits chemotherapy-induced colorectal cancer cell death. *Oncogene, 25,* 838-848.

Love, J.J., Li, X., Case, D.A., Giese, K., Grosschedl, R., & Wright, P.E. (1995). Structural basis for DNA bending by the architectural transcription factor LEF-1. *Nature, 376,* 791-795.

Low Dog, T. (2005). Menopause: a review of botanical dietary supplements. *The American Journal of Medicine, 118,* 98-108.

Lu, Q., Qiu, T.Q., & Yang, H. (2006). Ligustilide inhibits vascular smooth muscle cells proliferation. *European Journal of Pharmacology, 542,* 136-140.

Lu, N., Yang, Y., You, Q.D., Ling, Y., Gao, Y., Gu, H.Y., Zhao, L., Wang, X.T., & Guo, Q.L. (2007). Gambogic acid inhibits angiogenesis through suppressing vascular endothelial growth factor-induced tyrosine phosphorylation of KDR/Flk-1. *Cancer Letters, 258,* 80-89.

Mahalingam, D., Keane, M., Pirianov, G., Mehmet, H., Samali, A., & Szegezdi, E. (2009). Differential activation of JNK1 isoforms by TRAIL receptors modulate apoptosis of colon cancer cell lines. *British Journal of Cancer, 100,* 1415-1424.

Mak, D.H., Chiu, P.Y., Dong, T.T., Tsim, K.W., & Ko, K.M. (2006). Dang-Gui Buxue Tang produces a more potent cardioprotective effect than its component herb extracts and enhances glutathione status in rat heart mitochondria and erythrocytes. *Phytotherapy Research, 20,* 561-567.

Malemud, C.J. (2007). Inhibitors of stress-activated protein/mitogen-activated protein kinase pathways. *Current Opinions in Pharmacology, 7,* 1-5.

Malumbres, M., & Barbacid, M. (2003). RAS oncogenes: the first 30 years. *Nature Reviews. Cancer,*

3, 459-465.

Mansouri, A., Ridgway, L.D., Korapati, A.L., Zhang, Q., Tian, L., Wang, Y., Siddik, Z.H., Mills, G.B., & Claret, F.X. (2003). Sustained activation of JNK/p38 MAPK pathways in response to cisplatin leads to Fas ligand induction and cell death in ovarian carcinoma cells. *The Journal of Biological Chemistry, 278,* 19245-19256.

Martin, C., Connelly, A., Keku, T.O., Mountcastle, S.B., Galanko, J., Woosley, J.T., Schliebe, B., Lund, P.K., & Sandler, R.S. (2002). Nonsteroidal anti-inflammatory drugs, apoptosis, and colorectal adenomas. *Gastroenterology, 123,* 1770-1777.

Matsumoto, K., Akao, Y., Kobayashi, E., Ito, T., Ohguchi, K., Tanaka, T., Iinuma, M., & Nozawa, Y. (2003). Cytotoxic benzophenone derivatives from *Garcinia* species display a strong apoptosis-inducing effect against human leukemia cell lines. *Biological & Pharmaceutical Bulletin, 26,* 569-571.

Matsumoto, K., Akao, Y., Yi, H., Ohguchi, K., Ito, T., Tanaka, T., Kobayashi, E., Iinuma, M., & Nozawa, Y. (2004). Preferential target is mitochondria in alpha-mangostin-induced apoptosis in human leukemia HL60 cells. *Bioorganic & Medicinal Chemistry, 12,* 5799-5806.

Matsumoto, K., Akao, Y., Ohguchi, K., Ito, T., Tanaka, T., Iinuma, M., & Nozawa, Y. (2005). Xanthones induce cell-cycle arrest and apoptosis in human colon cancer DLD-1 cells. *Bioorganic & Medicinal Chemistry, 13,* 6064-6069.

Matuo, R., Sousa, F.G., Escargueil, A.E., Grivicich, I., Garcia-Santos, D., Chies, J.A., Saffi, J., Larsen, A.K., & Henriques, J.A. (2009). 5-Fluorouracil and its active metabolite FdUMP cause DNA damage in human SW620 colon adenocarcinoma cell line. *Journal of Applied Toxicology, 29,* 308-316.

Mayo, L.D., & Donner, D.B. (2001). A phosphatidylinositol 3-kinase/Akt pathway promotes translocation of Mdm2 from the cytoplasm to the nucleus. *Proceedings of the National Academy of Sciences of the United States of America, 98,* 11598-11603.

Mayo, C., & Mayol, X. (2009). Cyclin D1 negatively regulates the expression of differentiation genes in HT-29 M6 mucus-secreting colon cancer cells. *Cancer Letters, 281,* 183-187.

McA'Nulty, M.M., Whitehead, J.P., & Lippard, S.J. (1996). Binding of Ixr1, a yeast HMG-domain protein, to cisplatin-DNA adducts *in vitro* and *in vivo*. *Biochemistry, 35,* 6089-6099.

Melino, G., De Laurenzi, V., & Vousden, K.H. (2002). P73: friend or foe in tumorigenesis. *Nature Reviews. Cancer, 2,* 605-615.

Melino, G., Bernassola, F., Ranalli, M., Yee, K., Zong, W.K., Corazzari, M., Knight, R.A., Green, D.R., Thompson, C., & Vousden, K.H. (2004). p73 induces apoptosis via PUMA transactivation and Bax mitochondrial translocation. *The Jounal of Biological Chemistry, 279,* 8076-8083.

Meyer, J.P., & Gillatt, D.A. (2002). PC-SPES: a herbal therapy for the treatment of hormone refractory prostate cancer. *Prostate Cancer and Prostatic Diseases, 5,* 13-15.

Micheau, O., Solary, E., Hammann, A., & Dimanche-Boitrel, M.T. (1999). Fas ligand-independent, FADD-mediated activation of the Fas death pathway by anticancer drugs. *Journal of Biological Chemistry, 274,* 7987-7992.

Mitomi, H., Fukui, N., Tanaka, N., Kanazawa, H., Saito, T., Matsuoka, T., & Yao, T. (2010). Aberrant p16INK4a methylation is a frequent event in colorectal cancers: prognostic value and relation to mRNA expression and immunoreactivity. *Journal of Cancer Research and Clinical Oncology, 136,* 323-331.

Moggs, J.G., Szymkowski, D.E., Yamada, M., Karran, P., & Wood, R.D. (1997). Differential human nucleotide excision repair of paired and mispaired cisplatin-DNA adducts. *Nucleic Acids Research, 25,* 480-491.

Mok, T.S., Yeo, W., Johnson, P.J., Hui, P., Ho, W.M., Lam, K.C., Xu, M., Chak, K., Chan, A., Wong, H., Mo, F., & Zee, B. (2007). A double-blind placebo-controlled randomized study of Chinese herbal medicine as complementary therapy for reduction of chemotherapy-induced toxicity. *Annals of Oncology, 18,* 768-774.

Montorsi, M., Maggioni, M., Falleni, M., Pellegrini, C., Donadon, M., Torzilli, G., Santambrogio, R., Spinelli, A., Coggi, G., & Bosari, S. (2007). Survivin gene expression in chronic liver disease and hepatocellular carcinoma. *Hepatogastroenterology, 54,* 2040-2044.

Morgan, D.O. (1995). Principles of CDK regulation. *Nature, 374,* 131-134.

Mu, R., Lu, N., Wang, J., Yin, Y., Ding, Y., Zhang, X., Gui, H., Sun, Q., Duan, H., Zhang, L., Zhang, Y., Ke, X., & Guo, Q. (2010). An oxidative analogue of gambogic acid-induced apoptosis of human hepatocellular carcinoma cell line HepG2 is involved in its anticancer activity *in vitro*. *European Journal of Cancer Prevention, 19,* 61-67.

Muller, M., Strand, S., Hug, H., Heinemann, E.M., Walczak, H., Hofmann, W.J., Stremmel, W., Krammer, P.H., & Galle, P.R. (1997). Drug-induced apoptosis in hepatoma cells is mediated by the CD95 (APO-1/Fas) receptor/ligand system and involves activation of wild-type p53. *The Journal of Clinical Investigation, 99,* 403-413.

Muller, M., Wilder, S., Bannasch, D., Israeli, D., Lehlbach, K., Li-Weber, M., Friedman, S.L., Galle, P.R., Stremmel, W., Oren, M., & Krammer, P.H. (1998). P53 activates the CD95 (APO-1/Fas) gene in response to DNA damage by anticancer drugs. *The Journal of Experimental Medicine, 188,* 2033-2045.

Muscarella, D.E., & Bloom, S.E. (2008). The contribution of c-Jun N-terminal kinase activation and subsequent Bcl-2 phosphorylation to apoptosis induction in human B-cells is dependent on the mode of action of specific stresses. *Toxicology and Applied Pharmacology, 228,* 93-104.

Na, Y. (2009). Recent cancer drug development with xanthone structures. *Journal of Pharmacy and Pharmacology, 61,* 707-712.

Nagahara, H., Mimori, K., Ohta, M., Utsunomiya, T., Inoue, H., Barnard, G.F., Ohira, M., Hirakawa, K., & Mori, M. (2005). Somatic mutations of epidermal growth factor receptor in colorectal carcinoma. *Clinical Cancer Research, 11,* 1368-1371.

Nakayama, K., Ishida, N., Shirane, M., Inomata, A., Inoue, T., Shishido, N., Horii, I., Loh, D.Y., & Nakayama, K. (1996). Mice lacking p27Kip1 display increased body size, multiple organ hyperplasia, retinal dysplasia and, pituitary tumors. *Cell, 31,* 707-720.

Nehme, A., Baskaran, R., Aebi, S., Fink, D., Nebel, S., Cenni, B., Wang, J.Y., Howell, S., & Christen, R.D. (1997). Differential induction of c-Jun NH2-terminal kinase and c-Abl kinase in DNA mismatch repair-proficient and –deficient cells explosed to cisplatin. *Cancer Research, 57,* 3253-3257.

Nguyen, D.M., & Hussain, M. (2007). The role of the mitochondria in mediating cytotoxicity of anti-cancer therapies. *Journal of Bioenergetics and Biomembranes, 39,* 13-21.

Nie, F., Zhang, X., Qi, Q., Yang, L., Yang, Y., Liu, W., Lu, N., Wu, Z., You, Q., & Guo, Q. (2009). Reactive oxygen species accumulation contributes to gambogic acid-induced apoptosis in human hepatoma SMMC-7721 cells. *Toxicology, 260,* 60-67.

Nita, M.E., Nagawa, H., Tominaga, O., Tsuno, N., Fujii, S., Sasaki, S., Fu, C.G., Takenoue, T., Tsuruo, T., & Muto, T. (1998). 5-fluorouracil induces apoptosis in human colon cancer cell lines with

modulation of Bcl-2 family proteins. *British Journal of Cancer, 78,* 986-992.

Noordhuis, P., Holwerda, U., Van der Wilt, C.L., Van Groeningen, C.J., Smid, K., Meijer, S., Pinedo, H.M., & Peters, G.J. (2004). 5-Fluorouracil incorporation into RNA and DNA in relation to thymidylate synthase inhibition of human colorectal cancers. *Annals of Oncology, 15,* 1025-1032.

Nunes, I.S., Faria, J.M., Figueiredo, A.C., Pedro, L.G., Trindade, H., Barroso, J.G. (2009). Menthol and geraniol biotransformation and glycosylation capacity of *Levisticum officinal* hairy roots. *Planta Medica, 75,* 387-391.

Obolskiy, D., Pischel, I., Siriwatanametanon, N., & Heinrich, M. (2009). *Garcinia mangostana* L.: a phytochemical and pharmacological review. *Phytotherapy Research, 23,* 1047-1065.

O' Connell, J., Bennett, M.W., Nally, K., Houston, A., O'Sullivan, G.C., & Shanahan, F. (2000). Altered mechanisms of apoptosis in colon cancer: Fas resistance and counterattack in the tumor-immune conflict. *Annals of the New York Academy of Sciences, 910,* 178-195.

Oh, W.K., Kantoff, P.W., Weinberg, V., Jones, G., Rini, B.L., Derynck, M.K., Bok, R., Smith, M.R., Bubley, G.J., Rosen, R.T., DiPaola, R.S., & Small, E.J. (2004). Prospective, multicenter, randomized Phase II trial of the herbal supplement, PC-SPES, and diethylstilbestrol in patients with androgen-independent prostate cancer. *Journal of Clinical Oncology, 22,* 3705-3712.

Oh, J.E., Kim, M.S. Ahn, C.H., Kim, S.S., Han, J.Y., Lee, S.H., & Yoo, N.J. (2010). Mutational analysis of CASP10 gene in colon, breast, lung and hepatocellular carcinomas. *Pathology, 42,* 73-76.

Okamaoto, M., Ohsato, T., Nakada, K., Isobe, K., Spelbrink, J.N., Hayashi, J., Hamasaki, N., & Kang, D. (2003). Ditercalinium chloride, a pro-anticancer drug, intimately associates with mammalian mitochondrial DNA and inhibits its replication. *Current Genetics, 43,* 364-370.

Olszewski, U., & Hamilton, G. (2010). A better platinum-based anticancer drug yet to come? *Anti-cancer Agents in Medicinal Chemistry, 10,* 293-301.

Otto, A.M., Paddenberg, R., Schubert, S., & Mannherz, H.G. (1996). Cell-cycle arrest, micronucleus formation and cell death in growth inhibition of MCF-7 breast cancer cells by tamoxifen and cisplatin. *Journal of Cancer Research and Clinical Oncology, 122,* 603-612.

Ozer, J., Ratner, M., Shaw, M., Bailey, W., & Schomaker, S. (2008). The current state of serum biomarkers of hepatotoxicity. *Toxicology, 245,* 194-205.

Pagano, M., Tam, S.W., Theodoras, A.M., Beer-Romero, P., Del Sal, G., Chau, V., Yew, P.R., Draetta, G.F., & Rolfe, M. (1995). Role of the ubiquitin-proteasome pathway in regulating abundance of the cyclin-dependent kinase inhibitor p27. *Science, 269,* 682-685.

Pan, M.H., Chang, W.L., Lin-Shiau, S.Y., Ho, C.T., & Lin, J.K. (2001). Induction of apoptosis by garcinol and curcumin through cytochrome *c* release and activation of caspases in human leukemia HL-60 cells. *Journal of Agricultural and Food Chemistry, 49,* 1464-1474.

Pandey, M.K., Sung, B., Ahn, K.S., Kunnumakkara, A.B., Chaturvedi, M.M., & Aggarwal, B.B. (2007). Gambogic acid, a novel ligand for transferrin receptor, potentiates TNF-induced apoptosis through modulation of the nuclear factor-kappaB signaling pathway. *Blood, 110,* 3517-3525.

Panthong, A., Norkaew, P., Kanjanapothi, D., Taesotikul, T., Anantachoke, N., & Reutrakul, V. (2007). Anti-inflammatory, analgesic and antipyretic activities of extract of gamboges from *Garcinia hanburyi* Hook f. *Journal of Ethnopharmacology, 111,* 335-340.

Pedraza-Chaverri, Cardenas-Rodriguez, Orozco-Ibarra, & Perez-Rojas, J.M. (2008). Medicinal properties of mangosteen (*Garcinia mangostana*). *Food and Chemical Toxicology, 46,* 3227-3239.

Penaloza, C., Lin, L., Lockshin, R.A., & Zakeri, Z. (2006). Cell death in development: shaping the embryo. *Histochemistry and Cell Biology, 126,* 149-158.

Peng, H.Y., Du, J.R., Zhang, G.Y., Kuang, X., Liu, Y.X., Qian, Z.M., & Wang, C.Y. (2007). Neuroprotective effect of *z*-ligustilide against permanent focal ischemic damage in rats. *Biological & Pharmaceutical Bulletin, 30,* 309-312.

Persons, D.L., Yazlovitskaya, E.M., & Pelling, J.C. (2000). Effect of extracellular signal-regulated kinase on p53 accumulation in response to cisplatin. *The Journal of Biological Chemistry, 275,* 35778-35785.

Philp, A.J., Campbell, I.G., Leet, C., Vincan, E., Rockman, S.P., Whitehead, R.H., Thomas, R.J., Phillips, W.A. The phosphatidylinositol 3-kinase p85alpha gene is an oncogene in human ovarian and colon tumors. *Cancer Research, 61,* 7426-7429.

Piao, X.L., Park, J.H., Cui, J., Kim, D.H., & Yoo, H.H. (2007). Development of gas chromatographic/mass spectrometry-pattern recognition method for the quality control of Korean *Angelica*. *Journal of Pharmaceutical and Biomedical Analysis, 44,* 1163-1167.

Piersen, C.E. (2003). Phytoestrogens in botanical dietary supplements: implications for cancer. *Integrative Cancer Therapies, 2,* 120-138.

Pitti, R.M., Marsters, S.A., Lawrence, D.A., Roy, M., Kischkel, F.C., Dowd, P., Huang, A., Donahue, C.J., Sherwood, S.W., Baldwin, D.T., Godowski, P.J., Wood, W.I., Gurney, A.L., Hillan, K.J., Cohen, R.L., Goddard, A.D., Botstein, D., & Ashkenazi, A. (1998). Genomic amplification of a decoy receptor for Fas ligand in lung and colon cancer. *Nature, 396,* 699-703.

Polyak, K., Li., Y., Zhu, H., Lengauer, C., Willson, J.K., Markowitz, S.D., Trush, M.A., Kinzler, K.W., & Vogelstein, B. (1998). Somatic mutations of the mitochondrial genome in human colorectal cancers. *Nature Genetics, 20,* 291-293.

Prasad, S., Ravindran, J., Sung, B., Pandey, M.K., & Aggarwal, B.B. (2010). Garcinol potentiates TRAIL-induced apoptosis through modulation of death receptors and antiapoptotic proteins. *Molecular Cancer Therapeutics, 9,* 856-868.

Protiva, P., Hopkins, M.E., Baggett, S., Yang, H., Lipkin, M., Holt, P.R., Kennelly, E.J., & Bernard, W.I. (2008). Growth inhibition of colon cancer cells by polyisoprenylated benzophenones is associated with induction of the endoplasmic reticulum response. *International Journal of Cancer, 123,* 687-694.

Qi, Q., Gu, H., Yang, Y., Lu, N., Zhao, J., Liu, W., Ling, H., You, Q.D., Wang, X., Guo, Q. (2008a). Involvement of matrix metalloproteinases 2 and 9 in gambogic acid induced suppression of MDA-MB-435 human breast carcinoma cell lung metastasis. *Journal of Molecular Medicine, 86,* 1367-1377.

Qi, Q., Lu, N., Wang, X.T., Gu, H.Y., Yang, Y., Liu, W., Li, C., You, Q.D., & Guo, Q.L. (2008b). Anti-invasive effect of gambogic acid in MDA-MB-231 human breast carcinoma cells. *Biochemistry and Cell Biology, 86,* 386-395.

Qi, Q., You, Q., Gu, H., Zhao, L., Liu, W., Lu, N., & Guo, Q. (2008c). Studies on the toxicity of gambogic acid in rats. *Journal of Ethnopharmacology, 117,* 433-438.

Qiang, L., Yang, Y., You, Q.D., Ma, Y.J., Yang, L., Nie, F.F., Gu, H.Y., Zhao, L., Lu, N., Qi, Q., Liu, W., Wang, X.T., & Guo, Q.L. (2008). Inhibition of glioblastoma growth and angiogenesis by gambogic acid: an *in vitro* and *in vivo* study. *iochemical Pharmacology, 75,* 1083-1092.

Raitano, A.B., Halpern, J.R., Hambuch, T.M., & Sawyers, C.L. (1995). The Bcr-Abl leukemia

oncogene activates Jun kinase and requires Jun for transformation. *Proceedings of the National Academy of Sciences of the United States of America, 92,* 11746-11750.

Reutrakul, V., Anantachoke, N., Pohmakotr, M., Jaipetch, T., Sophasan, S., Yoosook, C., Kasisit, J., Napaswat, C., Santisuk, T., & Tuchinda, P. (2007). Cytotoxic and anti-HIV caged xanthones from the resin and fruits of *Garcinia hanburyi. Planta Medica, 73,* 33-40.

Riese, M.J., & Vaughn, D.J. (2009). Chemotherapy for patients with poor prognosis germ cell tumors. *World Journal of Urology, 27,* 471-476.

Rock, E., & DeMichele, A. (2003). Nutritional approaches to late toxicities of adjuvant chemotherapy in breast cancer survivors. *The Journal of Nutrition, 133,* 3785S-3793S.

Rodrigues, G.A., Park, M., & Schlessinger, J. (1997). Activation of the JNK pathway is essential for transformation by the Met oncogene. *The EMBO Journal, 16,* 2634-2645.

Romashkova, J.A., & Makarov, S.S. (1999). NF-kappaB is a target of AKT in anti-apoptotic PDGF signaling. *Nature, 401,* 86-90.

Rong, J.J., Hu, R., Qi, Q., Gu, H.Y., Zhao, Q., Wang, J., Mu, R., You, Q.D., & Guo, Q.L. (2009). Gambogic acid down-regulates MDM2 oncogene and induces $p21^{Waf1/CIP1}$ expression independent of p53. *Cancer Letters, 284,* 102-112.

Roos, W.P., & Kaina, B. (2006). DNA damage-induced cell death by apoptosis. *Trends in Molecular Medicine, 12,* 440-450.

Rosner, M.H. (2009). Urinary biomarkers for the detection of renal injury. *Advances in Clinical Chemistry, 49,* 73-97.

Rouleau, M., Patel, A., Hendzel, M.J., Kaufmann, S.H., & Poirier, G.G. (2010). PARP inhibition: PARP1 and beyond. *Nature Reviews. Cancer, 10,* 293-301.

Roy, S., & Nicholson, D.W. (2000). Cross-talk in cell death signaling. *The Journal of Experimental Medicine, 192,* F21-25.

Ruan, W.J., Lai, M.D., & Zhou, J.G. (2006). Anticancer effects of Chinese herbal medicine, science or myth? *Journal of Zhejiang University. Science. B., 7,* 1006-1014.

Rukachaisirikul, V., Phainuphong, P., Sukpondma, Y., Phongpaichit, S., & Taylor, W.C. (2005). Antibacterial caged-tetraprenylated xanthones from the stem bark of *Garcinia scortechinii. Planta Medica, 71,* 165-170.
34.

Russell, L., Hicks, G.S., Low, A.K., Shepherd, J.M., & Brown, C.A. (2002). Phytoestrogens: a viable option? *The American Journal of the Medical Sciences, 324,* 185-188.

Sadava, D., Ahn, J., Zhan, M., Pang, M.L., Ding, J., & Kane, S.E. (2002). Effects of four Chinese herbal extracts on drug-sensitive and multidrug-resistant small-cell lung carcinoma cells. *Cancer Chemotherapy and Pharmacology, 49,* 261-266.

Saif, M.W., Lansigan, F., Ruta, S., Lamb, L., Mezes, M., Elligers, K., Grant, N., Jiang, Z.L., Liu, S.H., & Cheng, Y.C. (2010). Phase I study of the botanical formulation PHY906 with capecitabine in advanced pancreatic and other gastrointestinal malignancies. *Phytomedicine, 17,* 161-169.

Saleh, H.A., Jackson, H., & Banerjee, M. (2000). Immunohistochemical expression of bcl-2 and p53 oncoproteins: correlation with Ki67 proliferation index and prognostic histopathologic parameters in colorectal neoplasia. *Applied Immunohistochemistry & Molecular Morphology, 8,* 175-182.

Sampath, P.D., & Kannan, V. (2009). Mitigation of mitochondrial dysfunction and regulation of eNOS expression during experimental myocardial necrosis by alpha-mangostin, a xanthonic derivative from *Garcinia mangostana. Drug and Chemical Toxicology, 32,* 344-352.

Sanchez-Prieto, R., Rojas, J.M., Taya, Y., & Gutkind, J.S. (2000). A role for the p38 mitogen-activated protein kinase pathway in the transcriptional activation of p53 on genotoxic stress by chemotherapeutic agents. *Cancer Research, 60,* 2464-2472.

Sarela, A.I., Scott, N., Ramsdale, J., Markham, A.F., & Guillou, P.J. (2001). Immunohistochemical detection of the anti-apoptosis protein, surviving, predicts survival after curative resection of stage II colorectal carcinomas. *Annals of Surgical Oncology, 8,* 305-310.

Schubbert, S., Shannon, K., & Bollag, G. (2007). Hyperactive Ras in developmental disorders and cancer. *Nature Reviews. Cancer, 7,* 295-308.
Sebolt-Leopold, J.S. (2000). Development of anticancer drugs targeting the MAPK pathway. *Oncogene, 19,* 6594-6599.

Sedletska, Y., Giraud-Panis, M.J., & Malinge, J.M. (2005). Cisplatin is a DNA-damaging antitumor

compound triggering multifactorial biochemical responses in cancer cells: importance of apoptotic pathways. *Current Medicinal Chemistry, 5,* 251-265.

Seimiya, H., Mashima, T., Toho, M., & Tsuruo, T. (1997). c-Jun NH2-terminal kinase-mediated activation of interleukin-1beta converting enzyme/CED-3-like protease during anticancer drug-induced apoptosis. *The Journal of Biological Chemistry, 272,* 4631-4636.

Seitz, H.K., & Becker, P. (2007). Alcohol metabolism and cancer risk. *Alcohol Research & Health, 30,* 38-41, 44-47.

Senderowicz, A.M. (2003). Small-molecule cyclin-dependent kinase modulators. *Oncogene, 22,* 6609-6620.

Shah, N., & Dizon, D.S. (2009). New-generation platinum agents for solid tumors. *Future Oncology, 5,* 33-42.

Sheaff, R.J., Groudine, M., Gordon, M., Roberts, J.M., & Clurman, B.E. (1997). Cyclin E-CDK2 is a regulator of p27Kip1. *Genes & Development, 11,* 1464-1478.

Sherr, C.J., & Roberts, J.M. (1999). CDK inhibitors: positive and negative regulators of G1-phase progression. *Genes & Development, 13,* 1501-1512.

Shiah, S.G., Chuang, S.E., & Kuo, M.L. (2001) Involvement of Asp-Glu-Val-Asp-directed, caspase-mediated mitogen-activated protein kinase kinase I cleavage, c-Jun N-terminal kinase activation, and subsequent Bcl-2 phosphorylation for paclitaxel-indcued apoptosis in HL-60 cells. *Molecular Pharmacology, 59,* 254-262.

Shang, P., Qian, A.R., Yang, T.H., Jia, M., Mei, Q.B., Cho, C.H., Zhao, W.M., & Chen, Z.N. (2003). Experimental study of anti-tumor effects of polysaccharides from *Angelica sinensis*. *World Journal of Gastroenterology, 9,* 1963-1967.

Sharif, S., O'Connell, M.J., Yothers, G., Lopa, S., & Wolmark, N. (2008). FOLFOX and FLOX regimens for the adjuvant treatment of resected stage II and stage III colon cancer. *Cancer Investigation, 26,* 956-963.

She, Q.B., Ma, W.Y., & Dong, Z. (2002). Role of MAP kinases in UVB-induced phosphorylation of p53 at serine 20. *Oncogene, 21,* 1580-1589.

Shen, A.Y., Wang, T.S., Huang, M.H., Liao, C.H., Chen, S.J., & Lin, C.C. (2005). Antioxidant and

antiplatelent effects on Dang-Gui-Shao-Yao-San on human blood cells. *The American Journal of Chinese Medicine, 33,* 747-758.

Shi, Y. (2006). Mechanical aspects of apoptosome assembly. *Current Opinion in Cell Biology, 18,* 677-684.

Shi, Y., He, L., & Wang. S. (2006). Determination of ligustilide in rat blood and tissues by capillary gas chromatography/mass spectrometry. *Biomedical Chromatography, 20,* 993-998.

Shimada, K., Nakamura, M., Ishida, E., Kishi, M., & Konishi, N. (2003). Roles of p-38 and c-jun NH2-terminal kinase-mediated pathways in 2-methoxyestradiol-induced p53 induction and apoptosis. *Carcinogenesis, 24,* 1067-1075.

Shtil, A.A., Mandlekar, S., Yu, R., Walter, R.J., Hagen, K., Tan, T.H., Roninson, I.B., & Kong, A.N. (1999). Differential regulation of mitogen-activated protein kinases by microtubule-binding agents in human breast cancer cells. *Oncogene, 18,* 377-384.

Singh, K.K., Russell, J., Sigala, B., Zhang, Y., Williams, J., & Keshav, K.F. (1999). Mitochondrial DNA determines the cellular response to cancer therapeutic agents. *Oncogene, 18,* 6641-6646.

Sinicrope, F.A., & Gill, S. (2004). Role of cyclooxygenase-2 in colorectal cancer. *Cancer Metastasis Reviews, 23,* 63-75.

Sinicrope, F.A. (2006). Targeting cyclooxygenase-2 for prevention and therapy of colorectal cancer. *Molecular Carcinogenesis, 45,* 447-454.

Slattery, M.L., Curtin, K., Wolff, R.K., Boucher, K.M., Sweeney, C., Edwards, S., Caan, B.J., Samowitz, W. (2009). A comparison of colon and rectal somatic DNA alterations. *Diseases of the colon and rectum, 52,* 1304-1311.

Sinha, D., Bannergee, S., Schwartz, J.H., Lieberthal, W., & Levine, J.S. (2004). Inhibition of ligand-independent ERK1/2 activity in kidney proximal tubular cells deprived of soluble survival factors up-regulates Akt and prevents apoptosis. *The Journal of Biological Chemistry, 279,* 10962010972.

Slee, E.A., Adrain, C., & Martin, S.J. (1999a). Serial killers: ordering caspase activation events in apoptosis. *Cell Death and Differentiation, 6,* 1067-1074.

Slee, E.A., Harte, M.T., Kluck, R.M., Wolf, B.B., Casiano, C.A., Newmeyer, D.D., Wang, H.G., Reed,

J.C., Nicholson, D.W., Alnemri, E.S., & Green, D.R., & Martin, S.J. (1999). Ordering the cytochrome c-initiated caspase cascade: hierarchical activation of caspases-2, -3, -6, -7, -8 and -10 in a caspase-9-dependent manner. *The Journal of Cell Biology, 144,* 281-292.

Small, E.J., Frohlich, M.W., Bok, R., Shinohara, K., Grossfeld, G., Rozenblat, Z., Kelly, W.K., Corry, M., & Reese, D.M. (2000). Prospective trial of the herbal supplement PC-SPES in patients with progressive prostate cancer. *Journal of Clinical Oncology, 18,* 3595-3603.

Soldani, C., & Scovassi, A.I. (2002). Poly(ADP-ribose) polymerase-1 cleavage during apoptosis: and update. *Apoptosis, 7,* 321-328.

Sovak, M., Seligson, A.L., Konas, M., Hajduch, M., Dolezal, M., Machala, M., & Nagourney, R. (2002). Herbal composition PC-SPES for management of prostate cancer: identification of active principles. *Journal of the National Cancer Institute, 94,* 1275-1281.

Sparber, A., Bauer, L., Curt, G., Eisenberg, D., Levin, T., Parks, S., Steinberg, S.M., Wootton, J. (2000). Use of complementary medicine by adult patients participating in cancer clinical trials. *Oncology Nursing Forum, 27,* 623-630.

Srivastava, R.K., Mi, Q.S., Hardwick, J.M., & Longo, D.L. (1999). Deletion of the loop region of Bcl-2 completely blocks paclitaxel-induced apoptosis. *Proceedings of the National Academy of Sciences of the United States of America, 96,* 3775-3780.

Stone, A.A., & Chambers, T.C. (2000). Microtubule inhibitors elicit differential effects on MAP kinase (JNK, ERK and p38) signaling pathways in human KB-3 carcinoma cells. *Experimental Cell Research, 254,* 110-119.

Sun, S.Y. (2005). Chemopreventive agent-induced modulation of death receptors. *Apoptosis, 10,* 1203-1210.

Sun, Y., Tang, J., Gu, X., & Li, D. (2005). Water-soluble polysaccharides from *Angelica sinensis* (Oliv.) Diels: preparation, characterization and bioactivity. *International Journal of Biological Macromolecules, 36,* 283-289.

Sung, J.J., Lau, J.Y., Young, J.P., Sano, Y., Chiu, H.M., Byeon, J.S., Yeoh, K.G., Goh, K.L., Sollano, J., Rerknimitr, R., Matsuda, T., Wu, K.C., Ng, S., Leung, S.Y., Makharia, G., Chong, V.H., Ho, K.Y., Brooks, B., Lieberman, D.A., & Chan, F.K. (2008). Asia Pacific consensus recommendations for colorectal cancer screening. *Gut, 57,* 1166-1176.

Tait, S.W., & Green, D.R. (2008). Caspase-independent cell death: leaving the set without the final cut. *Oncogene, 27,* 6452-6461.

Takahara, P.M., Rosenweig, A.C., Frederick, C.A., & Lippard, S.J. (1995). Crystal structure of double-stranded DNA containing the major adduct of the anticancer drug cisplatin. *Nature, 377,* 649-652.

Tang, J.C., Zhang, J.N., Wu, Y.T., & Li, Z.X. (2006). Effect of the water extract and ethanol extract from traditional Chinese medicines *Angelica sinensis* (Oliv.) Diels, *Ligusticum chuanxiong* Hort. And *Rheum palmatum* L. on rat liver cytochrome P450 activity. *Phytotherapy Research, 20,* 1046-1051.

Tao, Z., Zhao, Y., Lu, J., Duan, W., Qin, Y., He, X., Lin, L., & Ding, J. (2007). Caspase-8 preferentially senses the apoptosis-inducing action of NG-18, a gambogic acid derivative, in human leukemia HL-60 cells. *Cancer Biology & Therapy, 6,* 691-696.

Terzic, J., Grivennikov, S., Karin, E., & Karin, M. (2010). Inflammation and colon cancer. *Gastroenterology, 138,* 2101-2114.

Thomas, G.V., Szigeti, K., Murphy, M., Draetta, G., Pagano, M., & Loda, M. (1998). Down-regulation of p27 is associated with development of colorectal adenocarcinoma metastases. *The American Journal of Pathology, 153,* 681-687.

Tianniam, S., Bamba, T., & Fukusaki, E. (2009). Non-targeted metabolite fingerprinting of oriental folk medicine *Angelica acutiloba* roots by ultra performance liquid chromatography time-of-flight mass spectrometry. *Journal of Separation Science, 32,* 2233-2244.

Timofeev, O., Lee, T.Y., & Bulavin, D.V. (2005). A subtle change in p38 activity is sufficient to suppress in vivo tumorigenesis. *Cell Cycle, 4,* 118-120.

Treiber, D.K., Zhai, X., Jantzen, H.M., & Essigmann, J.M. (1994). Cisplatin-DNA adducts are molecular decoys for the ribosomal RNA transcription factor hUBF (human upstream binding factor). *Proceedings of the National Academy of Sciences of the United States of America, 91,* 5672-5676.

Triantafillidis, J.K., Nasioulas, G., & Kosmidis, P.A. (2009). Colorectal cancer and inflammatory bowel disease: epidemiology, risk factors, mechanisms of carcinogenesis and prevention strategies. *Anticancer Research, 29,* 2727-2737.

Tsai, N.M., Lin, S.Z., Lee, C.C., Chen, S.P., Su, H.C., Chang, W.L., & Harn, H.J. (2005). The

antitumor effects of *Angelica sinensis* on malignant brain tumors *in vitro* and *in vivo*. *Clinical Cancer Research, 11,* 3475-3484.

Tsai, N.M., Chen, Y.L., Lee, C.C., Lin, P.C., Cheng, Y.L., Chang, W.L., Lin, S.Z., & Harn, H.J. (2006). The natural compound *n*-butylidenephthalide derived from *Angelica sinensis* inhibits malignant brain tumor growth *in vitro* and *in vivo*. *Journal of Neurochemistry, 99,* 1251-1262.

Tsang, R.Y., Al-Fayea, T., & Au, H.J. (2009). Cisplatin overdose: toxicities and management. *Drug Safety, 32,* 1109-1122.

Tschopp, J., Irmler, M., & Thome, M. (1998). Inhibition of Fas death signals by FLIPs. *Current Opinion in Immunology, 10,* 552-558.

Upton, R. (2003). American Herbal Pharmacopoeia and Therapeutic Compendium: Dang Gui Root – *Angelica sinensis* (Oliv.) Diels. Scotts Valley, CA. 1-40.

Van Geelen, C.M., de Vries, E.G., & de Jong, S. (2004). Lessons from TRAIL-resistance mechanisms in colorectal cancer cells: paving the road to patient-tailored therapy. *Drug Resistance Updates, 7,* 345-358.

Vichi, P., Coin, F., Renaud, J.P., Vermeulen, W., Hoeijmakers, J.H., Moras, D., & Egly, J.M. (1997). Cisplatin- and UV-damaged DNA lure the basal transcription factor TFIID/TBP. *The EMBO Journal, 16,* 7444-7456.

Vickers, A., & Zollman, C. (1999). ABC of complementary medicine: herbal medicine. *BMJ (Clinical Research ed.), 319,* 1050-1053.

Vickers, A. (2002). Botanical medicines for the treatment of cancer: rationale, overview of current data, and methodological considerations for Phase I and II trials. *Cancer Investigation, 20,* 1069-1079.

Viglietto, G., Motti, M.L., & Fusco, A. (2002). Understanding $p27^{kip1}$ Deregulation in cancer: downregulation or mislocalization? *Cell Cycle, 1,* 394-400.

Violette, S., Poulain, L., Dussaulx, E., Pepin, D., Faussat, A.M., Chambaz, J., Lacorte, J.M., Staedel, C. & Lesuffleur, T. (2002). Resistance of colon cancer cells to long-term 5-fluouracil exposure is correlated to the relative level of Bcl-2 and Bcl-X(L) in addition to Bax and p53 status. *International Journal of Cancer, 98,* 498-504.

Vivanco, I., & Sawyers, C.L. (2002). The phosphatidylinositol 3-kinase AKT pathway in human cancer. *Nature Reviews. Cancer, 2,* 489-501.

Wang, T.H., Wang, H.S., Ichijo, H., Giannakakou, P., Foster, J.S., Fojo, T., & Wimalasena, J. (1998). Microtubule-interfering agents activate c-Jun N-terminal kinase/stress-activated protein kinase through both Ras and apoptosis signal-regulating kinase pathways. *The Journal of Biological Chemistry, 273,* 4928-4936.

Wang, T.H., Popp, D.M., Wang, H.S., Saitoh, M., Mural, J.G., Henley, D.C., Ichijo, H., & Wimalasena, J. (1999). Microtubule dysfunction induced by paclitaxel initiates apoptosis through both c-Jun N-terminal kinase (JNK)-dependent and –independent pathways in ovarian cancer cells. *The Journal of Biological Chemistry, 274,* 8208-8216.

Wang, X., Martindale, J.L., & Holbrook, N.J. (2000). Requirement for ERK activation in cisplatin-induced apoptosis. *The Journal of Biological Chemistry, 275,* 39435-39443.

Wang, Q., Ding, F., Zhu, N., He, P., & Fang, Y. (2003). Determination of the compositions of polysaccharides from Chinese herbs by capillary zone electrophoresis with amperometric detection. *Biomedical Chromatography, 17,* 483-488.

Wang, Z.Q., Chen, X.C., Yang, G.Y., & Zhou, L.F. (2004). U0126 prevents ERK pathway phosphorylation and interleukin-1beta mRNA production after cerebral ischemia. *Chinese Medical Sciences Journal, 19,* 270-275.

Wang, Y.L., Liang, Y.Z., Chen, B.M., He, Y.K., Li, B.Y., Hu, Q.N. (2005). LC-DAD-APCI-MS-based screening and analysis of the absorption and metabolite components in plasma from a rabbit administered an oral solution of danggui. *Analytical and Bioanalytical Chemistry, 383,* 247-254.

Wang, P.P., Zhang, Y., Dai, L.Q., & Wang, K.P. (2007). Effect of *Angelica sinensis* polysaccharide-iron complex on iron deficiency anemia in rats. *Chinese Journal of Integrative Medicine, 13,* 297-300.

Wang, L.L., Li, Z.L., Song, D.D., Sun, L., Pei, Y.H., Jing, Y.K., & Hua, H.M. (2008a). Two novel triterpenoids with antiproliferative and apoptotic activities in human leukemia cells isolated from the resin of *Garcinia hanburyi. Planta Medica, 74,* 1735-1740.

Wang, Y., Chen, Y., Chen, Z., Wu, Q., Ke, W.J., & Wu, Q.L. (2008b). Gambogic acid induces death inducer-obliterator 1-mediated apoptosis in Jurkat T cells. *Acta Pharmacologica Sinica, 29,* 349-354.

Wang, T., Wei, J., Qian, X., Ding, Y., Yu, L., & Liu, B. (2008c). Gambogic acid, a potent inhibitor of survivin, reverses docetaxel resistance in gastric cancer cells. *Cancer Letters, 262,* 214-222.

Wang, J., Liu, W., Zhao, Q., Qi, Q., Lu, N., Yang, Y., Nei, F.F., Rong, J.J., You, Q.D., Guo, Q.L. (2009). Synergistic effect of 5-fluorouracil with gambogic acid on BGC-823 human gastric carcinoma. *Toxicology, 256,* 135-140.

Watanapokasin, R., Jarinthanan, F., Jerusalmi, A., Suksamram, S., Nakamura, Y., Sukseree, S., Uthaisang-Tanethpongtamb, W., Ratananukul, P., & Sano, T. (2010). Potential of xanthones from tropical fruit mangosteen as anti-cancer agents: caspase-dependent apoptosis induction *in vitro* and in mice. *Applied Biochemistry and Biotechnology, DOI: 10.1007/s12010-009-8903-6.*

Watzka, S.B., Rauscher-Potsch, I., Nierlich, P., Setinek, U., Kostler, W.J., Potschger, U., Muller, M.R., & Attems, J. (2010). Concordance between epidermal growth factor receptor status in primary non-small-cell lung cancer and metastases: a post-mortem study. *European Journal of Cardio-thoracic Surgery, 38,* 34-37.

Wei, C.W., Lin, C.C., Yu, Y.L., Lin, C.Y., Lin, P.C., Wu, M.T., Chen, C.J., Chang, W.L., Lin, S.Z., Chen, Y.L., & Harn, H.J. (2009). *n*-Butylidenephthalide induced apoptosis in the A549 human lung adenocarcinoma cell line by coupled down-regulation of AP-2α and telomerase activity. *Acta Pharmacologica Sinica, 30,* 1297-1306.

Weingarten, M.A., Zalmanovici, A., & Yaphe, J. (2008). Dietary calcium supplementation for preventing colorectal cancer and adenomatous polyps. *Cochrane Database of Systematic Reviews, 1,* CD003548.

Werner, M.H., Huth, J.R., Gronenborn, A.M., & Clore, G.M. (1995). Molecular basis of human 46X, Y sex reversal revealed from the three-dimensional solution structure of the human SRY-DNA complex. *Cell, 81,* 705-714.

West, N.J., Courtney, E.D., Poullis, A.P., & Leicester, R.J. (2009). Apoptosis in the colonic crypt, colorectal adenomata, and manipulation by chemoprevention. *Cancer Epidemiology, Biomarkers & Prevention, 18,* 1680-1687.

Weston, C.R., & Davis, R.J. (2002). The JNK signal transduction pathway. *Current Opinion in Genetics & Development, 12,* 14-21.

Wheate, N.J., Walker, S., Craig, G.E., & Oun, R. (2010). The status of platinum anticancer drugs in the

clinical and in clinical trials. *Dalton Transactions.*

Wilasrusmee, C., Kittur, S., Siddiqui, J., Bruch, D., Wilasrusmee, S., & Kittur, D.S. (2002a). *In vitro* immunomodulatory effects of ten commonly used herbs on murine lymphocytes. *The Journal of Alternative and Complementary Medicine,* 8, 467-475.

Wilasrusmee, C., Siddiqui, J., Bruch, D., Wilasrusmee, S., Kittur, S., & Kittur, D.S. (2002b). *In vitro* immunomodulatory effects of herbal products. *The American Surgeon, 68,* 860-864.

Wilkes, G.M. (2005). Therapeutic options in the management of colon cancer: 2005 update. *Clinical Journal of Oncology Nursing, 9,* 31-44.

Wong, V.K., Yu, L., & Cho, C.H. (2008). Protective effect of polysaccharides from *Angelica sinensis* on ulcerative colitis in rats. *Inflammopharmacology, 16,* 162-167.

Wu, G.S. (2004). The functional interactions between the p53 and MAPK signaling pathways. *Cancer Biology & Therapy, 3,* 156-161.

Wu, S.J., Ng, L.T., & Lin, C.C. (2004a). Antioxidant activities of some common ingredients of traditional Chinese medicine, *Angelica sinensis, Lycium barbarum* and *Poria cocos. Phytotherapy Research, 18,* 1008-1012.

Wu, Z.Q., Guo, Q.L., You, Q.D., Zhao, L., & Gu, H.Y. (2004b). Gambogic acid inhibits proliferation of human lung carcinoma SPC-A1 cells *in vivo* and *in vitro* and represses telomerase activity and telomerase reverse transcriptase mRNA expression in the cells. *Biological & Pharmaceutical Bulletin, 27,* 1769-1774.

Wu, W.K., Sung, J.J., Lee, C.W., Yu, J., & Cho, C.H. (2010). Cyclooxygenase-2 in tumorigenesis of gastrointestinal cancers: an update on the molecular mechanisms. *Cancer Letters, 295,* 7-16.

Wyllie, A.H., Beattie, G.J., & Hargreaves, A.D. (1981). Chromatin changes in apoptosis. *The Histochemical Journal, 13,* 681-692.

Xie, J. & Itzkowitz, S.H. (2008). Cancer in inflammatory bowel disease. *World Journal of Gastroenterology, 14,* 378-389.

Xie, H., Qin, Y.X., Zhou, Y.L., Tong, L.J., Lin, L.P., Geng, M.Y., Duan, W.H., & Ding, J. (2009). GA3, a gambogic acid derivative, exhibits potent antitumor activities *in vitro* via apoptosis-involved

mechanisms. *Acta Pharmacologica Sinica, 30,* 346-354.

Xin, Y.F., Zhou, G.L., Shen, M., Chen, Y.X., Liu, S.P., Chen, G.C., Chen, H., You, Z.Q., Xuan, Y.X. (2007). *Angelica sinensis*: a novel adjunct to prevent doxorubicin-induced chronic cardiotoxicity. *Basic & Clinical Pharmacology & Toxicology, 101,* 421-426.

Xu, G., Feng, C., Zhou, Y., Han, Q.B., Qiao, C.F., Huang, S.X., Chang, D.C., Zhao, Q.S., Luo, K.Q., & Xu, H.X. (2008). Bioassay and ultraperformance liquid chromatography/mass spectrometry guided isolation of apoptosis-inducing benzophenones and xanthone from the pericarp of *Garcinia yunnanensis* Hu. *Journal of Agricultural and Food Chemistry, 56,* 11144-11150.

Xu, X., Liu, Y., Wang, L., He, J., Zhang, H., Chen, X., Li, Y., Yang, J., & Tao, J. (2009). Gambogic acid induces apoptosis by regulating the expression of Bax and Bcl-2 and enhancing caspase-3 activity in human malignant melanoma A375 cells. *International Journal of Dermatology, 48,* 186-192.

Xu, G., Kan, W.L., Zhou, Y., Song, J.Z., Han, Q.B., Qiao, C.F., Cho, C.H., Rudd, J.A., Lin, G., & Hu, H.X. (2010). Cytotoxic acylphloroglucinol derivatives from the twigs of *Garcinia cowa. Journal of Natural Products, 73,* 104-108.

Xue, T., & Roy, R. (2003). Studying traditional Chinese medicine. *Science, 300,* 740-741.

Yagi, H., Yotsumoto, F., Sonoda, K., Kuroki, M., Mekada, E., & Miyamoto, S. (2009). Synergistic anti-tumor effect of paclitaxel with CRM197, an inhibitor of HB-EGF, in ovarian cancer. *International Journal of Cancer, 124,* 1429-1439.

Yan, R., Li, S.L., Chung, H.S., Tam, Y.K., & Lin, G. (2005). Simultaneous quantification of 12 bioactive components of *Ligusticum chuanxiong* Hort. By high-performance liquid chromatography. *Journal of Pharmaceutical and Biomedical Analysis, 37,* 87-95.

Yan, R., Ko, N.L., Li, S.L., Tam, Y.K., & Lin, G. (2008). Pharmacokinetics and metabolism of ligustilide, a major bioactive component in Rhizoma chuanxiong, in the rat. *Drug Metabolism and Disposition, 36,* 400-408.

Yang, E., Zha, J., Jockel, J., Boise, L.H., Thompson, C.B., & Korsmeyer, S.J. (1995). Bad, a heterodimeric partner for Bcl-XL and Bcl-2, displaces Bax and promotes cell death. *Cell, 80,* 285-291.

Yang, T., Jia, M., Meng, J., Wu, H., & Mei, Q. (2006). Immunomodulatory activity of polysaccharide isolated from *Angelica sinensis*. *International Journal of Biological Macromolecules, 39,* 179-184.

Yang, X., Zhao, Y., Zhou, Y., Lv., Y., Mao, J., & Zhao, P. (2007a). Component and antioxidant properties of polysaccharide fractions isolated from *Angelica sinensis* (OLIV.) DIELS. *Biological & Pharmaceutical Bulletin, 30,* 1884-1890.

Yang, X., Zhao, Y., Lv, Y., Yang, Y., & Ruan, Y. (2007b). Protective effect of polysaccharide fractions from *Radix A. sinensis* against *tert*-butylhydroperoxide induced oxidative injury in murine peritoneal macrophages. *Journal of Biochemistry and Molecular Biology, 40,* 928-935.

Yang, X., Zhao, Y., Wang, H., & Mei, Q. (2007c). Macrophage activation by an acidic polysaccharide isolated from *Angelica sinensis* (Oliv.) Diels. *Journal of Biochemistry and Molecular Biology, 40,* 636-643.

Yang, Y., Yang, L., You, Q.D., Nie, F.F., Gu, H.Y., Zhao, L., Wang, X.T., & Guo, Q.L. (2007d). Differential apoptotic induction of gambogic acid, a novel anticancer natural product, on hepatoma cells and normal hepatocytes. *Cancer Letters, 256,* 259-266.

Yarom, N., Marginean, C., Moyana, T., Gorn-Hondermann, I., Birnboim, H.C., Marginean, H., Auer, R.C., Vickers, M., Asmis, T.R., Maroun, J., & Jonker, D. (2010). EGFR expression variance in paired colorectal cancer primary and metastatic tumors. *Cancer Biology & Therapy, 10,* Epub

Ye, Y.N., Liu, E.S., Li, Y., So, H.L., Cho, C.C., Sheng, H.P., Lee, S.S., & Cho, C.H. (2001a). Protective effect of polysaccharides-enriched fraction from *Angelica sinensis* on hepatic injury. *Life Sciences, 69,* 637-646.

Ye, Y.N., Koo, M.W., Li, Y., Matsui, H., & Cho, C.H. (2001b). *Angelica sinensis* modulates migration and proliferation of gastric epithelial cells. *Life Sciences, 68,* 961-968.

Ye, Y.N., Liu, E.S., Shin, V.Y., Koo, M.W., Li, Y., Wei, E.Q., Matsui, H., & Cho, C.H. (2001c). A mechanistic study of proliferation induced by *Angelica sinensis* in a normal gastric epithelial cell line. *Biochemical Pharmacology, 61,* 1439-1448.

Ye, Y.N., So, H.L., Liu, E.S., Shin, V.Y., & Cho, C.H. (2003). Effect of polysaccharides from *Angelica sinensis* on gastric ulcer healing. *Life Sciences, 72,* 925-932.

Yen, Y., So, S., Rose, M., Saif, M.W., Chu, E., Liu, S.H., Foo, A., Jiang, Z., Su, T., & Cheng, Y.C. (2009). Phase I/II study of PHY906/capecitabine in advanced hepatocellular carcinoma. *Anticancer Research, 29,* 4083-4092.

Yi, T., Leung, K.S., Lu, G.H., Zhang, H., & Chan, K. (2005). Identification and comparative determination of senkyunolide A in traditional Chinese medicinal plants *Ligusticum chuanxiong* and *Angelica sinensis* by HPLC coupled with DAD and ESI-MS. *Chemical and Pharmaceutical Bulletin, 53,* 1480-1483.

Yi, T., Yi, Z., Cho, S.G., Luo, J., Pandey, M.K., Aggarwal, B.B., & Liu, M. (2008). Gambogic acid inhibits angiogenesis and prostrate tumor growth by suppressing vascular endothelial growth factor receptor-2 signaling. *Cancer Research, 68,* 1843-1850.

Yi, L., Liang, Y., Wu, H., & Yuan, D. (2009). The analysis of Radix *Angelicae Sinensis* (Danggui). *Journal of Chromatography A, 1216,* 1991-2001.

Yip, K.W., Reed, J.C. (2008). Bcl-2 family proteins and cancer. *Oncogene, 27,* 6398-6406.

Youle, R.J., & Strasser, A. (2008). The Bcl-2 protein family: opposing activities that mediate cell death. *Nature Reviews. Molecular Cell Biology, 9,* 47-59.

Yu, C., Wang, S., Dent, P., & Grant, S. (2001). Sequence-dependent potentiate of paclitaxel-mediated apoptosis in human leukemia cells by inhibitors of the mitogen-activated protein kinase kinase/mitogen-activated protein kinase pathway. *Molecular Pharmacology, 60,* 143-154.

Yu, J., Guo, Q.L., You, Q.D., Lin, S.S., Li, Z., Gu, H.Y., Zhang, H.W., Tan, Z., & Wang, X. (2006). Repression of telomerase reverse transcriptase mRNA and hTERT promoter by gambogic acid in human gastric carcinoma cells. *Cancer Chemotherapy and Pharmacology, 58,* 434-443.

Yu, J., Guo, Q.L., You, Q.D., Zhao, L., Gu, H.Y., Yang, Y., Zhang, H.W., Tan, Z., & Wang, X. (2007). Gambogic acid-induced G2/M phase cell-cycle arrest via disturbing CDK7-mediated phosphorylation of CDC2/p34 in human gastric carcinoma BGC-823 cells. *Carcinogenesis, 28,* 632-638.

Yu, Y., Du, J.R., Wang, C.Y., & Qian, Z.M. (2008). Protection against hydrogen peroxide-induced injury by *z*-ligustilide in PC12 cells. *Experimental Brain Research, 184,* 307-312.

Yu, Y.L., Yu, S.L., Su, K.J., Wei, C.W., Jian, M.H., Lin, P.C., Tseng, I.H., Lin, C.C., Su, C.C., Chan, D.C., Lin, S.Z., Harn, H.J., & Chen, Y.L. (2010). Extended O6-methylguanine methyltransferase promoter hypermethylation following n-butylidenephthalide combined with 1,3-bis(2-chloroethyl)-1-nitrosourea (BCNU) on inhibition of human hepatocellular carcinoma cell growth. *Journal of Agricultural and Food Chemistry, 58,* 1630-1638.

Yujiri, T., Fanger, G.R., Garrington, T.P., Schlesinger, T.K., Gibson, S., & Johnson, G.L. (1999). MEK kinase I (MEKK1) transduces c-Jun NH2-terminal kinase activation in response to changes in the microtubule cytoskeleton. *The Journal of Biological Chemistry, 274,* 12605-12610.

Zha, J., Harada, H., Yang, E., Jockel, J., & Korsmeyer, S.J. (1996). Serine phosphorylation of death agonist BAD in response to survival factor results in binding to 14-3-3 not BCL-X(L). *Cell, 87,* 619-628.

Zhai, D., Jin, C., Shiau, C.W., Kitada, S., Satterthwait, A.C., & Reed, J.C. (2008). Gambogic acid is an antagonist of antiapoptotic Bcl-2 family proteins. *Molecular Cancer Therapeutics, 7,* 1639-1646.

Zamble, D.B., Mu, D., Reardon, J.T., Sancar, A., & Lippard, S.J. (1996). Repair of cisplatin-DNA adducts by the mammalian excision nuclease. *Biochemistry, 35,* 10004-10013.

Zhang, C.C., & Shapiro, D.J. (2000). Activation of the p38 mitogen-activated protein kinase pathways by estrogen or by 4-hydroxytamoxifen is coupled to estrogen receptor-induced apoptosis. *The Journal of Biological Chemistry, 275,* 479-486.

Zhang, H., & Sun, X.F. (2001). Loss of p27 expression predicts poor prognosis in patients with Dukes' B stage or proximal colorectal cancer. *International Journal of Oncology, 19,* 49-52.

Zhang, L., Du, J.R., Wang, J., Yu, D.K., Chen, Y.S., He, Y., & Wang, C.Y. (2009). Z-Ligustilide extracted from *Radix Angelica sinensis* decreased platelet aggregation induced by ADP *ex vivo* and arterio-venous shunt thrombosis *in vivo* in rats. *Yakugaku Zasshi, 129,* 855-859.

Zhang, Y., Zhou, L., Bao, Y.L., Wu, Y., Yu, C.L., Huang, Y.X., Sun, Y., Zheng, L.H., & Li, Y.X. (2010a). Butyrate induces cell apoptosis through activation of JNK MAP kinase pathways in human colon cancer RKO cells. *Chemico-Biological Interactions, 185,* 174-181.

Zhang, L.J., Chiou, C.T., Cheng, J.J., Huang, H.C., Kuo, L.M., Liao, C.C., Bastow, K.F., Lee, K.H., & Kuo, Y.H. (2010b). Cytotoxic polyisoprenyl benzophenonoids from *Garcinia subelliptica, 73,* 557-562.

Zhao, K.J., Dong, T.T., Tu, P.F., Song, Z.H., Lo, C.K., & Tsim, K.W. (2003). Molecular genetic and chemical assessment of Radix *Angelica* (Danggui) in China. *Journal of Agricultural and Food Chemistry, 51,* 2576-2583.

Zhao, L., Guo, Q.L., You, Q.D., Wu, Z.Q., & Gu, H.Y. (2004). Gambogic acid induces apoptosis and

regulates expressions of Bax and Bcl-2 protein in human gastric carcinoma MGC-803 cells. *Biological & Pharmaceutical Bulletin, 27,* 998-1003.

Zhao, Q., Yang, Y., Yu, J., You, Q.D., Zeng, S., Gu, H.Y., Lu, N., Qi, Q., Liu, W., Wang, X.T., & Guo, Q.L. (2008). Posttranscriptional regulation of the telomerase hTERT by gambogic acid in human gastric carcinoma 823 cells. *Cancer Letters, 262,* 223-231.

Zheng, J., & Ramirez, V.D. (2000). Inhibition of mitochondrial proton F0F1-ATPase/ATP synthase by polyphenolic phytochemicals. *British Journal of Pharmacology, 130,* 1115-1123.

Zheng, Y.Z., Choi, R.C., Li, J., Xie, H.Q., Cheung, A.W., Duan, R., Guo, A.J., Zhu, J.T., Chen, V.P., Bi, C.W., Zhu, Y., Lau, D.D., Dong, T.T., Lau, B.W., & Tsim, K.W. (2010). Ligustilide suppresses the biological properties of Danggui Buxue Tang: a Chinese herbal decoction composed of radix astragali and radix angelica sinensis. *Planta Medica, 76,* 439-443.

Zhou, B.P., Liao, Y., Xia, W., Spohn, B., Lee, M.H., & Hung, M.C. (2001). Cytoplasmic localization of p21Cip1/WAF1 by Akt-induced phosphorylation in HER-2/neu-overexpressing cells. *Nature Cell Biology, 3,* 245-252.

Zhuang, S., & Schnellmann, R.G. (2006). A death-promoting role for extracellular signal-regulated kinase. *The Journal of Pharmacology and Experimental Therapeutics, 319,* 991-997.